Determining changes in *Eucalyptus* litter during decomposition

by

Tsz Ching Christy Hung

A thesis submitted in

fulfilment of the requirements

for the degree of

Doctor of Philosophy

School of Life and Environmental Sciences

Faculty of Science

The University of Sydney

2026

Statement of originality

This is to certify that the content of this thesis is my own work. This thesis has not been submitted for any other degree or purpose.

I certify that the intellectual content of this thesis is the product of my own work, and that all assistance received in preparing this thesis and all sources have been acknowledged.

Tsz Ching Christy Hung

June 2026

Statement of contribution of others

Veronica Quintanilla Berjon and Dr. Danica Parnell collected litterfall and surface fuel litter samples in Wombat State Forest and Orbost State Forest, which are included in Chapter 2 and 4. Surface fuel litter samples used in Chapter 3 were collected by Dr. Meaghan Jenkins and Dr. Lai Fan Poon as part of their project. I am responsible for the experimental designs, collecting laboratory and field data, data analysis, and chapter writing.

This PhD research was conducted under the supervision of Associate Professor Tina Bell and Dr Malcolm Possell. They provided guidance on the research design, data collection and analysis, and offered critical feedback on the thesis development and writing.

Financial support was provided through a Postgraduate Research Scholarship from Natural Hazard Research Australia throughout the PhD candidature.

Tsz Ching Christy Hung

June 2026

Artificial intelligence

I (Tsz Ching Christy Hung) used Grammarly, Copilot, and ChatGPT for the purposes of text enhancement. The use of generative AI tool includes spelling corrections, minor sentence restructuring, and clarify enhancement. I confirm that where text was modified by generative AI, the content was reviewed for possible errors, inaccuracies, and bias. I take full responsibility for the submitted thesis, confirms the work is my own, and has used generative AI in accordance with University guidelines and policies.

Tsz Ching Christy Hung

June 2026

Dedication

To my maternal grandparents, whose journey has ended, yet your story continues to live through me and our family every day.

To my paternal grandparents, whose love embraced me when the story of my life was still a blank page – thank you for writing each chapter with me.

To my niece *Bethany*, soon to begin her own story in this world. I love you with all my heart. Remember: what is lost in the fire can be found in the ashes, and within those ashes, life finds its way back to bloom. May the ending of every chapter in your life nourish a new beginning.

Christy Hung

June 2026

Acknowledgement

I have never been a great storyteller – or at least, that is what my teddy bear used to tell me. I do not quite remember where this story began. Maybe it started when I was four, sitting behind my grandpa as he pedalled his bike through the street, the wind brushing past my cheeks. Or perhaps it was when I was six sneaking into the driver's seat and stealing the wheel while my dad stepped out to get food, imagining one day I would have my own car to drive around the city. It could have begun when I was twelve, riding on the back of my dad's motorcycle on the way to school, holding on tightly and feeling the world rush by. These moments have always stayed with me, ordinary, unforgettable. But if I had to say, I think this story truly began the day I arrived in Australia, chasing a childhood dream to study abroad. That moment marked the beginning of a journey filled with love, growth, and friendship.

Driving your own journey was not as easy as I thought when I was a kid, it was full of uncertainty and difficulties. Like all the greater adventure stories, mine began with two great heroes: Tina Bell and Malcolm Possell, my supervisors and instructors. We started this great journey together back in 2022 – from litterfall to litter decomposition, from the Bushfire Lab to Lansdowne to Batemans Bay. I am deeply grateful for your enormous amount of insights, patience, and unwavering support from my Honours year all the way to the end of my PhD. Thank you for giving me the freedom to steer my own wheel and choose our next destination, while always being there in the passenger seat to offer constructive feedback and encouragement. Thank you for putting your trust in me as a researcher even when I had no idea where we were headed. It has been my privilege to be your padawan, and I could never have achieved this without your guidance and trust.

I consider myself lucky to inherit the large litter samples from Dr. Meaghan Jenkins, Dr. Lai Fan Poon and Veronica Quintanilla Berjon. More importantly, Danica Parnell, as my daily supervisor during my professional development, this journey would not have started without you! These samples helped to build the roadmap for this great journey.

I still remember the day that I moved into Level 3 at ATP. No one was sitting in the open office area except me. But my time here was never dull, because I am part of the wonderful teaching support team. A big thank you to Adriana Hoxha, who welcomed me into this big family. Working alongside

with Iona Gyorgy, Svetlana Ryazanova, Dominic Cross, Jessica Maley, Evelyn Yin, Bridie Stanfield, and Amy Lin was one of the highlights of this journey. A special thanks to Carolina Cuenca Cardozo, who always encouraged me when I doubted myself, having you around was a blessing to me.

I spent countless hours with Tatjana Matic, who became my mentor, mother, best friend, and the best work partner I could ask for. You taught me anything that you knew, and I learned how to be a good scientist from you. You are always patience, listening to my struggles and hearing me out through all my whinges. More importantly, you generously shared your food with me, I am so grateful for the time we spent together – working in the lab, preparing for classes, and having pizza after all the hustles. Those days were unforgettable.

Learning to navigate this journey was never easy – especially when I was just learning how to drive. Spectroscopy was a whole new world and RStudio was always my weak point. I am truly grateful to Alexandre Wadoux for sharing your expertise and friendship. You taught me things I could never have learned alone, and I was lucky to have you around during the early part of my journey.

There were days when the engine would not start, and I was stranded in the middle of nowhere. Many thanks to all the 'mechanics' who helped me keep going. Special thanks to Michael Turner, the 'greatest mechanic of all', for your professional support with the Elementar, muffle furnace, spectrometers, and many more pieces of equipment. I was also lucky to receive help from Ann Ling at GeoSciences – your patience and kindness made this journey possible to continue.

The second year of my journey was full of sun and weeds, and I had two important partners in the field: Sami Hoxha and Anne Vervoort. The litterbag trial could not have been completed without your help and good company. I enjoyed every moment we spent together at Lansdowne and PBI – I have lost count of how many bags of snacks (and sandbag) we shared!

Throughout this journey, there were moments when I was exhausted and had to stop and rest before the next long drive. At those resting areas, I met my friends: José, Julia, Claires, Siska, Quentin, Marié, Yiji, Evelyn, Zongtang, Bright, Oscar, Sandra, Wartini, Mingming, Anita, Max, Harry, and Mikaela. Special thanks to Anne, Jay, Lloyd, Marliana, Yumi, Ricardo, Rachel, Julio, and Muqeet,

who always provided me with food, cake, chocolate, cookies, beers, and laughter. I am truly grateful for your love and encouragement, especially during the final stage when I was stuck in the mud and could not move forward. More importantly, thank you for cheering me on and celebrating with me when I finally reached my destination. This journey would not have been the same without you.

To all my friends at Lidcombe Anglican Church – Joyce, Alan, Ethan, Amelia, Maggy, Brian, Ben, Dilys, Hailey, Karen, Thomas, Charlotte, and many more. Thank you for always inviting me over for dinner when I needed a breather or felt homesick. I also want to thank my friends back in Hong Kong, especially Lucia, Ankie, Shita, and Faye, who have always been there for me since High School.

After 3.5 years of driving, the journey is finally coming to an end. I have saved the most precious for the last because they are there waving me to go home. I want to express my deepest gratitude to my family: Mum, Dad, Bernice, and especially my grandparents. This journey would not have been possible without your endless support, love, and belief in me. I am also grateful to my cousins Kiki and Angel, and especially my lovely niece – Bethany, who is soon to join us. The ‘good morning’ we exchanged every day became my motivation to finish this journey so I could come home and say it in person to Bethany. I love you endlessly.

Like all great stories, this one has an ending – but the memories, the lessons, and the love will stay with me forever.

Abstract

Eucalyptus dominates in nearly 80% of Australian native forests and their litter makes up a large proportion of the surface fine fuel layer (plant material < 6 mm in diameter) on the forest floor. The amount of fuel (i.e., fuel load) on this layer is controlled by the balance between litterfall and decomposition, and in turn, the litter layer significantly influences the spread of fire. Conversely, bushfires and prescribed burning affect the litter layer directly by reducing fuel load and altering its chemical and physical characteristics. In the longer term, fire effects on litter dynamics are mainly through changes in vegetation composition and the quality of the resulting litter.

The increasing risk of bushfire with climate change has led to widespread use of prescribed burning as a management tool across Australia. Consequently, many dry sclerophyll forests are now characterised by mosaics of recently burnt through to long-unburnt areas. Although research related to prescribed burning has examined the effects of fire on vegetation composition and soil properties, relatively little attention has been given to the changes in litter properties during and after fire events. The knowledge of the chemical quality of post-fire litter is essential for understanding litter dynamics and forest productivity in recently burnt areas. Therefore, the broad aim of this study was to investigate the changes of *Eucalyptus* litter quality in fire-prone ecosystems, with a particular focus on using infrared spectroscopy as a viable solution to complex laboratory-based analysis and the implications for analysing *Eucalyptus* litter quality.

A meta-analysis was conducted to provide a broad understanding of the effects of fire on *Eucalyptus* litter decomposition in Australian sclerophyll forests across a wide range of temporal and spatial scales. A systematic search of the peer-reviewed literature found that most Australian studies focused on the indirect ecological consequences of fires rather than its direct effects on decomposition rate. Although fire significantly influences litter dynamics, there were only limited empirical studies investigating post-fire litter decomposition. Collectively, *Eucalyptus* leaf litter decomposed more rapidly in bushfire-affected ecosystems (mean *k*-value of litter decomposition = 1.17 yr^{-1}), whereas decomposition following prescribed burning (mean *k*-value = 0.57 yr^{-1}) was slower than in unburnt areas (mean *k*-values = 0.77 yr^{-1}). However, the underlying mechanisms driving the differences among rates of litter decomposition remain unclear. The meta-analysis highlighted the need for more in-depth empirical studies to disentangle fire effects on litter dynamics, particularly changes in the rate of litter decomposition through alterations in litter quantity and litter quality.

It is well established that litter quality including carbon, nitrogen, cellulose, hemicellulose, and lignin content is a key driver of litter decomposition. However, traditional methods for measuring the components of litter rely on laboratory-based analysis, which are often complex, time-consuming, costly, and laborious. To address such limitations, mixtures of commercially available cellulose,

hemicellulose, and lignin were used as surrogates to investigate alternative methods for determining the chemical quality of *Eucalyptus* litterfall. The feasibility of using a plant mixture powder with visible-near-infrared (vis-NIR), near-infrared (NIR), and attenuated total reflectance Fourier transform infrared (ATR-FTIR) spectroscopy to predict the chemical quality of *Eucalyptus* litterfall was tested. Among the spectroscopic techniques used, NIR spectroscopy outperformed vis-NIR and ATR-FTIR for predicting the chemical quality of *Eucalyptus* litterfall, particularly for cellulose and lignin. Importantly, this study highlighted the potential of using spectroscopy as an effective tool for quantifying the litter chemical quality and set the scene for its broader application in understanding decomposition of forest litter.

Despite extensive research efforts to understand the dynamics of litter decomposition, most studies have focused exclusively on single-species or single-component leaf litter. However, this approach is not sufficient for understanding the dynamics of the forest litter layer since leaf and woody litter of different species may interact and decompose at different rates under natural conditions. A 15-month *in-situ* litterbag trial using overstorey *Eucalyptus* leaf litter, understorey vegetation, and surface fine fuel litter on the forest floor was done to test this hypothesis. The effect of fire was investigated by incorporating litter collected prior to a prescribed fire (PF) and 1-year after prescribed fire (1YAF). These materials were decomposed individually and in two- and three-component mixtures to understand the impacts of litter components, mixture composition, and time-since-fire on litter decomposition. Understorey litter alone and in combination with other litter components, had the greater mass loss, while *Eucalyptus* leaf litter alone had the lowest mass loss. At the end of the decomposition trial, litter collected 1-year after prescribed fire consistently decomposed at a faster rate (indicated by greater mass loss over time) than that collected prior to prescribed fire, with statistically significant differences found for *Eucalyptus* litter alone, *Eucalyptus* litter with understorey litter, understorey litter alone, and *Eucalyptus* leaf with decomposing litter. Understanding the synergistic effects of litter components on decomposition provides valuable insights for fire and fuel management strategies, particularly in ecosystems where prescribed burning is used regularly. Importantly, this study showed that ATR-FTIR spectroscopy provides more accurate predictions of carbon and nitrogen in litter during *in-situ* litterbag decomposition than NIR spectroscopy. This suggested that ATR-FTIR may be a more suitable technique to capture the complexity of and changes in chemical quality during natural litter decomposition.

Building on this work, a combustion experiment was conducted to examine the changes in litter properties during combustion, a process that often referred to as thermal decomposition. The aim of this study was to understand the effects of prescribed burning on litter mass loss and evaluate the performance of vis-NIR, NIR, and ATR-FTIR spectroscopy in predicting the carbon and nitrogen content of combustion residues (char and ash). To simulate temperatures typical of prescribed burning

in dry sclerophyll forests, surface fuel litter, including *Eucalyptus* leaf, twigs, and fine fuel litter were heated to or combusted at five different temperatures (200-600 ºC) in a muffle furnace. There was a clear pattern of increasing mass loss across the temperature gradient, with more than 70% of the initial litter mass loss at 600 ºC. Changes in total carbon and total nitrogen of surface fuel litter were more variable at lower temperatures. For example, nitrogen mineralisation occurred at lower temperature, followed by a sharp decline in both carbon and nitrogen content as combustion temperature increased. Spectroscopy, especially ATR-FTIR, demonstrated strong potential for predicting the chemical quality of combustion residues (i.e., validated R^2 = 0.97 for carbon and validated R^2 = 0.93 for nitrogen). This study highlights the powerful capability of spectroscopic techniques, especially ATR-FTIR spectroscopy, as a promising technology to characterise the chemical quality of naturally and thermally decomposed litter. ATR-FTIR offers a valuable opportunity to monitor post-fire nutrient dynamics to understand the ecological impacts of prescribed burning in *Eucalyptus* forests.

To the author's knowledge, this is the first comprehensive study to test all three commonly used spectral regions (vis-NIR, NIR, and ATR-FTIR) to analyse the chemical quality of *Eucalyptus* litter. The research demonstrates strong potential of spectroscopic techniques for predicting the chemical quality of *Eucalyptus* litter, including litterfall, during decomposition of litter, and combustion residues (i.e., char and ash) formed under laboratory conditions. The best spectroscopic techniques varied depending on the condition of the litter. For example, NIR spectroscopy provided a more accurate prediction for litterfall, while ATR-FTIR offered a better estimation for carbon and nitrogen prediction for biologically and thermally decomposed litter. These studies highlight the strength of each spectral region and their potential application in a broader ecological context. More importantly, this research has shown that sample-specific models provide more accurate predictions than a generalised (i.e., universal) model that was built using plant materials in other form. In addition, practical recommendations for model testing and a workflow based on different sample types are provided for researchers using spectroscopic methods in their studies.

Spectroscopy, when used alongside with laboratory analysis, is a rapid, accurate, and sustainable method for measuring litter chemical quality, particularly when dealing with large numbers of samples. With the rapid development in spectroscopic technology, future studies could explore the potential of spectroscopy in *in-situ* field conditions to examine its potential use in long-term fuel management. This study also highlights the potential of using spectroscopy in quantifying carbon and nitrogen content in litter and combustion residues. From a management perspective, this technique is useful in predicting the fire severity and the rate of forest recovery based on post-fire litter nutrient dynamics.

Overall, this study demonstrated that both natural and thermal decomposition alter litter carbon and nitrogen content and, consequently, decomposition rate. The results confirmed the

predominant role of climate in controlling litter decomposition, where rapid initial mass loss occurred under wet and warm conditions. At a regional scale, decomposition was governed by initial litter quality, particularly C/N ratio. For example, *Eucalyptus* litter with high C/N ratios decomposed more slowly than N-rich understorey litter. Under natural environment, where litter from various species usually decomposes as mixtures, the presence of N-rich litter facilitated the decomposition of *Eucalyptus* through nutrient transfer.

While being effective in fuel reduction, prescribed burning also plays a significantly role in regulating litter decomposition and nutrient dynamics. This study showed that litter collected 1-year after a prescribed fire decomposed more rapidly than litter collected prior to a prescribed fire, largely due to fire-induced changes in initial C/N ratios. In dry sclerophyll forests where prescribed burning is implemented, post-fire regeneration of understorey vegetation further enhanced litter decomposition rates, potentially providing a nutrient kick that can support forest recovery following fire. However, despite this facilitation of decomposition, carbon and nitrogen retained in surface fuel litter are redistributed through volatilisation and mineralisation, with consequence for terrestrial nutrient dynamics. From a management point of view, these findings highlight the importance of understanding how litter dynamics varies with fire regimes and understorey composition. These findings provide valuable guidance for site-specific fire and fuel management strategies that incorporate variation in litter quality, litter mixture composition, understorey vegetation, and fire regimes in fire-prone dry sclerophyll forests.

Table of Contents

Abbreviations

Abbreviation	Definition
1YAF	1-year after fire
ATR-FTIR	Attenuated total reflectance Fourier transform infrared
CV	Cross-validation
DL	Decomposing litter
EL	*Eucalyptus* leaf
EF	Elevated fuel
FF	Fine fuel
GA	Genetic algorithm
k-value	Decomposition rate constant
LCCC	Lin's Concordance Correlation Coefficient
LMM	Linear mixed model
LMR	Litter mass remaining
MIR	Mid-infrared
MSC	Multiplicative scatter correction
NIR	Near-infrared
Orbost SF	Orbost State Forest
PF	Prior to fire
PLSR	Partial least square regression
R^2	Coefficient of determination
R^2cv	Coefficient of determination of cross-validation
RF	Random forest
R^2v	Coefficient of determination of validation
RMSE	Root mean squared error
RMSECV	Root mean squared error of cross-validation
RMSEV	Root mean squared error of validation
SG	Savitzky-Golay
SNRs	Signal-to-noise ratios
SNV	Standard Normal variation
w	Window size
Wombat SF	Wombat State Forest
vis-NIR	Visible-near-infrared

Chapter 1

The effects of fire on litter decomposition in Australian *Eucalyptus* forests

1.1 Introduction

1.1.1 Sclerophyll forests in Australia

Forests are considered as one of the most valuable ecosystems on Earth, servicing as a nursey site for both flora and fauna by providing habitats, foods, and resources (e.g., Wood and Storer, 2009; Brockerhoff et al., 2017). Forests also play a critical role in regulating climate, acting as a global carbon (C) sink by absorbing atmosphere carbon dioxide (CO_2), a primary greenhouse gas, through photosynthesis, and releasing CO_2 back to the atmosphere through plant respiration (e.g., Führer, 2000). A fraction of carbon is retained in vegetation and soil, contributing to long-term carbon sequestration (e.g., Richards and Stokes, 2004).

According to the Food and Agriculture Organisation (FAO), a forest is defined as an area greater than 0.5 ha with trees taller than 5 m and a canopy cover more than 10% (Food and Agriculture Organisation, 2025). In contrast, a forest in Australia is recognised as being an area with tree height of more than 2 m with at least 20% of canopy cover (Australian Bureau of Agricultural and Resource Economics and Sciences, 2023). Under this national definition, Australia has approximately 133.6 million ha of forest, representing 17% of the total land area (Australian Bureau of Agricultural and Resource Economics and Sciences, 2023; Food and Agriculture Organisation, 2025). Forested areas can be categorised into native forests (98%), commercial plantations (1.5%), and other forest types (e.g., *Banksia* and *Callitris* forests; 0.5%). Broadly, Australian native forests are dominated by species of *Eucalyptus* (77%) and *Acacia* (8%), spanning a wide range of geographical and climatic conditions (Australian Bureau of Agricultural and Resource Economics and Sciences, 2023). *Eucalyptus* forests are often further categorised into dry and wet sclerophyll forests, defined by canopy structure, dominant species, and soil fertility (Webb et al., 1959; Ashton and Attiwill, 1994; Boland et al., 2006).

Wet sclerophyll forests (WSFs), also referred to as tall open forests, are characterised by tall trees (> 30 m) and a crown cover of 30-70% (Specht, 1970) (Table 1.1). Common species of *Eucalyptus* includes *E. grandis* (Flooded Gum), *E. delegatensis* (Alpine Ash), *E. obliqua* (Messmate Stringybark), and *E. pilularis* (Blackbutt). These forests are typically found in areas with mean annual

rainfall exceeding 1,000 mm with moderately fertile soil across high-altitudinal foothills, mountainous terrains, and deep gullies in southern Queensland, central, southern and northern New South Wales, central and southern Victoria, southern Tasmania, and southwest Western Australia (Ashton and Attiwill, 1994; Krishnan et al., 2019) (Table 1.1). Wet sclerophyll forests support development of a dense understorey of ferns, herbs, and rainforest associated species (Ashton and Attiwill, 1994; Stanton et al., 2014; Wardle-Johnson et al., 2017; Fensham et al., 2024).

In contrast, dry sclerophyll forests (DSFs), often referred to as open forests, are structurally more open and are characterised by a more diverse range of shrubs and grassy understorey species compared to WSFs (Ashton and Attiwill, 1994). Dominant trees are 10-30 m in height with canopy cover between 30-70%. Dry sclerophyll forests are widely distributed across Australia, typically occurring within 200 km of the coastline and on low fertility sandy, shallow soil (Ashton and Attiwill, 1994). Common *Eucalyptus* species in DSFs includes *E. marginata* (Jarrah), *E. sieberi* (Silvertop Ash), *E. globulus* (Blue Gum), and *E. radiata* (Narrow-leaved Peppermint).

It is important to acknowledge that forests classified under the same broad forest type can differ substantially across large spatial scales (Ashton and Attiwill, 1994). Variations in climatic and topographic conditions can result in distinct vegetation composition, litter dynamics, and fire regimes within the same broad forest type.

1.1.2 Fire and fire regimes in Australian sclerophyll forests

Bushfire, which is an Australian term equivalent to “wildfire”, “wildland fire” or “forest fire”, is a common disturbance in sclerophyll forests (Bowman, 1986; Bowman et al., 2009; Attiwill, 1994; Ashton and Attiwill, 1994; Bradstock et al., 2012; Sharples et al., 2016). Bushfire is defined as an unplanned and uncontained vegetation fire that can have significant economic, social, and environmental consequences (Cruz et al., 2018; McLauchlan et al., 2019). Fire has been a fundamental environmental element in Australia for 30 million years (Berad, 1977; Bowman, 1986; Bowman, 1998; Bowman et al., 2009; Attiwill, 1994; Ashton and Attiwill, 1994; Bradstock et al., 2012; Sharples et al., 2016; Morgan et al., 2020). Australian terrestrial ecosystems have been shaped by both natural fire and anthropogenic fire regimes, resulting in the dominance of fire-tolerant *Eucalyptus* in sclerophyll forests (Gill, 1975; Bowman, 1998; Burrows et al., 2013; Morgan et al., 2020).

In fire ecology and management, ‘fuel’ refers to the flammable material available for combustion (Cruz et al., 2018; McLauchlan et al., 2020). Forest fuels are primarily comprised of live and dead biomass including leaves, twigs, bark, and reproductive parts derived from both overstorey

and understorey species (Gould et al., 2011; Abram et al., 2021; Neumann et al., 2021). Such fuels are highly combustible and support regular fire; however fuel loads vary considerably among forest types (Murphy et al., 2013; Bowman et al., 2021). Bushfires typically occur in hot and dry summer months when fuel moisture content is low. In southeast Australia, bushfire seasons generally occur from spring through to autumn, coinciding with period of high temperature and low humidity (Cheney, 1976; Williamson et al., 2016; Abram et al., 2021). Dry sclerophyll forests typically experience frequent (~10 years) low-intensity surface fires, while crown fires (i.e., fire that burn through vegetation canopy) occur less regularly under extreme fire weather (Murphy et al., 2013; Bowman et al., 2021). In contrast, WSFs are characterised by infrequent fires (30-75 years) that range from low-intensity surface fires to high severity crown fires being generally constrained by relatively high fuel moisture content (Murphy et al., 2013; Bowman et al., 2021).

1.1.3 Changes in fire regimes

Fire regimes describe the long-term patterns and characteristics of fires including how often fire occurs (frequency), rate of energy release (intensity), time of year (seasonality), size of burnt area (extent), and the impact of fire on ecosystems (severity) (Gill, 1975; Keeley, 2009; Morgan et al., 2001; Barker and Price, 2018). Fire regimes are predominately driven by climate and its interaction with other factors such as vegetation composition, topography, and human-induced disturbances (Cheney, 1976; Thomas et al., 2014). Shift in fire regimes can have substantial immediate and long-term impacts on forest structure, vegetation composition, and the subsequent litter dynamics (Ashton and Attiwill, 1994; Cawson et al., 2018; Morgan et al., 2020; Muqqaddas and Lewis, 2020).

For thousands of years, Aboriginal people have used fire as a spiritual, cultural, and land management tool (e.g., Bowman, 1998; Kimber and Friedel, 2015; Fletcher et al., 2019). Indigenous fire which is characterised by low intensity and slow-moving fire was used to create mosaic of burnt and unburnt patches to promote regrowth and to reduce vegetation (Bowman, 1998; Morgan et al., 2020; Fletcher et al. 2021). Following European settlement, many Australian ecosystems have transitioned from Indigenous fire regimes to vastly different fire regimes with application of modern fire management practice which focus on fuel reduction (Bradstock et al., 2012; Morgan et al., 2020).

Bushfire seasons are extending as a consequence of anthropogenic climate change (Clarke et al., 2011; Filkov et al., 2020; Nolan et al., 2020; Abram et al., 2021). Hotter and drier weather conditions reduce fuel moisture content, increasing the possibility of ignitions and intensifying subsequent fire behaviour (Cawson et al., 2017; Abram et al., 2021). These effects were evident in 2019, when south-eastern Australia experienced record-breaking high temperatures coupled with

exceptionally low rainfall, producing dry fuel loads that contributed to the unprecedented scale and intensity of the 2019/20 Black Summer Bushfires (Filkov et al., 2020; Abram et al., 2021). Over 23% of the temperate forests in southeast Australia was burnt during the 2019/20 fire season (Nolan et al., 2020; Abram et al., 2021).

1.1.4 Determinants of fire behaviour

Fire behaviour is strongly influenced by meteorological conditions, topography, and fuel characteristics (Catchpole et al., 1998; Linn et al., 2007; Ganteaume et al., 2009; Bradstock et al., 2010; Gould et al., 2011; Hollis et al., 2015; Storey et al., 2016; Cruz et al., 2018; Hollis et al., 2025). Meteorological conditions and topography influence fire behaviour primarily through their effects on vegetation dynamics, which in turn determine fuel characteristics including fuel load and fuel moisture content (Bradstock et al., 2010; Matthews, 2014; Holsinger et al., 2016; Muscarella et al., 2019). Over large spatial and temporal scales, past climate and topography have interacted to shape forest structure and vegetation composition. At a local scale, weather and topography have a direct influence on fuel composition and moisture content, of which is a key driver of flammability (capacity to burn; Pauas et al., 2017). Consequently, under similar weather conditions for a given fuel load (i.e., dry biomass available to burn), fires tend to be more severe on ridges where fuel moisture is low, than in valleys, where fuels have higher moisture content (Penman et al., 2007; Bradstock et al., 2010; Cawson et al., 2017).

1.1.5 Prescribed burning as a fuel management strategy

Among all attributes of fire behaviour, fuel load is the only parameter that can be directly managed by humans. To mitigate the impact of bushfires, prescribed burning (also known as planned burning, controlled burning, hazard reduction burning, and fuel reduction burning) has been used as a management tool to reduce accumulated fuels on the forest floor (Burrows, 2008; Altangerel and Kull, 2013; McCaw, 2013; Price et al., 2022; Hashida et al., 2025). Prescribed burning is conducted during favourable weather conditions (March to May and September in southeast Australia; Clarke et al., 2019; Di Virgilio et al., 2020), including low wind speed, relatively high humidity, and cool temperature, to maintain low- to moderate fire intensity (usually < 4000 kW m^{-1}; Storey et al., 2016; Clarke et al., 2019). The extent of fuel consumption during a prescribed burn depends greatly on weather conditions, fire severity, fuel moisture content, and fuel composition (e.g., Fernandes and Botelho, 2003; Hollis et al., 2011; Sullivan et al., 2012; Di Virgilio et al., 2018). Drawing upon the synthesis by Price et al. (2022), prescribed burns typically remove 94% of near-surface fuel (i.e., low

lying vegetation, usually vertically oriented) and 68% of surface fine fuel (i.e., plant material < 6 mm in diameter) in DSFs (Raison et al., 1985; Hollis et al., 2011; Volkova and Weston, 2013; Volkova et al., 2014; Possell et al., 2015; Volkova and Weston, 2015; Jenkins et al., 2016; Volkova and Weston, 2019). Prescribed burning can immediately reduce bushfire risks by removing surface fuel and can substantially change natural fire regimes by directly altering fire seasonality and frequency, and indirectly influencing fuel dynamics (Bowman et al., 2011; Furlaud et al., 2023).

Despite the potential benefits of prescribed burning as a risk mitigation strategy, long-term use of prescribed burning can have deleterious ecological consequences (e.g., Fernandes and Botelho, 2003; Lewis et al., 2012; Althangerel and Kull, 2013; Burrows and McCaw, 2013; McCaw, 2013; Bennett et al., 2014; Cannon and Clemet, 2025). For example, declines in total C stocks have been documented in a DSF in Victoria (Bennett et al., 2014) and a WSF in south-east Queensland (Butler et al., 2020). In addition, long-term use of frequent fire to reduce fuel load can influence understorey composition (e.g., Birk and Bridges, 1989; Spence and Baxter, 2006; Lewis et al., 2012). For example, a study conducted in a long-term prescribed burning experimental site in a WSF in Queensland demonstrated that biennial and quadrennial burning increased the prevalence of grass (Lewis et al., 2012). In this case, an increase in highly flammable grass has the potential to increase the severity of future fire through the changes in understorey structure and composition (Lewis et al., 2012). Understandably, these studies have raised concerns regarding the long-term use of prescribed burning in sclerophyll forests under the current climate projections.

1.1.6 Fuel strata and layers in dry sclerophyll forests

For management purposes, Gould et al. (2011) established a rapid fuel assessment scheme for DSFs according to their vertical position above the ground (i.e., height) and fuel orientation (i.e., vertical or horizontal) (Gould et al., 2011; Cruz et al., 2018; Hollis et al., 2025).

Australian sclerophyll forests can be divided into five different fuel strata, which are (1) overstorey canopy of trees; (2) intermediate or understorey canopy trees; (3) elevated fuel layer; (4) near-surface fuel layer; and (5) surface fuel layer. Each fuel stratum contributes to fire behaviour differently, based on their vertical and horizontal continuity, physical state (i.e., live or dead), and bulk density (Gould et al., 2011; Cruz et al., 2018; Hollis et al., 2025). The flammability of the overstorey and intermediate canopy is strongly influenced by bark traits, particularly the presence of loose, fibrous bark that can act as ladder fuel which facilitate the spread of surface fire to the canopy layer (Gould et al., 2011; Grootemaat et al., 2017; Hollis et al., 2025). The elevated fuel layer consists of vertically oriented understorey vegetation, including live and dead shrubs and ferns, typically

ranging from 4-7 m tall. The near-surface fuel layer contains a mixture of vertically and horizontally oriented materials, including grasses, small shrubs, coarse woody debris, and freshly fallen plant material. The surface fuel layer, also known as the litter layer, is a horizontally arranged layer composed of freshly fallen leaves, twigs, bark, and reproductive material from both understorey and overstorey species.

Fine fuel within the surface fuel layer, which is defined as dead biomass < 6 mm in diameter and live biomass < 2 mm in diameter, serves as the primary ignition source and, when it burns, supplies the energy required for fire spread (Rogers and Westman, 1977; Fox et al., 1979; Woods and Raison, 1983; O'Connell, 1986; Birk and Bridges, 1989; Bridge, 2004; Gould et al. 2011; McCaw, 2013; Cawson et al., 2017; Pausas et al., 2017; Cruz et al., 2018; Neumann et al., 2021; Sullivan et al., 2021). Understanding the characteristics of the surface fuel layer is critical for effective fuel and fire management in sclerophyll forests (Cawson et al., 2017).

1.1.7 Litter dynamics

The importance of the surface fine fuel layer in ignition and spread of fire is a function of its characteristics, including thickness, continuity, bulk density, moisture content, and particle size (Gould et al., 2011; Thomas et al., 2014; Cawson et al., 2017). These characteristics, however, are highly variable over time and space (Cawson et al., 2017; Cruz et al., 2018). Under natural conditions, the amount (i.e., mass, depth) of surface fine fuel accumulated on the forest floor is primarily governed by the interplay between litterfall and litter decomposition processes (Olson, 1963; Birk and Simpson, 1980; Thomas et al., 2014; Neumann et al., 2021). These processes, in turn, are greatly dependent on climate (Ashton, 1975; Briggs and Maher, 1983), forest age (Ashton 1975), vegetation community (Sangha et al., 2006), and fire history (Fox et al., 1979; O'Connell et al., 1979). The balance between litterfall and decomposition is particularly importance in fire-prone landscapes where surface fine fuel litter exerts strong control over fire ignition and subsequent fire behaviour (McCaw et al., 2012).

Litterfall

Litterfall refers to the process by which dead plant materials (including leaves, twig, bark, and fruits) are abscised from vegetation and transferred to the forest floor (Bray and Gorham, 1964). Once shed, dead plant material is commonly referred to as litter (Facelli and Pickett, 1991), while the forest floor consisting of accumulated litter is often termed the litter layer (Spain, 1984). In Australian

sclerophyll forests, the rate of *Eucalyptus* litterfall is highly seasonal, primarily controlled by climatic factors such as temperature and rainfall (e.g., Ashton, 1975; Briggs and Maher, 1983; Adams and Attiwill, 1986; Pook et al., 1997; Turner and Lambert, 2022; Lamb, 2006; Penman and York, 2010). Typically, peak litterfall occurs during summer and early autumn, with lower rates in cooler months. *Eucalyptus* leaves are the main component of total litterfall (50-70%), followed by bark (10-20%), while twigs, flowers and fruits contribute smaller proportions (Ashton, 1975; Muqaddas and Lewis, 2020). Other factors such as vegetation composition, topography, and the frequency of disturbance including fire and drought also exert strong controls on litterfall dynamics (e.g., Ashton, 1975; Briggs and Maher, 1983; Adams and Attiwill, 1986; Pook et al., 1997; Turner and Lambert, 2022; Lamb, 2006; Penman and York, 2010; Muqaddas and Lewis, 2020). Variation in rate of litterfall influences the quantity and composition of litter on the forest floor, thereby affecting subsequent litter decomposition processes.

Litter decomposition

Litter decomposition refers to the breakdown and degradation of accumulated plant debris (i.e., litter) on the forest floor by detritivores and soil microorganisms (Aerts, 1997). During decomposition, litter is progressively reduced to form inorganic matter and nutrients that are available for plants and microorganism to take up (Baker, 1983; Coûteaux et al., 1995; Gartner and Cardon, 2004; Paudel et al., 2015). Litter decomposition therefore represents a key pathway in nutrient cycling, mediating the transfer of carbon and nitrogen from vegetation to soil (Attiwill, 1968; Ashton, 1975; O'Connell et al., 1978; Hingston et al., 1980, Baker et al., 1983; O'Connell and Menage, 1982; Coûteaux et al., 1995; Crockford and Richardson, 1998; Shammers et al., 2003; Sangha et al., 2006; Butler et al., 2020).

The rate of litter decomposition is regulated by complex interactions among environmental conditions (e.g., temperature and moisture availability), litter quantity, litter chemical quality (also known as litter quality, litter chemical composition, and litter chemical traits), and the soil microbial community (also known as decomposer community) (Meentemey et al., 1978; Melillo et al., 1982; Coûteaux et al., 1995; Aerts, 1997; Hättenschwiler et al., 2005; Cornwell et al., 2008; Paudel et al., 2015; Prieto et al., 2019; Wang et al., 2019b). In this context, litter chemical quality refers to the nutrient content and structural composition of plant litter, including concentrations of C, N, P, as well as other labile (e.g., sugars and cellulose) and recalcitrant (e.g., lignin and tannins) compounds that influence decomposition rate.

Over the last few decades, there has been substantial progress in understanding the key drivers of decomposition. A global meta-analysis of litter decomposition across multiple climatic zones found that the effects of climate and litter chemical quality (e.g., C, N, and lignin content) on leaf litter decomposition are hierarchical (Aerts, 1997). At a global scale, climate is the dominant control on decomposition, whereas at regional scales, litter chemical quality and microbial community become more dominant (e.g., Aerts, 1997; Zhang et al., 2008; Lam et al., 2021). For example, long-term climatic conditions strongly shape vegetation structure and plant functional traits, which subsequently influence the diversity and composition of the microbial community (Krishna and Mohan, 2017).

At the ecosystem scale, litter decomposition rate is predominantly driven by litter chemical quality including carbon:nitrogen (C/N) ratio and lignin content (Aert, 1997; Zhang et al., 2008; Paudel et al., 2015; Wang et al., 2022). The early stages of decomposition are largely controlled by concentrations of labile compounds and the C/N ratio, whereas lignin related traits (e.g., lignin:nitrogen (lignin/N) ratio) become more important in the later stages (Melillo et al., 1982; O'Connell, 1988; Berg and McClaugherty, 1989; Taylor et al., 1989; Aerts, 1997; Cornwell et al., 2008; Talbot et al., 2012). In this sense, high-quality litter (i.e., low C/N ratio and low lignin content) decomposes more readily than low-quality litter under warm and moist conditions (Zhang et al., 2008; Cuchietti et al., 2014).

Eucalyptus litter is generally expected to decompose slowly due to its high C/N ratio and high lignin content (O'Connell, 1986; Crockford and Richardson, 2002). Among *Eucalyptus* litter components, leaf litter is expected to decompose more readily than bark, as bark typically has a high C/N ratio (Paul and Polglase, 2004). Litter decomposition also varies substantially among species due to the difference in litter chemical quality. For example, high-quality litter from ferns and nitrogen fixing understorey legumes such as *Acacia* spp. decompose more rapidly than litter from *Eucalyptus* (e.g., O'Connell, 1986; Briones and Ineson, 1996; Xiang and Bauhus, 2007). In other ecosystems, leaves of herbaceous dicot species decompose more rapidly than monocot graminoid species (Cornelissen and Thompson, 1996).

1.1.8 Modelling litter accumulation and decomposition

Over the past several decades, a considerable number of fuel accumulation models have been developed to describe and predict the dynamics of vegetation, fuel loads, and fire behaviour (e.g., Jenny et al., 1949; Olson, 1963; Bunnell and Tait, 1974; Birk and Simpson, 1980; Zazali et al., 2021). From a fire management perspective, these models provide valuable guidance for determining appropriate intervals between prescribed burns based on the rate of surface fine fuel accumulation

(Raison et al., 1983; Hamilton et al., 1991; Fernandes and Botelho, 2003; Thomas et al., 2014). However, empirical measurements of litterfall and decomposition remain critical for effective forest and fire management.

Among existing models, the single negative exponential equation proposed by Jenny et al. (1949) and later modified by Olson (1963) was the first to mathematically described litter dynamics. The Olson model, also known as the 'Olson curve', has been widely applied to estimate litter decomposition rates and predict litter accumulation (e.g., Birk, 1979; Raison et al., 1986; Hart, 1995; McCaw et al., 1996; Tolhurst et al., 2008; Penman and York, 2010; Parsons et al., 2011; Thomas et al., 2014; Neumann et al., 2021).

The Olson model is based on a linear differential equation in which litter accumulates at a constant input rate (L) and decomposes at a decomposition rate constant (k; yr^{-1}; hereafter referred to as the k-value). The equilibrium fuel load or steady state (X_{ss}) is described by:

$$X_{ss} = \frac{L}{k} \qquad \text{Equation 1.1}$$

In the Olson model, the steady-state represents the balance between litterfall (i.e., input) and biomass loss through decomposition (i.e., output). This model suggested that decomposition rate can be explained by negative exponential pattern:

$$X_t = X_0\, e^{-kt} \qquad \text{Equation 1.2}$$

where X_t is the weight of litter remaining at time = t, X_0 is the initial weight of litter, and k is a decomposition rate constant (yr^{-1}).

The Olson model does not incorporate the contributions of understorey vegetation to the forest floor and their impacts on litter decomposition (e.g., Birk, 1979; Paul and Polglase, 2004; Lewis and Debuse, 2012; Gordon et al., 2017; Zazali et al., 2021; Adams and Neumann, 2024). More importantly, the Olson model assumes constant rates of litterfall and decomposition and the absence of disturbance, such as fires and drought. Under this assumption, the forest floor is expected reach a steady-state condition. However, these assumptions do not adequately reflect the spatio-temporal variability of litterfall and decomposition across species, forest types, and ecosystems (e.g., Ashton, 1975; Aerts, 1997). In Australia, where many forests are frequently disturbed by bushfires and prescribed burns, long fire-free intervals are required to reach a steady-state. Consequently, the Olson model might not be applicable in fire-prone DSFs.

To address these limitations, several modifications have been proposed to encapsulate fire, litter heterogeneity, and the role of litter chemical quality into the Olson model (e.g., Bunnell and Tait, 1974; Birk and Simpson, 1980; Raison et al., 1983; Rovira and Rovira, 2010; Zazali et al., 2021).

For example, Bunnell and Tait (1974) introduced a double exponential decay model that categorised litter into labile and recalcitrant components:

$$W_t = W_1 e^{-k1t} + (W_0 - W_1) e^{-k2t} \quad \text{Equation 1.3}$$

where W_t is the weight of litter at time t, W_1 is the amount of soluble component present, W_0 is the initial weight of litter, k_1 and k_2 are decomposition constant for labile and recalcitrant components, respectively. Although this model provides a more accurate prediction than the Olson model (O'Connell, 1987), the underlying mechanisms are not clearly explained and justified (Zazali et al., 2021).

Despite its limitations, the Olson model continues to be widely used to estimate fuel load and the decomposition rate constant (*k*-value) in Australian DSFs due to its simplicity (e.g., Fox et al., 1979; Birk, 1979; Birk and Simpson, 1980; McCaw, 2002; Tolhurst and Kelly, 2003; Gould et al., 2011; Parsons et al., 2011; Matthews et al., 2012; Volkova et al., 2019; Baietto et al., 2021; Burrows et al., 2023). In most existing studies, *k*-values were derived from litterbag experiments using the Olson model, based on litter mass loss measured over a known period of time (see Equation 1.2; e.g., Parsons et al., 2011). Decomposition rate constant (*k*-values) reported using this approach encapsulated the concurrent effects of climate and other environmental parameters on litter decomposition.

More recently, Neumann et al. (2021) conducted a meta-analysis to estimate decomposition rate constant (*k*-value) in unburnt sites (≥ 5 years since year) across Australia using an alternative implementation of the Olson model, in which *k*-value is calculated as a function of litterfall (LF) and standing litter (SL): k = LF/SL. In this context, litter including leaf, twigs, bark, fragmented, and partly decomposed litter accumulated on the forest floor were reported as standing litter. Although *k*-values derived from litterbag studies and those reported by Neumann et al. (2021) are conceptually equivalent, as both are calculated according to the Olson model, the latter assumes a steady-state litter pool and derived *k*-value from accumulated litter rather litter mass loss over time. At a continental scale, Neumann et al. (2021) reported mean *k*-values of 0.498 ± 0.435 yr^{-1} for total litter (i.e., litterfall and standing litter) and 1.093 ± 0.997 yr^{-1} for leaf litter.

Reliance on the Olson model without accounting for fire impacts on litterfall, decomposition, and forest structure may result in inaccurate prediction of fuel accumulation in fire-prone ecosystems (e.g., Zazali et al., 2021; Adams and Neumann, 2024). More sophisticated empirical studies are needed to fully understand the influence of fire on litter decomposition and to refine the application of the Olson model.

1.1.9 Fire effects on litter decomposition

Bushfires and prescribed burning increase the complexity of litter decomposition, primarily through direct and indirect alteration of vegetation composition, soil properties, and microbial activities (O'Connell 1987b; Certini, 2005; Brennan et al., 2009; Guinto et al., 2011; Lewis et al., 2012; Toberman et al., 2014; Muqaddas et al., 2016; Ficken and Wright, 2017; Butler et al., 2020; Liechty and Reinke, 2020). The extent to which fire alters litter decomposition depends greatly on forest type, forest structure, and more importantly, fire intensity, frequency, and severity (e.g., Raison et al., 1986; Bennett et al., 2014; Butler et al., 2017a; Ficken and Wright, 2017; Butler et al., 2020).

Bushfires can reduce decomposition rates by causing an immediate decline in microbial biomass (e.g., Dooley and Treseder, 2012). In contrast, frequent prescribed burning may accelerate decomposition indirectly by altering the understorey layer. Repeated fires often reduce woody understorey vegetation, hence increasing light penetration to the forest floor and promote the growth of ferns and nitrogen fixing legumes such as *Acacia* (e.g., Birk and Bridge, 1989; Spence and Baxter, 2006; Lewis et al., 2012; Muqaddas and Lewis, 2020). However, frequent fire may also negatively affect decomposition by altering the stoichiometry (i.e., balance) of C, N, P in plant and soil (e.g., Bui and Henderson, 2013; Toberman et al., 2014; Butler et al., 2019). In addition, prescribed burning aimed at reducing fuel loads can lead to rapid re-accumulation of surface litter within 5 years (e.g., Raison et al., 1986; McCaw et al., 1996), with slower subsequent decomposition due to reduced litter thickness (McCaw et al., 1996).

Despite substantial research, findings on fire effects on litter decomposition and environmental factors, including understorey vegetation richness and composition, soil properties, and microbial activity often lead to divergent conclusions (e.g., Certini et al., 2011; Meira-Castro et al., 2015; Ficken and Wright, 2017; Butler et al. 2020; Muqaddas and Lewis, 2020). Such discrepancies may be partly due to differences in fire history, fire regimes, and site-specific factors. Consequently, the lack of consistent results limits our ability to understand the long-term consequences of fire on the litter decomposition in sclerophyll forests. It is also important to consider the impact of fire on understorey vegetation composition and their resulting litter quality to fully understand the influence of fire on litter decomposition and nutrient release.

1.1.10 Objective and research questions

This chapter employed a meta-analysis approach to evaluate the effects of fire on litter decomposition in DSFs and WSFs across Australia. Specifically, this review examined the concurrent influences of site-specific factors including climate, landscape position (i.e., inland vs. coastal), litter

component (e.g., leaf, twig, bark, and total litter), and fire type (i.e., unburnt, prescribed burning, and bushfire) on the rate of litter decomposition. The research questions below form the basis of this review:

1. How does the rate of *Eucalyptus* litter decomposition vary among fire type (i.e., prescribed burning versus bushfire) as a function of forest type?
2. How does the rate of *Eucalyptus* litter decomposition vary among different types of surface fine fuel litter (e.g., leaves, twigs, total litter) as a function of fire type?
3. How does fire influence potential drivers (i.e., vegetation composition, litter quality and quantity, soil properties, and microbial activity) of litter decomposition?

1.2 Materials and methods

1.2.1 Literature search and data extraction

A systematic literature search was conducted using research databases: Web of Science Core Collections, BIOSIS Previews, and CAB Abstracts with keywords: "Fire and *Eucalyptus* decomposition", "Fire and litter decomposition", "Fire and litter dynamics", "Fire and litter quality", "Fire and soil", "Fire and decomposer", "Fire and understorey", "Post-fire and understorey", "Pre-fire and understorey". Peer-reviewed literature that met the following criteria were included:

1. Conducted in Australian *Eucalyptus* dominated forests or plantations;
2. Details of fire type, fire history, fire intensity, time-since-fire, or fire regimes were included;
3. The rate of decomposition (expressed as decomposition rate constant: *k*-value);
4. The impacts of fire on vegetation composition, litter dynamics (i.e., fine fuel loads, litterfall, and litter accumulation), litter quality, soil properties, and microbial activity were considered.

The reference list of selected publications was also searched to identify key literature. After screening, 30 publications were selected for review and meta-analysis. Selected papers were coded for reference purposes. Specifically, publications that reported measurements conducted in more than one forest location were treated as separate studies for each location and coded accordingly to account for the influence of spatial and geographical heterogeneity in post-fire litter decomposition. As a result, the 30 publications yielded a total of 33 studies in 20 study areas (see Table A1 in Appendix A).

Studies that used a chronosequence sampling approach (sampling varied with time-since-fire) to compare the effects of fires on environmental factors were considered as a single study. In addition,

studies that were conducted in the same study site were coded with the same alphabetical letter to account for site-specific environmental conditions. More importantly, litter decomposition rates were analysed explicitly using a meta-analysis approach, whereas fire effects on vegetation composition, litter quality, soil properties, and microbial activity were reviewed qualitatively and summarised (see Table A2 in Appendix A).

Original data were extracted directly from text and tables of the selected publications, or digitised from figures using PlotDigitizer (PlotDigitizer, version 3.1.4, 2022; www.plotdigitizer.com; PORBITAL). Site characteristics including forest name and location within Australia (state), latitude and longitude, elevation (m asl), distance from the coast, mean annual temperature (MAT), and mean annual precipitation (MAP) were extracted from the literature. Where elevation, landscape position (i.e., inland/coastal), and distance from the coast were not reported, these data were derived using Google Earth based on the geographic coordinates provided in the literature. When MAT and MAP were not available from the literature, climatic data were obtained from the nearest weather station operated by the Australian Bureau of Meteorology.

Study sites were classified into forest types based on vegetation structures, precipitation, vegetation structure, soil fertility, fire regimes, and distribution in Australia (Specht, 1970; Ashton and Attiwill, 1994; Cruz et al., 2018; Table 1.2). Study sites were further classified into inland or coastal forests based their physical distance to the coast (i.e., landscape position). In this study, inland forest was defined as > 50 km from the coast.

Data on decomposition rate constant (*k*-value; yr^{-1}) of individual *Eucalyptus* litter components (i.e., leaf, twig, bark, fruits, and total litter) were extracted directly from the literature or calculated from percentage litter mass loss over known exposure periods in litterbag studies using the Olson model (Equation 1.2). Data availability varied among litter components, with *k*-values for non-leaf components (i.e., twig, bark, fruit, and total litter) derived from only two studies involving prescribed burning. For analysis purposes, *k*-values from prescribed-burnt sites were further categorised into leaf, woody litter (i.e. bark + twigs + fruits), and total litter (hereafter *k*-values for prescribed-burnt site).

Hence, data relating to (1) litter dynamics (including litter dynamics (including fuel loads, litterfall, and litter accumulation); (2) litter quality (including concentrations of C, N, P, S, K, Ca, Mg, Na, Cl, Mn, Zn, Cu, C/N, C/P, and N/P); (3) soil properties (including soil pH, soil total C, soil organic C, soil total N, soil total P, soil K, soil Ca, soil Mg, soil Na, soil Al, soil C/N, soil C/P, and soil N/P); (4) microbial activity (including microbial C, microbial N, microbial P, microbial C/N, microbial C/P, and microbial N/P; (5) fire regimes (including fire type: unburnt, prescribed burning or bushfire, fire

intensity: low- or high-intensity, time-since-fire); and (6) experimental factors (including initial mass of litter, litterbag mesh size, litter bag exposure time, litter mass loss) (Table 1.2) were extracted from the selected studies. These variables were not included in the meta-analysis; however, they were systemically summarised and reviewed to examine the fire effects on the potential drivers of litter decomposition (see Table A2 in Appendix A).

Table 1.1: Classification of forest type based on precipitation, vegetation community, soil fertility, and fire regimes (Specht, 1970; Ashton and Attiwill, 1994; Gill, 1994; Keith, 2004; Wiltshire, 2004; Attiwill et al., 2013; Thomas et al., 2014; Cruz et al., 2018). QLD = Queensland; NSW = NSW; VIC = Victoria; TAS = Tasmania; WA = Western Australia.

Forest type	**Precipitation**	**Overstorey canopy**	**Understorey vegetation**	**Soil fertility**	**Fire regimes**	**Distribution in Australia**
Wet sclerophyll forest (WSF; also known as tall open forest)	Mean average precipitation < 1000 mm yr^{-1}	Tall (> 30 m), open canopy (30-70% cover) Dominant *Eucalyptus* species include *E. sieberi*, *E. marginata*, *E. obliqu, E. grandis, E. pilularis, E. regnans, E. delegatensis, E. diversicolor*, *E. cloeziana, E. microcorys, E. viminalis, E. smithii, E. paniculata, E. saligna, E. cypellocarpa, E. ovata, E. jacksonii,* and *E. guilfoylei*	Dense understoreys of short shrubs, pachycauls, lianes, ground ferns, herbs, rainforest associated species and grassy understorey species	Moderately fertile	Fire prone and supports frequent (~10 years) low-intensity surface fire. High severity crown fire may occur under extreme fire weather	Southern QLD and northern NSW, central and southern NSW, central and southern VIC, southern TAS, southwest WA

Table 1.1 continued.

Forest type	Precipitation	Overstorey canopy	Understorey vegetation	Soil fertility	Fire regimes	Distribution in Australia
Dry sclerophyll forest (DSF; also known as open forest)	Mean average precipitation >1000 mm yr^{-1}	Open canopy (30-70%) with tree heights from 10-30 m. Dominant *Eucalyptus* species include *E. pilularis, E. maculata, E. sieberana, E. gummifera, E. piperita, E. fastigata, E. cypellocarpa, E. radiata, E. pauciflora, E. marginata,* and *E. gomphocephala*	Diverse range of sclerophyll shrubs and grassy understorey, including *Acacia, Daviesia, Hakea, Hibbertia, Leptospermum, Leucopogon*, and herbaceous species including *Dianella, Lepidosperma, Lomandra*, and fern including *Adiantum* and *Pteridium*	Generally infertile	Fire-prone, characterised by infrequent fires (30-75 years). Fire intensity ranges from low-intensity surface fire to high severity crown fire	Coastal and subcoastal southeast Australia (from SA to QLD), TAS, and southwestern corner of Western Australia

Table 1.2: Description of variables extracted from selected publications.

	Variable	Definition	Data type/unit
Details of publication	Reference	Publications used in this study	Text
	Authors	Authors and year of publication	Text
	Year of study	Year when the study was conducted	Year
Geographical variables	Location	Australian states and territory where study was conducted	Text
	Forest	Forest where study was conducted	Text
	Forest type	Dry sclerophyll forest (DSF) or wet sclerophyll forest (WSF)	Categorical
	Distance to the coast	Physical distance to the coast	km
	Landscape position (Inland/coastal)	Based on physical distance to the coast (inland: > 50 km from the coast)	Categorical
Climatic variables	Latitude	Latitude of study site	Decimal
	Longitude	Longitude of study site	Decimal
	Elevation	Metres above sea level	m asl
	Climate zone	According to the classification published by the Australian Bureau of Meteorology	Text
	Temperature	Mean annual temperature (MAT) of the study site	°C yr^{-1}
	Precipitation	Mean annual precipitation (MAP) of the study site	mm yr^{-1}
Vegetation and litter types	Species	Dominant *Eucalyptus* species in study site	Categorical
	Litter type	*Eucalyptus* leaf, twigs, bark, fruit, and total litter	Categorical
Fire regimes	Time-since-fire	Time interval between last fire	Years
	Fire type	Unburnt, prescribed burn or bushfire	Categorical
	Fire intensity	Low-intensity or high-intensity	Categorical
Experimental factors	Mesh size	Mesh size of the litterbag	mm
	Initial litter mass	Mass of litter inside the litterbag at the beginning of the litter decomposition experiment	g
	Litterbag exposure time	Exposure time of the litterbag to the forest floor	Days
	Mass remaining	The mass of remaining litter at a specific time	g

Table 1.1 continued.

	Variable	Definition	Data type/unit
Litter dynamics	Decomposition rate constant (*k*-value)	Calculated using exponential equation	yr^{-1}
	Fine fuel	Mass of surface fine fuel layer	$t\ ha^{-1}$
	Litterfall	Average mass of litterfall on the forest floor or litterfall trap	$t\ ha^{-1}$
Microbial activity	Microbial biomass	Microbial C, N, P	$mg\ kg^{-1}$
	Microbial stoichiometry	Microbial C/N, C/P, N/P	Ratio
Litter chemical quality	Litter quality	Litter C, N, P, S, K, Ca, Mg, Na, Cl	%
	Litter quality	Litter Mn, Zn, Cu	$mg\ kg^{-1}$
	Litter stoichiometry	Litter C/N, C/P, N/P	Ratio
Soil properties	Soil pH	Indication of soil acidity or alkalinity	pH unit
	Soil properties	Soil organic carbon (SOC), total carbon (TC), total nitrogen (TN)	%

1.2.2 Statistical analysis

Data were statistically analysed in Jamovi (Version 1.6, 2022; The Jamovi Project, Sydney, Australia) to evaluate the effects of fire regimes and related environmental drivers on *Eucalyptus* litter decomposition rate. All available *k*-values (n = 55) were tested for normality and homogeneity using the Shapiro-Wilk test and Levene's test, respectively, and were log-transformed to meet these assumptions. One-way, two-way, and three-way Analysis of Variance (ANOVA) were used to explore the main effects and interactions among forest types (i.e., dry and wet sclerophyll forests), landscape position (i.e., inland and coastal), and fire type (i.e., unburnt, prescribed burning, and bushfire) on (1) leaf litter *k*-values across all fire types (n = 44) and (2) *k*-values for prescribed burnt sites only (n = 36). Where statistically significant effects were detected ($\alpha = 0.05$), pairwise comparisons among groups were conducted using Games-Howell Post-Hoc test.

Linear mixed models (LMMs) were used to further examine the effects of forest type, fire type, landscape position, litter component, and site characteristics on *Eucalyptus* litter decomposition rate. Decomposition rate constants (*k*-values) were treated as the response variable in all models.

For analysis of leaf litter, forest type, fire type, and landscape position were specified as fixed effects. For analyses restricted to prescribed-burnt sites, fixed effects included forest type, litter component, and landscape position. In all models, site-specific characteristics (i.e., climatic and environmental variations among study sites) were included as random effects. Model performance was evaluated by marginal R^2 which represent the proportion of variance explained by fixed effects only, and conditional R^2 which represent the proportion of variance explained by both fixed effects and random effects.

1.3 Results

1.3.1 Description of publication reviewed

A total of 30 key literature published between 1979 and 2020 were reviewed. The literature search suggested that most of the existing studies focused on fire effects on understorey composition, litter quality, and soil properties. Of the 30 publications reviewed, only 13 reported direct measurements of fire effects on the rate of *Eucalyptus* litter decomposition, and eight of these studies were published before 1993. Hence, the number of published studies increased considerably with the occurrence of major bushfire events (Figure 1.1). For example, a total of eight studies were published between 1983 and 1990 after the 1983 Ash Wednesday bushfires, while more than half (n = 16) of the publication reviewed were published after the 2009 Black Saturday bushfire (Figure 1.1).

However, most of these focused on the effects of bushfire on understorey vegetation regrowth, while only five studies examined the direct impact of bushfire on *Eucalyptus* litter decomposition rate constant (*k*-values; see Table A1 in Appendix A).

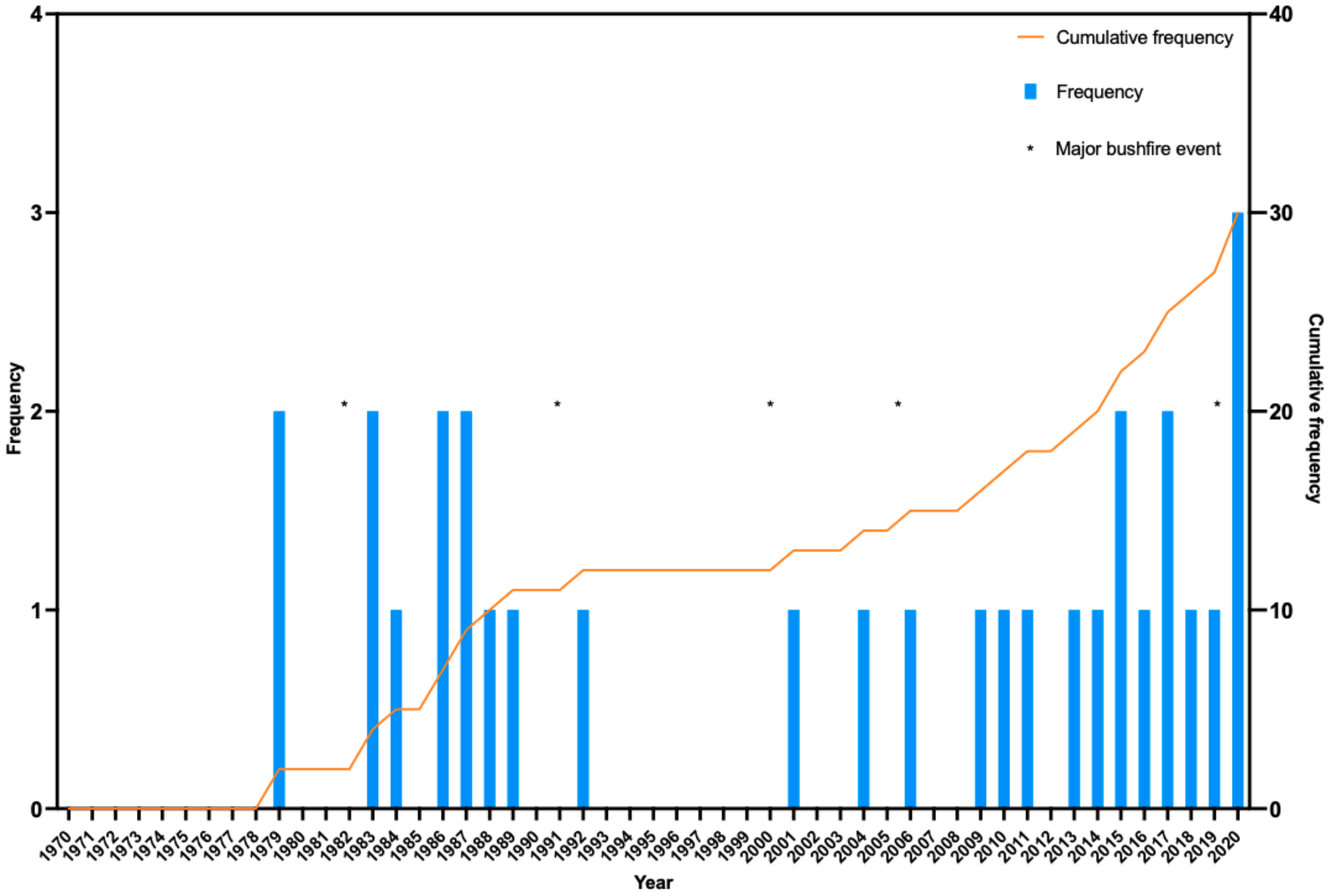

Figure 1.1: Annual total and cumulative frequency of the number of publications (n = 30) examining the effects of fire on *Eucalyptus* litter decomposition and its important drivers in Australia by publication year. Years marked with * indicate major bushfire events in Australia.

1.3.2 Description of studies reviewed

Publications that included replicated treatments across different forests were considered as separate studies for each forest to account for variability in site-specific factors, including climate, soil properties, vegetation community, and fire regimes. In this case, a total of 33 studies were identified in 30 publications (see Table A1 in Appendix A). Of these, 11 were done in Queensland and a further eight and seven studies were based in Western Australia and New South Wales, respectively (Figure 1.2a). Despite Victoria having experienced some of the extensive bushfire events (e.g., Ash Wednesday, Black Saturday, and Black Summer bushfires; Attiwill and Adams, 2013; Dave and Sarre, 2020), relatively few relevant studies (n = 4) were identified (Figure 1.2a). Most of the studies reviewed (76%; n = 26) were done in WFSs, with the remainder done in DSFs (n = 7; Figure 1.2b). Of all the studies examined, 26 studies were in coastal forests, while only seven were in inland forests (Figure 1.2b).

The majority of the studies focused on short-term (1-5 years) fire effects on environmental factors and litter decomposition rate constant (*k*-values; see Table A1 in Appendix A). However, only two studies reported immediate (< 1 month) effects of prescribed burning on soil P (Huang et al., 2013), C and N in litter and soil (Krishnaraj et al., 2016). All studies included a long-unburnt site as a control for comparison with burnt sites. Long-unburnt sites were located as close as possible to the burnt areas to represent pre-fire environmental conditions. However, the definition of 'long-unburnt' varied among studies and was dependent on study objectives. In short-term studies, long-unburnt sites were generally defined as those unburnt for more than 15 years, whereas studies employing a chronosequence sampling approach (e.g., 2, 5, 10, and 20 years after fires) classified long-unburnt sites as those unburnt for at least 40 years.

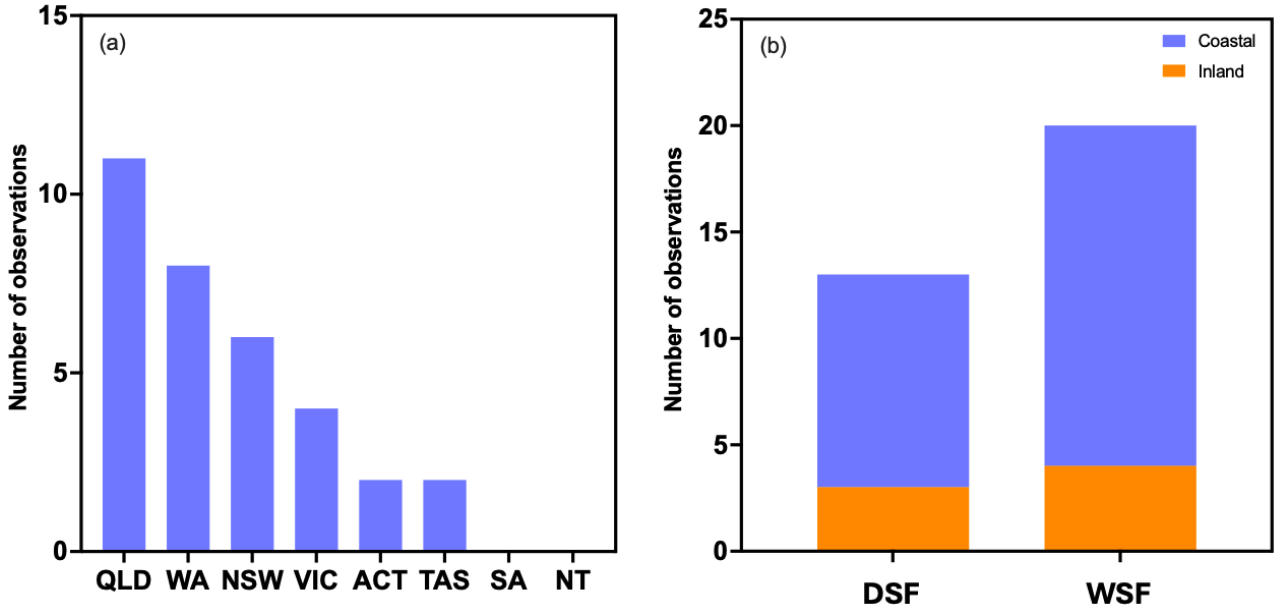

Figure 1.2: Geographical distribution of studies reviewed (n = 33) (a) according to region (Australian states and territory): QLD = Queensland; WA = Western Australia; NSW = New South Wales; VIC = Victoria; ACT: Australian Capital Territory; TAS; Tasmania; SA = South Australia; NT = Northern Territory; (b) according to forest type and landscape position: DSF = dry sclerophyll forest; WSF = wet sclerophyll forest.

1.3.3 Litter decomposition rate constants (*k*-values) datasets

Although the number of studies published increased following major bushfire event (Figure 1.1), there were few publications (n = 7) that specifically examined the effect of bushfire on litter decomposition and its driving factors. Of these, only three studies were replicated in parallel with prescribed-burnt sites for direct comparison between fire types. In contrast, most studies identified (n = 27) focused on the effects of prescribed burning on litter decomposition and potential drivers including litter dynamics, understorey vegetation, soil properties, and microbial activity. Many of these studies specifically investigated the long-term effects of fire frequency (i.e., biennially and quadrennial burns) on litter chemical quality and soil properties (see Table A1 in Appendix A).

Across all selected studies, a total of 55 litter decomposition rate constants (*k*-values) were extracted directly from the literature or calculated using single or double exponential equations (Equation 1.2; Equation 1.3; Figure 1.3). Most studies reported *k*-values for *Eucalyptus* leaf litter (n = 49), whereas only two studies explicitly examined the decomposition rate of non-leaf litter component (n = 6), both of which were conducted in prescribed-burnt sites (Fox et al., 1979; O'Connell, 1987b). Collectively, the dataset included 49 *k*-values for leaf litter, two for twigs, two for total litter (comprising leaf, twig, bark, fruit, and understorey litter), one for bark, and one for

fruit. As non-leaf *k*-values were exclusively derived from prescribed-burnt sites, twig, bark, and fruit *k*-values were aggregated to represent woody litter in prescribed-burnt ecosystems (n = 4).

Within prescribed-burnt sites, *k*-values of leaf litter ranged from 0.19-1.55 yr^{-1}, with a mean of 0.57 yr^{-1}, while *k*-values of woody litter spanned from 0.12-0.23 yr^{-1} with a mean of 0.20 yr^{-1}. Total litter *k*-values ranged from 0.31-0.40 yr^{-1} with a mean of 0.36 yr^{-1} (Figure 1.3b).

Among all fire types, *k*-values for leaf litter in unburnt sites (n = 14) spanned from 0.32-1.53 yr^{-1}, with a mean of 0.77 yr^{-1}. In prescribed-burnt sites, leaf litter *k*-values (n = 26) showed a slightly lower mean (0.57 yr^{-1}), with values ranging from 0.19-1.55 yr^{-1}. In contrast, bushfire-affected sites showed greater variability, with *k*-values ranging from 0.39-2.06 yr^{-1} and a mean of 1.17 yr^{-1}. Specifically, *k*-values for bushfire-affected sites were predominantly derived from WSFs, with no available data from DSF for comparison.

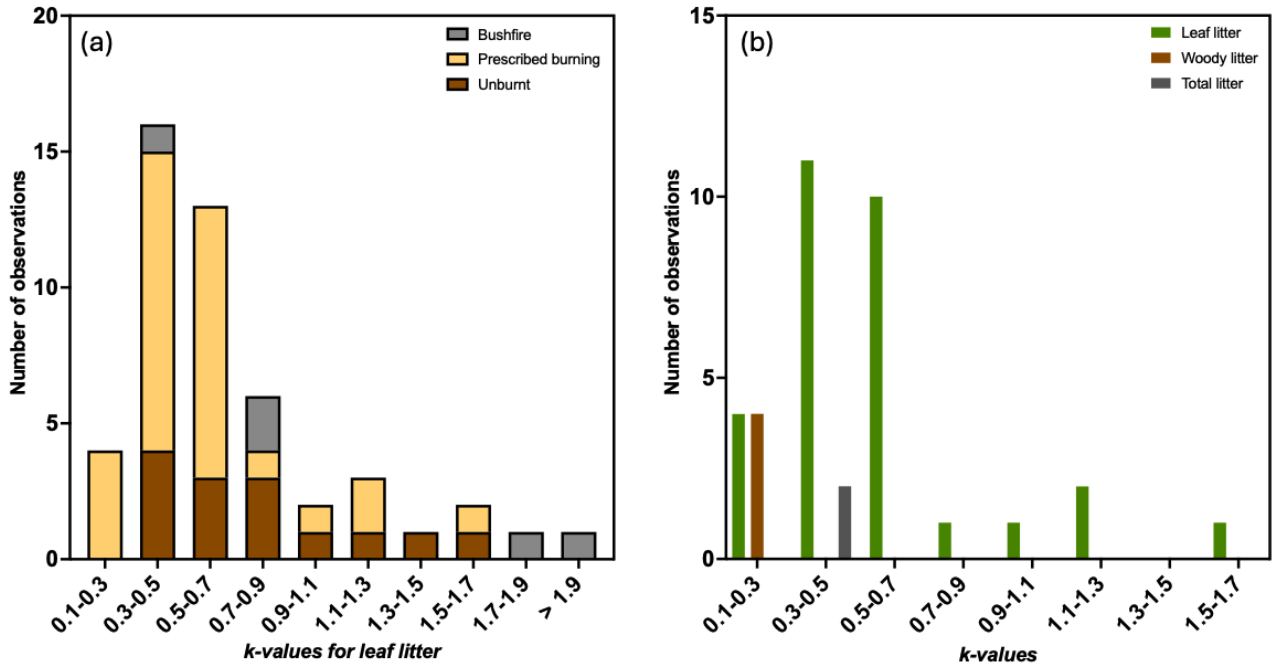

Figure 1.3: Frequency distribution of (a) leaf litter decomposition rate constants (*k*-values) among all fire types and (b) litter decomposition rate constants (*k*-values) of leaf litter, woody litter, and total litter in prescribed-burnt sites.

1.3.4 Litter decomposition rate constants

*Leaf litter decomposition rate constants (*k*-values) among all fire types*

Landscape position (i.e., inland/coastal) and fire type (i.e., unburnt, prescribed burn, and bushfire) showed little influence on *Eucalyptus* leaf litter decomposition rate constants (One-way ANOVA; $p > 0.05$; Table 1.3). In contrast, *k*-values of leaf litter differed significantly between forest type (One-way ANOVA; $p = 0.026$; Table 1.3), with DSFs having significantly higher mean *k*-values (0.34 yr^{-1}) than WSFs (0.23 yr^{-1}). Despite this difference, linear mixed model analysis indicated that forest type alone only explained a small proportion of the variability in leaf litter *k*-values (LMM; R^2 marginal = 0.08; Table 1.4). Although the addition of study site as a random factor increased the variance explained, the LMM was insufficient to explain variation in *k*-values (LMM; R^2 conditional = 0.25; Table 1.4).

Interaction terms in the LMM involving fire type could not be evaluated due to singular models fits arising from multicollinearity among predictors, thus leading to no interaction effects detected by two-way and three-way ANOVA models (p = N.A.; Table 1.3). Consequently, LMMs were used to examine the combined effects among forest type, landscape position, and fire type (i.e., as fixed effects) on leaf litter decomposition rate constants while accounting for site-specific variability (i.e., as random effect; Table 1.4). This model indicated that fixed effects accounted for 17% of the variance in leaf litter *k*-values (LMM; marginal $R^2 = 0.17$; Table 1.4), whereas the addition of site-specific characteristics increased the explained variance to 52% (LMM; conditional $R^2 = 0.52$; Table 1.4).

*Litter decomposition rate constants (*k*-values) in prescribed-burnt sites only*

For prescribed-burnt sites, *k*-values varied significantly among litter components (One-way ANOVA; $p = 0.033$; Table 1.3). In particular, woody litter showed significantly higher mean *k*-values (0.72 yr^{-1}) than leaf litter (mean *k*-values = 0.31 yr^{-1}; $p < 0.001$). Like the dataset of *k*-values for leaf litter, two-way and three-way ANOVA models for prescribed-burnt sites could not be assessed due to singular fits caused by linear dependence among predictors (Two- and three-way ANOVA; p = N.A.; Table 1.3). A LMM indicated that litter component alone had a strong influence on *k*-values, explaining 41% of the variance in *k*-values (LMM; marginal $R^2 = 0.41$; Table 1.4). In contrast, the combined addition of forest type, landscape position, and litter component as fixed effects accounted for a slightly lower proportion of the variance in *k*-values (LMM; marginal $R^2 = 0.39$; Table 1.4). When site-specific variability was included as a random effect, the proportion of variance explained increased (LMM; conditional $R^2 = 0.58$; Table 1.4).

*Litter decomposition rate constants (*k*-values) in unburnt and prescribed-burnt sites*

Since the *k*-values for bushfire-affected sites were only available for WSFs, an additional comparison was conducted between unburnt and prescribed-burnt sites to further investigate the effects of forest type and fire type on leaf litter decomposition rate constants (*k*-values; Table 1.4). Leaf litter *k*-values differed significantly between both forest type and fire type (One-way ANOVA; Table 1.3). Specifically, DSFs had significantly higher mean *k*-value (0.34) than WSFs (mean *k*-value = 0.23; $p = 0.033$; Table 1.3). Prescribed-burnt sites had significantly higher mean *k*-value (0.31) than unburnt sites (mean *k*-value = 0.21; $p = 0.049$; Table 1.3). However, the interaction between forest type and fire type did not significantly influence leaf litter *k*-values (two-way ANOVA; $p > 0.05$; Table 1.3). Despite this, the LMM indicated that forest type and fire type when considered individually as fixed effects, explained only a small proportion of the variance in leaf litter *k*-value (LMMs; marginal $R^2 \leq 0.10$; Table 1.4). In contrast, the model that incorporated forest type and fire type as fixed effects, together with study sites as random effect accounted for a greater proportion of the variance in *k*-values (LMMs; marginal $R^2 = 0.19$; conditional $R^2 = 0.37$; Table 1.4).

Table 1.3: Results of one-way, two-way, and three-way ANOVA examining the effects of forest type, landscape position (i.e., inland/coastal), fire type (unburnt, prescribed-burnt, and bushfire-affected sites), and their interactions on log-transformed leaf litter *k*-values. This table also presents ANOVA results for prescribed-burnt sites only to understand the effects of forest type, landscape position, litter component (i.e., leaf, woody litter, and total), and their interactions on log-transformed *k*-values. In addition, ANOVA results for unburnt and prescribed-burnt sites to understand the effects of forest type, fire type, and their interactions log-transformed leaf litter *k*-values is presented. *Indicates statistical significance ($p < 0.05$). N.A. indicates the interaction effects could not be evaluated due to singular fit encountered arising from multicollinearity among predictors.

Variables	***p***
***k*-values for leaf litter across all fire types**	
Forest type	< 0.026*
Landscape position	0.78
Fire type	0.16
Forest type × Landscape position	0.74
Forest type × Fire type	N.A.
Landscape position × Fire type	N.A.
Forest type × Landscape position × Fire type	N.A.
***k*-values for prescribed-burnt sites**	
Forest type	0.26
Landscape position	0.52
Litter component	0.033*
Forest type × Landscape position	N.A.
Forest type × Litter component	N.A.
Forest type × Landscape position × Litter component	N.A.
***k*-values for leaf litter in unburnt and prescribed-burnt sites**	
Forest type	0.033*
Fire type	0.049*
Forest type × Fire type	0.11

Table 1.4: Linear mixed models were used to investigate the effects of forest type (dry and wet sclerophyll forests), fire type (unburnt, prescribed-burnt, and bushfire-affected sites), landscape position (inland/coastal), litter component (leaf, woody litter, and total litter), and their combined effects on log-transformed *k*-values. Decomposition rate constants (*k*-values) were treated as the dependent variable, while forest type, fire type, landscape position, and litter component were included as fixed effects. Site-specific characteristics (i.e., study site) were included as random effects. Marginal R^2 represents the proportion of variance explained by fixed effects, while condition R^2 represents the proportion of variance explained by both fixed and random effects.

Variables	R^2 marginal	R^2 conditional
***k*-values for leaf litter across all fire types**		
Log(*k*-value) ~ 1 + Forest type + (1| Study site)	0.08	0.25
Log(*k*-value) ~ 1 + Forest type + Fire type + Landscape position (1| Study site)	0.17	0.52
***k*-values for prescribed-burnt sites only**		
Log(*k*-value) ~ 1 + Litter component + (1| Study site)	0.41	0.48
Log(*k*-value) ~ 1 + Forest type + Litter component + Landscape position + (1| Study site)	0.39	0.58
***k*-values for leaf litter in unburnt and prescribed-burnt sites**		
Log(*k*-value) ~ 1 + Forest type + (1| Study site)	0.10	0.27
Log(*k*-value) ~ 1 + Fire type + (1| Study site)	0.07	0.27
Log(*k*-value) ~ 1 + Forest type + Fire type + (1| Study site)	0.19	0.37

1.4 Discussion

This study synthesised a subset of 33 studies described in 30 publications that reported the direct or indirect effects of prescribed burning and bushfire on *Eucalyptus* litter decomposition in Australian sclerophyll forests. The preliminarily systematic literature search revealed that most published studies have focused on the effect of fire on potential drivers of litter decomposition, such as litter composition, understorey vegetation, soil properties, and microbial activity, with far less attention on the determination of decomposition rate constants (*k*-values). Furthermore, most studies focused on prescribed burning, with relatively few studies reporting data on the effect of bushfire on litter decomposition (O'Connell et al., 1979; O'Connell, 1988; O'Connell and Menage, 1983; Birk and Bridges, 1989; Buckingham et al., 2015; Butler et al., 2017a; Cawson et al., 2018). This imbalance likely reflects the high frequency of prescribed burning across Australia, compared with the sporadic occurrence of bushfire. The literature examined spanned from 1970 to 2020, with 13 studies published after 2010, indicating an increase in recent research attention. Additional studies have been published following the 2019/2020 Black Summer bushfires; however, these studies fell outside the temporal scope of this review and were not included in this synthesis. In addition, a substantial body of relevant grey literature, including government reports and research theses was not included in this review. Consequently, the results of this synthesis do not fully reflect the litter decomposition rate in fire-affected ecosystems across Australia, particularly those impacted by bushfire events.

It is also important to note that there was a strong bias towards WSFs and coastal regions, whereas data availability for DSFs and inland forests were limited. This is likely due to the fact that a considerable amount of data derived from long-term prescribed burning experiments conducted in Peachester State Forest, a coastal forest in Queensland (Guinto et al., 2001; Bastias et al., 2006; Toberman et al., 2014; Butler et al., 2017a; Butler et al., 2019; Muqaddas et al., 2015; Muqaddas and Lewis, 2020). Hence, comparisons among forest types and landscape position rely on limited field data, so caution is required when interpreting the findings of this study.

1.4.1 Fire effects on litter decomposition rate

Overall, leaf litter decomposition rate constants (*k*-values) followed the pattern: bushfire-affected site > unburnt sites > prescribed-burnt sites. Broadly, prescribed burning was associated with reduced rates of leaf litter decomposition, while bushfire was associated with enhanced decomposition rates. Reduced decomposition rates following prescribed burning have been reported in *Eucalyptus pilularis* forest, where rapid litter re-accumulation was observed after fire, with this effect diminishing as time-since-fire increased (Birk and Bridges, 1989). In contrast, enhanced

decomposition rates in bushfire-affected site have been attributed to increased concentrations of P and N in litterfall in the first year following fire (O'Connell, 1979; Birk and Bridges, 1989). These post-fire nutrient pulses are likely driven by disruption of nutrient translocation caused by high-intensity crown fires, resulting in greater nutrient retention in senesced leaf litter (O'Connell, 1979; Birk and Bridges, 1989). In addition, the higher decomposition rate constants in bushfire-affected ecosystems may be explained by an increase in soil P availability after fire (Butler et al., 2017a). This interpretation is consistent with previous studies demonstrating positive correlations among litter decomposition and P concentration in soil and litter (e.g., Aerts, 1997; Zhang et al., 2008; Liu et al., 2024).

As noted previously, substantial gaps remain in understanding the effects of bushfire on decomposition rate constants in fire-prone DSFs. To address this limitation, comparisons were made explicitly between unburnt and prescribed-burnt sites. In this analysis, mean leaf litter *k*-values was higher in DSFs compared to WSFs. This finding contrasted with previous studies reporting slower decomposed rates under warm and dry conditions (e.g., Thomas et al., 2014). Such differences may reflect the broader geographical scope of this study, where studies were included from South Australia, Western Australia, and Tasmania – regions characteristics by distinct climate and environmental conditions. The divergence in decomposition could also be attributed to differences in fire regimes as the long-term prescribed burning studies in WSFs were included in the analysis.

Leaf litter decomposed slowly in prescribed-burnt sites compared to unburnt sites. This result aligned with previous findings where faster rates of *Eucalyptus* decomposition were measured in unburnt sites than in prescribed-burnt sites (e.g., Raison et al., 1986; O'Connell, 1987; Butler et al., 2020), potentially due to higher soil N availability with long-term fire exclusion (Butler et al., 2020). Fire frequency further influenced decomposition dynamics, as long-term frequent burning often led to depletion in soil N and P pools, resulting in lower decomposition with prescribed burns every four years compared with biennial burns (Butler et al., 2020). In addition, frequent burning has been shown to promote the growth of bracken fern, herbaceous plant, grasses, and mosses (Lewis et al., 2012, Muqaddas and Lewis, 2020), which may intensify competition for soil nutrients and further constrain litter decomposition. In comparison, long-term fire suppression can facilitate soil N accumulation over time, potentially enhancing litter decomposition processes (Butler et al., 2020).

Collectively, findings of this review demonstrated that site-specific variability including micro-climate, soil properties, vegetation composition, and microbial activity are of considerable importance in regulating the rate of litter decomposition in burnt and unburnt *Eucalyptus* ecosystems. However, limited research has examined how fire regimes influence site-specific factors and how these factors, in turn, regulate litter decomposition in fire-prone ecosystems. Consequently, more in-

depth empirical research is required to improve our knowledge of litter decomposition under current and future climate scenarios.

1.4.2 Fire effects on environmental factors

In contrast to the paucity of information describing litter decomposition rate constants (*k*-values), the effect of fire on key drivers of litter decomposition are well documented. For example, bushfire has been shown to have a major influence on decomposer communities. High-intensity bushfire reduces the abundance of macroinvertebrate assemblages due to removal of surface litter, increased soil temperature and reduced soil moisture (Buckingham et al., 2015). In addition, high-intensity bushfires cause substantial loss of overstorey canopy which often leads to increased light penetration to promote the growth of understorey ferns, legumes, and moss (e.g., Birk and Bridges, 1989; Spencer and Baxter, 2006; Lewis et al., 2012; Lewis and Debuse, 2012; Buckingham et al., 2015; Table A2 in Appendix A). This understorey vegetation can contribute to rapid accumulation of surface litter fuel during the first year after fire despite comparatively lower litterfall rates (e.g., Birk and Bridges, 1989; Bridges, 2004).

In comparison, frequent prescribed burning has been shown to reduce the density and growth of woody shrubs, often resulting in a grassy-dominated understorey (e.g., Lewis et al., 2012; Muqaddas and Lewis, 2020). However, the effects of prescribed burning on litterfall rate remain unclear since existing research is often divergent. For example, prescribed burning had minimal effects on litterfall rates in a DSF in New South Wales (Birk and Bridges, 1989), whereas it significantly reduced annual litterfall in WSFs in Queensland (Muqaddas and Lewis, 2020) and DSFs in Western Australia (Abbott et al., 1984). Similarly, the effects of prescribed burning on litter chemical quality are inconsistent across studies. For example, leaf litter from frequently burnt sites (i.e., biennial and quadrennial burns) has been reported to have higher C/N ratio than litter from unburnt sites (e.g., Toberman et al., 2014; Butler et al., 2019; Muqaddas and Lewis, 2020), while other studies observed little to no differences between unburnt and burnt sites (e.g., Abbott et al., 1984). Prescribed burning often leads to an increase in soil pH (e.g., Guinto et al., 2001; Huang et al., 2013; Bulter et al., 2017a) and soil available P (e.g., Close et al., 2011; Butler et al., 2017a), with noticeable decrease in soil total C and N content (e.g., Bastias et al., 2006; Muqaddas et al., 2015; Butler et al., 2017a).

1.5 Future prospects

This review demonstrates that there is a limited body of research addressing the direct effects of fire on *Eucalyptus* litter decomposition, with much of the existing literature focusing on the consequence of prescribed burning on vegetation composition and soil properties. The available literature also shows a strong bias towards WSFs, despite DSFs experiencing more frequent prescribed burning as a management strategy to mitigate the severity of bushfire. Furthermore, this review highlights that site-specific factors such as climate, litter dynamics, soil properties, and microbial activity can have major impacts on litter decomposition. As decomposition studies are often labour-intensive and require long timeframes, our current knowledge of fire effects on litter decomposition across Australian sclerophyll forests remains limited.

Many questions remain – how does fire history, especially time-since-fire, affect litter decomposition, and how does post-fire understorey vegetation affect surface fine fuel decomposition in *Eucalyptus* forests? The research presented in this thesis will follow these two lines of enquiry to advance the current understanding on the dynamics of litter decomposition in terrestrial ecosystems to provide valuable insight into fuel management. Empirical data describing post-fire litter decomposition and fuel dynamics can ultimately help forest and fire managers to understand forest recovery, as well as

Chapter 2

Determination of litter chemical quality by infrared spectroscopy

---

2.1 Introduction

Accurate quantification of chemical characteristics (i.e., carbon, nitrogen, cellulose, hemicellulose, and lignin) of litter is important for predicting the rate of litter decomposition, accumulation, and their subsequent effects on fire behaviour (e.g., Aerts, 1997; Cornelissen et al., 2017; Ficken and Wright, 2017). However, such analyses often involve complex chemical procedures, which can limit their widespread application in ecological research. As a result, relatively few studies have documented the concentration of lignocellulosic compounds in *Eucalyptus* litter due to the cost and complexity of analytical methods involved.

To date, one of the most comprehensive studies to address this gap is a meta-analysis done by Paul and Polglase (2004), which summarised data from 13 litterbag decomposition studies conducted across *Eucalyptus* forests in Australia (e.g., Briggs and Maher, 1983; O'Connell and Menagé, 1982; Wood and Raison, 1983; Maheswaran and Attiwill, 1987; Spain and le Feuvre, 1987; O'Connell, 1988; Polglase and Attiwill, 1992; O'Connell, 1994; O'Connell, 1997; Crockford and Richardson, 1998a; Crockford and Richardson, 1998b; Hooda, 1998; Wedderburn and Carter, 1999). For freshly fallen *Eucalyptus* litter samples, cellulose content averaged 25.1% in leaf litter, 43.3% in bark, and 48.8% in dead wood. Lignin content averaged 41.1% in leaf litter, 15.7% in bark, and 22.1% in dead wood. The average C/N ratios for *Eucalyptus* leaf litter, bark, and dead wood materials were 74.0, 102.1, and 102.6, respectively. Noticeably, among these 13 litterbag studies, only O'Connell (1997) explicitly reported cellulose and lignin content in *Eucalyptus* bark, suggesting that this meta-analysis may not fully represent the variability of litter chemical quality across different climatic or geological regions. This underscores the need for further research to provide empirical and regional-specific data on the chemical quality of *Eucalyptus* litter. This knowledge would be particularly valuable for effective forest and fire management, as it could be used to increase the understanding regarding nutrient cycling, and it would support the development of efficient fuel reduction strategies under current and projected climate change scenarios.

Conventional laboratory analysis, which involves the use of chemicals and destructive procedures such as extraction and combustion, is costly, inefficient, and requires considerable effort in sample preparation (Murphy and Riley, 1962; Van Soest, 1963; Bachega et al., 2016). For example, the Dumas dry combustion method using an elemental analyser (also known as a CHN analyser) is commonly employed as a standard technique to quantify the amount of C, N, and H in soil and plant samples (McLellan et al., 1991b; Jimenez and Ladha, 1993; Sieper et al., 2006; Chintala et al., 2013). This technique is based on complete combustion of samples at high temperature (above 1,000 °C) with subsequent oxidation (using O_2 gas) and reduction reaction of gaseous products (Chintala et al., 2013).

Despite its reliability and repeatability, the preparation of samples and use of a CHN analyser is laborious, and expensive, which restricts analysis of large numbers of samples (Jimenez and Ladha, 1993). For elemental analysis, samples need to be ground to a fine particle size and weighed (approximately 40 milligrams (mg) for plants and 150 mg for soil samples) to make a pellet housed in a tin capsule. The number of samples that can be analysed is limited by the capacity of the autosampler and the time for analysis of each sample, which typically ranges from 5 to 10 minutes per element (Sieper et al., 2006; Chintala et al., 2013). A primary limitation of this method is its high operational cost. This includes the initial investment required to purchase a CHN analyser, ongoing maintenance expenses, such as consumables (e.g., reagents and columns) and the replacement of carrier gases. Although commercial laboratories offer an alternative to in-house analysis, the cost per sample remains high, typically ranging from AUD $24 to $154, due to labour, consumables, and sampling handling time. These financial constraints pose a significant challenge to the feasibility of long-term ecological studies, such as litter decomposition and litterfall research that require the collection and analysis of samples over extended periods.

Compared to conventional laboratory analysis, infrared (IR) spectroscopy is a sustainable analytical technique that does not involve the use of chemicals. Visible- (vis), near- (NIR), and mid- (MIR) infrared spectroscopy is a promising technique that could be used for making fast and repeatable sample measurements with a high level of accuracy. Infrared spectrometers, which require simple to no sample preparation, are easy to operate and more applicable to studies that involve a large sample set (Ono et al. 2003; Parsons et al. 2011; Steinwandter et al., 2019; Prananto et al., 2021). Rapid and precise measurements are greatly beneficial for researchers and practitioners to characterise the biochemical composition of plant samples through interpretation of spectral signals (McLelln et al., 1991b; Joffre et al., 1992; Gillon et al, 1993; Gillon et al., 1999; Ono et al., 2003; Parsons et al., 2011; Steinwandter et al. 2019). Spectroscopy combined with chemometric methods (mathematical and statistical analysis) has been successfully employed in forestry (McLellan et al.,

1991b; Joffre et al., 1992; Gillon et al., 1993; Gillon et al., 1999; Haberhauer and Gerzabek, 1999; Schimleck et al., 2000; Ono et al., 2003; Richardson et al., 2004; Alchanatis et al., 2005; Kumar et al., 2007; Parsons et al., 2011; Chen et al., 2015; Ferreira et al., 2018; Steinwandter et al., 2019; Md Salim et al., 2021; Xiao et al., 2022; Barotto et al., 2023; Bao et al., 2024), soil science (Ben-Dor, 1995; McCarty et al., 2002; Cécillon et al., 2009; Chodak, 2008; Minasny et al., 2008; Ramirez-Lopez et al., 2018; Hutengs et al., 2019; Gomat et al., 2024; Jeon et al., 2024), agriculture (De Alencar Figueiredo et al., 2016; Prananto et al., 2021; Walsh et al., 2020) and the food industry (Cheng and Sun, 2017; Johnson et al., 2022) to predict and quantify the chemical and physical properties of samples from their spectra.

2.1.1 Principles of infrared spectroscopy

Infrared (IR) spectroscopy is a powerful technique that detects the molecular vibrations resulting from the absorption of infrared radiation by atoms within a molecule (Agelet and Hurburgh, 2010). The wavelengths at which IR radiation is absorbed correspond to specific molecular bonds and structures. This allows identification of multiple chemical properties from a single spectral measurement, making it a valuable analytical tool for reliable and quick sample analysis.

Visible and near-infrared spectroscopy

Visible (vis-) spectroscopy involves the direct measurement of light absorption within the visible spectrum, ranging from 380-780 nanometres (nm), corresponds to colours that can be perceived by the human eye, such as violet, blue, green, yellow, orange, and red. Visible spectroscopy is useful for providing objective and accurate colour measurement of a sample, serving as a more reliable alternative than subjective visual assessment. In contrast, near-infrared (NIR) spectroscopy is based on the overtone (i.e., higher-order, lower-intensity vibration; Reichenbächger and Popp, 2012) and combination of the foundation function groups such as O-H, C-H, N-H, and C=O, which originate in the mid-infrared (MIR) region (Richardson et al., 2004; Rossel et al., 2006; Chodak, 2008; Agelet and Hurburgh, 2010). Spectra from NIR spectroscopy typically consist of broad, overlapping absorption bands that cannot be interpreted visually or directly assigned to specific chemical bonds (Agelet and Hurburgh, 2010). Therefore, spectral pre-processing techniques are generally required to resolve overlapping features and improve the accuracy of calibration models developed from NIR spectra.

Fourier transform infrared spectroscopy

Fourier transform infrared (FTIR) spectroscopy lies in the mid-infrared (MIR) region, covering wavenumbers from 4,000 to 400 cm^{-1} (2,500 to 25,000 nm). This technique measures molecular vibration (i.e., stretching, bending, twisting, and scissoring) between chemical bonds in organic compounds such O-H, C-H, N-H, S-H, and C=O (Haberhauer and Gerzabek, 1999; Blum and John, 2012; Soriano-Disla et al., 2013; 2014). As a result, FTIR spectroscopy provides more detailed and direct information regarding the chemical structure and composition of a sample compared to vis-NIR spectroscopy (Lee et al., 2017).

Spectral pre-processing and chemometrics

Spectral pre-processing and chemometrics are important step in spectroscopic analysis. Spectral pre-process (also known as spatial transformation or pre-treatment method) is a technique that used to improve the quality of spectra by reducing scatter effects and instrument noise (Agelet and Hurburgh, 2010). Spectral pre-processing involves applying multiple mathematical techniques to spectral data to reduce noise, enhance signal features, correct baseline drift, and compensate for light scattering effects (Savitzky and Goley, 1964; Rinnan et al., 2009; Brown et al., 2000; Engel et al., 2013; Wadoux et al., 2021). The most commonly used pre-processing techniques include smoothing, Savitzky-Golay (SG) derivatives, standard normal variate (SNV). In most cases, the steps of spectra pre-processing include: (1) noise removal, (2) baseline correction, (3) scatter correlation, and (4) scaling (Rinnan et al., 2009; Engel et al., 2013; Wadoux et al., 2021). The order and combinations of pre-processing techniques depend largely on the type of samples and the quality of spectral data. However, a simple spectral pre-processing approach is generally recommended to preserve important spectra (Engel et al., 2013; Wadoux et al., 2021). Excessive smoothing may increase the apparent accuracy of the calibration model, it may also reduce the model's sensitivity to external datasets, a problem that often known as overfitting (Agelet and Hurburgh, 2010).

Chemometrics refer to the application of mathematical and statistical methods to extract meaningful information from complex data (Agelet and Hurburgh, 2010). For spectroscopic analysis, chemometric modelling is essential for developing calibration models that can predict the chemical or physical properties of unknown samples (Agelet and Hurburgh, 2010). For this method, absorbance spectra from a representative set of samples are correlated with reference values obtained from laboratory analysis or from standard reference materials. The most common chemometric methods used in spectroscopic analysis for calibration model development include partial least square

regression (PLSR), principal component analysis (PCA), Cubist, and random forest (e.g., Chodak, 2008; Wadoux et al., 2021; Ramírez et al., 2023; Jeon et al., 2024).

Once a calibration model is developed, its performance must be evaluated through validation, which indicates how well the model predicts the properties of interest of an independent set of samples that were not used during calibration. Model validation is crucial to avoid overfitting and ensure model robustness and generalisability (Agelet and Hurburgh, 2010). Preparing an independent set of samples often requires extensive sample collection and laboratory analysis. Cross-validation is often used as a practical alternative, which involves partitioning the available sample set into two subsets: (1) a training set for calibration model development and (2) a testing set for validation model development, which also known as "train-test split".

The important steps in predicting chemical properties using spectroscopy include: (1) collecting spectra from a representative sample set, (2) pre-processing of spectra data, (3) laboratory analysis of a representative sample set, (4) multivariate analysis (e.g., regression model or machine learning techniques), (5) calibration model development, and (6) model validation.

2.1.2 Limitations of infrared spectroscopy

Absorption in the NIR region is typically weak, broad, and overlaps due to overtone and combination bands of O-H, C-H, N-H, and C=O in the MIR region (Richardson et al., 2004; Rossel et al., 2006; Chodak, 2008; Agelet and Hurburgh, 2010). As a result, NIR spectra are non-specific and require careful interpretation. Chemometric methods are usually used to resolve overlapping and broad NIR spectra bands (Barnes et al., 1989; Rinnan et al., 2009; Zhou et al., 2011; Zimmermann and Kohler, 2013). A key challenge is that the effectiveness of these techniques is highly dependent on the quality of the spectral data, and there is no standard (i.e., universal) protocol for spectral analysis (Engel et al., 2013). In all applications, the selection of an optimal pre-processing technique is not straightforward and requires prior knowledge of the spectral characteristics with a basic understanding of each pre-processing technique. Similarly, choosing an appropriate modelling method is complex and require careful consideration on the dataset size, spectral features, and the intended application.

A major constraint of vis-NIR spectroscopy is its sensitivity to the nature of the sample including particle size and moisture content, and external factors such temperature and incident light (Barnes et al., 1989; Coops et al., 2002; Kumar, 2007; Rotbart et al., 2013; Xu et al., 2019; Prananto et al., 2021). Variations in temperature and incident light can reduce signal intensity, degrade the signal-to-noise ratio (SNR), and spectral resolution (Rotbart et al., 2013; Xu et al., 2019). Similarly,

high moisture content and heterogenous particle size can affect the accuracy and robustness of calibration models (Rotbart et al., 2013; Janik et al., 2016; Prananto et al., 2021).

2.1.3 Spectroscopy in analysing chemical quality of plant material

Despite these limitations, vis-NIR, NIR-, and FTIR have been widely used to analyse chemical properties of soil and plant samples. Spectroscopy has been used to characterise plant species, assess wood quality and leaf moisture content, and to quantify plant litter chemical quality (Foley et al., 1998; Wang et al., 2021; Tsuchikawa et al., 2023). For example, vis-NIR spectroscopy has been used to detect the moisture content of six dominant *Eucalyptus* species in Sydney, Australia (Kumar, 2007) and to determine leaf nutrient concentration in a *Eucalyptus* plantation in Brazil (Oliveira et al., 2019). Several other studies have contributed convincing evidence in the application of vis-NIR spectroscopy for the measurement of N concentration in foliage, demonstrating strong correlations between vis-NIR predictions and N data obtained from laboratory analysis (e.g., McLellan et al., 1991b; Rotbart et al., 2013; Terhoeven-Urselmans et al., 2006).

Successful applications of vis-NIR and FTIR spectroscopy for analysing the content of C, N, and lignocellulosic compounds in forest litter have been well documented. Numerous studies have used spectroscopic techniques to estimate and predict the chemical quality of fresh and decomposing litter materials with high accuracy (R^2 ranging from 0.86 to 0.98; Elvidge, 1990; McLellan et al., 1991b; Joffre et al., 1992; Gillon et al., 1999; Coops et al., 2002; Ono et al., 2003; Richardson et al., 2004; Poke et al., 2005; Terhoeven-Urselmans et al., 2006; Ono et al., 2007; Ono et al., 2008; Parsons et al., 2011; Ferreira et al., 2018; Oliveira et al., 2019; Steinwandter et al., 2019; Kothari et al., 2024; Zou et al., 2024). In addition to chemical quality, several studies have successfully applied spectroscopic techniques to predict the decomposition of forest litter (e.g., Gillon et al., 1993; Parsons et al., 2011). These studies support the use of vis-NIR spectroscopy as a powerful and reliable technique to be used alongside laboratory analysis to quantify the chemical quality of plant litter.

Previous studies have also reported the successful application of FTIR spectroscopy in predicting the chemical quality of forest litter in various decomposition stages (Rodrigues et al., 1998; Nault et al., 2009; Zhou et al., 2011; Duboc et al., 2012; Chen et al., 2015; McKee et al., 2016; Fan et al., 2017; Constantine et al., 2021; Zhang et al., 2024). For example, FTIR spectroscopy has been used to predict the lignin content in *Eucalyptus globulus* wood samples with high accuracy (Rodrigues et al., 1998). Similarly, FTIR spectroscopy has also been applied to predict C content in leaf litter from *Betula platyphylla* (Japanese White Birch; Zhang et al., 2024), N content in decomposing leaf litter of various species (Nault et al., 2009), and lignocellulosic compounds in

decomposing litter of *Andropogon geradii* (Big Bluestem Grass; McKee et al., 2016). These studies confirmed the feasibility of using FTIR spectroscopy in quantifying the chemical quality of decomposing litter from different vegetation types. More recently, attenuated total reflectance Fourier transform infrared (ATR-FTIR) spectroscopy has been successfully used to determine the intensity of past fire events using charcoal derived from dominant tree species in Australia (Constantine et al., 2021). This study has demonstrated the potential use of ATR-FTIR in analysing the chemical quality of charred materials produced from fire events. Collectively, these studies have demonstrated that FTIR spectroscopy is a viable technique to understand the chemical quality of plant materials at various stages, including charred materials.

2.1.4 Recent advancements in spectroscopy

Traditional measurements of MIR spectra are acquired using a FTIR potassium bromide (KBr) pellet (Zhou et al., 2011). The disadvantage of this method (FTIR-KBr) is the use of chemicals, and the time spent on sample preparation such as grinding and mixing individual samples with KBr. An important advancement for measuring MIR spectra is attenuated total reflectance Fourier transform infrared (ATR-FTIR) spectroscopy which utilises the total internal reflection of IR light to allow direct interactions with the sample surface to facilitate detection of chemical bonds (Haberhauer and Gerzabek, 1999; Blum and Johnson, 2012; Md Salim et al., 2021). This method allows measurement in the form of liquids, solution, pastes, powders, and solids without complex sample preparation (Blum and Johnson, 2012). Despite its great success in forensic science and the food industry (Manheim et al., 2016; Johnson et al., 2022), there are few published studies that have used ATR-FTIR to determine chemical properties of plant and soil samples (e.g., Haberhauer and Gerzabek, 1999; Zhou et al., 2011; Chen et al., 2015; Mckee et al., 2016; Md Salim et al., 2021).

With the development of technology and increased research efforts in spectroscopy, vis-NIR spectrometers have evolved from expensive benchtop instrument to low-cost research grade portable devices. The use of portable spectrometers demonstrates great potential in making *in-situ*, real-time, fast, and accurate prediction of properties of soil, crops, and plant litter samples (Dos Santos et al., 2013; Soriano-Disla et al., 2017; Hutengs et al., 2019; Prananto et al., 2021; Sandak et al., 2020; Tang et al., 2020). In practice, portable NIR spectrometers (wavelength range from 1,300 to 2,500 nm) have been used successfully *in-situ* to predict the concentration of N in cotton leaves (R^2 = 0.94; Prananto et al., 2021). Portable vis-NIR and MIR spectrometers have also been used to estimate the nutrient content (e.g., N, Ca, K, and Mg) of sorghum and maize leaves in *in-situ* condition (Silva et al., 2013). However, as evidence of this being very much a developing technology, the performance

of portable spectrometers is limited by sample conditions, including moisture content, particle size, short spectral range, and low spectra resolution (e.g., Dos Santos et al., 2013; Rotbart et al., 2013; Gałuszka et al., 2015; Prananto et al., 2021). For example, a study conducted by Prananto et al. (2021) demonstrated the influence of moisture content and particle size on vis-NIR spectra, showing that dried and finely ground samples produced more accurate and reliable calibration models than models using fresh and unground samples. Additionally, environmental factors such as temperature, light, and humidity can affect the analytical performance of portable spectrometers and may influence spectral quality and reduce model accuracy (e.g., Roger et al., 2003; Minasny et al., 2011). Despite these limitations, portable spectrometers offer the advantage of real-time measurements and are highly desirable in environmental studies to rapidly predict the chemical and physical properties of soil and plant materials. Testing the potential of portable spectrometers to measure fresh and unground samples in field applications is of particular interest since drying and grinding of samples is labour intensive and time consuming.

2.1.5 Objective and research questions

Over the last few decades, the body of research focusing on the use of spectroscopy for characterising soil and plant properties, particularly using the vis-NIR (400-2,500 nm) and ATR-FTIR (2,500-25,000 nm) spectroscopy, has increased. These spectral regions contain rich information relevant to predicting the chemical composition of samples. However, the use of spectroscopic techniques to examine changes in chemical quality during litter decomposition, especially for *Eucalyptus* species, has received little attention. To reduce analytical costs, recent studies have explored more economically viable methods for estimating the chemical quality of forest litter. One approach uses commercially available mixtures of cellulose, hemicellulose, and lignin as a reference powder, with simplex-lattice mixture design to represent their proportion in plant biomass (Oh et al., 2005; Krasznai et al., 2012; Fan et al., 2017). This method coupled with infrared spectroscopy and multivariate analysis, has been used as a cost-efficient alternative for predicting the content of lignocellulosic compounds in plant samples.

In this context, this study explored the feasibility of using commercially available cellulose, hemicellulose, and lignin mixture with benchtop vis-NIR, NIR, and ATR-FTIR spectrometers to predict the chemical quality of *Eucalyptus* litter as the starting point for understanding forest decomposition processes. Calibration models developed using different spectral pre-processing techniques were compared to evaluate the influence of pre-processing on model performance.

Litterfall samples from two different dry sclerophyll *Eucalyptus* forests (i.e., an inland forest and a coastal forest) were characterised using both qualitative (vis-NIR, NIR-, and ATR-FTIR spectroscopy) and quantitative (chemometric methods) analyses to determine litter chemical quality (i.e., C, N, cellulose, hemicellulose, and lignin). Calibration models were developed to predict the chemical quality of litterfall samples collected across different months from the same *Eucalyptus* forest sites. To assess the feasibility and accuracy of using spectroscopic methods to analyse chemical properties of plant material, the following research questions were formulated:

1. How does litterfall samples from the same forest type but in different geographic locations (i.e., inland and coastal) vary in chemical quality?
2. Which spectral regions (vis-NIR, NIR, or ATR-FTIR) are the most suitable to determine the C, N, cellulose, hemicellulose, and lignin in samples of *Eucalyptus* litterfall?
3. Which pre-processing techniques produce the best calibration model?

2.2 Materials and methods

2.2.1 Description of study areas

In this study, *Eucalyptus* litterfall samples collected from a previous litterfall experiment were used. Samples were collected in Wombat State Forest (Wombat SF) and Orbost State Forest (Orbost SF) located in Victoria, Australia from July 2018 to August 2019. Despite being more than 400 km apart, both sites were broadly described as dry sclerophyll forests (DSFs) with tree 10-30 m in height and a canopy cover of 30-70% (Department of Sustainability and Environment, 2004). Both study sites have a fire history of being long-unburnt with a minimum of 15 years of time since last fire.

Wombat State Forest

Wombat State Forest (Wombat SF) is located in central western Victoria (33°41' S, 144°46' E) and is characterised by a temperate climate with warm summers and cold winters. During the sampling period (2018-2019), the mean minimum and maximum temperature were 12.3 °C and 32.9 °C, respectively, with a total rainfall of 755.2 mm. The lowest daily temperature during the sampling period was 9 °C, while the highest reached 40.2 °C (Australian Bureau of Meteorology, 2021).

Wombat SF is classified as DSF (Ecological Vegetation Class 20: Heathy Dry Forest) with dominant *Eucalyptus* species including *E. goniocalyx* (Long-leaf Box), *E. macrohyncha* (Red Stringybark), *E. dives* (Broad-leaved Peppermint), *E. radiata* (Narrow-leaved Peppermint), and *E. obliqua* (Messmate Stringybark) (Department of Sustainability and Environment, 2004). The

understorey layer is composed of small to medium shrub including *Acacia pycnantha* (Golden Wattle), *A. paradoxa* (Hedge Wattle), *Phyllanthus hirtellus* (Thyme Spurge), and *Leucopogon virgatus* (Common Beard-heath) (Department of Sustainability and Environment, 2004b). The forest covers an area of 70,000 ha and occurs on shallow and rocky yellow podozol derived from Ordvician sediment. The terrain consists of foothills with an average elevation of 790 m above sea level and a ground slope of <15° (Department of Sustainability and Environment, 2004).

Orbost State Forest

Orbost State Forest (Orbost SF) is in East Gippsland in eastern Victoria (37°30' S, 148°45' E), approximately 10 km from the coast. Orbost SF is characterised by a mild temperate climate with warm summers and cool winters. During the sampling period, the mean minimum and maximum temperature were 15.2 °C and 28.2 °C, respectively, with a total rainfall of 557.8 mm. The lowest daily temperature was 10.9 °C, while the highest reached 44.5 °C (Australian Bureau of Meteorology, 2021).

Orbost SF is a DSF (Ecological Vegetation Class: 16: Lowland Forest) with dominant *Eucalyptus* species of *E. obliqua* (Messmate Stringybark), *E. muelleriana* (Yellow Stringybark), *E. globoidea* (White Stringybark), *E. consideniana* (Yertchuk) (Department of Sustainability and Environment, 2004a). The understorey was dominated by *Acacia terminalis* (Sunshine Wattle), *Kunzea ericoides* (Burgen), and *Pteriduim esculentum* (Bracken Fern) (Department of Sustainability and Environment, 2004a). Orbost SF occurs on Ordovician sediment and has an elevation between 50-503 m above sea level (Jenkins et al., 2016).

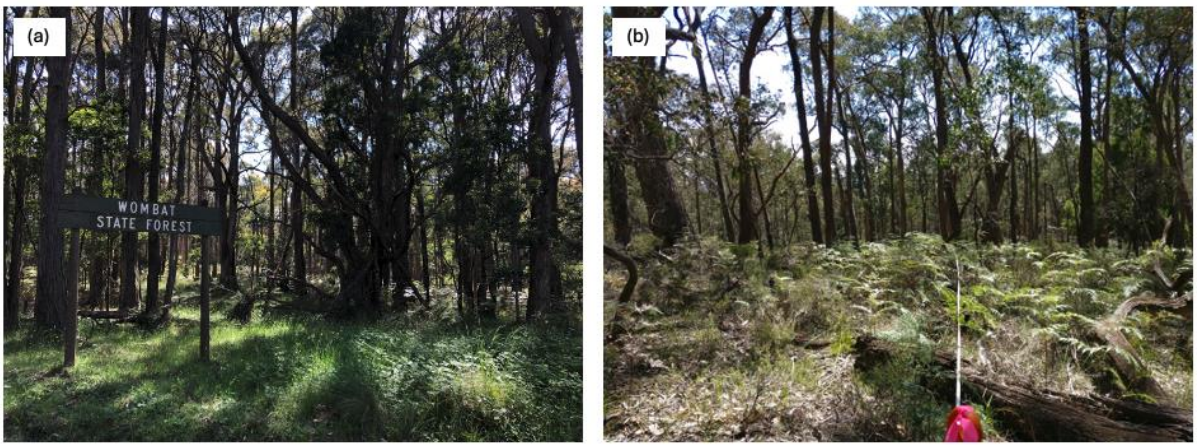

Figure 2.1: Example of study areas in (a) Wombat State Forest and (b) Orbost State Forest, Victoria during litterfall sampling in December 2017.

Litterfall collection

During August 2018 and July 2019, four transects were established in Wombat SF and Orbost SF. Transects in Wombat SF were established along a fire trail at Bullarto North (BN) with two transects in an east facing position and two transects in a west facing position. Transects in Orbost SF were established along a road at Bonang Road (BR) in west and north facing positions and at Donald Knob (DK) in west and north facing positions. In each transect, three plots (ridge, mid-slope, and bottom) were stratified according to topographic differences (i.e., slopes).

In each plot, five square litterfall traps (61 x 61 cm frame with a 56 x 56 cm mesh base) were installed approximately 5 cm above the forest floor using the roving and fixed sampling technique (Wilm, 1946) to capture small scale variation within the study area in each plot. To account for variation in litterfall, two litterfall traps were fixed in one location throughout the sampling period (referred to fixed litterfall traps), while three litterfall traps were repositioned randomly within the plot after each litterfall collection (referred to as roving litterfall traps).

Litterfall samples were collected bimonthly (n = 7 collections) from 24 plots (5 litterfall traps from per plot) between August 2018 to July 2019. Litterfall samples were stored in labelled paper bags, transported to the laboratory, and oven-dried at 60 °C for a minimum of one week (Model TD-78T-2D, Thermoline Scientific, Wetherill Park, NSW, Australia). Litterfall samples were into fractions, including overstorey *Eucalyptus* leaves, twigs (> 6 mm diameter), fine twigs (< 6 mm diameter), bark of *Eucalyptus*, and fruits. Dry weight of the total litterfall and individual component were weighed and recorded.

Average annual litterfall

Total litterfall rate in Wombat SF and Orbost SF between August 2018 and July 2019 was 3.7 t ha^{-1} yr^{-1} and 4.7 t ha^{-1} yr^{-1}, respectively. Litterfall in Wombat SF followed a seasonal trend with maximum in summer and minimum in winter. In contrast, maximum litterfall in Orbost SF was in autumn and winter, with a minimum spring. Despite the difference in litterfall patterns, leaf litter and bark of *Eucalyptus* were the two major components of litterfall, accounting for 64-66% and 9-11% of the total annual litterfall, respectively.

2.2.2 Selection of calibration and validation sets

Calibration samples set for lignocellulosic compounds

In this study, powdered samples of cellulose (α-cellulose; product number: C8002; hereafter referred to as 'x1'), hemicellulose in the form of xylan (extracted from Beechwood, product number: X4252; hereafter referred to as 'x2'), and alkaline lignin (product number: 471003; hereafter referred to as 'x3'), purchased from Sigma-Aldrich Chemie GmbH (Sigma-Aldrich Corporation, St. Louis, Missouri, USA), were used to represent the proportion of cellulose, hemicellulose, and lignin in *Eucalyptus* litterfall samples. Each powdered standard (x1, x2, and x3) was chemically pure, representing 100% of each component.

A simplex-lattice design {*q,m*} (SLD) developed by Scheffé (1958) was adopted to generate the possible proportion of cellulose, hemicellulose, and lignin in *Eucalyptus* litterfall. In this design, *q* represents the number of components (i.e., factors; x1, x2, x3), where *m* is the level that used in the design (Lambrakis, 1968). This model obtains all the possible formulations (i.e., mixture blends) by changing the proportion of components in the mixture while the sum of their concentration always equal to 100%. In a simplex-lattice design (SLD), the design space (*m* + 1) has unconstrained and is defined by equally spaced component proportions ranging from 0-1 in a *q* - 1 dimension (Lambrakis, 1968). The SLD model can be expressed as:

$$x_i = 0, \frac{1}{m}, \frac{2}{m}, \ldots, 1 \; for \; i = 1, 2, \ldots, q \qquad \text{Equation 2.1}$$

where x_i is the proportion of components in the blend, *i* varied from the value of 0-*m* and the sum of the blend is 1. In addition, the number of mixture blends (design points) in the simplex-lattice design is calculated by:

$$\frac{(q+m-1)!}{(m!(q-1)!)} \qquad \text{Equation 2.2}$$

The SLD model was generated using the package '*mixexp*' implemented in the open-source statistical programming software RStudio (version 4.2.1, RStudio Team, 2022) to determine the number of experimental runs and the proportion of the three components. A {3,5} SLD model was used to yield a total of 21 mixture blends represented by a two-dimensional triangle, including the three single component mixture blends (i.e., pure mixture, 100% of x1, x2, x3; vertices of the triangle), 12 two-component mixture blends (edges of the triangle), and six three-component mixture blends (points inside the triangles) (Figure 2.1).

A total of 21 mixture blends (1 g for each formulation) were prepared by mixing a relative proportion of x1, x2, x3 to a total of 100% (Figure 2.1; Table 2.1). The proportion of cellulose,

hemicellulose, and lignin in the blend was used as independent variables in the experimental design. The spectra of the mixture blends (n = 21) were measured using vis-NIR, NIR, and ATR-FTIR spectrometers (see Section 2.2.5) to assist in assessing the cellulose, hemicellulose, and lignin concentration in *Eucalyptus* leaf and bark litterfall samples.

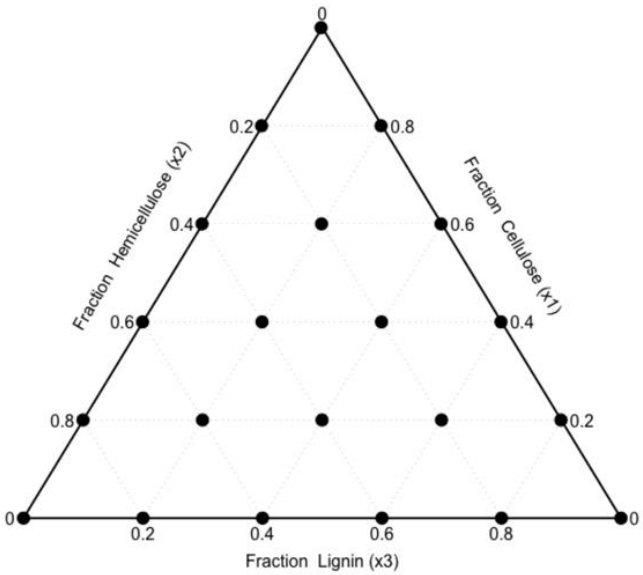

Figure 2.2: Example of a simplex-lattice design {3,5} for modelling the relationship between the proportion of cellulose, hemicellulose, and lignin in *Eucalyptus* litterfall samples. The vertices of the triangle represent pure components (i.e., 100% of x1/x2/x3), while the edges of the triangle represent the mixture blends that made up of the components at both edges (the component at the opposite edge is absent). The points inside the triangle represent the mixture blends containing all three components (i.e., cellulose, hemicellulose, and lignin).

Validation sample selection for lignocellulosic compounds

Leaf and bark litterfall samples from Wombat SF and Orbost SF were selected to represent the dominant component of surface fine fuel. A representative subset (n = 42) of litterfall samples collected during the period of maximum litterfall was used to validate the calibration models for predicting cellulose, hemicellulose, and lignin content. The number of samples included in this subset was primarily constrained by the processing capacity of the external laboratory conducting the chemistry analysis (see Section 2.2.3 for analysis details), but also by cost. To minimise the total number of samples for laboratory analysis, leaf and bark litterfall samples from the five litterfall traps within each plot (including both fixed and roving litterfall traps) were bulked to create composite samples. This resulted in a total of 12 leaf and 12 bark composite samples from Wombat SF collected in April 2019, and nine leaf and nine bark samples from Orbost SF collected in August 2018.

Table 2.1: The 21 mixture blends generated using the simplex-lattice design. Each mixture blend was prepared by mixing the corresponding powdered samples of cellulose (x1), hemicellulose (x2), and lignin (x3) to a total weight of 1 g. The table list all the possible formulations including the three pure components (vertices of the triangle), the 12 two-component mixture blends (edges of the triangle), and the six three-component mixture blends (points inside the triangles).

	Mass (g)		
Mixture	**Cellulose (x1)**	**Hemicellulose (x2)**	**Lignin (x3)**
1	1	0	0
2	0.8	0.2	0
3	0.6	0.4	0
4	0.4	0.6	0
5	0.2	0.8	0
6	0	1	0
7	0.8	0	0.2
8	0.6	0.2	0.2
9	0.4	0.4	0.2
10	0.2	0.6	0.2
11	0	0.8	0.2
12	0.6	0	0.4
13	0.4	0.2	0.4
14	0.2	0.4	0.4
15	0	0.6	0.4
16	0.4	0	0.6
17	0.2	0.2	0.6
18	0	0.4	0.6
19	0.2	0	0.8
20	0	0.2	0.8
21	0	0	1

Calibration and validation sample selection for carbon and nitrogen content

The 21 mixture blends and the 42 representative litterfall samples were used to construct a calibration model for prediction of total carbon (TC) and total nitrogen (TN) content. This calibration dataset included a total of 63 samples. An additional subset of 207 litterfall samples, including 105 litterfall samples from Wombat SF (56 leaf and 48 bark samples) and 102 litterfall samples form Orbost SF (59 leaf and 43 bark samples) were selected to validate the TC and TN calibration models. Litterfall samples were dried at 60 °C for a minimum of 48 h in a fan-forced oven (Model TD-78T-2-D, Thermoline Scientific, Wetherill Park, NSW, Australia), ground using a food-grade grinder (Breville Coffee and Spice Grinder; model BCG200BSS; Breville Pty, Sydney, Australia) to pass through a 1 mm sieve. Ground samples were stored in labelled plastic containers prior to laboratory analysis.

2.2.3 Laboratory analysis of litterfall chemical quality

Determination of carbon and nitrogen content

The total carbon (TC) and total nitrogen content (TN) of the mixture blends (n = 21) and litterfall samples (n = 249) were analysed using an Elementar analyser (Elementar Vario Max CNS, Analysensystem GmbH, Hanau, Germany). Phenylalanine was used as a standard to calibrate the instrument prior to sample analysis and was analysed at an interval of every 20 samples to ensure analytical accuracy.

Determination of cellulose, hemicellulose and lignin content in Eucalyptus *litterfall samples*

Representative subsets of leaf (n = 21) and bark (n = 21) samples were selected for conventional chemical analysis to validate the calibration models developed using vis-NIR, NIR-, and ATR-FTIR spectral data. A total of 42 litterfall samples were submitted to the New South Wales Department of Primary Industry (NSW DPI) Feed Quality Service Laboratory in Wagga Wagga, NSW, Australia for determination of fibre fractions. The analysis included direct measurement of acid detergent fibre (ADF-D), sequential measurement of ADF (ADF-seq), neutral detergent fibre (NDF), and acid detergent lignin (ADL). Fibre fractions were determined using acid detergent extraction methods following Van Soest et al. (1991), with the ANKOM 200 Fibre Analyser (Ankom Technology Inc., Macedon, NY, USA). *Eucalyptus* leaf and bark litterfall samples were pre-soaked in acetone for 10 min prior to analysis to avoid overestimation of ADF content (McArthur, 1988; Makkar et al., 1995; Tahir et al., 2019). Hemicellulose content in *Eucalyptus* litterfall samples was determined by subtracting ADF-seq from NDF, while cellulose content was determined by subtracting ADL from ADF. Lignin content was quantified as the acid detergent lignin (ADL) fraction.

2.2.4 Statistical analysis of litterfall chemical quality

Statistical analyses were performed using Jamovi (Version 2.3, 2024; The Jamovi Project, Sydney, Australia). One-way analysis of variance (ANOVA) was conducted to test the effects of position in landscape (i.e., inland vs. coastal), followed by Games-Howell Post-Hoc tests where significant differences were identified ($\alpha = 0.05$).

2.2.5 Spectral analysis

Visible-near-infrared (vis-NIR) and near-infrared (NIR) spectra were collected using Black-Comet-CXR-SR (Channel 1: vis-NIR spectrum between 219 and 1,100.5 nm at a resolution of 0.5 mm; 1,770 variables) and RED-Wave-NIRSX-SR spectrometers (Channel 2: NIR spectrum between 863 and 1,754 nm at a resolution of 1.75 nm; 517 variables) with a RFX-3D reflectance base (StellaNet Inc. Oldsmar, Florida, USA) under constant room temperature. The RFX-3D reflectance base is an upward looking accessory equipped with an integrated light source containing a 10-watt halogen bulb. Visible-NIR and NIR spectrometers were warmed up for at least 15 min prior to scanning to reduce instrumental noise. Spectrometers were calibrated using a white ceramic reflectance standard (RS50 white standard) prior to scanning of samples. A dark scan was acquired by placing the white ceramic standard on top of the RFX-3D reflectance base with no light source, while a white reference scan was acquired with the light on. Samples were scanned under Absorbance Mode with an integration time 500 millisecond (ms) for vis-NIR spectra measurement and 100 ms for NIR spectra measurement. Dried and ground samples were placed on a clean glass Petri dish and placed on top of the RFX-3D reflectance base for spectra measurement. Five sub-samples of each sample were scanned using both vis-NIR and NIR spectrometers. Sample spectra were exported from SpectraWiz software (version 6.2, StellarNet Inc., 2023) and imported into RStudio (version 2022.07.1+554, RStudio Team, 2022). To reduce random noise and improve spectral reliability, the mean spectum of the five sub-samples was calculated (Terhoeven-Urselmans et al., 2006, Yang et al., 2017; Xiao et al., 2022).

Mid-infrared (MIR) spectra were acquired using the attenuated total reflectance Fourier transform infrared (ATR-FTIR) spectrometer (4500a portable FTIR spectrometer; Agilent Technology Inc., Santa Clara, California, USA) in the wavenumber ranges from 4,000 to 650 cm^{-1} (equal to wavelength ranges from 2,500 to 25,000 nm) with a resolution of 3.75 cm^{-1}, which generated a total of 899 variables. The ATR-FTIR spectrometer was connected to a laptop equipped with MicroLab PC software (version 2.9.3, Agilent Technologies Inc., 2023). The spectrometer was warmed up for at least 15 min prior to scanning to reduce instrumental noise. Spectra of a clean ATR crystal against air was used as a background and acquired prior to each sample scan. Samples were loaded on the ATR diamond sampling window and secured with the sample press tip. The sample window was cleaned with lint-free laboratory-grade tissue (Kimtech Science Kimwipes 34155; Kimberly-Clark Inc.) after each scan to avoid cross-contamination. Five sub-samples of each sample were scanned using the ATR-FTIR spectrometer. Spectra were exported from MicroLab and imported into RStudio to calculate the mean spectrum for each sample. The final spectrum for each sample was

obtained by averaging the spectra of the five subsamples, resulting in one representative spectrum per sample.

2.2.6 Pre-processing of spectra

Pre-processing of vis-NIR, NIR, and ATR-FTIR spectra was done in RStudio using the guidelines and R code from Wadoux et al. (2021). Detailed descriptions of each pre-processing technique used are presented here.

Trimming

Spectra trimming is usually performed after transformation of reflectance to absorbance values. Trimming aims to remove wavelengths that do not contain useful information for spectra analysis (Wadoux et al., 2021). In most cases, wavelengths at the edge of the sensor range are removed due to their low signal-to-noise ratios (Wadoux et al., 2021). In this study, wavelengths from 219-500 nm and 1,000.5-1,100.5 nm were removed from vis-NIR spectra acquired using the vis-NIR spectrometer, while wavelengths from 863-1,000 nm and 1,651-1,754 nm were removed from NIR spectra acquired using the NIR spectrometer. After trimming, a total of 999 wavelengths in the vis-NIR region and 371 wavelengths in the NIR region were retained for model development. The complete ATR-FTIR spectral range (4,000 to 650 cm^{-1}) was used due to its high SNRs (899 wavenumbers). Visible-NIR and NIR spectral trimming was done using the function *trimSpec* () in RStudio (Wadoux et al., 2021) to remove spectral regions with low SNRs.

Savitzky-Golay smoothing filter

The Savitzky-Golay (SG) smoothing filter is a pre-processing technique that fits a polynomial regression within a given window size to reduce spectral noise (Zimmermann and Kohler, 2013). Spectrum smoothing is achieved by fitting a polynomial regression to the whole raw spectra within a given window size (w), where w represents the number of wavelengths used in the local polynomial regression. Although a high polynomial degree and a large window size can effectively reduce spectral noise, the use of a large window size may suppress spectral signals that contain important chemical information and thus have deleterious effects on the performance of the calibration models (Rinnan et al., 2009; Wadoux et al., 2021). Therefore, in this study, a second order polynomial and a set of low window size (w = 3, 5, and 7) were used on trimmed vis-NIR (999 wavelengths), NIR- (371 wavelengths), and ATR-FTIR (899 wavenumbers) spectra, respectively. Savitzky-Golay

smoothing was done by *sgolayfilt* () function in the '*prospectr*' R package in RStudio (Wadoux et al., 2021).

Baseline correction

Multiplicative scatter correction (MSC) and standard normal variation (SNV) are two most widely used methods to minimise the scatter effects caused by light scattering and particle size (Rinnan et al., 2009; Wadoux et al., 2021). Both techniques lead to similar results, however, MSC requires a reference spectrum for scatter correction. Therefore, in most cases, SNV is preferred over MSC and was chosen for this study.

Multiplicative scatter correction

Multiplicative scatter correction (MSC) is a spectral pre-processing technique that used to correct both additive and multiplicative effects by fitting each spectrum to a reference spectrum using a linear least square regression. Ideally, the reference spectrum is a spectrum that has not been affected by scatter effects. However, in most cases, a reference spectrum is referred to as the mean spectrum of the whole spectra. This method assumes that the effects of particle size and light scattering will be reduced by averaging the spectra. The method of MSC can be described as:

$$X_i = a_i + b_i X_{ref} + \in_i \qquad \text{Equation 2.3}$$

$$X_i^{msc} = \frac{X_i - a_i}{b_i} \qquad \text{Equation 2.4}$$

where *a* and *b* are the intercept and slop of the linear model, X_{ref} reference spectrum, in this case, is the mean of the whole spectra, and ϵ is the residuals of the spectrum, *i* (Wadoux et al., 2021). In this study, MSC was not applied since an independent reference spectrum that is unaffected by scatter effects was not available.

Standard normal variation

Standard normal variation (SNV) transformation, also known as *z*-transformation or centering and scaling, is a technique that used to correct for single light scattering (Wadoux et al., 2021). Standard normal variation is used to transform each spectrum individually (operating in row-wise manner), where each spectrum (ρ) is normalised to a mean of zero ($\bar{\rho}$) and standard deviation of 1 (σ_ρ):

$$SNV = \frac{\rho - \bar{\rho}}{\sigma\rho}$$ Equation 2.5

In this study, SNV was done using the *snvBLC* () function in the '*prospectr'* R package in RStudio (Wadoux et al., 2021).

Wavelength selection

To optimise the model performance, a genetic algorithm (GA) was used as a feature wavelength (for vis-NIR and NIR) and wavenumber (for ATR-FTIR) selection technique (also known as variable selection) to reduce data dimensionality. This approach identifies a subset of informative wavelengths from the trimmed vis-NIR and NIR spectra and the full ATR-FTIR spectra, prior to calibration model development. The GA feature selection is a method inspired by the Darwinian evolutionary theory – the concept of 'survival of the fitness' (Lestander et al., 2003; Koljonen et al., 2007; Fan et al., 2021). This technique uses a partial least square regression (PLSR) model to select a subset of wavelengths that best explain the variance in the targeted chemical properties. In brief, an initial population of potential solutions – chromosomes (i.e., set of wavelengths or wavenumbers) – are generated randomly. The fitness of each individual chromosome is evaluated by a fitness function based upon the performance of a partial least square regression (PLSR) model. Chromosomes with the best fitness scores in each generation are chosen to reproduce to form a new population that has the highest potential to solve the problem. Through an iterative process, the GA feature selection identifies the most meaningful wavelengths for model development. Ferreira et al. (2018) demonstrated that the GA feature selection method significantly improves the predictivity of calibration models in estimating the chemical quality of *Eucalyptus* litterfall samples. In this study, GA feature selection was done using the *ga_pls* () function in the 'plsVarSel' package in RStudio using an initial population of 100 wavelengths (or wavenumbers) with 10 iterations.

Spectral pre-processing combinations

A series of spectral pre-processing combinations were applied to vis-NIR, NIR, and ATR-FTIR spectra prior to calibration model development. These included the use of Savitzky-Golay (SG) smoothing and Standard Normal Variate (SNV) transformation. Specifically, the following combinations were teste:

- Raw spectra (vis-NIR and NIR spectra were trimmed; the full ATR-FTIR spectra was retained)

- SG smoothing (window size 3 + polynomial order of 2) followed by SNV
- SG smoothing (window size 5 + polynomial order of 2) followed by SNV
- SG smoothing (window size 7 + polynomial order of 2) followed by SNV

A range of small window size was selected to prevent excessive smoothing and preserve important spectral features.

In this study, two sets of calibration models were developed. The first set used the above pre-processing combinations alone, while the second set incorporated GA feature selection following the same pre-processing steps. The performance of both sets of models was compared and evaluated to identify the most effective approach for predicting C, N, cellulose, hemicellulose, and lignin content in litterfall samples.

2.2.7 Calibration model development

Following spectral pre-processing, multivariate analysis techniques were used to model the relationship among spectra and laboratory measured values of chemical properties of interest. In other studies, the most commonly used multivariate analyses include partial least square regression (PLSR), Bootstrap with bagged PLSR (Bootstrap PLSR), Cubist, and random forest (RF) (e.g., Chodak, 2008; Ng et al., 2019; Wadoux et al., 2021; Jeon et al., 2024). Of these methods, PLSR is widely considered as one of the most powerful due to its simplicity, robustness, and interpretability, especially when dealing with high-dimensional spectral data. However, due to the widespread adoption of machine learning in soil spectroscopy (e.g., Ramírez et al., 2023; Wadoux et al., 2023; Jeon et al., 2024), Cubist and RF were also included in this study to evaluate and compare their effectiveness as modelling techniques for prediction of litter chemical quality.

Partial least square regression

Partial least square regression is a chemometric technique that combines principal component analysis (PCA) and multiple linear regression (MLR) to model the relationship among predictors and response variables (Wold et al., 2001; Chodak, 2008; Wadoux et al., 2021). This technique is designed to handle multicollinearity, where predictor variables are highly correlated, such as spectral data. Partial least square regression has been used extensively in spectral analysis to correlate soil and plant properties with complex spectral features (e.g., Joffre et al., 1992; Parsons et al., 2011; Janik et al., 2016; Jeon et al., 2024). This technique reduces spectral data dimensionality by extracting a set of principle components (PCs), also referred to as latent variables, that maximise the covariance between

predictors and response variables. In this study, PLSR models were developed using spectral data as predictor variables and laboratory measured values as response variables. Internal cross-validation (CV) was done to determine the optimal number of PCs for model development to predict properties of litterfall samples. The maximum number of PCs in the PLSR model was set to 30, while the optimal number of PCs for the calibration model was selected based on the root mean squared error (RMSE). In this study, PLSR models were developed using the *plsr* () function within the '*pls' package* in RStudio.

Bootstrap bagged partial least squares regression

Bootstrap bagged partial least squares regression (bootstrap PLSR) is a technique that combines PLSR and bootstrap aggregation (also known as bagging). Bootstrap aggregation is a resampling technique that generates multiple subsets of the original calibration data set (bootstrap samples) by randomly sampling with replacement. Each bootstrap is considered as an independent dataset and is used to train a PLSR model. The final prediction is obtained by averaging the outputs of all the individual models (Wadoux et al., 2021). In this study, bootstrap PLSR models were developed using the *fitBagPlsr* () function in RStudio.

Cubist

Cubist is a rule-based ensemble algorithm that is used to develop predictive models by generating a set of conditional rules (Quinlan, 1993). These rules are used to build decision trees, where each terminal node is fitted with a linear regression model to make predictions. In this study, Cubist models were developed using *cubist* () function within the 'cubist' package in RStudio.

Random forest

Random forest (RF) is an ensemble machine learning algorithm that builds multiple decision trees using bootstrap sampling techniques (random sampling the calibration dataset with replacement; Breiman, 2001). In the forest, each tree is trained using a unique subset of bootstrap samples, and at each tree node, a random subset of predictor variables is considered for splitting until pre-defined criteria are met. The final prediction is obtained by averaging the output of all decision trees. In this study, RF models were developed using the *randomForest* () function within the '*randomForest*' package in RStudio with the default number of tree set to 500 (ntree = 500).

2.2.8 Model evaluation metrics

The performance and the accuracy of the cross-validation and validation models were evaluated using several statistical metrics, including the coefficient of determination (R^2), root mean squared error (RMSE), and Lin's Concordance Correlation Coefficient (LCCC) value.

Coefficient of determination

The coefficient of determination (R^2) is a measure of the proportion of variance in the observed values that is explained by the models. The coefficient of determination (R^2) is a value between 0 and 1, where values closer to 1 indicate a better model fit. In this study, R^2 was calculated for both cross-validation and validation models using the following equation:

$$R^2 = 1 - \frac{\sum_{i=1}^{n}(y_i - \hat{y}_i)^2}{\sum_{i=1}^{n}(y_i - \bar{y}_i)^2} \quad \text{Equation 2.6}$$

According to Saeys et al. (2005), a R^2 value between 0.61 and 0.81 indicates moderate prediction accuracy, whereas a R^2 between 0.82 and 0.9 is considered good, and values above 0.91 are considered excellent.

Root mean squared error

Root mean squared error (RMSE) is the standard deviation (SD) of the differences between observed and predicted values. This value indicates how closely the predicted value fits to the observed values. In this study, root mean squared error (RMSE) of the cross-validation and validation models was calculated using the following equation:

$$RMSE = \sqrt{\frac{1}{n}\sum_{i=1}^{n}(y_i - \hat{y}_i)^2} \quad \text{Equation 2.7}$$

Lin's Concordance Correlation Coefficient

Lin's Concordance Correlation Coefficient (LCCC) assesses the agreement between the prediction and measured values along the 1:1 line (Lawrence and Lin, 1989). This measure ranges from -1 to +1, where a value closer to +1 indicates strong agreement. A positive LCCC value (0 to +1) indicates a positive linear relationship, while a negative LCCC values (0 to -1) indicates a negative linear relationship. In this study, LCCC was calculated for both validation and cross-validation models using the following equation (Wadoux et al., 2021):

$$\rho_c = \frac{2r\sigma_{pred}\sigma_{obs}}{\sigma_{obs}^2 + \sigma_{pred}^2 + (\mu_{obs} - \mu_{pred})^2} = rC_b$$ Equation 2.8

For each litter chemical quality (i.e., C, N, cellulose, hemicellulose, and lignin) and spectral range (vis-NIR, NIR, and ATR-FTIR), the model with the highest R^2 and LCCC values, along with the lowest RMSE was considered the best performing model.

2.3 Results

2.3.1 Litterfall chemical quality

Overall, litterfall from Orbost SF had greater proportions of lignocellulosic compounds (i.e., cellulose, hemicellulose, and lignin) than litterfall from Wombat SF, but contained lower TC and TN (Figure 2.2). The total amount of N, C/N ratio, and hemicellulose in leaf litterfall did not vary significantly between the two forests (One-way ANOVA; $p > 0.05$; Figure 2.2b, c, e), and bark litterfall from both locations showed comparable hemicellulose and lignin content (One-way ANOVA; $p > 0.05$; Figure 2.2e, f).

Leaf litterfall from Wombat SF had significantly higher TC content (57.56 ± 6.43%) compared to Orbost SF (53.16 ± 4.05%; One-way ANOVA; $p < 0.001$; Figure 2.2a). In contrast, bark litterfall from Wombat SF had significantly lower TC than that from Orbost SF (43.49 ± 4.05% and 46.88 ± 2.65%, respectively; One-way ANOVA; $p < 0.001$; Figure 2.2a). Total N in leaf and bark litterfall from Wombat SF was greater than samples from Orbost SF, but only TN in bark was statistically significant different (One-way ANOVA; $p < 0.001$; Figure 2.2b). The mean TN content of bark from Wombat SF (0.58 ± 0.21%) was approximately three times greater than that of bark from Orbost SF (0.21 ± 0.13%), but the former had considerable variability (Figure 2.2b). The mean C/N ratio of bark from Orbost SF was three times greater (274.72 ± 38.53%) than that of Wombat SF bark (One-way ANOVA; $p < 0.001$ Figure 2.2c).

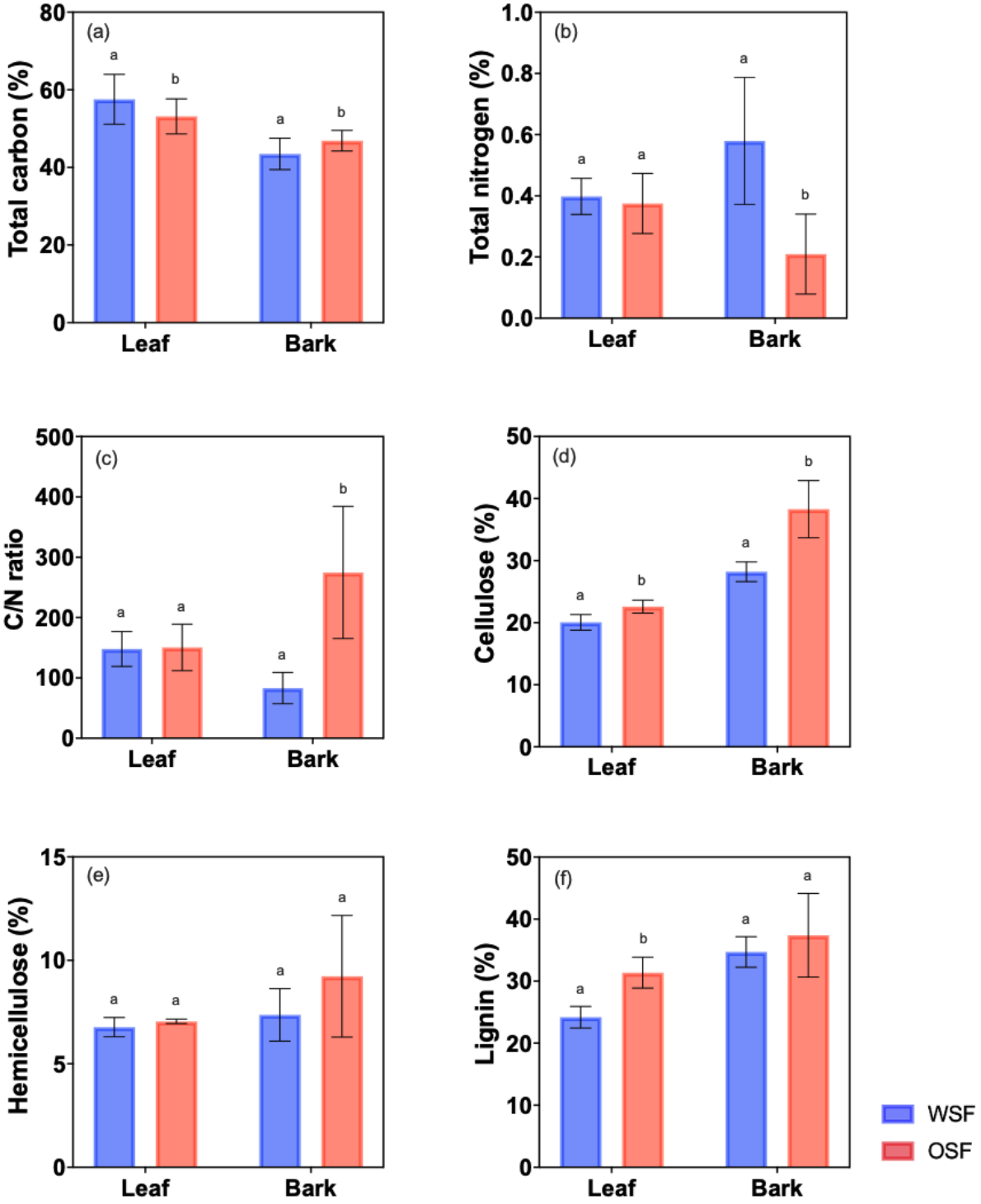

Figure 2.3: Chemical quality of *Eucalyptus* litterfall from two dry sclerophyll forests in Victoria, Australia (Wombat State Forest (Wombat SF; bars in blue) and Orbost State Forest (Orbost SF; bars in red). (a) total carbon; (b) total nitrogen; (c) carbon:nitrogen (C/N) ratio; (d) cellulose; (e) hemicellulose; and (f) lignin content. Bars represent mean value and error bars indicate standard deviation. Statistical comparison between forests was identified using one-way ANOVA followed by Games-Howell Post-Hoc test ($\alpha = 0.05$). For each litterfall component, means with the same letter are not significantly difference ($p > 0.05$).

In terms of lignocellulosic compounds, litterfall from Orbost SF had greater content of cellulose, hemicellulose, and lignin compared to Wombat SF. Leaf litter from Orbost SF had statistically higher cellulose and lignin (One-way ANOVA; $p < 0.001$; Figure 2.2d, f), while Orbost SF bark had significantly more cellulose than those from Wombat SF (One-way ANOVA; $p < 0.001$; Figure 2.2d).

2.3.2 Predicting litter chemical quality with vis-NIR, NIR, and ATR-FTIR spectroscopy

Calibration and validation dataset

The calibration dataset for TC and TN in *Eucalyptus* litterfall comprised 63 samples, including 21 mixture blends and 42 representative litterfall samples collected from Wombat State Forest (Wombat SF) and Orbost State Forest (Orbost SF). Total carbon of the calibration dataset ranged widely from 38.06 to 70.03%, with a mean of 45.83%, while TN spanned from 0.022 to 0.71%, with a mean of 0.26% (Table 2.2). Notably, the maximum TC value (70.03%) was identified as an outlier (points outside the whiskers in a box-and-whisker plot; data not shown here). Although the calibration dataset captured a wide range of TC and TN, it did not fully cover the variation measured in the validation dataset. The validation dataset (n = 207 litterfall samples) had a broader range of TC (37.29 to 80.22%), including a lower minimum and two outliers that exceeded the maximum TC in the calibration dataset. Total N of the validation dataset covered a comparable range, but the mean value was higher (0.40%), and several outliers exceeded the maximum TN values of the calibration dataset (Table 2.2).

For cellulose, hemicellulose, and lignin content, the calibration dataset comprised of 21 mixtures formulated using a simplex-lattice design. As a result, the proportions of each component in the mixtures were fixed, ranging from 0 to 100%, with a mean of 33.33%. This design covered a broad distribution of cellulose, hemicellulose, and lignin content to ensure that the calibration model could capture the putative variation in the validation dataset and unknown samples. In the validation dataset, cellulose content of *Eucalyptus* litterfall samples spanned from 18.01 to 46.39%, with a mean of 26.83%, while lignin ranged from 21.45 to 49.95%, with a mean of 31.55% (Table 2.2).

Table 2.2: Descriptive statistics of total carbon (TC), total nitrogen (TN), cellulose, hemicellulose, and lignin content in leaf and bark litterfall samples for the whole, calibration and validation datasets. For TC and TN content, the whole dataset comprised 21 mixture blends, 42 representative litterfall samples, and an additional 207 litterfall samples. In contrast, the dataset for cellulose, hemicellulose, and lignin included the 21 mixture blends and the LB litterfall samples only. Abbreviations: *N* = number of samples; Min = minimum, 1st Qu = first quartile; 3rd Qu = third quartile; Max = maximum.

Model 1: Calibration model using litterfall samples

	N	**Min**	**1st Qu**	**Median**	**Mean**	**3rd Qu**	**Max**
Total carbon							
Whole dataset	270	37.29	45.30	48.41	50.48	56.70	80.22
Calibration	63	38.06	42.51	46.13	45.83	48.11	70.03
Validation	207	37.29	47.28	49.73	51.88	57.63	80.22
Total nitrogen							
Whole dataset	270	0.02	0.25	0.36	0.36	0.47	1.30
Calibration	63	0.02	0.06	0.33	0.26	0.43	0.71
Validation	207	0.08	0.30	0.37	0.40	0.48	1.30

Model 2: Calibration model using synthetic mixtures

	N	**Min**	**1st Qu**	**Median**	**Mean**	**3rd Qu**	**Max**
Cellulose							
Whole dataset	63	0	20.00	24.44	29.00	37.33	100.00
Calibration	21	0	0	20.00	33.33	60.00	100.00
Validation	42	18.01	21.33	24.45	26.83	29.72	46.39
Hemicellulose							
Whole dataset	63	0	6.78	7.09	16.13	12.34	100.00
Calibration	21	0	0	20.00	33.33	60.00	100.00
Validation	42	4.01	6.81	7.00	7.53	7.19	12.53
Lignin							
Whole dataset	63	0	24.11	32.39	32.15	37.77	100.00
Calibration	21	0	0	20.00	33.33	60.00	100.00
Validation	42	21.45	26.04	32.45	31.55	34.76	49.95

Datasets representing both cellulose and lignin included an outlier that exceeded the upper range of the validation dataset, yet these values were fully covered by the calibration dataset. In contrast, hemicellulose had a narrower range in the validation dataset, ranging from 4.01 to 12.53%, with a mean of 7.53% (Table 2.2). Notably, there were several outliers that exceeded both the lower and upper range of the validation dataset.

Model performance

Model evaluation statistics from calibration and validation datasets suggested that partial least square regression (PLSR) models outperformed bootstrap PLSR, Cubist, and random forest (RF) in predicting the chemical quality of *Eucalyptus* litterfall samples, as evidence by higher R^2 and LCCC, and lower RMSE (Table 2.3). The only exception was the ATR-FTIR model developed for prediction of cellulose content, where the RF model had a better predictive value than PLSR. In most cases, the application of spectral pre-processing techniques including Savitzky-Golay (SG) smoothing and standard normal variate (SNV) transformation significantly improved model prediction accuracy. In contrast, genetic algorithm (GA) feature selection had a limited effect on predicting the chemical quality of *Eucalyptus* litterfall. The use of GA-based model was only effective for cellulose prediction in conjunction with ATR-FTIR spectra (Table 2.3).

Table 2.3: Comparative performance of the best models selected from vis-NIR, NIR, and ATR-FTIR spectra for predicting total carbon (TC), total nitrogen (TN), cellulose, hemicellulose, and lignin content in *Eucalyptus* litterfall. Calibration models were developed using multivariate modelling analysis including partial least squared regression (PLSR), bootstrap PLSR, Cubist, and random forest (RF). Models were selected based on the highest coefficient of determination (R^2), the lowest root mean squared error (RMSE), and the highest Lin's Concordance Correlation Coefficient (LCCC) value after testing different pre-processing combinations (raw spectra, SG smoothing, SNV, and GA feature wavelength selection). SG = Savitzky-Golay smoothing; w = window size (number following indicate the size of the applied window); k = polynomial order; SNV = standard normal variate transformation; R^2cv = coefficient of determination of cross-validation model; RMSECV = root mean squared error of cross-validation model; LCCCcv = Lin's Concordance Correlation Coefficient of cross-validation model; R^2v = coefficient of determination of validation model; RMSEV = root mean squared error of validation model; LCCCv = Lin's Concordance Correlation Coefficient of validation model.

	Spectra	Best model	Pre-processing technique	Calibration dataset			Validation dataset		
				R^2cv	RMSECV	LCCCcv	R^2v	RMSEV	LCCCv
Total Carbon	vis-NIR[a]	PLSR	Raw trimmed vis-NIR spectra	0.02	6.44	0.16	0.48	5.02	0.63
	NIR[b]	PLSR	Raw trimmed NIR spectra	0.12	5.83	0.33	0.60	4.40	0.75
	ATR-FTIR[c]	PLSR	SG (w = 7, k = 2), SNV	0.72	5.52	0.24	0.72	3.96	0.80
Total Nitrogen	vis-NIR[a]	PLSR	SG (w = 3, k = 2), SNV	0.65	0.13	0.80	0.61	0.11	0.73
	NIR[b]	PLSR	SG (w = 5, k = 2), SNV	0.72	0.11	0.78	0.51	0.12	0.69
	ATR-FTIR[c]	PLSR	SG (w = 5, k = 2), SNV	0.77	0.10	0.86	0.51	0.13	0.66
Cellulose	vis-NIR[a]	PLSR	Raw trimmed vis-NIR spectra	0.74	15.02	0.84	0.62	5.32	0.78
	NIR[b]	PLSR	SG (w = 3, k = 2), SNV	0.99	2.00	0.99	0.89	2.44	0.94
	ATR-FTIR[c]	RF	SG (w = 5, k = 2), SNV, GA	0.96	6.36	0.97	0.77	5.30	0.82
Hemicellulose	vis-NIR[a]	PLSR	SG (w = 3, k = 2), SNV	0.70	16.31	0.80	0.36	5.88	0.35
	NIR[b]	PLSR	Raw trimmed NIR spectra	0.99	3.07	0.99	0.32	2.53	0.55
	ATR-FTIR[c]	PLSR	SG (w = 3, k = 2), SNV	0.97	4.68	0.99	0.30	2.94	0.50
Lignin	vis-NIR[a]	PLSR	Raw trimmed vis-NIR spectra	0.99	3.04	0.99	0.83	2.49	0.91
	NIR[b]	PLSR	SG (w = 3, k = 2), SNV	0.99	2.00	0.99	0.89	2.44	0.94
	ATR-FTIR[c]	PLSR	Raw FTIR spectra	0.94	7.04	0.97	0.45	4.74	0.68

[a] The wavelength range for the vis-NIR spectral regions was 500.5-1,000 nm.
[b] The wavelength range for the NIR spectral region was 1,000.5-1,650 nm.
[c] The wavenumber range for the MIR infrared region was 4,000-650 cm^{-1} (wavelength: 2,500-25,000 nm).

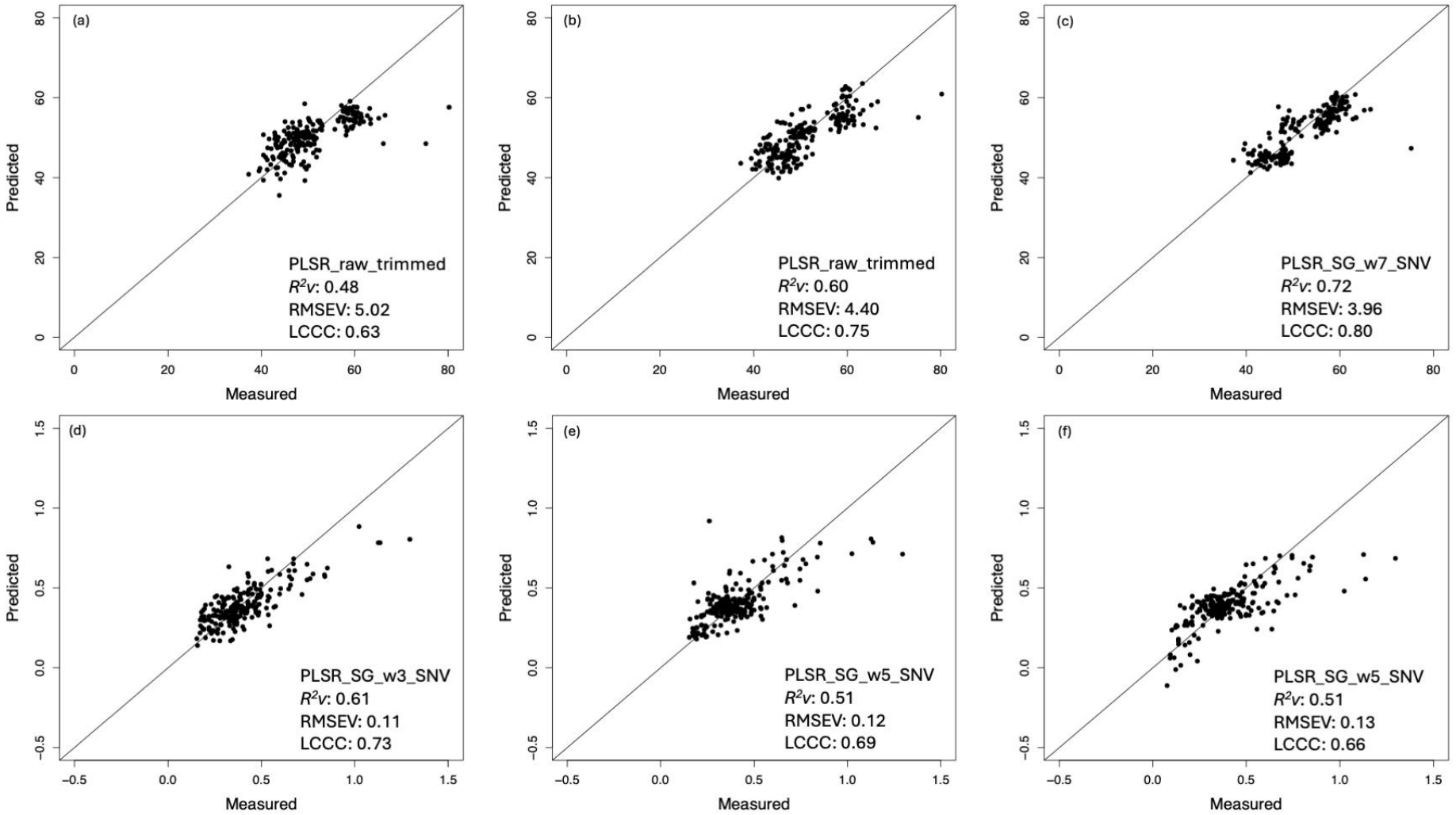

Figure 2.4: Validation results for predictions of total carbon (TC) and total nitrogen (TN) in *Eucalyptus* litterfall using vis-NIR, NIR, and ATR-FTIR spectra. Scatterplots show laboratory measured values against the predicted values for the validation dataset. The top row show shows the best-performing models for prediction of TC content using (a) vis-NIR; (b) NIR; and (c) ATR-FTIR spectra. The bottom row shows the best performing models for prediction of TN content using (d) vis-NIR; (e) NIR; and (f) ATR-FTIR spectra. In each panel, the solid line represents the 1:1 line. PLSR = partial least square regression; SG = Savitzky-Golay smoothing; *w* = window size; SNV = standard normal variate transformation; R^2v = coefficient of determination of validation model; RMSEV = root mean square error of validation model; LCCC = Lin's Concordance Correlation Coefficient.

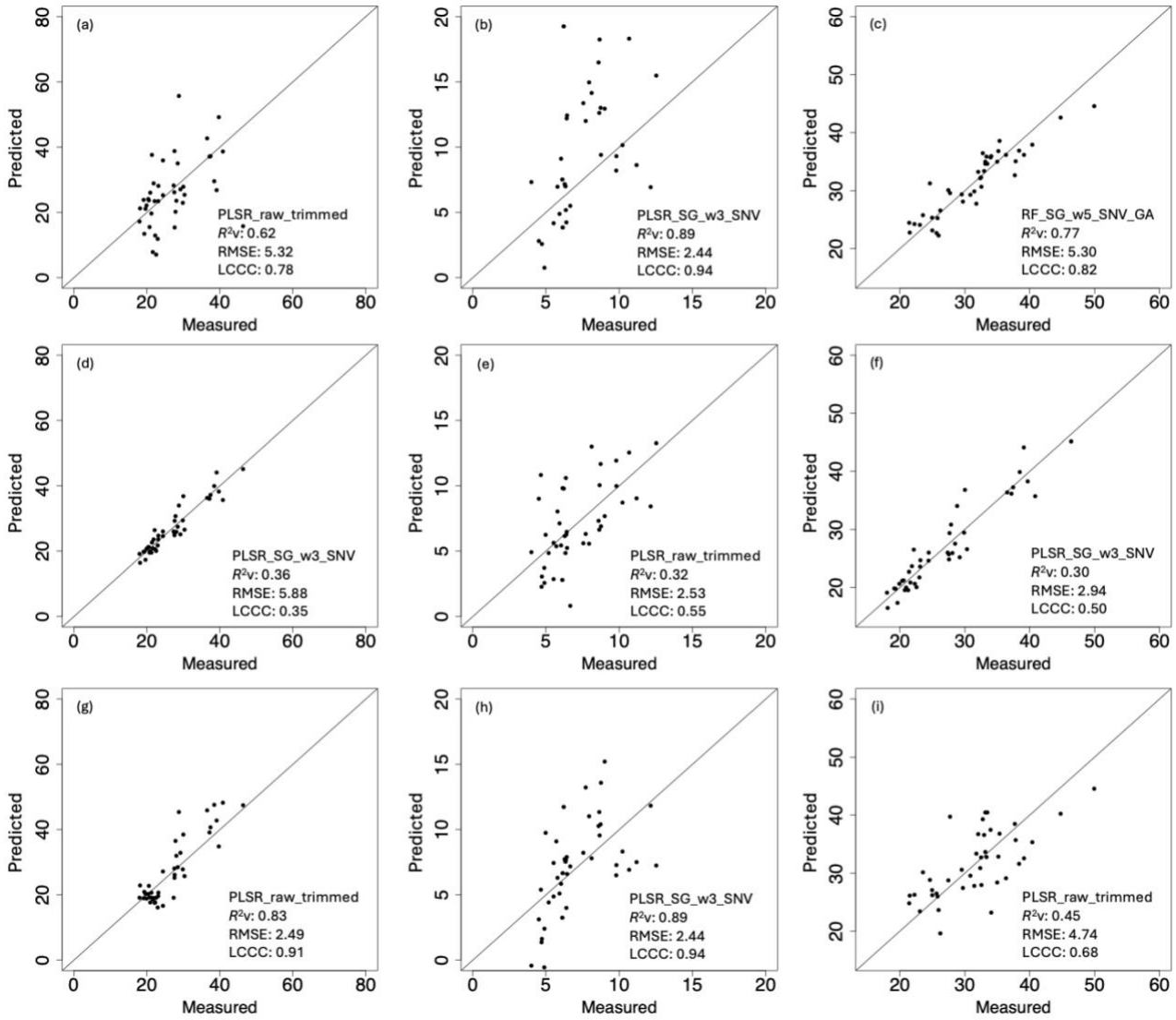

Figure 2.5: Validation results for predictions of cellulose, hemicellulose, and lignin content in *Eucalyptus* litterfall samples using vis-NIR, NIR, and ATR-FTIR spectra. Scatterplots show laboratory measured values against the predicted values for the validation set. The top row shows the best-performing model for prediction of cellulose content using (a) vis-NIR; (b) NIR; and (c) ATR-FTIR spectra. The middle row shows the best-performing models for prediction of hemicellulose content were (d) vis-NIR; (e) NIR; and (f) ATR-FTIR spectra. The bottom row shows the best-performing models for prediction of lignin content were (g) vis-NIR; (h) NIR; and (i) ATR-FTIR spectra (bottom row). In each panel, the solid line represents the 1:1 line. PLSR = partial least square regression; SG = Savitzky-Golay smoothing; *w* = window size; SNV = standard normal variate transformation; R^2v = coefficient of determination of validation model; RMSEV = root mean squared error of validation model; LCCC = Lin's Concordance Correlation Coefficient.

The use of vis-NIR and NIR spectroscopy for predicting TC in *Eucalyptus* litterfall was unsatisfactory (Table 2.3). Although the PLSR models developed using raw and trimmed vis-NIR and NIR spectra performed better than those built from pre-processed spectra, their overall performance was poor (see Table B1 in Appendix B), with substantially low R^2cv and high RMSECV. In contrast,

the PLSR model based on ATR-FTIR spectra achieved a moderate performance in both calibration and validation datasets (Table 2.3; Figure. 2.3c).

In comparison, prediction of TN was more reliable than TC, with substantially higher R^2 and lower RMSE and higher LCCC from both calibration and validation dataset (Table 2.3). The best performing model was achieved with pre-processed vis-NIR spectra, which produced a R^2v of 0.61, considered to reflect a moderate level of accuracy. Comparable performance was found for PLSR models trained on pre-processed (SG_*w*5_SNV) NIR and ATR-FTIR spectra (R^2v of 0.51), while the ATR-FTIR model had a marginally higher RMSEV and lower LCCC. Both NIR and ATR-FTIR models tended to underestimate TN content at higher concentration (greater than 0.8%), specifically, the ATR-FTIR model produced negative predictions at low concentrations. Despite showing moderate prediction accuracy, the RMSEV of all models was relatively high given the low TN content in the validation dataset (0.08-1.30%, Table 3.2).

Among all litter chemical qualities tested, the best predictions were achieved for cellulose and lignin using a PLSR model built from pre-processed NIR spectra (SG_*w*3_SNV). Both models had a R^2v of 0.89, a RMSEV of 2.44 and a LCCCv of 0.94 (Table 3.2), and the scatterplot showed strong agreement between predicted and measured values (Figure 2.4b, h). In contrast, the PLSR model using raw and trimmed vis-NIR spectra showed lower accuracy, and the scatterplot (Figure 2.3b) showed a tendency for overprediction of cellulose content. Interestingly, the vis-NIR model which performed poorly for cellulose, yielded a good prediction for lignin content (R^2v of 0.83), with strong agreement along the 1:1 line (Figure 2.3g). The performance of the RF model trained on ATR-FTIR spectra with GA selected wavelength outperformed PLSR models based on full ATR-FTIR spectral and achieved a moderate prediction in cellulose content ($0.61 < R^2 < 0.81$) (Table 2.3).

Prediction accuracy for hemicellulose was the lowest among all litter chemical qualities tested. Despite showing promising calibration results (R^2cv of 0.7, 0.99, and 0.97 for vis-NIR, NIR, and ATR-FTIR models, respectively), validation performance was poor across all spectral regions, with R^2v ranging from 0.3 to 0.36 (Table 2.3).

2.4 Discussion

2.4.1 Chemical quality of litterfall according to location

The first question posted for this chapter was to determine if litterfall samples from the same forest type (i.e., dry sclerophyll forest) but in different geographic locations (i.e., inland and coastal) vary in chemical quality. Although the effects of regional and large-scale spatial variations in litterfall

pattern are well documented (e.g., O'Connell, 1987), variability within and between forests of the same region or same forest type is often overlooked when estimating annual litterfall and its subsequent decomposition and accumulation rate. This implies a significant limitation in forest and fire management with the assumption of constant or steady litterfall rate in most Australian forests. This may result in significant over- or underestimation of the amount of accumulated litter.

In this study, leaf and bark litterfall were collected as part of a litterfall study that investigated the rate of rate and pattern of *Eucalyptus* litterfall in two DSFs in contrasting location. Contrary to the general assumption of stronger seasonal control, spatial heterogeneity was found to have a crucial role in *Eucalyptus* litterfall dynamics. Litterfall in the coastal forest (Orbost SF) was highly variable and was not directly correlated with rainfall or temperature but strongly influenced by extreme weather events such as wind and storms (Hung et al., 2021; unpublished data). In contrast, litterfall in the Wombat SF was strongly seasonal and followed expected patterns. These differences in litterfall dynamics suggested potential differences in chemical quality. Specifically, higher nitrogen content was expected in litterfall from Orbost SF, as wind-induced abscission may prevent nutrient resorption (i.e., translocation) prior to litterfall, which is a common mechanism in *Eucalyptus* species (Crous et al., 2019). However, the results did not support this expectation. Instead, litterfall from Orbost SF had higher C/N ratio and higher lignocellulosic compounds concentration compared to Wombat SF litterfall. In contrast, Wombat SF litterfall showed higher TC and TN contents, with the exception of TC content in bark. The extremely high C/N ratio in Orbost SF bark is of particular interest, suggesting potential nutrient limitation in the study area. These findings are particularly important because litter chemical quality has strong controls on litter decomposition rate (e.g., Melillo et al., 1982; Salamanca et al., 1998; Talbot and Treseder, 2012), especially C/N ratio and lignin content. The high C/N ratio and lignin content in Orbost SF litterfall suggested that litterfall from Orbost SF may decompose faster than those from Wombat SF. These variations in nutrient content may be attributed to differences in soil properties, plant species composition, stand age, and climatic condition. However, the corresponding data were not collected and analysed as these variables were beyond the scope of the present study, which limits the ability to examine their influence on litterfall chemical quality.

More importantly, this study demonstrates that despite differences in litterfall dynamics, the chemical quality of litterfall from DSFs across a large spatial scale were broadly similar. Although this was not the expected outcome, this suggests that a calibration model developed using litterfall from these forests could be representative for *Eucalyptus* litterfall from other forests. Specifically, future studies could explore the robustness and applicability of the calibration models developed here in a broader application, for example, on surface fine fuel litter.

2.4.2 Suitability of spectral regions for determining chemical quality of litterfall

Direct determination of litter chemical quality by laboratory analysis is often expensive and time-consuming. This study demonstrates the feasibility of using spectroscopic techniques to quantify the chemical quality of plant materials to provide insights into the chemical quality of *Eucalyptus* litterfall. This study has shown that vis-NIR, NIR, and ATR-FTIR spectroscopy can offer an accurate and repeatable measurement of the chemical quality of litterfall samples. These results highlight the potential for the broader application of spectroscopy in ecological research, including studies on litter decomposition and nutrient cycling.

Spectroscopy has been widely used for the rapid determination of the chemical quality of plant litter (e.g., McLellan et al., 1991b; Joffre et al., 1992; Gillon et al., 1993; Gillon et al., 1999; Ono et al., 2003; Poke et al., 2005; Lammer et al., 2009; Ferreira et al., 2018; Oliveira et al., 2019; Steinwandter et al., 2019; Zou et al., 2024), but this is the first study to compare and evaluate the model performance of the three most commonly used spectral regions – vis-NIR, NIR, and MIR using the ATR-FTIR to characterise the chemical quality of *Eucalyptus* litterfall. Given the limited number of studies focused specifically on *Eucalyptus* and its related species, the findings of this study are discussed in the context of plant litter spectroscopy across a wide range of litter components (e.g., leaf, bark, and wood), plant species, and ecosystems.

Overall, the models developed in this study achieved moderate to strong performance for the chemical qualities of interest. The predictive performance of each spectral region varied depending on the litter chemical quality assessed. Near-infrared (NIR) spectroscopy showed strong prediction for compounds including cellulose and lignin, however, the prediction accuracy for hemicellulose was consistently poor across all spectral regions used. Visible-NIR spectroscopy has provided moderate success in predicting hemicellulose content in broadleaf angiosperms and needleleaf conifers (Kothari et al., 2024) and with more reliability for wood samples (Chen et al., 2010; Zhou et al., 2015).

Hemicellulose

Although vis-NIR had the highest R^2cv value among the three spectral regions, it showed the highest RMSECV and RMSEV. This disagreement between the R^2 and RMSE values suggested that vis-NIR spectroscopy is not reliable in hemicellulose prediction. The relatively low prediction accuracy of hemicellulose in the ATR-FTIR region is not surprising because the spectra of cellulose and hemicellulose are very similar, making it difficult to distinguish using ATR-FTIR spectroscopy (Kostryukov et al., 2023). Consequently, an indirect correlation is recommended for hemicellulose

prediction using ATR-FTIR spectroscopy, which adds further complexity to model development. The poor performance of the hemicellulose models in this study is likely due to the relatively low variation within the validation dataset (ranging from 4.0-12.5%), which contrasts with the much broader range observed in the calibration dataset (0-100%). Although the validation dataset is fully encompassed within the calibration set, this large discrepancy in ranges may lead to overestimation of hemicellulose, potentially leading to the relatively high RMSE values due to the limited number of data points representing lower hemicellulose contents of litterfall samples.

Cellulose and lignin

This study showed that NIR spectroscopy is effective for estimating the cellulose and lignin content in *Eucalyptus* litterfall. Although a narrow NIR spectral range (500.5-1,000 nm) was used, the accuracy of the NIR model for cellulose and lignin content was within the range used in other studies which employed the full NIR spectra (1,100-2,500 nm). For example, similar prediction accuracy for cellulose was obtained for decomposing forest litter (R^2v = 0.87; McLellan et al., 1991b; Table 2.4) and wood samples of *Eucalyptus globulus* (Raymond and Schimleck, 2002; R^2v between 0.78 and 0.94; Table 2.4). The lignin model presented in this study is comparable with that of Ono et al. (2003), who reported a R^2v of 0.87 for fresh, litterfall, and decomposing material using full vis-NIR spectra (400-2,500 nm; Table 2.4). The accuracy of the model for lignin was lower than that reported by Ferreira et al. (2018) for decomposing litter of *Eucalyptus* (R^2v = 0.93 for Klason lignin and 0.97 for acid soluble lignin; Table 2.4), by Parsons et al. (2011) for Australian tropical rainforest species (R^2v = 0.96 and 0.94 for litterfall and decomposing litter, respectively; and 0.90 for a combined model; Table 2.4), by Poke et al. (2005) for *Eucalyptus globulus* wood samples (R^2v = 0.83 for acid-soluble lignin, 0.97 for Klason lignin; Table 2.4), by Joffre et al. (1992) for leaf litter from various plant species (R^2v = 0.96; Table 2.4), and by Vávřová et al. (2008) for leaf and branch litter (R^2v = 0.98; Table 2.4).

The high R^2v, low RMSEV, and high LCCC values achieved in this study (see Table 2.3) suggest that a calibration model built on a restricted wavelength range (1,000.5-1,650 nm) with commercially available plant powder is robust enough for predicting cellulose and lignin content in *Eucalyptus* litterfall. McLellan et al. (1991b) and Ono et al. (2003) both identified four major wavelengths for lignin calibration using stepwise multiple linear regression (i.e., 1,438, 2,154, 1,708, 2,320 nm; and 1,960, 2,320, 1,352, 1,716 nm, respectively). Due to the restricted NIR spectral range used, only two of these wavelengths were included – 1,352 and 1,438 nm – yet the NIR model still achieved excellent prediction accuracy for lignin content. This suggests that other important lignin-

related wavelengths may exist in the region of 1,000.5-1,650 nm, but further investigation is needed to confirm this hypothesis. In addition, future studies should explore how different analytical methods for measuring lignin influences overall model performance and predictivity to identify the most suitable method for lignin quantification in plant materials for use in spectroscopic modelling.

In contrast to the NIR model, the ATR-FTIR model did not perform well, particularly for predicting lignin content. The low accuracy of the ATR-FTIR models was unexpected, since the spectral range used covered the major absorption bands in the FTIR region between 6,261 and 7,042 nm (1,597 to 1,420 cm^{-1}; Popescu et al., 2011, Chen et al., 2013). Surprisingly, the best performing ATR-FTIR model for predicting lignin was based on non-pre-processed spectra (but still with low R^2v and high RMSEV). High RMSE values suggested potential overfitting of the calibration model, which likely contributed to poor model performance. Javier-Astete et al. (2021) achieved good prediction of lignin in wood samples using ATR-FTIR spectra pre-processed with 1st derivate and 2nd derivate transformations. The best result for lignin prediction using an ATR-FTIR model (R^2v > 0.95) was reported by Zhou et al. (2015) for wood samples from various hardwood species, including *Eucalyptus* (Table 2.4). For this, the 1st derivate transformation was combined with MSC and SNV with PLSR for development of the calibration model (Zhou et al., 2015). Thus, the pre-processing combinations used in this study might not be suitable for predicting lignin using ATR-FTIR spectroscopy and, before abandoning it as a useful method, other pre-processing techniques such as derivatives should be used to investigate improved model predictivity. It should also be kept in mind that the studies by Javier-Astete et al. (2021) and Zhou et al. (2015) focused on wood samples which may have different absorption bands compared to leaf and bark litterfall. Extending the current study to compare the performance of using ATR-FTIR for quantifying lignin concentration in wood samples (e.g., the twig component of litterfall) could provide useful insight into the use of ATR-FTIR spectroscopy for sample analysis.

Table 2.4: Summary of the studies that employed spectroscopy to analyse the chemical quality of plant materials. Only plant materials that were comparable to *Eucalyptus* were selected. Sample size includes both calibration and validate dataset. R^2v = coefficient of determination of validation model. For lignin content, acid soluble lignin (ASL) was measured using UV/VIS spectrometer, while Klason insoluble lignin was measured using 72% sulphuric acid (Klason method).

Carbon content

Sample type	Sample size	R^2v	Spectral range	Laboratory analysis	Source
Decomposing deciduous and conifers litter	51	0.95-0.98	1,100-2,500 nm	CHN analyser	Joffre et al., (1992)
Pine needles	87-525	0.86-0.99	400-2,500 nm	CHN analyser	Gillon et al. (1999)
Leaf and branch of various species	25&78	0.41 & 0.91	350-2,500 nm	CHN analyser	Vávřová et al. (2008)
Australian rainforest species	865 & 2,860	0.88-0.94	780-2,780 nm	CHN analyser	Parson et al. (2011)
Decomposing *Eucalyptus* litter	308	0.94	1,100-2,500 nm	Oxidation with $K_2Cr_2O_7$ in concentrated H_2SO_4	Ferreira et al. (2018)
Deciduous and conifers litter	322	0.76-0.89	350-2,500 nm	CHN analyser	Kothari et al. (2024)
Birch leaf litter	267	0.84	400-2,500 nm	CHN analyser	Zhang et al. (2024)

Nitrogen content

Sample type	Sample size	R^2v	Spectral range	Laboratory analysis	Source
Decomposing deciduous and conifers litter	51	0.95-0.98	1,100-2,500 nm	CHN analyser	Joffre et al., (1992)
Leaf and branch of various species	25 & 76	0.83 & 0.88	350-2,500 nm	CHN analyser	Vávřová et al. (2008)

Table 2.4 continued.

Nitrogen content

Sample type	Sample size	R^2v	Spectral range	Laboratory analysis	Source
Australian rainforest species	865 & 2,860	0.95-0.98	780-2,780 nm	CHN analyser	Parson et al. (2011)
Loblolly leaf litter	144	0.81	350-2,500 nm	CHN analyser	Stein et al. (2014)
Deciduous and conifers litter	322	0.91-0.95	350-2,500 nm	CHN analyser	Kothari et al. (2024)

Cellulose content

Sample type	Sample size	R^2v	Spectral range	Laboratory analysis	Source
Deciduous and conifers	169	0.90	1,100-2,500 nm	UV/VIS spectrometer and Klason method	McLellan et al. (1991b)
Eucalyptus wood	40	0.78-0.94	1,100-2,500 nm	Diglyme method of Wallis et al. (1997)	Raymond and Schimleck (2002)
Hard- and softwood	12	0.99	4,000-400 cm^{-1}	Van Soest analysis	Chen et al. (2010)
Decomposing *Eucalyptus* litter	308	0.99-1.00	1,100-2,500 nm	Kjeldahl distillation	Ferreira et al. (2018)
Capirona and Bolania woods	100 & 150	0.74 & 0.97	4,000-400 cm^{-1}	Van Soest analysis	Javier-Astete et al. (2021)

Table 2.4 continued.

Lignin content

Sample type	Sample size	R^2v	Spectral range	Laboratory analysis	Source
Deciduous and conifers	169	0.91	1,100-2,500 nm	UV/VIS spectrometer and Klason method	McLellan et al. (1991b)
Decomposing beech and oak litter	92	0.92-0.98	1,100-2,500 nm	Sulphate-hydrolysis	Ono et al. (2003)
Eucalyptus globulus wood	61	0.83-0.99	1,100-2,500 nm	UV/VIS spectrometer and Klason method	Poke et al. (2005)
Leaf and branch of various species	25 & 56	0.54 & 0.85	350-2,500 nm	Klason method	Vávřová et al. (2008)
Hard- and softwood	12	0.98	4,000-400 cm^{-1}	Van Soest analysis	Chen et al. (2010)
Australian rainforest species	865 & 2,860	0.90-0.96	780-2,780 nm	Fiber analyser	Parson et al. (2011)
Hardwood species	37	> 0.95	10,000-4,000 cm^{-1}	Klason method	Zhou et al. (2015)
Decomposing *Eucalyptus* litter	308	0.93-0.99	1,100-2,500 nm	UV/VIS spectrometer and Klason method	Ferreira et al. (2018)
Capirona and Bolania woods	100 & 150	0.74 & 0.97	4,000-400 cm^{-1}	Van Soest analysis	Javier-Astete et al. (2021)

For models built using GA selected wavelengths, only the prediction of cellulose content showed improved accuracy with ATR-FTIR spectra when coupled with the RF modelling technique. Despite the excellent R^2cv value (0.96), the relatively high RMSECV (5.30), the model may have been overfitted considering the small variation in cellulose content within the dataset. This contrasts with findings from Javier-Astete et al. (2021), who reported strong prediction of cellulose in wood samples using predictive modelling based on ATR-FTIR with PLSR (R^2v of 0.74 and 0.97, respectively; Table 2.4). As for lignin content, the poor prediction performance of any cellulose model may be attributed to the range of pre-processing techniques used. The use of GA feature selection to optimise the wavelength range used may have improved model performance, however more in-depth comparison is required before a unanimous conclusion can be drawn.

The novel use of commercially available powders as surrogates for lignocellulosic compounds used in conjunction with spectroscopic techniques to predict the chemical quality of plant material has proven to be exceptionally useful for predictive modelling efforts. Extending the use of commercially available powder as reference materials for other forms of plant material (e.g., decomposing or burnt litter) and other plant species such as *Acacia* and pine is warranted.

2.4.3 Predictive potential for total carbon and nitrogen

Carbon

The performance of spectroscopic models for predicting TC were not as good as anticipated. In particular, the vis-NIR and NIR models had extremely low values for R^2cv and the moderate R^2v (see Table 2.3). The weak correlation between the calibration and validation models suggests that vis-NIR and NIR spectroscopy are not useful for predicting TC content in *Eucalyptus* litterfall. Poor performance of vis-NIR and NIR models was also reported by Richardson and Reeves III (2005) for TC in conifer foliage with R^2 values of 0.37 and 0.26 for vis-NIR and NIR models, respectively. In contrast with other ecological studies, vis-NIR and NIR spectroscopy has successfully predicted C content for various plant species and plant parts with high accuracy. For example, excellent performance has been found for models for predicting C in pine needles from recently burnt ecosystem (R^2v = 0.99; Gillon et al., 1999; Table 2.4), leaf and branch litter from various plant species (R^2v = 0.95 and 0.88, respectively; Vávřová et al., 2008; Table 2.4), and intact and ground leaf litter of different species (R^2v = 0.76 and 0.69, respectively; Kothari et al. 2024; Table 2.4).

In contrast to vis-NIR and NIR spectroscopy, TC content in *Eucalyptus* litterfall was predicted with good accuracy using ATR-FTIR spectroscopy (see Table 2.3). Although the model performance was lower than values reported for dried conifer leaf litter (R^2v = 0.92; Richardson and Reeves III,

2015) and for birch leaf litter (R^2v = 0.84; Zhang et al., 2024; Table 2.4), the results presented here demonstrate good prediction performance. While ATR-FTIR spectroscopy has been shown to be a powerful tool for TC prediction in plant material, its application in ecological processes remains limited, with only a few studies having explored its use in biological decomposition (Steinwander et al., 2019) and thermal decomposition (Lammer et al., 2009). A rich area for future investigations lies in application of ATR-FTIR spectroscopy in decomposition studies.

Nitrogen

While many studies have documented the potential of vis-NIR, NIR, and ATR-FTIR spectroscopy in prediction of TN, the models developed using *Eucalyptus* litterfall performed poorly compared to previous research. For example, good prediction was found for TC in leaf and branch litter (R^2v = 0.88; Vávřová et al., 2008; Table 2.4) and loblolly pine needles (R^2v = 0.81; Stein et al., 2014; Table 2.4) using the full vis-NIR spectrum. Excellent accuracy in N prediction was found for intact leaves and ground litter (R^2v = 0.92 and 0.95, respectively; Kothari et al., 2024; Table 2.4), deciduous and coniferous litter (R^2v = 0.97; McLellan et al., 1991b), pine litter (R^2v = 0.98; Gillon et al., 1999; Table 2.4), and litter from various species (R^2v = 0.99; Joffre et al., 1992; Table 2.4), also using the full vis-NIR spectrum. Despite using a relatively narrow range of vis-NIR spectra (400-900 nm), Oliveira et al. (2019) reported an excellent result for prediction of TN in leaf litter from *Eucalyptus urophylla* (R^2v = 0.96; Table 2.4). These studies suggest that prediction accuracy does not necessarily improve when the full spectrum is used.

2.4.4 Spectral pre-processing and multivariate statistical analysis

For several of the litter chemical quality parameters assessed in this study, calibration models developed on spectra with no pre-processing yielded more accurate predictions than models constructed with transformed spectra. For example, the use of raw vis-NIR spectra achieved considerably accuracy in the prediction of cellulose and lignin in *Eucalyptus* litterfall. This means that spectral pre-processing does not always lead to an improve in the predictivity of a calibration model. This is not a common result since the majority of literature regarding soil and plant spectroscopy indicate that pre-processing is necessary to remove noise, and baseline and light scattering (e.g., Foley et al., 1998; Chodak, 2008; Rinnan et al., 2009; Zhang et al., 2024). For example, the study conducted by Zhang et al. (2024) showed that models built on pre-processing ATR-FTIR spectra performed better than that of raw spectra. One possible reason could be the pre-

processing techniques used at this stage of the overall study may have removed important spectral features critical for the prediction of litter chemical properties.

Savitzky-Golay (SG) smoothing and standard normal variate (SNV) are the most commonly used pre-processing techniques in plant spectroscopy (e.g., Vávřová et al., 2008; Pearsons et al., 2011; Ishizuka et al., 2014). Both methods were used prior to calibration model development to minimise baseline scattering and enhance spectral signals in some instances although there was no universal spectral transformation suitable for all litter chemical quality parameters assessed. The selection and effectiveness of spectral pre-processing depends largely on the chemical properties of interest. Furthermore, it was shown that a large window size does not necessarily improve or degrade the model performance with the maximum window used in this study being 7. As indicated earlier, many studied have achieved good prediction strength using 1st and 2nd derivatives (e.g., Gillon et al., 1993; Zhou et al., 2015; Javier-Astete et al., 2021) but this method was not applied in this study to minimise the risk of overfitting and noise enhancement, especially when working with such a small calibration dataset (Huang et al., 2010; Krasznai et al., 2012). Additionally, the use of derivatives often requires fine-tuning of moving window size and polynomial order which can lead to excessive manipulation of spectral data (Rinnan et al., 2009).

The use of wavelength selection as part of the spectral pre-processing technique to remove redundant wavelength prior to calibration model development has increased recently. The most common spectral variable selection methods are competitive adaptive reweighted sampling (CARS), successive projections algorithm (SPA), and genetic algorithm (GA; Ferreira et al., 2008; Xiaobo et al., 2010; Fan et al., 2021; Ai et al., 2022; Zhang et al., 2024). In this study, GA feature wavelength selection was used to identify a subset of the most informative wavelengths for calibration model development. Ferreira et al. (2018) demonstrated the effectiveness of GA-selected wavelength in predicting the chemical quality of *Eucalyptus* harvest residues during decomposition. However, GA feature wavelength selection did not improve model prediction accuracy for *Eucalyptus* litterfall in this study. An exception was the prediction of cellulose content using ATR-FTIR spectra, where the GA-based random forest model performed slightly better than the full-spectrum model. However, the improvement was marginal, with only minor improvement in R^2v and RMSEV. This was somewhat unexpected considering the successful application of GA feature selection for other *Eucalyptus* materials. Further investigation is warranted to assess the method using other plant materials and biological or ecological applications.

With the development in spectroscopy and machine learning, Cubist and random forest (RF) have been widely used to predict soil properties such as carbon and nitrogen content (e.g., Dangal et al., 2019; Ramírez et al., 2023; Wadoux et al., 2023; Zhang et al., 2023; Canero et al., 2024; Jeon et

al., 2024). Despite successful applications of Cubist and RF modelling for in prediction of soil properties, PLSR remains the mainstream modelling technique in plant spectroscopy. In support of this, PLSR outperformed bootstrap PLSR, Cubist, and RF in estimating the chemical quality of *Eucalyptus* litterfall, except for cellulose content. The dataset used was relatively small, especially the calibration dataset, which can limit the performance of 'tree-based' models that rely on large sample size to build decision trees (Ng et al., 2019). In contrast, PLSR is a simple linear regression technique which provides a more accurate and robust fit with smaller datasets and is less prone to overfitting (Martins et al., 2024).

2.4.5 Limitation of calibration dataset and pre-processing techniques

Most of the existing literature in this area have focused on a single spectral region, or at most two – which usually capture both vis- and NIR spectra as a continuous spectrum using a single spectrometer (also referred to as vis-NIR spectrometer). In contrast, NIR and MIR are generally acquired using separate, specialised instrument due to differences in the radiation sources and detectors required (Freitage et al. 2022). In most cases, vis-NIR spectrometer cover a full range from 350-2,500 nm, while ATR-FTIR spectrometers spans from 2,500 to 25,000 nm (4,000-400 cm^{-1}). However, the actual spectral coverage depends largely on the specific spectrometer used. One of the limitations of this study is the relatively narrow spectral range used, compared to the full range that was employed in many previous studies (from 350-2,500 nm for vis-NIR and 1,100-2,500 nm for NIR; Joffre et al., 1992; Gillon et al., 1993; Kothari et al., 2024). Specifically, the vis-NIR and NIR spectrometers used in this study only covered the range from 500.5-1,100 nm and 1,000.5-1,650 nm, respectively, in particularly, the NIR spectral region is relatively narrow when compared to other studies. In order to improve model performance and reduce spectral noise, trimming was applied to remove the low SNRs regions at the two ends of the spectrum, which further reduces the total number of wavelengths used for calibration model development (999 wavelengths for vis-NIR and 371 for NIR spectrum). Despite these constraints in spectral range, models developed in this study illustrated good to strong promise of predicting litter properties of interest, particularly cellulose (calculated by subtracting ADL from ADF) and lignin (expressed as ADL). This suggested despite the wavelength of the vis-NIR and NIR spectrometers used here is limited, they remain useful for determining certain chemical properties of interest.

Prior to calibration model development, it is common practice to select a subset of representative samples and apply statistical techniques such as Mahalanobis distance (*H*) to detect outliers (e.g., Gillon et al., 1999; Chodak, 2008; Pearsons et al., 2011). However, in this study, a

simplex-lattice design was employed to formulate all possible combinations of commercially available powder to represent the varying lignocellulosic concentration in plant material. This approach resulted in 21 mixture blends (ranging from 0-100%) to represent the cellulose, hemicellulose, and lignin concentration in *Eucalyptus* litterfall for calibration model development. The aim of this approach is to use synthetic mixture as an economic alternative to cover a wide chemical composition range in unknown samples to increase the reproducibility and generalisation of the calibration model. As a result, Mahalanobis distance or other statistical techniques were not applied to select representative samples for calibration model establishment, since the 21 mixture blends were designed to cover the range from 0 to 100%.

Unfortunately, due to time and budget constraints, it was not possible to include litterfall samples with a broader range of chemical composition in the calibration model, which limited the development of a more robust model. Consequently, the performance of the model presented here may be restricted by the relatively small calibration dataset size, particularly for lignocellulosic compounds, where only 42 samples were used. For soil carbon prediction, Lucà et al. (2017) recommended a minimum of 130 samples for reliable PLSR calibration. A study conducted by Ng et al. (2019) further demonstrated that the size of the calibration dataset has significant influence on the performance of the prediction accuracy of vis-NIR spectroscopy in predicting soil properties, including sand, silt, and clay content. This study suggested that the performance of PLSR and Cubist model for soil prediction reach a plateau when the calibration model consist of 4,000 and 5,000 samples, respectively. This number is substantially higher than the sample size used in the present study. It can be presumed that increasing the number of samples in the calibration dataset is expected to improve the robustness of the model. However, this is not always the case as the model performance also depends greatly on the sample representativeness, the order and combination of the pre-processing techniques employed (Ng et al., 2019) Since there are no standardised protocol or one-size fits all approach, the selection of the pre-processing techniques for spectroscopic modelling remains highly dataset dependent, and to some extent, subjective. Therefore, when comparing the results presented here with previous studies, it is necessary to account for the concurrent effects of the calibration sample size and the different pre-processing techniques employed across studies.

In addition, the use of commercially available chemical mixture with significantly low nitrogen content or the relatively low hemicellulose level to present the chemical composition of real plant materials may contribute to model overfitting or reduce the overall reproducibility when applying to a new dataset, especially when the value is beyond the range covered in the calibration model (Kothari et al., 2024). We also acknowledge that different studies may have employed various laboratory analysis techniques in the determination of chemical composition. For example, for lignin

determination, some studies have used the Van Soest methods (Ai et al., 2022), some have employed the Klason methods (e.g., Ono et al., 2003; Ishizuka et al., 2012), while other have considered the acid soluble lignin. The same situation also happened to nitrogen quantification where nitrogen was determined with an CHN elemental analysis (e.g., Joffre et al., 1992; Gillon et al., 1993; Parson et al., 2011) or Kjeldahl method (Oliveira et al., 2019). These differences in analytical procedure may result in significant discrepancies in the lignin content, potentially contributing to the variability across studies. As such, extra cautions were practiced when extrapolating existing knowledge directly to the context of *Eucalyptus* litterfall materials, as well as when interpreting the performance of the predictive models constructed in this study.

To obtain a more accurate prediction of chemical quality in plant materials, future studies could include samples from a wide range of plant species, litter components, as well as litter at different stages, such as intact leaves, fresh litterfall, decomposing litter, and mixtures with other plant species. However, applying spectroscopy in a wider ecological setting maybe challenging due to the increase of complexity and variability in chemical composition.

Chapter 3

The role of chemical quality and litter components in decomposition

3.1 Introduction

Litter decomposition that occurs on the soil surface represents a major pathway of nutrient cycling from plant to soil (e.g., Attiwill, 1968; O'Connell et al., 1978; Bulter et al., 2020) and has profound effects on the accumulation of available fine fuel (plant debris < 6 mm in diameter; also known as surface fine fuel; see Section 1.1.7) for combustion (e.g., McCaw et al., 2012). The importance of surface fine fuel in fire behaviour and the rate of fire spread are a function of its depth, continuity, and moisture content (e.g., Gould et al., 2011). In the absence of fire, the rate and extent of litter decomposition are primarily controlled by climate, vegetation type, and as the microbial community, and are highly geographically and seasonally variable (e.g., Meentemeyer, 1978; Aerts, 1997; Cornwell et al., 2008; Zhang et al., 2008; Wu et al., 2025).

Prescribed burning as a disturbance adds further complexity to litter decomposition processes in dry sclerophyll forests (Fox et al., 1979; Woods and Raison, 1983; O'Connell, 1988; Birk and Bridges, 1989; Gunito et al., 2011; Muqaddas et al., 2015; Butler et al., 2017a; Butler et al., 2017b; Ficken and Wright, 2017; Butler et al., 2020; Liechty and Reinke, 2020; see Chapter 1). Changes in litter dynamics are mainly through direct and indirect alteration of vegetation composition, soil properties, and microbial activities, and may vary with fire regimes, forest types, locations, fire history, and environmental conditions (O'Connell, 1987a; Brennan et al., 2009; Guinto et al., 2011; Lewis et al., 2012; Toberman et al., 2014; Ficken and Wright, 2017; Butler et al., 2020; Liechty and Reinke, 2020).

Frequent fires in Australian forests often lead to a temporary shift in understorey vegetation structure and composition through the removal of woody shrubs, resulting in a flammable understorey layer dominated by *Acacia*, grasses, and ferns (Adams and Attiwill, 1984; Spencer and Baxter, 2006; Wanthongchai et al., 2008; Lewis and Debuse, 2012; Lewis

et al., 2012; Bassett et al., 2017; Gordon et al., 2017; Zylstra et al., 2023). As understorey vegetation regrows, it contributes litter and other plant materials to the surface and near-surface fuel layers. Understorey vegetation, which may be rich in nutrients, produces litter with low C/N ratios, contains recalcitrant compounds (i.e., lignin), and usually decompose more rapidly than litter from woody shrub in the mid-storey layer (Landuyt et al., 2019). A shift in vegetation type and litter quality can have profound effects on litter decomposition through the alteration of litterfall patterns and decomposition rate. In addition, the contribution of understorey litter may accelerate forest regeneration through the release of important nutrients such as N and P during decomposition (O'Connell, 1983; Xiang and Bauhus, 2007; Zhao et al., 2013). Despite extensive research on understanding the regeneration and composition of understorey vegetation after fire (e.g., Fox and Fox, 1986; Lewis et al., 2012; Reverchon et al., 2012; Lewis, 2020), little is known about the role of post-fire vegetation in contributing to nutrient pools. Since long-unburnt forests are becoming scarcer and regenerating forests are dominating across the landscape (von Takach et al., 2022), improved knowledge of post-fire understorey vegetation and their resulting litter quality will be crucial for understanding litter decomposition processes in Australian forests.

To date, the effects of climate and litter chemistry on decomposition of single-species leaf litter are well established. In recent decades, there has been a growing interest in understanding the interactions among leaf litter of different species during decomposition (Briones and Ineson, 1996; Cornelissen, 1996; Bauhus et al., 2000; Gartner and Cardon, 2004; Xiang and Bauhus, 2007; Cuchietti et al., 2014; Liu et al., 2020). These studies have shown that mixed species leaf litter often decompose at non-additive rates – either faster (synergistically) or slower (antagonistically) than decomposition of single-species litter. Synergistic effects are particularly common, with faster decomposition rates due to nutrient transfer from high quality litter to low quality litter (e.g., Xiang and Bauhus, 2007; Cuchietti et al., 2014; Liu et al., 2020). For example, a study conducted in a mixed plantation in Victoria, Australia found that the presence of *Acacia* spp. facilitated early-stage decomposition of leaf litter from *Eucalyptus* spp. and was recognised as a potential underlying mechanism for an increase in N availability (Xiang and Bauhus, 2007).

There is a critical knowledge gap as the measurement of leaf litter alone does not fully represent the dynamics of forest litter since leaf litter and woody material of different species (e.g., *Eucalyptus*, *Acacia*, and bracken fern) usually interact and decompose together. Hence, there is a need to understand the decomposition dynamics of surface fine fuel, particularly in

fire-prone ecosystems where fuel loads are tightly related to fire behaviour (Gould et al., 2011; Thomas et al., 2014; Cawson et al., 2017). More importantly, while most of the existing studies have focused on the decomposition of leaf litterfall (e.g., O'Connell, 1986; Xiang and Bauhus, 2007; Ferreira et al., 2021), the interactions between freshly fallen litter and partially decomposed litter on the forest floor remain largely unexplored. Since surface fine fuel layers are made up of litter of various ages (e.g., Burrows, 2001), this highlights a significant gap in the current understanding of decomposition processes.

As described in Chapter 2, visible (vis-), near- (NIR), and mid-infrared (MIR) spectroscopy is an inexpensive, rapid, and accurate technique that is widely used in agriculture and forestry to determine the chemical composition (functional groups) of samples (e.g., Gillon et al., 1993; Ferreira et al., 2018; Chapter 2). Unlike traditional laboratory analysis, this technique does not require extensive sample preparation and the use of chemicals. In addition, this fast and precise technique is particularly useful in litter decomposition experiments because of the rapidity, repeatability, and precision of measurements. Several studies have successfully employed vis-NIR and FTIR spectroscopy to predict the rate of leaf litter decomposition (Gillon et al., 1993; Gillon et al., 1999; Gillon and David, 2001; Parsons et al., 2011; McKee et al., 2016). These studies highlight the potential of spectroscopy for quantifying the chemical quality of litter and sets the scene for future forest decomposition research.

3.1.1 Objective and research questions

Empirical data describing the effects of prescribed burning on litter quality (i.e., total C and total N content) and the subsequent decomposition rate of surface fine fuel is scarce. Therefore, this study aims to quantify the chemical quality of *Eucalyptus* litter, understorey biomass, and surface fine fuel before and 1-year after a low-intensity prescribed burning. An *in-situ* litterbag decomposition trial was conducted over a period of 15 months to examine the putative effects of litter chemical quality, litter component, prescribed fire, and their combined effects on mixed species litter decomposition. Following on from analytical methods investigated in Chapter 2, this study also explores the application of spectroscopy for predicting the chemical quality of decomposing litter.

To understand the underlying factors of mixed species litter decomposition and the feasibility of using spectroscopy in quantify the changes of litter chemical quality during decomposition, the following research questions were formulated:

1. How does the initial chemical quality of litter collected prior to a prescribed burn differ from that collected 1-year after fire?
2. How does understorey vegetation affect the decomposition rate of *Eucalyptus* leaves? Can litter from understorey species (high quality litter) enhance the decomposition rate of *Eucalyptus* leaf litter (i.e., low quality litter)?
3. Can vis-NIR, NIR, and ATR-FTIR spectroscopy be used to measure the changes of chemical quality during mixed-species litter decomposition? Which spectral regions are the most suitable for detecting change?
4. How transferrable is the calibration model developed for spectroscopy in Chapter 2 using synthetic mixtures and litterfall? Can it be used to predict the chemical quality of decomposing litter

3.2 Materials and methods

3.2.1 Site characteristics

An *in-situ* litterbag decomposition trial was conducted at Lansdowne Farm of the University of Sydney, Cobbitty, NSW, Australia (34°02'S, 150°66'E). The farm area has previously been used for growing crops (e.g., barley, corns, and beans) for research and teaching purposes. There is no recorded fire history for the farm area. The topography of the study area is flat with an elevation of 64 m above sea level. The soil in Cobbitty is characterised as Cambisol with a loose and sandy texture according to the Australian Soil Classification (Keith et al., 2016).

Climate data

Weather data including long-term annual rainfall, mean maximum and minimum temperature, as well as the total monthly rainfall, mean maximum and minimum monthly temperature during the study period (September 2023 to November 2024) were obtained from the Australian Bureau of Meteorology from the Camden Airport weather station (weather station number: 068192; 34°04'S, 150°69'E), which is located 3.1 km away from Lansdowne Farm, Cobbitty. Local temperature and soil moisture data during the study period were monitored using a portable weather station (ATMOS 41; METER Group, Inc., Pullman, WA,

USA) that was installed in the middle of the study area at a height of 2 m. Soil moisture was recorded at 10 cm depth.

3.2.2 Litter material and litterbag preparation

The litterbag technique was used to measure the *in-situ* changes of litter mass and chemical quality over time (Bokhorst and Wardle, 2013; Krishna and Mohan, 2017). Litterbags (15 x 15 cm) were made of commercial use fiberglass fly screen (Model number: 529573; Cyclone Screening, Australia) with a mesh size of 0.53 mm to exclude soil meso- and macro-invertebrate fauna yet allow the entry of soil microbial organisms and small invertebrates (< 0.53 mm) to facilitate the process of decomposition (Bokhorst and Wardle, 2013).

Samples collected from a previous studies were used for an *in-situ* litter decomposition trial. Detailed descriptions of the study sites and the methods used for sample collection are provided in Jenkins et al. (2016). In brief, litter samples were collected from four study sites located west of Orbost State Forest, south-eastern Victoria, Australia, before (1-2 months prior) and 1-year after a prescribed burn applied during autumn in 2011 (Jenkins et al., 2016). The four study sites were: Frogs Hollow (FH), Pettmans (PETT), South Boundaries (SB), and Upper Tambo (UT). Prescribed burns at all sites were low-intensity with flame height < 2 m with similar fire weather conditions and fuel moisture content (Jenkins et al., 2016).

All study sites are broadly described as *Eucalyptus* low open dry sclerophyll forest (DSFs) with 30-70% foliage coverage (Jenkins et al., 2016). Vegetation composition and density varied across study sites. Generally, the overstorey was dominated by *Eucalyptus muelleriana (*Yellow Stringybark), *E. globoidea (*White Stringybark), and *E. consideniana* (Yertchuk). The understorey was comprised of *Acacia* spp., *Pteridium esculentum* (Bracken Fern), *Kunzea* spp., and grasses.

At each site, surface fuel litter (< 25 mm in diameter; without mineral soil) and elevated fuel (i.e., understorey vegetation) were collected using a 1 x 1 m quadrat 1-2 months before (hereafter referred to as prior to fire) and 1-year after a prescribed burn (hereafter 1-year after fire). Samples were dried in a fan-forced oven (60 ºC for a minimum of 48 h; Model TD-78T-2-D, Thermoline Scientific, Wetherill Park, NSW, Australia) and sorted into fractions (overstorey *Eucalyptus* leaves, elevated fuel, and surface fine fuel litter). Overstorey *Eucalyptus* leaves (EL; hereafter *Eucalyptus* leaf) collected from the forest floor were largely intact and did not pass through a 25 mm sieve. Elevated fuel (EF) consisted of living and dead plant biomass clipped at ground level and collected from within the litter ring. Surface fine fuel

litter (< 9 mm in diameter; FF; see Section 1.1.7 for definition) was a mix of fragmented leaves, bark, twigs, and fruits. Sorted samples were stored in labelled paper bags at ambient conditions in the laboratory until required.

A simplex-lattice design (see Section 2.2.2) was used to generate all possible single, two-, and three-component (*Eucalyptus* leaf, elevated fuel, and surface fine fuel) mixtures to investigate the decomposition rate and nutrient release from forest litter. This resulted in a total of 10 mixture combinations: three single-component (10 g) mixtures, six two-component (6.7 g and 3.3 g) mixtures, one three-components (3.33 g for each component) mixtures (Table 3.1) for two time-since-fire collections (i.e., prior to fire and 1-year after fire). Lucerne hay (10 g) was chosen as a reference material to assess whether the experimental setup was operating as intended. Three sides of each litter bag were sealed using an impulse heat sealer (Model number: VHIB400C; QIS Packaging, Queensland, Australia), filled with the required sample, and the fourth side sealed. Each litterbag was identified with a labelled aluminium tag. There were six replicates for most of the combinations, except for three prior to fire (PF) combinations (6, 7, 9), and six 1-year after fire (1YAF) combination (2, 3, 4, 6, 7, 9) due to insufficient amounts of elevated fuels available (Table 3.1). There were four replicates for these combinations. A total of 560 litterbags (2 time-since-fire collections x 11 combinations x 5 collection days x 6 (or 4) replicates) were prepared. Litterbags were laid flat and stored in a plastic storage box for transport to the study site. Due to the fine texture (small particle size), litterbags containing lucerne hay were reweighed in the field prior to installation to record the exact initial weight. Based on the size of litter fractions, this step was not required for other litter bags. An additional 40 litterbags filled with lucerne hay was prepared for a second installation on the third collection day (11 June 2024) due to their rapid mass loss. A total of 600 litterbags were prepared for the *in-situ* litterbag decomposition trial. As lucerne hay was used as a reference material, litterbags containing lucerne hay were not included in any further analysis, therefore, data on the lucerne hay are not presented (See Figure C1 in Appendix C).

3.2.3 Site preparation

An area of 12 x 78 m was established in a fenced area at the Lansdowne Farm on 11-12 September 2023. The area was cleared by manually removing weeds and other debris on the soil surface 1 week prior to the start of the *in-situ* litterbag decomposition trial. Soil samples to a depth of 10 cm were collected using a steel soil core (5.5 cm radius) at every 10 m within

the area (n = 3 for every 10 m), stored in zip lock bags, transported to the laboratory, and sieved to 1 mm. Weed matting was installed and anchored using pins and sandbags to minimise the growth of weeds. To ensure that litterbags maintain contact with the soil surface, weed mat was cut into a 45 x 45 cm opening at the position where the litterbags were placed (Figure 3.1a, b). Typical annual weeds at the site included *Raphanus raphanistrum* (Wild Radish), *Silybum marianum* (Milk Thistle), *Erigeron bonariensis* (Fleabane), and *Echinochloa* spp. (Barnyard Grass).

The *in-situ* litterbag decomposition trial was set up as a randomised block design with three blocks (A, B, and C) spaced 2 m apart from each other (Figure 3.1a). Each block contained 57 sampling points (45 x 45 cm) with a 60 cm interval, yielding a total of 171 plots. Four or six replicates of each litter combination was randomly assigned for a collection day (collection day = 5). Litterbags assigned to the same collection day were arranged in a group of four, randomly allocated to a sampling point (sampling point = 57), placed on the soil surface, and secured to the ground with wire and bamboo stakes on the four corners (Figure 3.1b). A total of 560 litterbags were placed in position on 15-16 September 2023. An additional 40 litterbags filled with lucerne hay were placed in position on 11 June 2024.

Table 3.1: *Eucalyptus* leaf (EL), elevated fuel (EF), and surface fine fuel (FF) collected prior to fire (PF) and 1-year after fire (1YAF) were used to prepare litterbag for *in-situ* litterbag decomposition trial. The 10 litter mixture combinations were generated using a simplex-lattice design (SLD). Lucerne hay was used as a reference material. Each litterbag was filled with the corresponding litter materials to a total of 10 g.

	Materials (g)				Number of replicates	
Combination	**EL**	**EF**	**FF**	**Lucerne**	**PF**	**1YAF**
EL100	10	0	0	0	6	4
EL67:EF33	6.7	3.3	0	0	6	4
EL33:EF67	3.3	6.7	0	0	6	4
EF100	0	10	0	0	6	4
EL67:FF33	6.7	0	3.3	0	6	6
EL33:EF33:FF33	3.3	3.3	3.3	0	4	4
EF67:FF33	0	6.7	3.3	0	4	4
EL33:FF67	3.3	0	6.7	0	6	6
EF33:FF67	0	3.3	6.7	0	4	4
FF100	0	0	10	0	6	6
Lucerne	0	0	0	10	6	6

Figure 3.1: Details of the set-up of the *in-situ* litterbag decomposition trial (a) an area of 12 x 78 m at Lansdowne Farm, Cobbitty, NSW, Australia was prepared. Three blocks were established: A (left), B (middle), and C (right). Each block contained 57 sampling points; each contained four litterbags; (b) an example of the arrangement of litterbags at each sampling point. The top left litterbag represents EL100 (filled *Eucalyptus* leaf only), the top right represents EF100 (filled with elevated fuel only), the bottom left represents EL33:EF33: FF33 (filled with *Eucalyptus* leaf, elevated fuel and surface fine fuel), the bottom right represents Lucerne (filled with lucerne hay only).

At each collection day (91, 179, 274, 364, and 443 days after the start of the trial), a total of 112 litterbags (including lucerne hay) from 29 sampling points were collected. An additional 20 litterbags filled with lucerne hay were collected at Day 364 and Day 443 from the second installation. All litterbag samples were stored in labelled paper bags, transported to the laboratory, and dried at 60 °C for a minimum of 48 h in a fan-forced oven (Model TD-78T-2-D, Thermoline Scientific, Wetherill Park, NSW, Australia). Over the trial period, a total of 483 litterbags sample from both time-since-fire collections were harvested from the *in-situ* litterbag decomposition trial, with loss of only 17 litterbags. Litterbag samples were cleaned with gentle brushing to remove soil and hand sorted to remove weeds and roots if needed. Cleaned samples were weighed to calculate litter mass loss over time.

The proportion of litter mass remaining (%LMR) as a function of time was calculated using the equation:

$$\%LMR = \frac{M_t}{M_0} \times 100\% \qquad \text{Equation 3.1}$$

where %LMR is percentage litter mass remaining from the original litter weight, M_t is the weight of litter remaining at the day of collection, and M_0 is the initial weight of litter inside the litterbag.

After weighing, litterbag samples were ground using a food-grade grinder (Breville Coffee and Spice Grinder; BCG200BSS; Breville Pty, Botany, Australia) to pass through a 1 mm sieve and stored in labelled plastic bags until further analysis.

3.2.4 Soil analysis

Soil samples collected prior to the litterbag decomposition trial (see Section 3.2.3) were air-dried, sieved through a 1 mm sieve, and analysed for total carbon (TC) and total nitrogen (TN) using an Elementar Analyser (Elementar Vario Max CNS Analysensysteme GmbH, Hanau, Germany). Soil acidity (pH) and electrical conductivity (EC) of soil were measured at a soil:water ratio of 1:5 using a pH (SevenCompact^{TM} S210, Mettler Toledo, Columbus Ohio, United State) and EC meter (SevenCompact^{TM} S230, Mettler Toledo). Approximately 2 g of air-dried soil was added to 10 mL of deionised water and shaken for 1 h, left to settle for 15 min prior to pH and EC measurements.

3.2.5 Litterbag spectral analysis

Spectral scans of litterbag samples using visible-near-infrared (vis-NIR), near-infrared (NIR), and attenuated total reflectance Fourier transform infrared (ATR-FTIR) spectrometers were obtained as described in Chapter 2 (see Section 2.2.5; Wadoux et al., 2021). In brief, five sub-sample from each litterbag samples were scanned and imported into RStudio for processing. The final spectrum for each sample was calculated by averaging the five sub-sample spectra, resulting in one representative spectrum per litterbag sample per each spectral region. Visible-NIR and NIR spectra of litterbag samples were acquired using the Black-Comet-CXR-SR and RED-Wave-NIRSX-SR spectrometer (StellarNet Inc. Oldsmar, Florida, USA), respectively. While ATR-FTIR absorbance spectra were obtained using the 4500a portable FTIR spectrometers (Agilent Technology Inc., Santa Clara, California, USA).

Spectral pre-processing

All vis-NIR, NIR, and ATR-FTIR spectra were pre-processed using the same combination of techniques described in Chapter 2 (see Section 2.2.6; Wadoux et al., 2021), including spectral trimming, Savitzky-Golay (SG) smoothing, and standard normal variate (SNV) correction. As discussed in Section 2.4.4, the 2nd derivative is a commonly used pre-processing technique to enhance spectral features (e.g., Gillon 1993; Javier-Astete et al., 2021). However, unlike Chapter 2, where the sample size was limited (see Section 2.2.2 and 2.2.3) the substantially larger sample set available in this study allowed the use of the 2nd derivative to improve spectral quality and the calibration model performance. The second derivative was calculated using the Savitzky-Golay smoothing function by *sgolayfilt* () function in the '*prospectr*' R package in RStudio (Wadoux et al., 2021).

3.2.6 Calibration model development and evaluation

Generalised calibration model

To evaluate the performance and generalisability of the calibration models developed for total carbon (TC) and total nitrogen (TN) in Chapter 2 (Model 1; see Section 2.3.2), these models were applied to predict TC and TN content in litterbag samples (Model 3). This approach was used to assess the applicability of models developed using commercially available sources of cellulose and lignin and representative leaf and bark litterfall samples for predicting TC and TN content across varying states of biological decomposition.

In this context, the calibration dataset of Model 3 was constructed using synthetic mixtures and litterfall samples (see Section 2.3.2), whereas the validation dataset consisted of litterbag samples, which service as an external independent dataset.

Sample-specific calibration model

To compare and evaluate the performance of the generalised model (Model 3) with a sample-specific approach, a cross-validation model was developed using train-test split method (Model 4). Litterbag samples were randomly partitioned into calibration (n = 337) and validation dataset (n = 146) using a 70:30 train-test split.

Model evaluation

The performance of Model 3 and Model 4 was compared and evaluated to determine whether a generalised model developed using synthetic mixtures and representative litterfall materials was sufficient to predict TC and TN in decomposing litter, or whether a sample-specific model was required to achieve a more accurate prediction of TC and TN during decomposition (Model 4). Model performance was evaluated using the coefficient of determination (R^2), Lin's Concordance Correlation Coefficient (LCCC), and root mean squared error (RMSE). The model with the highest R^2 and LCCC values, and the lowest RMSE was considered the best performing model (see Section 2.2.8).

3.2.7 Statistical analysis

Statistical analyses were done using Jamovi (Version 2.3, 2024; The Jamovi Project, Sydney, Australia) to test the combined effects of litter mixture combinations and litterbag collection day on the proportion of litter mass remaining (%LMR). Data from missing samples were removed from the data set to protect statistical power and reduce bias. One-way and two-way analysis of variance (ANOVA) were done to test (1) differences in topsoil properties across the study area established at Lansdown Farm, and (2) the effects and interactions among litter mixture combinations and litterbag collection day on %LMR. Where statistically significant effects were detected ($\alpha = 0.05$), pairwise comparisons among groups were conducted using Games-Howell Post-Hoc test.

Linear mixed model (LMM) was used to examine the effects of litter mixture combinations and litterbag collection day on %LMR (fixed effects). Time-since-fire collection (i.e., prior to fire (PF) and 1-year after fire (1YAF) was considered as random effects. The values of R^2 (explained by fixed effects) and R^2 condition (explained by fixed effects and random effect) are reported to compare model fits.

3.3 Results

3.3.1 Site characteristics

Long-term and monthly weather data

Cobbitty, NSW is characterised by a warm and temperate climate with a long-term (1971-2024) average maximum and minimum temperatures of 23.8 °C and 10.3 °C, respectively (weather station number: 068192, Camden Airport, 3.1 km from Lansdowne Farm; Australian Bureau of Meteorology, 2024). The long-term (1943-2024) average annual precipitation is 819.6 mm, with most of the rain falling during summer months of January to March.

As anticipated from the long-term average, during the *in-situ* litterbag decomposition trial, the study site experienced a hot, wet summer and a cool, dry winter, with excessive rainfall observed in April and June 2024 (Figure 3.2a). During the first two months of litterbag trial, rainfall was relatively low with only 17 mm in September and 19 mm in October 2023, while the temperature fluctuated daily between minimum and maximum temperatures (5 °C and 30 °C, respectively; Figure 3.2a, b). Total rainfall remained high over the summer months, followed by a decline after January 2024. The highest monthly temperature was recorded in December, at 41.8 °C (Figure 3.2b). The highest rainfall event occurred in April (185.6 mm), dropped to 71.4 mm in May, and increased to 135.6 mm in June. The lowest monthly temperature was observed in June 2024. Rainfall from July to October 2024 was consistently low (19.6-33.4 mm), before an increase again in November, reflecting the typical seasonal trend observed in the long-term data. The first spring (i.e., September and October 2023) was slightly drier and hotter than the second spring in 2024 (Figure 3.2a, b).

Soil

Soil moisture content (0-10 cm), which was monitored locally using a soil moisture probe, was relatively low during the first three months of incubation (September-November 2023) and showed a steady decline (Figure 3.2a). Soil moisture content increased substantially following summer rainfall, reached a plateau in February 2024, followed by a drop in March. Due to consistent rain in April and June 2024, soil moisture remained high (above 0.2 m^3/m^3) throughout autumn and declined slowly during winter and spring, with the lowest soil moisture content measured from September to November 2024 (Figure 3.2a).

Prior to the *in-situ* litterbag decomposition trial, TC, TN, C/N ratio, and EC of topsoil (0-10 cm) was similar across the study area (One-way ANOVA; $p > 0.05$; Table 3.2). The only statistically significant difference was for soil pH, between topsoil collected at sampling distances of 10 m and 50 m (One-way ANOVA; $p = 0.017$; Table 3.2) and between 10 m and 70 m (One-way ANOVA; $p = 0.031$; Table 3.2). In general, soil pH ranged between 5.8 and 6.2, while the EC ranged from 146.3 to 213.9 µS cm^{-1} indicating that properties of the topsoil were homogeneous across the study area.

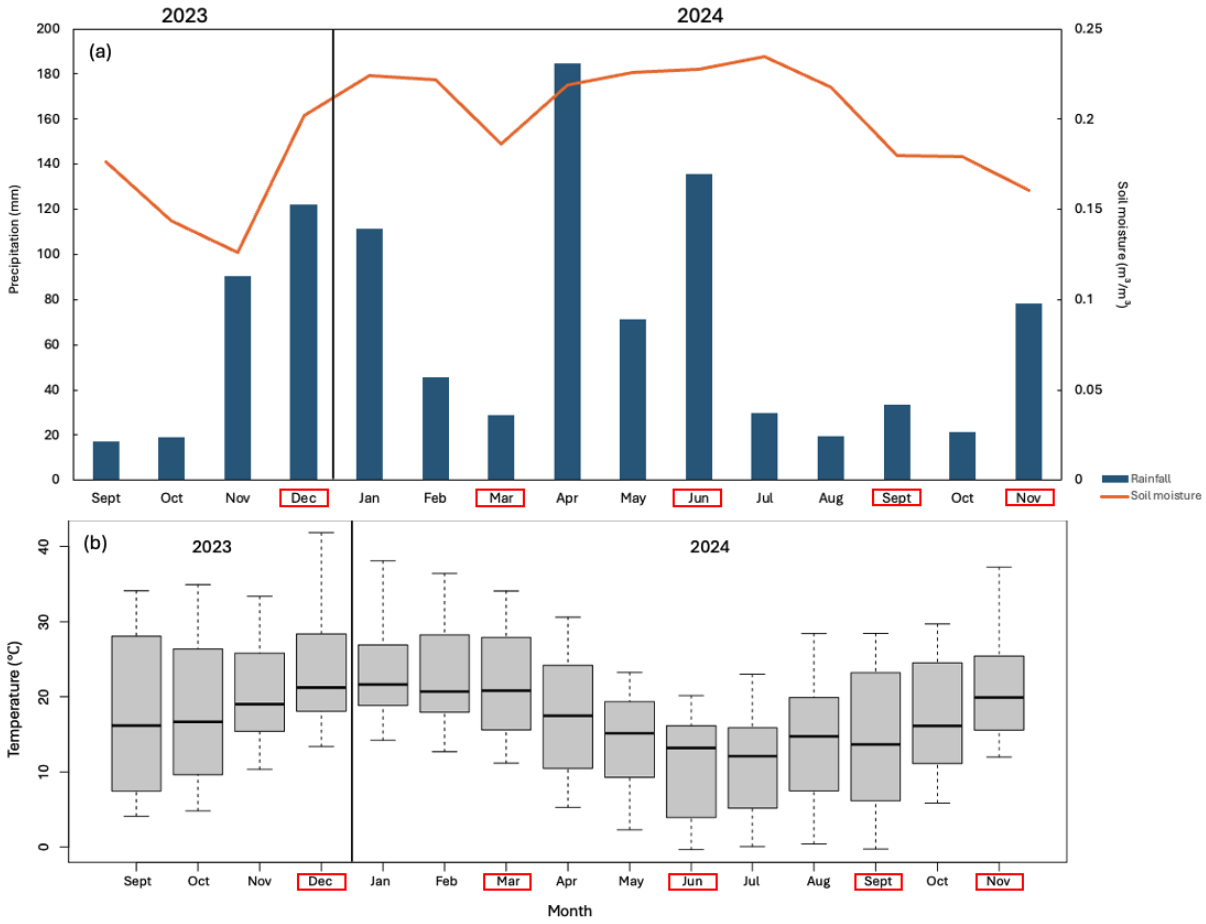

Figure 3.2: Weather conditions in Cobbitty, NSW during the *in-situ* litterbag decomposition trial (September 2023 to December 2024). (a) Total monthly rainfall (dark blue bars; data from Bureau of Meteorology 2025, weather station number 068192, Camden Airport, 3.1 km from Lansdowne Farm) and soil moisture (orange line; data from local weather station; ATMOS 41; Edaphic Scientific Pty Ltd, Victoria, Australia); (b) Box-and-whiskers plot of monthly temperature recorded by the local weather station. The black line within each box represents the median monthly temperature, the top whisker represents the mean monthly maximum temperature, and the bottom whisker represents the mean monthly minimum temperature. Months corresponding to dates of litterbag collection are marked with red box.

Table 3.2: Summary statistics of total carbon (TC), total nitrogen (TN), carbon:nitrogen (C/N) ratio, pH, and electric conductivity (EC) in topsoil (0-10 cm) collected from the study site in Lansdown Farm, Cobbitty, NSW, Australia (34°02'S, 150°66'E), prior to *in-situ* litterbag decomposition trial in September 2023. Topsoil was sampled at every 10 m with one replication per block (Block A, B, and C). Data are presented as mean ± standard deviation (n = 3 for every 10 m). Statistical comparisons along the transect was identified using one-way ANOVA followed by Games-Howell Post-Hoc test (α = 0.05). For each soil property, mean with the same superscript letter within a column are not significantly different ($p > 0.05$).

Sampling distance (m)	TC (%)	TN (%)	C/N	pH	EC (µS cm^{-1})
10	1.27 ± 0.20^{a}	0.087 ± 0.013^{a}	14.67 ± 1.08^{a}	6.21 ± 0.14^{a}	213.90 ± 81.17^{a}
20	1.25 ± 0.27^{a}	0.091 ± 0.024^{a}	13.90 ± 0.79^{a}	6.10 ± 0.14^{ab}	202.03 ± 98.20^{a}
30	1.02 ± 0.05^{a}	0.073 ± 0.004^{a}	13.96 ± 0.16^{a}	5.98 ± 0.08^{ab}	201.33 ± 22.50^{a}
40	1.06 ± 0.14^{a}	0.077 ± 0.014^{a}	13.88 ± 0.87^{a}	6.01 ± 0.005^{ab}	146.30 ± 83.44^{a}
50	0.97 ± 0.06^{a}	0.068 ± 0.010^{a}	14.47 ± 1.27^{a}	5.77 ± 0.21^{ab}	149.77 ± 22.70^{a}
60	1.01 ± 0.02^{a}	0.072 ± 0.004^{a}	13.95 ± 0.98^{a}	5.88 ± 0.15^{ab}	170.90 ± 54.09^{a}
70	0.95 ± 0.07^{a}	0.069 ± 0.007^{a}	13.76 ± 0.32^{a}	5.80 ± 0.12^{b}	177.85 ± 92.90^{a}

3.3.2 *In-situ* litterbag decomposition trial

Initial litterbag chemistry

Prior to prescribed burning, litter mixtures with *Eucalyptus* leaf (EL100) showed relatively high carbon content (TC content > 47%) than those comprised of elevated fuel (EF) and surface fine fuel (FF; TC content ≤ 45%) (Table 3.3). Of these, EL100 and EL67:EF33 had the highest TC content, with EF100 and EF67:FF33 containing the lowest TC content. Litter mixtures comprised of 33% *Eucalyptus* leaf had similar TN content (66-67%), while those containing 67% or 100% EL had a higher TN content, ranging from 71-76%. Of all litter mixtures, EF100 had the lowest TN content and the highest C/N ratio, while EF mixed with 67% fine fuel (FF) had the highest TN content and the lowest C/N ratios.

One year after fire litter mixtures comprised of EL and EF had relatively higher carbon content (> 46%) than those comprised of EF and FF (< 42%). Among these litter mixtures, EL67:FF33 had the highest carbon content, with no significant differences when compared to the pre-fire condition (One-way ANOVA; $p > 0.05$; Table 3.3). Litter mixtures with high amounts of surface fine fuel had the lowest TC and TN content. Among all, EL67:FF33 and the three-component mixtures had the highest C/N ratios, while EF100 had the lowest value.

One-year after fire, TC content in the three single-component mixture were lower, with significant differences found for EF100 (One-way ANOVA; $p = 0.026$; Table 3.3) and FF100 (One-way ANOVA; $p = 0.022$; Table 3.3). In addition, a significant difference in TN content was found for EL100 (One-way ANOVA; $p < 0.001$; Table 3.3) and EF100 (One-way ANOVA; $p = 0.003$; Table 3.3). In contrast, FF100 collected 1-year after fire had lower TN content than comparable samples collected prior to fire (One-way ANOVA; $p > 0.05$; Table 3.3).

Total C and TN content varied depending on litter mixture composition. Generally, surface fine fuel collected prior to prescribed fire had higher TC content, while fine fuels collected 1-year after fire tended to have higher TN content, and this corresponded to differences in C/N ratios.

Table 3.3: Initial total carbon (TC), total nitrogen (TN), and carbon:nitrogen (C/N) ratios in litter mixtures composed of *Eucalyptus* leaf (EL), elevated fuel (EF), and surface fine fuel (FF) collected prior to fire (PF) and 1-year after fire (1YAF). A simplex-lattice design was used to generate 10 possible single, two-, and three-component litter mixtures for both time-since-fire collections. Data are presented as mean ± standard deviation (n = 3). Statistical comparisons among time-since-fire collections were identified using one-way ANOVA followed by Games-Howell Post-Hoc test (α = 0.05). For each litter mixture in time-since-fire collections, means with the same superscript letter within a column are not significantly different ($p > 0.05$).

Time-since-fire collection	Litter mixture	TC (%)	TN (%)	C/N ratio
Prior to fire (PF)	EL100	52.18 ± 0.63[a]	0.71 ± 0.013[a]	73.98 ± 0.57[a]
	EL67:EF33	51.89 ± 0.32[a]	0.72 ± 0.030[a]	72.63 ± 2.70[a]
	EL33:EF67	49.59 ± 0.44[a]	0.67 ± 0.024[a]	73.95 ± 1.97[a]
	EF100	44.97 ± 0.89[a]	0.55 ± 0.020[a]	82.40 ± 1.53[a]
	EL67:FF33	49.05 ± 5.48[a]	0.76 ± 0.13[a]	66.30 ± 17.00[a]
	EL33:EF33:FF33	47.81 ± 1.21[a]	0.66 ± 0.073[a]	73.48 ± 10.64[a]
	EF67:FF33	44.62 ± 1.18[a]	0.70 ± 0.097[a]	64.51 ± 7.91[a]
	EL33:FF67	47.09 ± 1.19[a]	0.67 ± 0.04[a]	70.21 ± 2.51[a]
	EF33:FF67	45.01 ± 0.86[a]	0.82 ± 0.05[a]	55.28 ± 2.50[a]
	FF100	45.21 ± 0.33[a]	0.80 ± 0.05[a]	56.59 ± 3.46[a]
1-year after fire (1YAF)	EL100	49.29 ± 1.56[a]	0.88 ± 0.02[b]	55.98 ± 0.77[b]
	EL67:EF33	47.67 ± 0.23[b]	0.79 ± 0.02[b]	60.68 ± 1.23[b]
	EL33:EF67	46.07 ± 0.81[b]	0.85 ± 0.07[b]	54.22 ± 3.75[b]
	EF100	42.64 ± 0.51[b]	0.78 ± 0.04[b]	54.46 ± 2.90[b]
	EL67:FF33	50.23 ± 1.37[a]	0.74 ± 0.05[a]	67.66 ± 3.59[a]
	EL33:EF33:FF33	49.13 ± 0.54[a]	0.75 ± 0.06[a]	65.68 ± 5.01[a]
	EF67:FF33	40.42 ± 3.03[a]	0.72 ± 0.08[a]	56.53 ± 2.31[a]
	EL33:FF67	39.91 ± 1.40[b]	0.67 ± 0.03[a]	59.49 ± 3.18[b]
	EF33:FF67	39.87 ± 2.08[b]	0.64 ± 0.08[b]	63.15 ± 5.30[a]
	FF100	38.70 ± 1.81[b]	0.63 ± 0.09[a]	61.92 ± 6.28[a]

Mass loss of litter mixtures

For all litter mixtures and time-since-fire collections, litter decomposition followed a similar pattern with a rapid initial mass loss (ranging from 12.9-29.8%) during the early stage of decomposition (first 179 days) which gradually slowed over time (Figure 3.3).

During the first 179 days, regardless of time-since-fire, EL100 had the highest %LMR (PF = 87.1%; 1YAF = 81.3%; Figure 3.3a), while EF100 had the lowest %LMR (PF = 70.2%; 1YAF = 72.3%; Figure 3.3d). Differences in litter mass loss between time-since-fire collections were most pronounced between Day 91 and Day 179. As decomposition continued, the rate of litter mass loss slowed, and in some cases, significant differences in %LMR were found between Day 179 and Day 274 (e.g., PF EL33:DL67; Figure 3.3h). In the later stage of decomposition (after 179 days), litter mass loss began to plateau and there were no significant differences among collection day and time-since-fire collections (One-way ANOVA; $p > 0.05$; Figure 3.3), except for EL67:EF33 and EL100,

where significant differences among prior to fire and 1-year after fire collections were observed on Day 364 (One-way ANOVA; $p = 0.027$; Figure 3.3) and Day 443 (One-way ANOVA; $p = 0.015$; Figure 3.3), respectively.

The remaining proportional litter weight after 15 months of decomposition ranged from 60.0 to 75.6%. Most litter mixtures retained less than 70% of their original weight, except for EL100 from both time-since-fire collections, two-component EL67:EF33 and EL67:FF33 collected prior to fire, and FF100 collected 1-year after fire. Among all mixtures, EL100 from prior to fire collection retained more than 75% of its original mass at Day 443, significantly higher than the corresponding 1-year after fire collection (One-way ANOVA; $p = 0.015$; Figure 3.3a). A general trend was evident; litterbags with EF showed a lower %LMR, while litterbags with EL showed a higher %LMR, whereas the three-component litter mixtures showed intermediate rates of decomposition (Figure 3.3f). In particular, litterbags containing EF resulted in highest mass loss, in the order of single-component > two-component > three-component litter mixtures. Single-component litterbags with EF had the fastest mean decomposition rate, with both time-since-fire collections with more than 40% of its original mass lost at the end of the decomposition trial (Figure 3.3d).

Nutrient dynamics

For all litter mixtures and time-since-fire collections, changes in TC content followed a similar pattern found for litter mass loss, where carbon content decreased gradually over time (Figure 3.4). The most substantial changes in TC content were in the early stages of decomposition. At Day 179, TC content in litter mixtures ranged from 59.4 to 96.0%. At this stage, EF100 collected prior to fire had the lowest TC content (Figure 3.4d), while FF100 collected 1-year after fire had a significantly higher TC content (One-way ANOVA; $p < 0.001$; Figure 3.4j). As found for litter mass loss, changes in TC content after the initial period (179 days) were not significant among litter mixtures in most cases.

At the end of 443 days of decomposition, TC remaining spanned from 51.1 to 94.2%, with the highest TC in FF100 and the lowest in EF100, both from 1-year after fire collection. Throughout the 15 months of *in-situ* litterbag decomposition, EL67:FF33 collected prior to fire consistently had significantly higher TC content than that from 1-year after fire collection (One-way ANOVA; $p <$ 0.001-0.007; Figure 3.4i). Similarly, FF100 collected 1-year after fire had significantly higher TC content than those from prior to fire collection (One-way ANOVA; $p < 0.001$-0.007; Figure 3.4j). This pattern was consistent except for the initial 91 days where differences were not significant (One-way ANOVA; $p > 0.05$; Figure 3.4j). Overall, changes in TC content in FF100 collected 1-year after

fire were minimal, with 94% of TC remaining at the end of the decomposition period, with no significant differences in TC content between the first (Day 91) and the last collection (Day 443) (One-way ANOVA; $p > 0.05$; Figure 3.4j). A similar pattern was also observed in the three-component mixture (EL33:EF33:FF33), where no significant differences in TC content were found among time-since-fire collections (One-way ANOVA; $p > 0.05$; Figure 3.4f). In contrast, EF100 from both time-since-fire collections showed the greatest changes in TC during *in-situ* decomposition, with almost half of initial C content lost by the end of the decomposition period (Figure 3.4f).

A different pattern was found for TN in litter mixtures which increased up to 30% during the early stage of decomposition (Figure 3.5). The exception to this pattern was found for EL100 (Figure 3.5d), and several two-component mixtures (EL67:EF33 from both time-since-fire collections and EL67:FF33 from the prior to fire collection). Notably, TN content in EL100 from both time-since-fire collections showed a negligible decrease during the first 91 days of decomposition followed by an increased in the next collection period (Figure 3.5a). In particular, EL100 collected prior to fire showed an increase in TN from 76.3 to 96.1%, while the increase in TN of EL100 collected 1-year after fire was less pronounced (Figure 3.5a).

The amount of nitrogen in many of the decomposing litter mixtures increased over time (Figure 3.5). At the end of 15 months, the amount of TN in litter mixtures from 1-year after fire collection exceeded the initial level, except for mixtures that included a high ratio of *Eucalyptus* leaf litter (i.e., EL100 (75.5 ± 4.2%; Figure 3.5a), EL67:EF33 (99.9% ± 1.9; Figure 3.5b), and EL67:FF33 (96.0 ± 5.1%; Figure 3.5e). The pattern of change in samples collected prior to fire were less obvious, while some litter mixture combinations had a decreased in TN content at the end of the decomposition (e.g., EL100, EF67:FF33; EF33:FF67; FF100). No statistically significant differences were found for TN content in EL67:EF33, EL33:EF67, EF100, EF67:FF33, and EF33:FF67 among collection day from both time-since-fire collections (One-way ANOVA; $p > 0.05$; Figure 3.5).

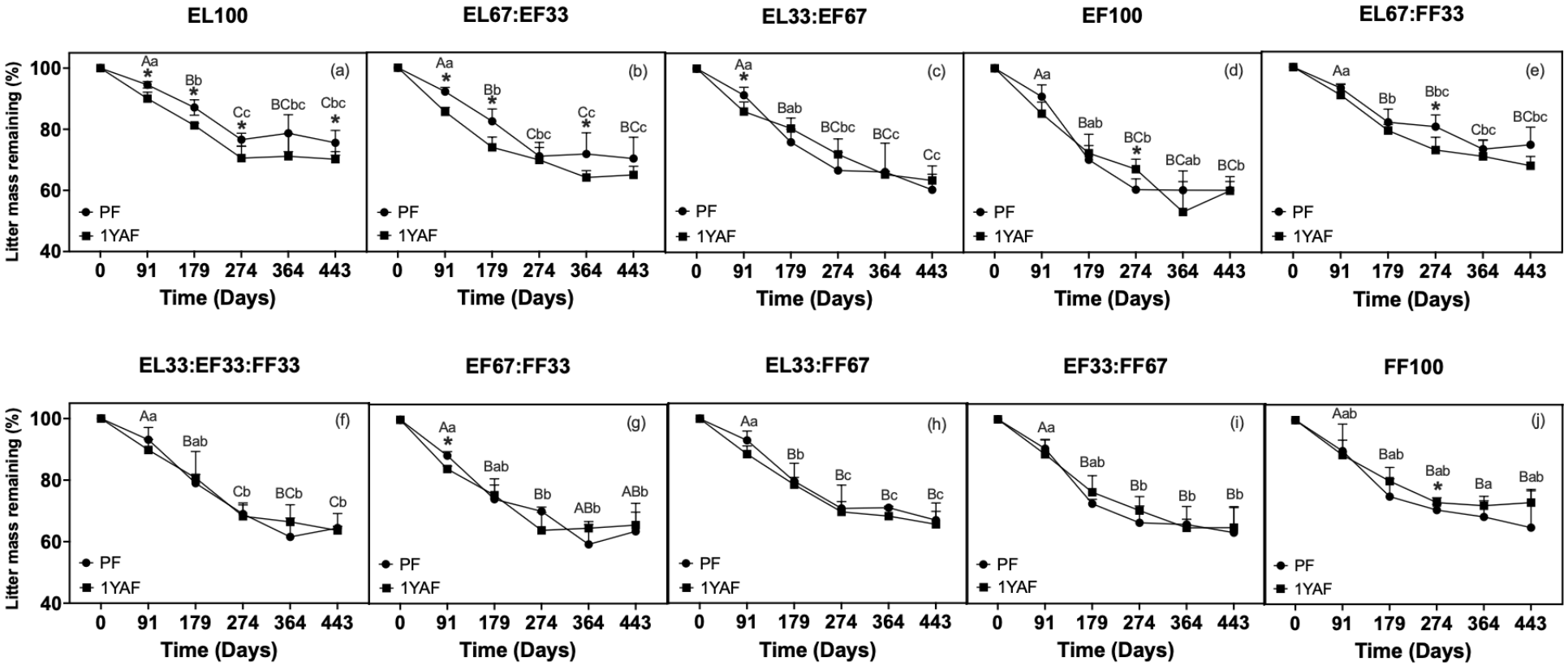

Figure 3.3: Percentage of the initial litter mass remaining (%LMR) of litter mixtures over the course of 15 months of *in-situ* litterbag decomposition. Litter mixtures were composed of *Eucalyptus* leaf (EL), elevated fuel (EF), and surface fine fuel (FF) and were collected prior to fire (PF) and 1-year after fire (1YAF). A simplex-lattice design (SLD) was used to generate 10 possible single-, two-, three-component litter mixtures for both time-since-fire collections. Each plot compares the %LMR of the same litter mixture combination under the two time-since-fire collections. Points represent mean value of %LMR and error bars indicate standard deviation. Statistical comparisons within and between collection day were identified using one-way ANOVA followed by Games-Howell Post-Hoc test ($\alpha = 0.05$). *indicates significant differences between time-since-fire collections for each collection day ($p < 0.05$). Within each plot, means with the same letter are not significantly different ($p > 0.05$). Uppercase letters represent the statistical differences within the PF collection, while lowercase letters represent the statistical differences within the 1YAF collection.

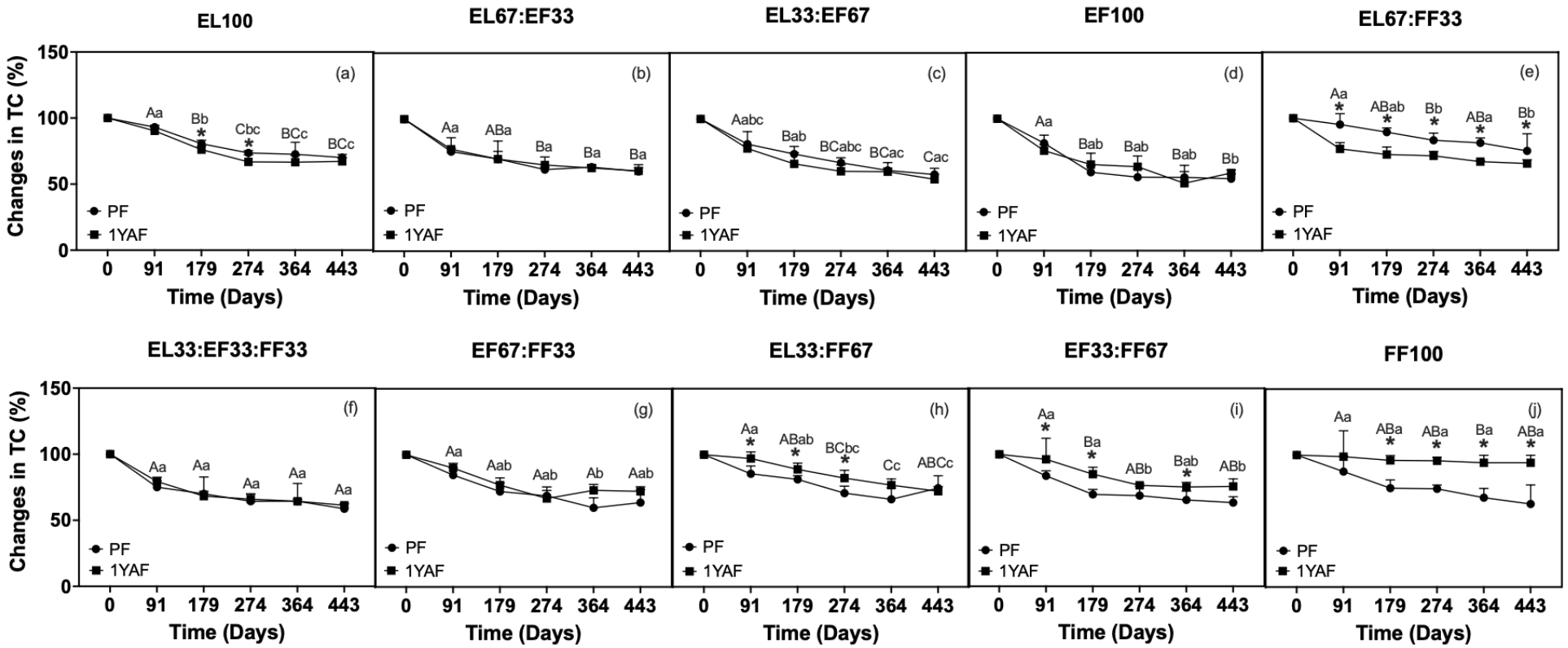

Figure 3.4: Percentage changes of total carbon (TC) in litter mixtures over the course of 15 months of *in-situ* litterbag decomposition. Litter mixtures were composed of *Eucalyptus* leaf (EL), elevated fuel (EF), and surface fine fuel (FF) and were collected prior to fire (PF) and 1-year after fire (1YAF). A simplex-lattice design (SLD) was used to generate 10 possible single-, two-, three-component litter mixtures for both time-since-fire collections. Each plot compares the total carbon content of the same litter mixture combination under the two time-since-fire collections. Points represent mean value of TC and error bars indicate standard deviation. Statistical comparisons within and between collection day were identified using one-way ANOVA followed by Games-Howell Post-Hoc test ($\alpha = 0.05$). *indicates significant differences between time-since-fire collections for each sampling time ($p < 0.05$). Within each plot, means with the same letter are not significantly different ($p > 0.05$). Uppercase letters represent the statistical differences within the PF collection, while lowercase letters represent the statistical differences within the 1YAF collection.

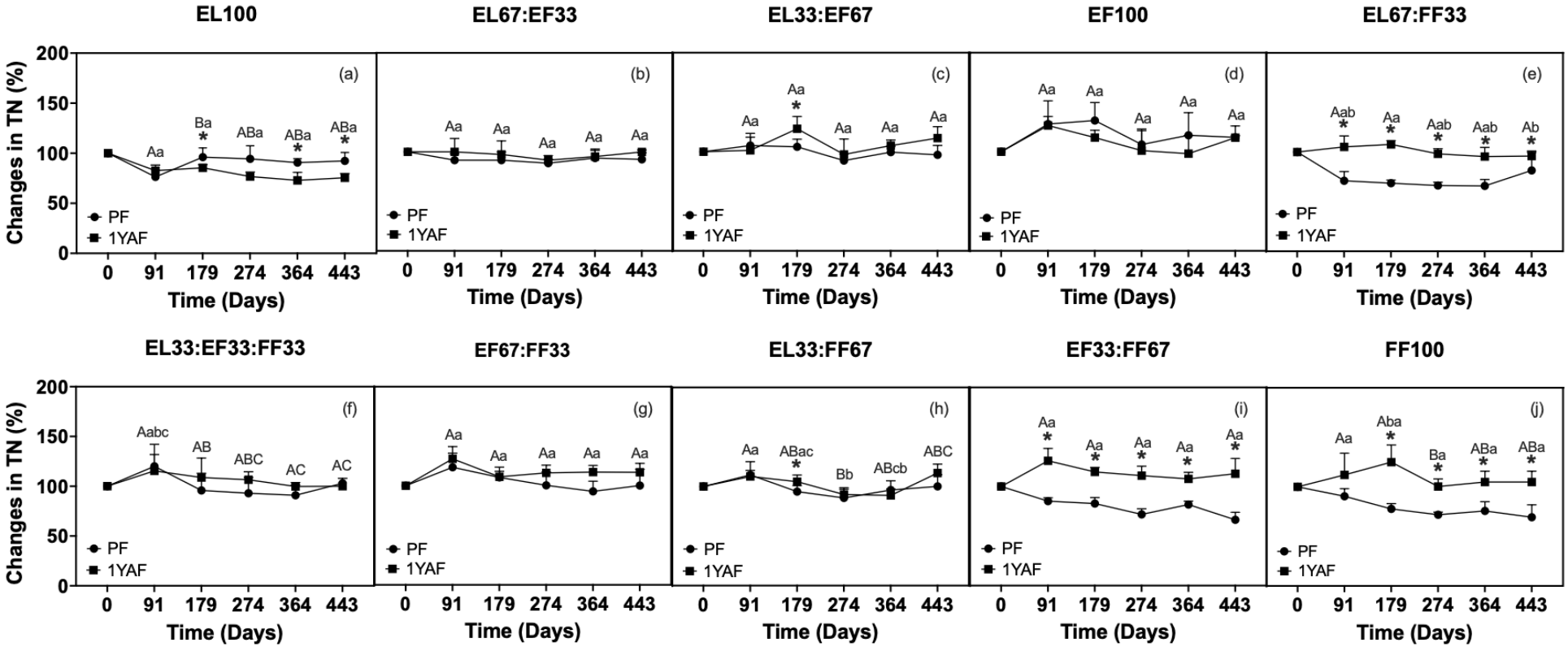

Figure 3.4: Percentage changes of total nitrogen (TN) in litter mixtures over the course of 15 months of *in-situ* litterbag decomposition. Litter mixtures were composed of *Eucalyptus* leaf (EL), elevated fuel (EF), and surface fine fuel (FF) and were collected prior to fire (PF) and 1-year after fire (1YAF). A simplex-lattice design (SLD) was used to generate 10 possible single-, two-, three-component litter mixtures for both time-since-fire collections. Each plot compares the total nitrogen content of the same litter mixture combination under the two time-since-fire collections. Points represent mean value of TN and error bars indicate standard deviation. Statistical comparisons within and between collection day were identified using one-way ANOVA followed by Games-Howell Post-Hoc test ($\alpha = 0.05$). *indicates significant differences between time-since-fire collections for each sampling time ($p < 0.05$). Within each plot, means with the same letter are not significantly different ($p > 0.05$). Uppercase letters represent the statistical differences within the PF collection, while lowercase letters represent the statistical differences within the 1YAF collection.

Effects of litter mixture combinations and incubation time on percentage litter mass remaining

The linear mixed model (LMM) demonstrated a good model fit, with a marginal R^2 of 0.76 and conditional R^2 of 0.78 (LMM; Table 3.4). This indicated that fixed effects alone explained 76% of the variance, however the inclusion of time-since-fire (i.e., prior to fire and 1-year after fire) as a random effect had a limited impact on the overall model fit (LMM; conditional R^2 = 0.78; Table 3.4). The substantially low intra-class correlation coefficient (ICC) of time-since-fire collections suggests that the differences between prior to fire and 1-year after fire only attributed 8% of the total variance in percentage litter mass remaining (%LMR) after *in-situ* litterbag decomposition (LMM; ICC = 0.08; Table 3.5). In addition, the high residual variance suggested that there is a substantial proportion of variation in %LMR remains unexplained by the LMM model.

The fixed effects Omnibus test from the LMM (Table 3.6) showed that both litter mixture combination and collection date had statistically significant main effects on %LMR (LMM; F = 16.02 and 355.91, respectively; $p < 0.01$; Table 3.6). However, their interaction did not significantly affect %LMR during the *in-situ* litterbag decomposition trial (LMM; F = 0.97; p = 0.53; Table 3.6).

Table 3.4: Summary of linear mixed model (LMM) results examining the effects of litter mixture combinations, collection day (i.e., incubation time), and their combined interactions on percentage litter mass remaining (%LMR) after 15 months of *in-situ* litterbag decomposition trial. The dependent variable, %LMR was log-transformed to meet model assumptions. Fixed effects included litter mixtures combinations, collection dates, and their combined interactions, while time-since-fire collections were included as random effects. Marginal R^2 represents the proportion of variance explained by fixed effects alone, while conditional R^2 represents the proportion of variance explained by the fixed and random effects.

Variables	**Marginal R^2**	**Conditional R^2**
Log%MR ~ 1 + Litter mixture combinations + Collection day + Litter mixture combinatios:Collection day + (1+|Time-since-fire collections)	0.76	0.78

Table 3.5: Summary of random effects of the linear mixed model (LMM). Variance, standard deviation (SD), and intra-class correlation coefficient (ICC) of time-since-fire collections intercept are presented. ICC value represents the proportion of variance that could be explained by the random effects, while residue variance represents the unexplained variations in %LMR after accounting for both fixed and random effects in the LMM.

Groups	**Name**	**Variance**	**SD**	**ICC**
Time-since-fire collections	(Intercept)	0.0099	0.099	0.080
Residual		0.11	0.34	

*Number of observations: 483; number of groups: time-since-fire collections = 2.

Table 3.6: Summary of fixed effects Omnibus test showing the effects of litter mixtures combinations, collection day, and their combined interactions on %LMR after 15 months *in-situ* litterbag decomposition trial.

	***F* values**	**df**	***p***
Litter mixture combinations	16.02	9	< 0.001
Collection day	355.91	4	< 0.001
Litter mixtures combinations × Collection day	0.97	36	0.53

3.3.3: Predicting total carbon and total nitrogen of decomposing litter with spectroscopy

Dataset characteristics

The calibration dataset for the generalised model (Model 3) was comprised of a total of 63 samples, including 21 mixture blends (synthetic mixtures) and 42 representative litterfall samples (Table 3.6; see Section 2.2.2). This dataset covered a broad range of TC content (38.1-70.0%, mean = 45.8%) which generally encompassed the TC range of the validation dataset (litterbag samples from all sampling dates, n = 483). In contrast, the TN range in the calibration dataset was narrower (0.22-0.71%, mean = 0.26%) and did not fully capture the full variation in the validation dataset. For the validation dataset of Model 3, TC ranged from 30.5 to 51.5%, with a mean of 44.4%, TN ranged from 0.5 to 1.6%, with a mean of 0.9%, with the maximum TN value exceeded the value in the calibration dataset (Table 3.7).

In comparison, Model 4 used a train-test split decomposing litter mixture samples, with 70% of samples assigned to the calibration dataset (n = 337) and 30% to the validation dataset (n = 146; Table 3.6). The TC and TN content of the validation dataset was well represented by the calibration dataset (30.5-51.3% with a mean of 44.4% for TC, and 0.5-1.6%, mean of 0.89% for TN).

Table 3.7: Descriptive statistics of total carbon (TC) and total nitrogen (TN) content in decomposing litter mixtures from *in-situ* litterbag decomposition trial. The calibration model developed in Chapter 2 (Model 1, see Section 2.3.2) was used in Model 3, while the validation dataset represents litter mixtures from *in-situ* litterbag decomposition study from each sampling date. Model 3 was contrasted using train-test split (i.e., a random 70:30 internal data split). Abbreviations: *N* = number of samples; Min = minimum, 1st Qu = first quartile; 3rd Qu = third quartile; Max = maximum.

Model 3: Generalised model using synthetic mixtures and litterfall

	N	**Min**	**1st Qu**	**Median**	**Mean**	**3rd Qu**	**Max**
Total carbon							
Whole dataset	546	30.51	42.01	44.89	44.53	47.18	70.03
Calibration	63	38.06	41.66	45.66	45.80	48.27	70.03
Validation	483	30.51	42.15	44.86	44.37	47.10	51.53
Total nitrogen							
Whole dataset	546	0.22	0.73	0.84	0.81	0.95	1.64
Calibration	63	0.22	0.065	0.33	0.26	0.43	0.71
Validation	483	0.50	0.78	0.86	0.89	0.97	1.64

Model 4: Calibration model using train-test split

	N	**Min**	**1st Qu**	**Median**	**Mean**	**3rd Qu**	**Max**
Total carbon							
Whole dataset	483	30.51	42.18	44.89	44.41	47.15	51.53
Calibration	337	30.51	41.95	44.83	44.36	47.21	51.33
Validation	146	32.56	42.25	45.18	44.52	46.69	51.16
Total nitrogen							
Whole dataset	483	0.50	0.78	0.86	0.89	0.97	1.64
Calibration	337	0.50	0.78	0.86	0.89	0.97	1.64
Validation	146	0.62	0.77	0.87	0.88	0.97	1.45

3.3.4: Model performance

For both models, partial least square regression (PLSR) models based on pre-processed vis-NIR, NIR, and ATR-FTIR spectra outperformed bootstrap PLSR, Cubist, and random forest (RF), as indicated by the higher coefficients of determination (R^2) and Lin's concordance correlation coefficients (LCCC), and the lower root mean square error (RMSE; Table 3.8). The only exception was observed in the generalised model (Model 3), where non-pre-processed NIR spectra produced a better N prediction than the pre-processed spectra.

In most cases, the PLSR model using NIR spectra pre-processed with Savitzky-Golay (SG) smoothing and standard normal variate (SNV) transformation yielded the best TC and TN prediction. However, in the sample-specific model (Model 4), the use of 2nd derivative with SG smoothing and SNV increased the model accuracy and performed better than the models that used only SG smoothing and SNV transformation. These results indicate the spectral pre-processing techniques, including SG smoothing, 2nd derivatives, and SNV transformation have a positive impact on model accuracy and predictivity. However, the use of genetic algorithm (GA) feature wavelength selection

did not improve performance over model using the full spectral range for both carbon and nitrogen prediction in decomposing litter mixtures.

For both models, ATR-FTIR spectroscopy outperformed vis-NIR and NIR in predicting the TC and TN content in decomposing litter mixtures (Table 3.8). Predictions of TC and TN achieved acceptable accuracy, with R^2v of 0.67 for TC and 0.77 for TN in the generalised model (Model 3), and R^2v of 0.68 for TC and 0.73 for TN in the sample-specific model (Model 4). Although the generalised model (Model 3) achieved a relatively high R^2v for TC prediction, its calibration performance was weak with low R^2cv and high RMSECV.

The predictive performance of vis-NIR and NIR spectroscopy for TC was moderate to unsatisfactory. In particular, the use of synthetic mixtures and litterfall samples (Model 3) failed to produce reliable carbon prediction, yielded a very low R^2cv and high RMSECV. In addition, the scatterplot showed that NIR predicted TC values was poorly aligned with laboratory measurement, with points clustered horizontally along the diagonal line, indicating poor prediction (Figure 3.5b). In contrast, this model performed better for TN prediction, with higher R^2cv, R^2v and lower RMSECV and RMSEV values than for TC. However, TN prediction using vis-NIR and NIR remained weak, with a R^2v of 0.33 and 0.46, respectively (Figure 3.6d, e).

In contrast, the sample-specific model (Model 4), which was constructed using litterbags samples and train-test split approach, provided a more reliable prediction of carbon content of decomposing litter mixtures. However, the scatterplot (Figure 3.7) of the validation results showed that all models had the tendency to overestimate the TC content when measured values below 40%. In contrast, the performance of the sample-specific model for nitrogen prediction only yielded a better performance than the generalised model (Model 3) with vis-NIR spectra. In all other cases, the generalised model showed better accuracy in nitrogen prediction than the 70:30 split.

Table 3.8: Comparative performance of the best models selected from vis-NIR, NIR, and ATR-FTIR spectra for predicting total carbon (TC) and total nitrogen (TN) content in decomposing litter mixtures from *in-situ* litterbag decomposition trial. Calibration models were developed using multivariate modelling analysis including partial least squared regression (PLSR), bootstrap PLSR, Cubist, and random forest (RF). Models were selected based on the highest coefficient of determination (R^2), the lowest root mean squared error (RMSE), and the highest Lin's Concordance Correlation Coefficient (LCCC) value after testing different pre-processing combinations (raw spectra, SG smoothing, SNV, 2nd derivative, and GA feature wavelength selection). SG = Savitzky-Golay smoothing; *w* = window size (number following indicate the size of the applied window); *k* = polynomial order; *m* = order of derivatives; SNV = standard normal variate transformation; R^2cv = coefficient of determination of cross-validation model; RMSECV = root mean squared error of cross-validation model; LCCCcv = Lin's Concordance Correlation Coefficient of cross-validation model; R^2v = coefficient of determination of validation model; RMSEV = root mean squared error of validation model; LCCCv = Lin's Concordance Correlation Coefficient of validation model.

Model 3: Generalised model using synthetic mixture and litterfall samples (from Chapter 2)

	Spectra	Best model	Pre-processing technique	Calibration dataset			Validation dataset		
				R^2cv	RMSECV	LCCCcv	R^2v	RMSEV	LCCCv
Total carbon	vis-NIR[a]	PLSR	SG (*w* = 7, *k* = 2), SNV	0.19	5.04	0.34	0.58	2.43	0.73
	NIR[b]	PLSR	SG (*w* = 3, *k* = 2), SNV	0.07	5.58	0.10	0.05	3.64	0.10
	ATR-FTIR[c]	PLSR	SG (*w* = 7, *k* = 2), SNV	0.33	3.77	0.55	0.67	2.13	0.80
Total nitrogen	vis-NIR[a]	PLSR	SG (*w* = 7, *k* = 2), SNV	0.43	0.18	0.63	0.33	0.14	0.54
	NIR[b]	PLSR	Raw trimmed NIR spectra	0.71	0.11	0.83	0.46	0.12	0.64
	ATR-FTIR[c]	PLSR	SG (*w* = 7, *k* = 2), SNV	0.84	0.08	0.92	0.77	0.08	0.87

Table 3.8 continued.

Model 4: Sample-specific model using litterbag samples (train-test split)

	Spectra	Best model	Pre-processing technique	Calibration dataset			Validation dataset		
				R^2cv	RMSECV	LCCCcv	R^2v	RMSEV	LCCCv
Total Carbon	vis-NIR[a]	PLSR	SG (w = 7, k = 2), SNV	0.50	2.62	0.67	0.48	2.67	0.66
	NIR[b]	PLSR	SG (w = 3, k = 2, m = 2), SNV	0.51	2.62	0.68	0.55	2.41	0.71
	ATR-FTIR[c]	PLSR	SG (w = 5, k = 2), SNV	0.73	1.94	0.84	0.68	2.04	0.81
Total Nitrogen	vis-NIR[a]	PLSR	SG (w = 3, k = 2), SNV	0.50	0.12	0.64	0.35	0.13	0.57
	NIR[b]	PLSR	SG (w = 7, k = 2, m = 2), SNV	0.30	0.13	0.51	0.59	0.11	0.73
	ATR-FTIR[c]	PLSR	SG (w = 3, k = 2), SNV	0.76	0.08	0.86	0.73	0.08	0.85

[a] The wavelength range for the vis-NIR spectral regions was 500.5-1,000 nm

[b] The wavelength range for the NIR spectral region was 1,000.5-1,650 nm

[c] The wavenumber range for the MIR infrared region was 4,000-650 cm^{-1} (wavelength: 2,500-25,000 nm)

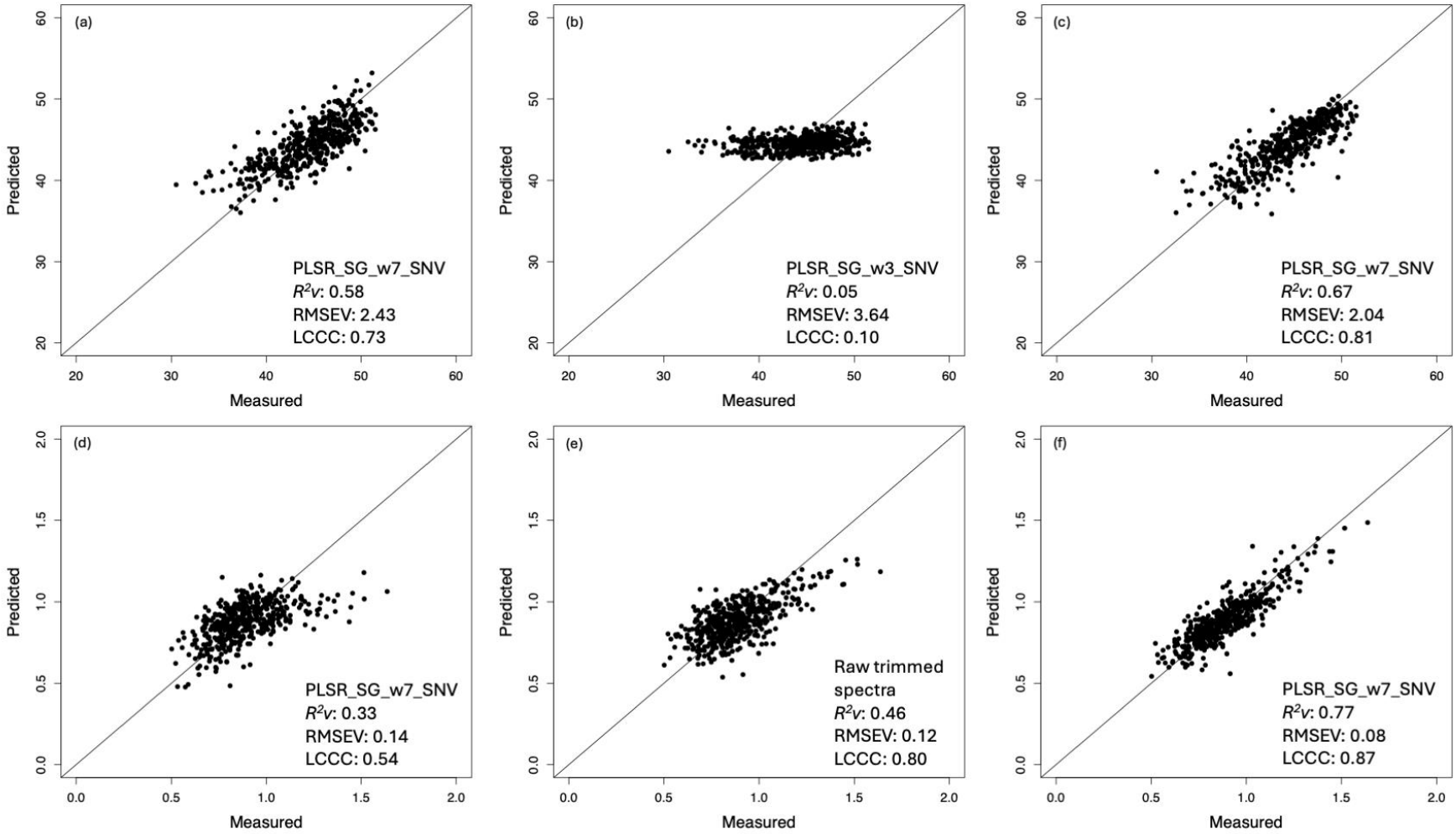

Figure 3.6: Validation results for predictions of total carbon (TC) and total nitrogen (TN) in decomposing litter mixtures from *in-situ* litterbag decomposition trial using synthetic mixtures and litterfall samples from Chapter 2 (Model 3; as a generalised model) with vis-NIR, NIR, and ATR-FTIR spectra. Scatterplots show laboratory measured values against the predicted values for the validation dataset. The top row shows the best-performing models for prediction of TC content using (a) vis-NIR; (b) NIR; and (c) ATR-FTIR spectra. The bottom row shows the best performing models for prediction of TN content using (d) vis-NIR; (e) NIR; and (f) ATR-FTIR spectra. In each panel, the solid line represents the 1:1 line. PLSR = partial least square regression; SG = Savitzky-Golay smoothing; *w* = window size; SNV = standard normal variate transformation; R^2v = coefficient of determination of validation model; RMSEV = root mean square error of validation model; LCCC = Lin's Concordance Correlation Coefficient.

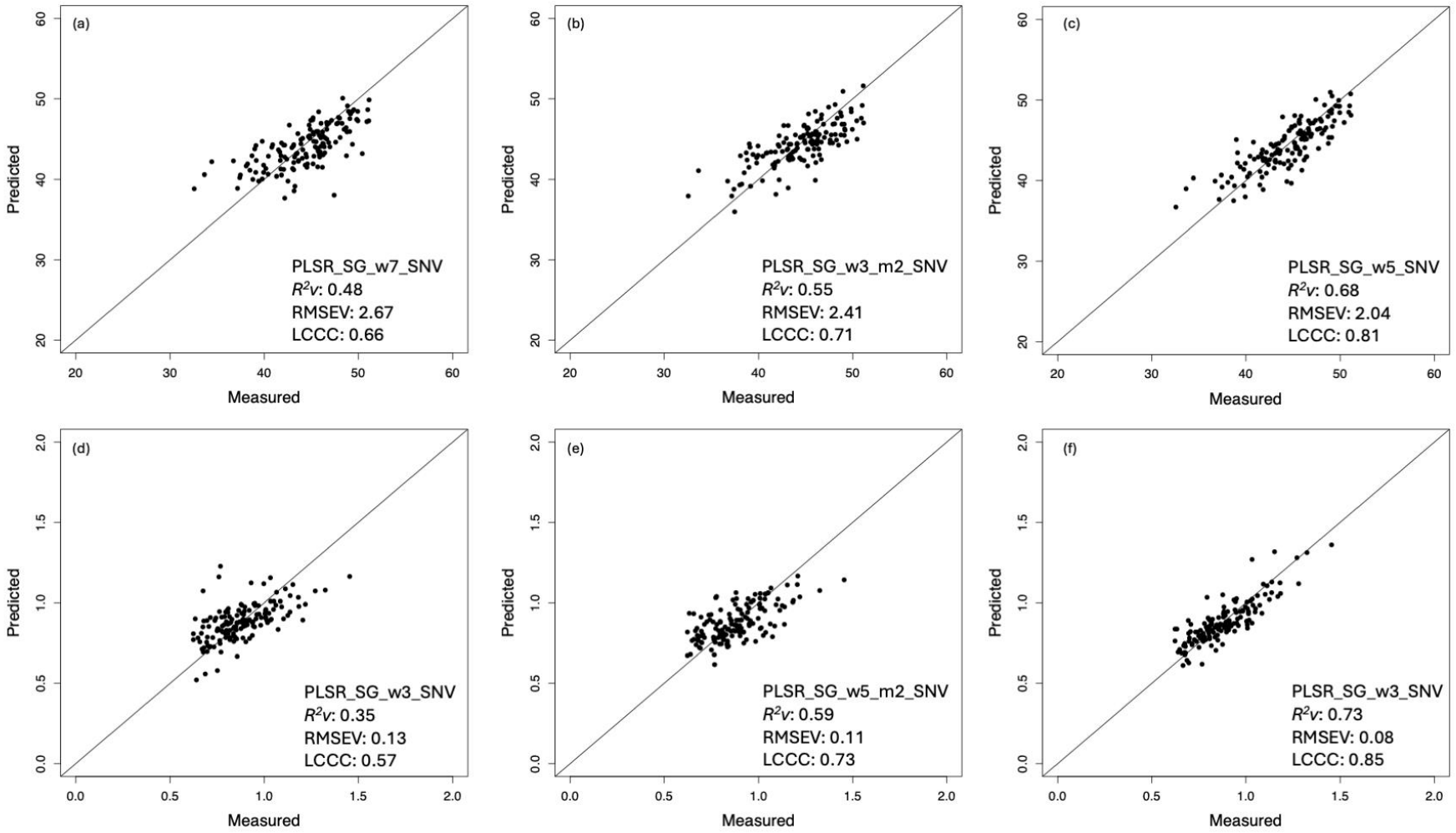

Figure 3.7: Validation results for predictions of total carbon (TC) and total nitrogen (TN) in decomposing litter mixtures from *in-situ* litterbag trial with vis-NIR, NIR, and ATR-FTIR spectra. Calibration models were developed using a train-test data split. Scatterplots show laboratory measured values against the predicted values for the validation dataset. The top row shows the best-performing models for prediction of TC content using (a) vis-NIR; (b) NIR; and (c) ATR-FTIR spectra. The bottom row shows the best performing models for prediction of TN content using (d) vis-NIR; (e) NIR; and (f) ATR-FTIR spectra. In each panel, the solid line represents the 1:1 line. SG = Savitzky-Golay smoothing; *w* = window size; *m* = order of derivatives; R^2v = coefficient of determination of validation model; RMSEV = root mean square error of validation model; LCCC = Lin's Concordance Correlation Coefficient.

3.4 Discussion

3.4.1 Fire history and litter quality

This study demonstrates that the carbon and nitrogen content of *Eucalyptus* leaf litter, understorey species, and decomposing litter present after a prescribed burning is distinctly different from that of samples collected prior to the burn. One year after fire, the TC content of litter was lower compared to those collected prior to fire, while the TN content was higher resulting in a lower C/N ratio. This pattern is consistent with the hypothesis that prescribed burning alters the chemical composition of the litter layer, which may subsequently affect the rate of litter decomposition and nutrient recycling. This pattern was also found for a DSF in southeastern Queensland, Australia, where *Eucalyptus* leaf litter collected after prescribed burning contained more TN and had lower C/N ratios (Butler et al., 2017a). However, repeated prescribed burning at 2-4 years intervals in *Eucalyptus* forests may increase litter C/N ratio (Butler et al., 2020). Fire-induced changes in understorey composition, microbial communities, and soil properties are expected to affect plant growth and subsequent litter chemical quality.

The response of understorey vegetation to prescribed burning and evidence for a putative increase in N availability in litter following fire varies across DSFs in Australia. For example, a study conducted by Bulter et al. (2017a) showed that the response of litter N content varied between the two *Eucalyptus* forests examined, reflecting the potential influence of site variability on post-fire responses. In other locations, the understorey layer of vegetation may be dominated by nitrogen rich *Acacia* spp. and bracken ferns which contribute to higher quality litter post-fire (Jenkins et al., 2016). It is widely assumed that litter from understorey vegetation, particularly nitrogen-fixing *Acacia* produce litter with higher N than *Eucalyptus* leaf litter. For example, in a long-term plantation forest, *Acacia mearnsii* had considerably higher initial N content than *E. globulus* leaf litter (Xiang and Bauhus, 2007). Although infrequent prescribed burning is unlikely to cause vegetation shift (Lewis and Debuse, 2012), in some forest types, it is likely to promote the regrowth of nitrogen-rich understorey species, leading to an increase in N in understorey litter. It should also be noted that freshly fallen litter tends to have higher TC content, whereas older litter may have a relatively lower nutrient content due to leaching and early decomposition processes (O'Connell, 1986).

3.4.2 Litter decomposition

Findings from this study are consistent with the general trend described above, where litter mixtures with an initial C/N ratio less than 60 showed a rapid mass loss in the first 91 days of *in-situ*

litterbag decomposition trial. This was particularly evident for the pure understorey litter collected prior to fire (PF EF100), which had the highest C/N ratio among all litter mixtures (Table 3.2) and the lowest mass loss after 91 days (Figure 3.2). In contrast, pure understorey litter collected 1-year after fire (1YAF EF100) had the lowest initial C/N ratio among all litter mixtures (Table 3.2) and the highest mass loss at Day 91 (Figure 3.2). This suggests that litter initial C/N ratio may explain the differences in litter mass loss in early decomposition of single-component litter. Initial litter C/N ratio has been used in other studies to understand early decomposition in litter mixtures. For example, Xiang and Bauhus (2007) reported that *Eucalyptus* litter with a higher initial C/N ratio decomposed significantly slower than *Acacia* litter and *Eucalyptus*:*Acacia* mixture (i.e., lower initial C/N ratio) over 110 days of incubation. Similarly in this study, litter mixtures with an initial C/N ratio less than 60 had mass loss comparable with 1YAF EF100 after 91 days of decomposition (Table 3.3; Figure 3.3). However, for both single-component and litter mixtures, the influence of initial litter C/N ratio appeared to diminish over time. Taken together, these results suggested that differences in mass loss among litter collected before and after fire can be attributed to initial chemical quality.

Regardless of mixture combinations, litter mass loss was greatest during the first stages of decomposition and then slowed down with little change over time. This pattern of mass loss is consistent with previous studies which reported a trend of rapid loss in many other *Eucalyptus* ecosystems (e.g., O'Connell, 1998; Guo and Sims, 1999; Crockford and Richardson, 2002; Ribeiro et al., 2002; Ferreira et al., 2021). While the greatest mass loss occurred between spring and early autumn (September 2023 to June 2024), continued rainfall and high soil moisture content during the summer months extended the latter stages of litter decomposition (Day 91 through to Day 274). This aligns with another study where cool and moist condition favoured microbial activity leading to a rapid rate of decomposition of *Eucalyptus* (Guo and Sims, 1999). In addition, some litter mass loss is likely due to sustained leaching of soluble materials (O'Connell and Menagé, 1982; O'Connell, 1986; Bernhard-Reversat, 1999).

Despite following a similar pattern, loss in dry weight of pure *Eucalyptus* leaf litter after 3 months (5-10%) was less than that of *in-situ* decomposition for the same period of time in a short rotation *Eucalyptus* forest (16-34%; Guo and Sims, 2002), and substantially lower than for incubation in a dry *Eucalyptus macrocarpa* forest (33%; Maheswaran and Attiwill, 1987). Mass loss reported here was also less than that after 4 months of *in-situ* decomposition in a mixed *Eucalyptus* forest (Crockford and Richardson, 2002) and decomposition of *Eucalyptus* litter under laboratory microcosm conditions (37%; Briones and Ineson, 1996).

Decomposition of *Eucalyptus* litter is relatively slow due to high C/N and lignin/N ratios, as well as the presence of essential oil and tannins (Wood, 1974; Adams and Attiwill, 1986). Differences

in mass loss during decomposition may also be related to the species examined, climate, fire history, and initial litter chemical quality (e.g., Coûteaux et al., 1995; Zhang et al. 2008). Rate of litter decomposition has also been attributed to microbial community, which exerts strong influences on a local scale (e.g., Zhang et al., 2008; Krishna and Mohan, 2017). In relation to this study, the home field advantage hypothesis (HFA) suggests that litter decomposes more rapidly in its native ecosystem due to interactions between site-specific (locally adapted) soil microbial communities and environmental factors such as climate, soil properties, and microclimate (Gholz et al., 2000). Although the HFA in litter decomposition is not always evident (e.g., Bachega et al., 2016; Bani et al., 2019; Song et al., 2019), and was beyond the logistical scope of this study, relocating litter from its native habitat to another ecosystem can alter litter mass loss through several mechanisms. For example, in this study, forest litter may have decomposed more slowly than if it were in a forest location due to differing microbial communities, the absence of understorey shading, interaction with weeds. However, at this stage, there is not enough evidence to attribute differences in litter mass loss among studies to a single factor.

Other factors such as litter age and particle size, mesh size, and material used for the litterbag, and the season of litterbag installation may also have influenced litter mass loss and nutrient release (O'Connell and Menagé, 1982; Toberman et al., 2014; Krishna and Mohan, 2017). There is no standard protocol for litterbag experiments and decomposition studies have employed a range of styles of litterbags and litter components. For example, many studies have used freshly senescent *Eucalyptus* leaves collected using litterfall traps (O'Connell, 1986; O'Connell, 1988; Crockford and Richardson, 2002; Ribeiro et al., 2002; Xiang and Bauhus, 2007; Toberman et al., 2014; Ferreira et al., 2021; Rachid et al., 2023) or from the forest floor (Briones and Ineson, 1996; Guo and Sims, 2002; Skorupa et al., 2015; Butler et al., 2020; Baietto et al., 2021). *Eucalyptus* litter collected from the forest floor may have already gone through soluble carbon release without showing any signs of damage (Bernhard-Reversat, 1999) and would be expected to decompose more slowly than fresh leaf litterfall materials (Toberman et al., 2014).

The mesh size of litterbags is an important factor controlling the rate of litter decomposition. Krishna and Mohan (2017) concluded that a mesh size of 1-2 mm is the most suitable for litterbag decomposition studies as it allows the entry of microbes, microfauna, as well as the leaching of organic compound (Bradford et al., 2002; Bokhorst and Wardle, 2013; Xie, 2020). Despite this, litterbag mesh size still varies greatly among studies, typically ranging from 0.1-4.0 mm. In the present study, litterbags with a mesh size of 0.53 mm may have restricted the movement of some microbes and limited the entry of macrofauna. The relatively fast decomposition rate reported in other studies may be, in part, due to the use of litterbags with a larger mesh size (e.g., O'Connell, 1988;

Guo and Sims, 2002; Butler et al., 2020; Ferreira et al., 2021), which allow the access of macrofauna and the loss of litter fragments during decomposition. Mass loss of *Eucalyptus* litter in fine mesh bags (0.2 mm) was 5% less than for litter in coarse mesh bags (3 mm) after 18 months of *in-situ* decomposition (O'Connell and Menagé, 1982). This difference in mass loss highlights the importance of carefully considering litterbag mesh size and that caution is required when comparing litter mass across studies that employed different litterbag mesh size.

3.4.3 Litter decomposition and nutrient cycling

Temporal patterns of change in litter chemical quality during *in-situ* decomposition trial in this study agree with the general picture of a decline in TC over time (e.g., Maheswaran and Attiwill, 1987; Ribeiro et al., 2002; Goya et al., 2008; Toberman et al., 2014; Butler et al., 2020). Similarly, substantial increases in TN, phosphorus, calcium, and magnesium have been found during decomposition of *Eucalyptus* litter (O'Connell, 1988; Guo and Sims, 2002; Goya et al., 2008). Nitrogen in litter increases during decomposition and leads to a subsequent decrease in litter C/N ratio under both long-unburnt and recently burnt regimes (Maheswaran and Attiwill, 1987; Ribeiro et al., 2002; Goya et al., 2008; Toberman et al., 2014; Butler et al., 2020). At the end of the decomposition process, low C/N ratios indicate potential nitrogen immobilisation, a common characteristic of *Eucalyptus* forests in Australia (Adams and Attiwill, 1986; Corbeels et al., 2003). This is partly due to differences in soil nutrient content among sites, where soils in long-unburnt sites often have high N content compared to frequently burnt sites, suggesting less N resorption by plants which then accumulates in the litter (Wright and Westoby, 2003; Butler et al., 2020).

Litter mass loss was more rapid in litter mixtures (two- and three-component litter mixtures) compared with single-species litter decomposition. This supports the notion of synergistic effects of litter mixtures leading to faster than average decomposition (Gartner and Cardon, 2004; Xiang and Bauhau, 2007; Cuchietti et al., 2014; Liu et al., 2020). For example, the presence of *Acacia* litter facilitated the decomposition of *Eucalyptus* litter which was otherwise constrained by relatively low N concentration (Xiang and Bauhau (2007). Mixing *Eucalyptus* litter with *Acacia* with a low C/N ratio enhanced N mineralisation through nutrient transfer during the initial stage of decomposition. This was further supported by the initial mass loss and TN enrichment found in *Eucalyptus* and *Acacia* litter mixtures. Accelerated mass loss, enhanced N mineralisation, and increases in K and Ca concentration were also reported when *Eucalyptus* decomposed in mixture with European broad-leaved tree species (Briones and Ineson, 1996). These patterns are supposed to be the result of nutrient transfer from high quality to low quality litter which can facilitate the overall decomposition rate

(Schimel and Hättenschwiler, 2007; Schimel et al., 2007; Ferreira et al., 2012). Several studies have suggested that N transfer is mainly through leaching and microbial activity, particularly involving fungal mycelia (Briones and Ineson, 1996; Schimel et al., 2007; Lummer et al., 2012). However, the underlying mechanisms of nutrient transfer among litter of different quality are complicated and yet to be resolved.

Decomposition studies focusing solely on single-component litter may underestimate the temporal variations in litter mass loss and overall nutrient dynamics. While a substantial amount of C is released during litter decomposition the pattern of loss is generally universal among litter components. The dynamics of N in decomposing litter is more complex, especially in litter mixture where N from high quality can transfer to low quality to enhance the overall rate of decomposition. This emphasises the importance of considering the role of other dominant litter types in the ecosystems when investigating the decomposition of *Eucalyptus* litter in fire-affected ecosystems, with implications for nutrient cycling and fire behaviour under the current climate.

3.4.4 Performance of vis-NIR, NIR, and ATR-FTIR spectroscopy

In this study, decomposing litter mixtures were used an as external independent test dataset (also known as external validation) to evaluate the performance of the calibration model developed in Chapter 2 and its accuracy in predicting the chemical quality of a set of unknown litter samples. This provides an unbiased evaluation of the generalisation of the model for wider application. External validation has been recognised as a crucial step in building a robust calibration model (e.g., Chodak, 2008; Esbensen and Geladi, 2010), but it is not widely practiced owing in part to economic and time constraints. External validation often requires sampling from an independent study site, as well as providing an additional effort in sample preparation and spectral screening. Many studies used internal train-test splitting (e.g., 70:30 random splitting) and it has become a common validation practice (e.g., McLellan et al., 1991b; Ferreira et al., 2018). In some cases, only cross-validated results were reported (e.g., Joffre et al., 1992; Gillon et al., 1999). These practices may lead to heavily biased results (i.e., artificially good validation results) due to fitting the calibration model with highly similar datasets. This raises the question of whether a calibration model built using representative samples (i.e., generalised model) is sufficient to predict the properties of interest in a set of new samples. In this context, the following discussion focusses on whether the model constructed in Chapter 2 could be confidently applied across a wide variety of plant species and plant materials or a sample-specific model is required to achieve acceptable accuracy.

This study demonstrated that attenuated total reflectance Fourier transform infrared (ATR-FTIR) can predict the general patterns of change in TC and TN in decomposing litter mixtures (Table 3.8). Specifically, the performance of the ATR-FTIR calibration model developed using synthetic mixture and litterfall (Model 3; developed in Chapter 2; Table 3.8; Figure 3.6) and the model developed using train-test split (Model 4; Table 3.8; Figure 3.7) for N prediction were highly similar. Interestingly, cross-validation results indicated that the generalised model (Model 3) provided slightly more accurate N predictions than the sample-specific model (Model 4). This was unexpected as a generalised model is assumed to perform less well than a sample-specific model. This may be because the generalised model (Model 3) incorporated a much larger validation dataset than the sample-specific model (Model 4) which relied on internal data splitting. Although the generalised model (Model 3) showed considerable predictive ability for TN content, its performance for predicting TC was not promising. This is because the cross-validation results did not fall within the acceptable range, suggesting an inaccurate prediction for TC. This is consistent with earlier findings, where the use of synthetic mixtures and litterfall with vis-NIR and NIR spectroscopy also performed poorly in TC prediction (see Section 2.3.2).

The generalised ATR-FTIR calibration model developed in Chapter 2 was found to be reliable for TN prediction and it can be concluded that it can be applied to various forms of *Eucalyptus* litter with acceptable accuracy. However, its use for TC prediction remains uncertain and requires further validation to confirm its reproducibility and reliability. Nevertheless, it was demonstrated that ATR-FTIR has strong potential to support the development of a universal calibration for predicting nitrogen content. In this case, constructing sample-specific calibration models may not be necessary. The notion that a generalised, well-calibrated ATR-FTIR model could be used to efficiently predict N in *Eucalyptus* litter materials has great value for forest management and ecological research.

In contrast to ATR-FTIR spectroscopy, the vis-NIR and NIR model developed in Chapter 2 did not reliably predict TC and TN content in decomposing litter. Several studies have obtained excellent prediction accuracy for TC and TN in decomposing leaf litter from various species using NIR spectroscopy (e.g., McLellan et al., 1991b; Joffre et al. 1992). This discrepancy could be due to the relatively narrow spectral range and the use of a synthetic mixture which may not have captured the important absorbance bands associated with to the TC and TN content in decomposing litter. In response, the usefulness of predictive models developed using vis-NIR, NIR, and ATR-FTIR will be explored further in the following chapter using the context of thermal decomposition rather than biological decomposition of litter.

Chapter 4

Understanding thermal decomposition of *Eucalyptus* litter using spectroscopy

---

4.1 Introduction

The increase in bushfire frequency and intensity under climate change (Di Virgilio et al., 2019; Bowman et al., 2020; Abram et al., 2021; van Oldenborgh et al., 2021) has led to an increased use of prescribed burning to mitigate the impacts of fire on humans and the environment (Price et al., 2022). From a management perspective, prescribed burning is an effective tool for mitigating bushfire risk through fuel load reduction (Bowman et al., 2011; McCaw, 2013; See Chapter 1.1.6). Although prescribed fires are generally of lower intensity than bushfires, they are often implemented more frequently with a fire return interval from 3 to 12 years, depending on forest type, to maintain fuels at low hazard level (e.g., Guinto et al., 2001; Butler et al., 2020; Penman et al., 2011; Price et al., 2022; also see Chapter 1). For example, prescribed burning in dry sclerophyll forests (DSFs) is typically conducted on a 3-4 year cycle (e.g., Guinto et al., 2001). Over the long-term, repeated fires can have ecological consequences through changes in vegetation communities (e.g., Lewis et al., 2012; see Chapter 3), soil properties, and nutrient dynamics (e.g., Close et al., 2011; Guinto et al., 2011; Bennett et al., 2014; Muqaddas et al., 2016; Butler et al., 2017a).

While effective in reducing fuel loads, prescribed fire can substantially influence soil organic matter and litter nutrient dynamics (Guinto et al., 2011; Certini, 2005; Goforth et al., 2005; Knicker, 2007; Muqaddas et al., 2019). During a fire, large quantities of C and N stored in vegetation, litter, and soil are released to the atmosphere through volatilisation and mineralisation, resulting in shifts in ecosystem C and N stocks (Raison et al., 1985a; Flannigan et al., 2009; Cheng et al., 2013; Possell et al., 2015). For example, the increased use of prescribed burning to reduce fire hazard has led to declines in total ecosystem C stock in Wombat State Forest, a DSF in Victoria, Australia (Bennett et al., 2014; also see Chapter 2 for site description). Similarly, long-term prescribed burning has negatively influenced C dynamics in wet sclerophyll forest (WSF) in Queensland, through alterations to litterfall dynamics and soil properties (Butler et al., 2020; Muqaddas and Lewis, 2020). Quantifying fire-induced C and N loss remains a challenge due to the spatiotemporal heterogeneity of fuel structure and fire behaviour (e.g., Bradstock et al., 2010; Gould et al., 2011; Matthews et al., 2012).

Since the quantity and composition of fuel prior to fires are often unknown, one approach to estimate the changes in C and N is to quantify the amount and characteristics of combustion residues – char and ash.

Following a fire, a heterogeneous layer of combustion residues composed of organic and inorganic materials is deposited on the soil surface, ranging from C-rich char and charcoal to mineral-rich ash (Bodí, 2014; Sánchez-García et al., 2023). The chemical quality, morphology, and colour of these residues vary markedly as a function of (1) fuel load, (2) fuel type, and (3) combustion completion (Bodí, 2014; Safdari et al., 2018; Sánchez-García et al., 2023). Combustion completeness refers to the degree of which organic material is oxidised during combustion and is primarily controlled by combustion temperature and duration (Bodí, 2014).

For a given fuel load and fuel type, plant biomass initially undergoes drying and partial thermal degradation at low temperatures (≤ 100 °C), with minimal chemical transformation. As temperature increases under oxygen-limited conditions (~250-450 °C; lower combustion completeness), thermal degradation intensified, and biomass undergoes pyrolysis and smouldering combustion. Progressive pyrolysis results in the formation of a continuum of C-rich organic residues, ranging from slightly charred materials to char and charcoal (Schmidt and Noack, 2000; Masiello, 2004; Bodí, 2014; Safdari et al., 2018).

In the literature, the term ‘char’ and ‘charcoal’ are sometimes used interchangeably, however, in some contexts, char often refer to residues that are pyrolysed to a lesser degree than charcoal (Han et al., 2020). In this context, char retains some of its structure, whereas charcoal is chemically and physically more distinct from its parent biomass due to a higher degree of aromatic condensation (Masiello, 2004). Collectively, C-rich organic residues from pyrolysis are often referred to as pyrogenic carbon (PyC) or black carbon (BC) (Schmidt and Noack, 2000; Masiello, 2004). Since the chemical reactions governing pyrolysis are beyond the scope of this study, the term ‘char’ is used to describe the continuum of pyrogenic carbon described above, this includes slightly charred materials, char, and charcoal.

Under high combustion completeness (> 450 °C), where carbon is highly volatised, biomass burning can result in inorganic, white, powdery ash (Goforth et al., 2005; Gray and Dighton, 2006; Pereira et al., 2012; Bodi, 2014; Sánchez-García et al., 2023). Ash is generally alkaline and rich in cations and nutrients such as phosphorus and calcium with little nitrogen due to its high susceptibility to volatilisation at high temperature (Raison et al., 1985a; Pitman, 2006; Úbeda et al., 2009; Hogue and Inglett, 2012; Yusiharni and Gilkes, 2012; Bodi, 2014; Sánchez-García et al., 2023). As temperatures increase, pH and electrical conductivity (EC) of ash also increases (Úbeda et al., 2009;

Pereira et al., 2012; Bodi, 2014; Sánchez-García et al., 2023). The deposition of ash on the soil surface can therefore temporarily increase soil pH and cation availability (Khanna et al., 1994; Guinto et al., 2011; Bodí, 2014). Despite the loss of soil organic matter, fire can provide a short-term nutrient pulse through ash deposition, commonly referred to as the 'ash-bed effect' (Chambers and Attiwill, 1994; Certini, 2005; Gray and Dighton, 2005; Úbeda et al., 2009, Pereira et al., 2014; Agbeshie et al., 2022).

Characteristics of ash, particularly colour and nutrient content, are useful indicators of fire behaviour (Goforth et al., 2005; Úbeda et al., 2009; Dūdaitė et al., 2011; Pereira et al., 2012; Bodi, 2014; Sánchez-García et al., 2023). For example, ash colour has been associated with nutrient content and pH (Pereira et al., 2012) with the prevalence of lighter coloured ash and higher pH indicating greater fire intensity. Arguably, ash colour has limited usefulness in field observations because the structure of surface fine fuel is complex, and combustion completeness often varies spatially and temporally. Low-intensity prescribed burning often results in the formation of a heterogeneous layer of ash with lighter-colour ash deposited over charred materials (Bodí, 2014), making it difficult to assess ash nutrient content and fire severity solely on ash colour.

Sampling ash after fire is challenging due to safety concerns, ash mobility, rapid redistribution, and incorporation into the soil (Bodí, 2014; Sánchez-García et al., 2023). To address this, laboratory-based muffle furnaces have been used extensively to stimulate ash production under controlled temperature and oxygen conditions (Raison et al., 1985a; Gray and Dighton, 2006; Lammers et al., 2009; Qian et al., 2009; Úbeda et al., 2009; Galang et al., 2010; Gabet and Bookter, 2011; Mukherjee et al., 2011; Hogue and Inglett, 2012; Constantine et al., 2021; Myers-Pigg., 2024). However, laboratory produced char and ash do not fully represent those produced from naturally occurring fires due to restriction on oxygen availability and combustion conditions, which can influence combustion completeness and, consequently, the extent of thermal alteration (also known as charring intensity) (e.g., Hogue and Inglett, 2012; Kaal et al., 2012; Santín et al., 2017; Belcher et al., 2018; Constantine et al., 2021). For example, a study conducted by Santín et al. (2017) indicated that charcoal derived from natural fire has more a condensed aromatic structure than that produced from combustion in a laboratory muffle furnace. In addition, combustion of single-species fuels using a muffle furnace does not capture the complexity of the forest floor which is comprised of litter from multiped plant species that lay horizontally and vertically (e.g., Hogue and Inglett, 2012; Constantine et al., 2021). Despite the above limitations, the use of laboratory muffle furnace offers a consistent and replicable method for exploring the comparative effects of combustion temperature on the chemical and physical characteristics of char and ash (e.g., Raison et al., 1985a; Gray and Dighton, 2006; Hogue and Inglett, 2012; Constantine et al., 2021).

A key challenge remains in characterising the chemical composition of combustion residues in a quick and reliable manner. As discussed previously (see Chapter 2 and 3), determining the chemical quality of litter using laboratory analysis for measuring C and N content is expensive and time-consuming. Spectroscopy has the advantage of being low-cost and reliable. Although visible-near-infrared (vis-NIR), near-infrared (NIR) and mid-infrared (MIR) spectroscopy are widely used to study the changes in litter C and N during natural decomposition (Gillon et al., 1999; Parsons et al., 2011; McKee et al., 2016; Steinwandter et al., 2019), there are comparatively few studies exploring the application of spectroscopy for predicting the properties of char and ash derived from plant materials. Previous studies that have used spectroscopy to characterise combustion residues have primarily focused on analysing and interpretating specific features of ash including wettability (Dlapa et al., 2013), carbohydrate chemistry (Lammers et al., 2009), and chemical quality of charcoal (Minatre et al., 2024). Other studies have used FTIR spectroscopy to analyse the properties of charcoal derived from fire (e.g., Guo et al., 1998; Ramalho et al., 2017; Constantine et al., 2021; Ryan et al., 2024; Ryan et al., 2025), but not from controlled combustion trials. Collectively, these studies highlight the potential of FTIR spectroscopy as an effective technique to determine the chemical quality of combustion residues (i.e., char and ash) derived from prescribed burning, bushfires, and under laboratory conditions.

4.1.1 Objective and research questions

With future climate projection indicating an ongoing need to increase the use of prescribed burning for risk mitigation, DSFs in Australia will remain as a complex mosaic of forest ages and regeneration states. This raises the important question of whether fire history affects the chemical quality of ash produced during fire in dry sclerophyll forests. To address this, the following research questions were formulated:

1. Does litter type (leaves, twigs, and surface fine fuel) and fire history (long-unburnt and recently burnt) influence litter mass loss at different combustion temperatures?
2. How does C and N in litter change during combustion?
3. Can vis-NIR, NIR-, and ATR-FTIR spectroscopy be used to predict C and N content in combustion residues produced across a temperature gradient?
4. How transferrable are calibration models developed for predicting C and N in litter? Can they predict the chemistry of combustion residues or is a sample-specific calibration model required for accurate predictions?

A laboratory-based combustion experiment was done using a muffle furnace to simulate temperatures reached during prescribed burning (200, 300, 400, 500, 600 °C). This combustion temperature profile was determined based on a study conducted by Watton et al. (2012) where the flame temperature of fires in Australian DSFs was 300-400 °C. However, in the natural environment, flame temperatures of a prescribed burn can vary according to air temperature, humidity, fuel load, and fuel structure (e.g., Sullivan et al., 2012). The temperature range used in this study aimed to capture a wider range of possible fire temperatures during prescribed burning.

In this study, *Eucalyptus* leaf, twigs, and surface fine fuel litter from two long-unburnt forests (> 15 years) and a recently burnt forest (approximately 4 years) were used to represent the dominant components of the surface fine fuel layer. Samples were analysed using vis-NIR, NIR, and ATR-FTIR spectroscopy to predict TC and TN content of combustion residues (see Chapter 2 and 3). The best performing calibration models from previous studies (i.e., models developed in Chapter 3) were used to assess their applicability and robustness. Another set of calibration models were developed using combustion residues produced from muffle furnace combustion and evaluated using an external independent test dataset. The purpose of this approach was to determine whether a generalised model is sufficiently robust for broader application or if sample-specific calibration is required for reliable estimation of TC and TN content in combustion residues.

4.2 Materials and methods

4.2.1 Sample collection

Long-unburnt sites

Bulk samples of litter were collected from long-unburnt areas in Wombat State Forest (33°41’S, 114°46’E) and Orbost State Forest (37°30’S, 148°45’E), Victoria, Australia in December 2018 (summer). Detailed description of the site characteristics of Wombat State Forest (Wombat SF) and Orbost State Forest (Orbost SF) can be found in Chapter 2 (see Section 2.2.1). In brief, surface fine fuel litter (here after surface fine fuel) was collected using a circular litter ring (0.1 m^2 area) within established plots. Samples were dried in a fan-forced oven (60 °C for a minimum of 48 h; Model TD-78T-2-D, Thermoline Scientific, Wetherill Park, NSW, Australia) and sorted into fractions, including overstorey *Eucalyptus* leaves (hereafter referred to as leaf litter), bark, twigs, and fine fuel litter. Sorted samples were stored in labelled paper bags in a cool dry environment in the laboratory until required.

Recently burnt site

Surface fuel litter including leaves, twigs, bark and surface fine fuel (see Section 1.1.7 for definitions of surface fuel litter and surface fine fuel) was collected from a completely independent site in Big Bit Road (BBR), Boyne State Forest, south-eastern New South Wales, Australia (35°62'S, 150°24'E) in April 2024 (mid-autumn). The sampling area was located on the boundary between two logging compartments along an access road (Durras Road). Prior to the 2019/20 Black Summer bushfires, this area was considered as long-unburnt, with the last recorded fire event being a prescribed burning in 1986-1987. The fire at this location was classified as moderate to high severity, with partial to complete canopy scorch and partial canopy consumption (NSW Government Data Portal - SEED, 2025). At the time of sampling, the site was classified as 4 years after high-moderate severity bushfire with regrowth of both overstorey and understorey vegetation (Figure 4.1a).

The Boyne State Forest covers an area of 6,400 hectares and forms part of a large contiguous area of forest managed by state government agencies and private landholders. The sampling site was located at 168 m above sea level (a.s.l). The region is characterised as a temperate climate with warm to hot summers, cool winters, and high precipitation throughout the year. Long-term (1991-2024) monthly mean maximum and minimum temperatures are 21.8 °C and 10.0 °C, respectively; the long-term (1985-2024) average monthly precipitation is 919 mm (Australian Bureau of Meteorology, 2024; weather station: 069134). The forest is broadly classified as open tall (15-25 m tree height) dry sclerophyll forest, dominated by *Corymbia maculata* (Spotted Gum), *Eucalyptus pilularis* (Blackbutt), *E. paniculata* (Scattered Grey Ironbark), *E. globoidea* (White Stringybark), *E. consideniana* (Yertchuk) and *E. gummifera* (Bloodwood) (Rueegger et al., 2018). Understorey vegetation is dominated by Burrawang (*Macrozamia communis*), *Acacia decurrens* (Black Wattle), *A. longissimi* (Narrow-leaf Wattle), *A. falciformis* (Broad-leaf Hickory), Bracken Fern (*Pteridium esculentum*), and grasses.

To characterise surface fuel litter and elevated fuel (live biomass above the surface) at Big Bit Road (BBR), samples were collected from within a circular steel ring (0.1 m^2 area) placed randomly throughout the study area (Figure 4.1b). At each sampling point, topsoil samples (0-10 cm) were also collected using a steel soil core (5.5 cm radius) and stored in labelled plastic bags (Figure 4.1b). A total of 19 surface fuel litter and topsoil samples were collected from the site. Surface fuel samples (n = 19) were dried at 60 °C for a minimum of 48 h in a fan-forced oven (Model TD-78T-2-D, Thermoline Scientific, Wetherill Park, NSW, Australia), sorted into fractions including leaf litter, twigs, bark, understorey litter, elevated fuel (live biomass), and surface fine fuel litter (< 9 mm in diameter; FF). Sorted samples were stored in labelled paper bags in an ambient condition in the laboratory until required. An additional set of bulk surface fuel litter (i.e., leaf litter, twigs, and bark)

were collected for combustion studies within the sampling area, sample were oven-dried at 60 °C for a minimum of 48 h in a fan-forced oven.

Figure 4.1: (a) The sampling area in Big Bit Road (BBR), Boyne State Forest, south-eastern NSW, Australia (35°62'S, 150°24'E). The area was dominated by dense *Acacia* spp. and *Eucalyptus* regrowth after the 2019/20 Black Summer bushfires; (b) A steel ring (0.1 m^2 area) was placed in randomly selected locations along either side of the access track and surface fuel litter and soil were collected from within the ring.

4.2.2 Soil analysis

Soil samples were air-dried, passed through a 1 mm sieve, and analysed for total carbon (TC) and total nitrogen (TN) by dry combustion method (Elementar Vario Max CNS Analysensysteme GmbH, Hanau, Germany). Soil acidity (pH) and electrical conductivity (EC) of topsoil were measured at a soil:water ratio of 1:5 using a pH (SevenCompact^{TM} S210, Mettler Toledo, Columbus Ohio, United State) and EC meter (SevenCompact^{TM} S230, Mettler Toledo). Approximately 2 g of air-dried soil was added with 10 mL of deionised water, shaken for 1 h, and left to settle for 15 min prior to measurement.

4.2.3 Laboratory-based combustion of surface fuel litter

All surface fuel litter samples (leaf litter, twigs, and surface fine fuel) from Wombat SF, Orbost SF, and BBR were cut to 1-2 cm pieces to maximise sample homogeneity prior to combustion, dried at 60 °C for a minimum of 48 h in a fan-forced oven (Model TD-78T-2-D, Thermoline Scientific, Wetherill Park, NSW, Australia) and stored in the oven until required. Sub-samples of each surface fuel litter (approximately 5 g, n = 8) were weighed into aluminium foil trays and stored in a desiccator

to prevent moisture absorption from the atmosphere. Foil trays containing samples were placed in a rectangular steel tray (14 x 5 x 2 cm) and introduced to the muffle furnace (Muffle furnace; CEMLL-SD; LABEC, Sydney, Australia) once it had reached the desired temperature (Figure 4.2a). For each litter type, a total of five batches (n = 5) were combusted at 200, 300, 400, 500, and 600 °C for 1 h. To account for the small-scale spatial variation in temperature distribution within the muffle furnace, samples were arranged in two rows, with a total of eight samples in each batch (Figure 4.2a). Consequently, each litter type at each temperature had a total of 40 replicates (5 runs x 8 samples per batch). A total of 1,800 residues samples were obtained (3 locations x 3 fuel types x 5 temperatures x 8 replicates x 5 batches). A subset of unburnt, air-dried samples of each litter type was used as a control. Samples were removed from the muffle furnace, carefully transferred to a desiccator, cooled until safe to handle and reweighed to obtain mass loss. Cooled samples were stored in labelled plastic bags for further analysis.

The proportional mass loss (%ML) after combustion in the muffle furnace was calculated using the equation:

$$\%ML \frac{Initial\ mass\ (g) - final\ mass(g)}{Initial\ mass\ (g)} x\ 100\% \qquad \text{Equation 4.1}$$

Average mass loss of each surface fuel litter at each combustion temperature was calculated (n = 40).

4.2.4 Statistics analysis

Statistical analyses were conducted using Jamovi (Version 2.6.17.0, 2025, The Jamovi Project, Sydney, Australia). Data from missing samples were removed from the dataset to protect the statistical power and reduce bias.

One-way analysis of variance (One-way ANOVA) was used to test differences in % litter mass loss among each surface fuel litter at each combustion temperature. Where statistically significant effects were detected ($\alpha = 0.05$), pairwise comparisons among groups were conducted using Games-Howell Post-Hoc test.

Linear mixed models (LMMs) were used to test the effects of site (forest location: Wombat SF, Orbost SF, BBR), litter types (leaf litter, twigs, and surface fine fuel), combustion temperatures (200, 300, 400, 500, 600 °C), and their combined effects on litter mass loss (n = 1,800). For all models, percentage mass loss (%ML) were treated as the response variable, while site of origin, litter types, and combustion temperature were considered as fixed effects. Batch effects and positional effects

were considered as random effects to account for the variation between batches and the variation between positions within batch, respectively. The impact of batch effects and positional effects on litter mass loss were assessed separately and in combination. The model fit was assessed using marginal R^2 and conditional R^2. Marginal R^2 indicates the proportion of variance explained by fixed effects, while the conditional R^2 indicates the variance explained by both fixed and random effects.

4.2.5 Formation of composite samples

To account for the effects of small-scale variation in temperature distribution within the muffle furnace, samples on the opposite end were paired to form a composite sample (hereafter combustion residues) to minimise any potential bias. In each batch, sample 1 was paired with sample 6, sample 2 was paired with sample 5, sample 3 was paired with sample 4, and sample 7 was paired with sample 8 (Figure 4.2b). Each pair was ground together using a mortar and pestle to pass through a 1 mm sieve. After pairing, the number of samples was reduced by half (n = 900).

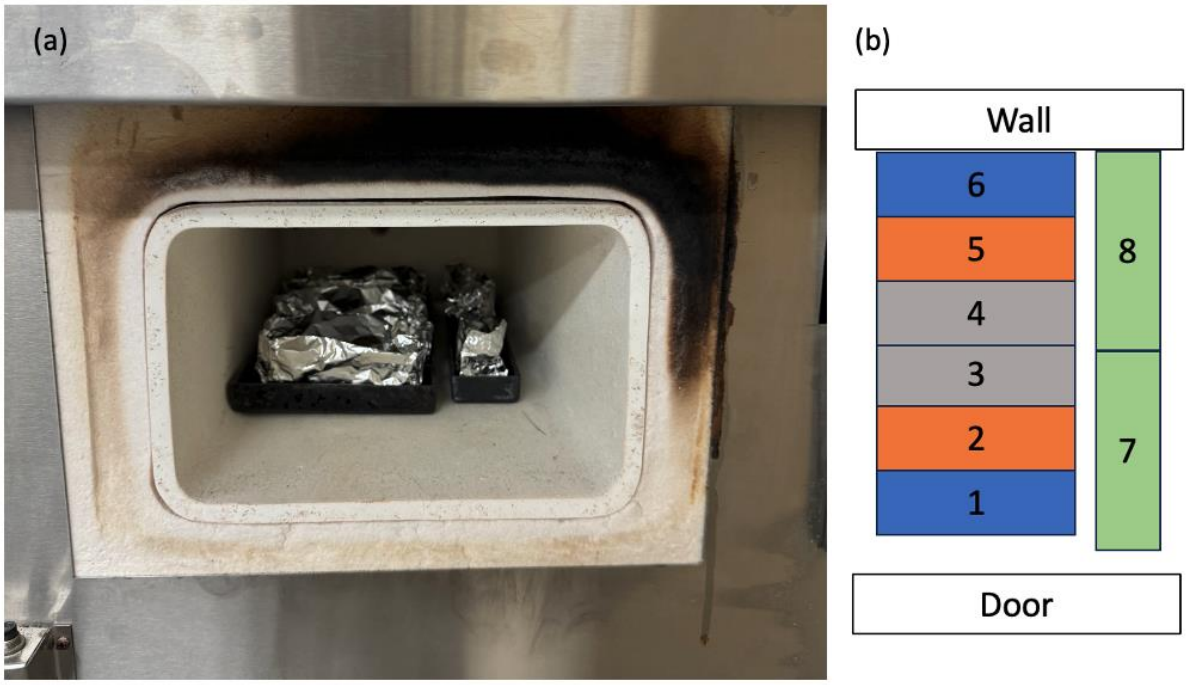

Figure 4.2: The arrangement of samples inside the muffle furnace. (a) Approximately 5 g of samples were weighed into aluminium foil trays (open top) and placed in a rectangular steel tray to allow airflow; (b) Schematic of the arrangement of samples inside the muffle furnace. In each batch, a total of eight samples were combusted (n = 1,800 samples in total). Samples on the opposite end were combined to form a composite sample (n = 900; hereafter combustion residues) to account for variation in furnace temperature during combustion. The colour coding represents the pairing system, sample with the same colour were ground together to pass through a 1 mm sieve for spectra and chemical analysis.

4.2.6 Total carbon and total nitrogen after combustion

An estimation of change in total carbon (TC) and total nitrogen (TN) content in surface fuel litter after combustion was made by comparing the TC and TN content before and after combustion. To do this, a subset (n = 5) of unburnt leaf litter, twigs, and surface fine fuel litter from Wombat SF, Orbost SF, and BBR were ground using a food-grade grinder (Breville Coffee and Spice Grinder; BCG200BSS; Breville Pty, Sydney, Australia), passed through a 1 mm sieve and stored in labelled plastic bags prior to laboratory analysis.

Total C and TN (% dry mass) content of unburnt litter (n = 5 per litter type) and combustion residues were determined using an Elementar analyser (Elementar Vario Max CNS, Analysensysteme GmH, Hanua, Germany). Mean TC and TN of unburnt surface fuel litter (n = 5 per litter type) were used as reference values (expressed as % dry mass). Initial TC and TN (g) in unburnt litter were calculated by converting reference value to mass fraction (divided by 100) and multiplied by the initial sample mass (Equation 4.2).

$$Initial\ TC/TN\ (in\ g) = \left(\frac{Reference\ value\ (\%\ dry\ mass)}{100}\right) \times Initial\ sample\ mass\ (g) \quad \text{Equation 4.2}$$

The TC and TN content (g) in ash composite were calculated using the same approach but based on the weight of composite sample:

$$\left(\frac{Reference\ value\ (\%\ dry\ mass)}{100}\right) \times Weight\ of\ combustion\ residues\ (g) \quad \text{Equation 4.3}$$

The percentage of TC and TN content remaining (%) after combustion was calculated using as the ratio of TC or TN content (g) in composite samples to initial content (g) in unburnt litter:

$$\left(\frac{TC\ or\ TN\ in\ composite\ sample\ (in\ g)}{Initial\ TC\ or\ TN\ (in\ g)}\right) \times 100\% \quad \text{Equation 4.4}$$

One-way analysis of variance (ANOVA) was conducted to test (1) difference in initial litter quality among study sites, and (2) differences in total carbon (TC) and total nitrogen (TN) remaining after combustion. Where statistically significant effects were detected ($\alpha = 0.05$), pairwise comparisons were conducted using Games-Howell Post-Hoc test to identify difference between variables tested.

4.2.7 Spectral and chemical analysis

Spectral scanning and pre-processing

Spectral scans of composite residues using visible-near-infrared (vis-NIR), near-infrared (NIR), and attenuated total reflectance Fourier transform infrared (ATR-FTIR) spectrometers were obtained as described in Chapter 2 (see Section 2.2.5). In brief, five sub-samples from each residue composite sample were scanned and imported into RStudio for processing. The final spectrum for each sample was calculated by averaging the five spectra for each sub-sample, resulting in one representative spectrum per composition sample per each spectral range. Visible-NIR and NIR spectra were acquired using the Black-Comet-CXR-SR and RED-Wave-NIRSX-SR spectrometers (StellarNet Inc. Oldsmar, Florida, USA), respectively. Attenuated total reflectance Fourier transform infrared absorbance (ATR-FTIR) spectra were obtained using a 4500a portable FTIR spectrometer (Agilent Technology Inc., Santa Clara, California, USA). All vis-NIR, NIR, and ATR-FTIR spectra were pre-processed using the same combinations (i.e., trimming, SG smoothing, and SNV) described in Chapter 2 and 3 (see Section 2.2.6 and Section 3.2.5; Wadoux et al., 2021).

Generalised calibration model

To evaluate the applicability of a generalised model, the calibration model developed using litterbag samples (Model 4; train-test split; see Section 3.2.6) was applied to predict TC and TN content in combustion residues. In this context, the calibration dataset of Model 4 was constructed using litterbag samples (n = 337; see Section 3.2.6), whereas the validation dataset consisted of combustion residues from the muffle furnace experiment (n = 893), which service as an external independent dataset.

Sample-specific calibration model

To assess if a sample-specific calibration model could provide a more accurate prediction, combustion residue samples from long-unburnt forests (Wombat SF and Orbost SF; n = 595) were used to develop a sample-specific calibration model (Model 5). Combustion residues from the recently burnt site (BBR; n = 298) were used as an external independent test dataset to evaluate the performance of the sample-specific calibration model.

Model evaluation

Four regression models were used to develop calibration models: partial least squares regression (PLSR), bootstrap bagged PLSR, Cubist, and random forests (RF). Genetic algorithm (GA) feature selection was also employed to select the most wavelengths for prediction (see Section 2.2.7). The performance of each regression model was compared and evaluated by R^2 and RMSE. Model with the highest R^2 and lowest RMSE were selected. In addition, the performance of the generalised calibration model (from Chapter 3) and the sample-specific calibration model (built using ash residue samples) were compared and evaluated using the coefficient of determination (R^2) and Lin's Concordance Correlation Coefficient (LCCC) (see Section 2.2.8).

4.3 Results

4.3.1: Mass loss after combustion

For all study sites and litter types, %ML of surface fuel litter increased across the temperature gradient until a plateau was reached at 500-600 °C (Figure 4.3). The most substantial changes in %ML occurred when temperature increased from 200-300 °C, during which more than one third of the litter mass was lost. The increase in %ML was smaller between 300-400 °C and 400-500 °C with very small losses as the temperate increased to 600 °C. Leaf litter from Wombat SF had statistically greater %ML across the temperature gradient (One-way ANOVA; $p < 0.001$-0.028; Figure 4.3a) compared to all other sites, except at 300 °C, where %ML of Wombat SF and BBR were statistically similar (One-way ANOVA; $p > 0.05$; Figure 4.3a). At 600 °C, more than 80% of the initial weight was lost during thermal degradation, with significant differences in %ML among study sites (One-way ANOVA; $p < 0.001$-0.028; Figure 4.3a).

Twigs followed a similar pattern to leaf litter, with an increase in %ML across the temperature gradient (Figure 4.3b). The differences in %ML between 300 and 400 °C among sites were smaller compared to those for leaf litter. Twigs had the lowest %ML at 200 °C and the highest %ML at 600 °C (85% loss), with no statistical differences among study sites (One-way ANOVA; $p > 0.05$; Figure 4.3b). In comparison, surface fine fuel litter showed the greatest variability in %ML, with significant differences among study sites at all temperatures, except for 400 °C (Figure 4.3c; One-way ANOVA; $p < 0.001$-0.033; Figure 4.3c). Among all litter types, surface fine fuel litter had the lowest %ML at all combustion temperatures, with 75% of the original mass lost at 600 °C.

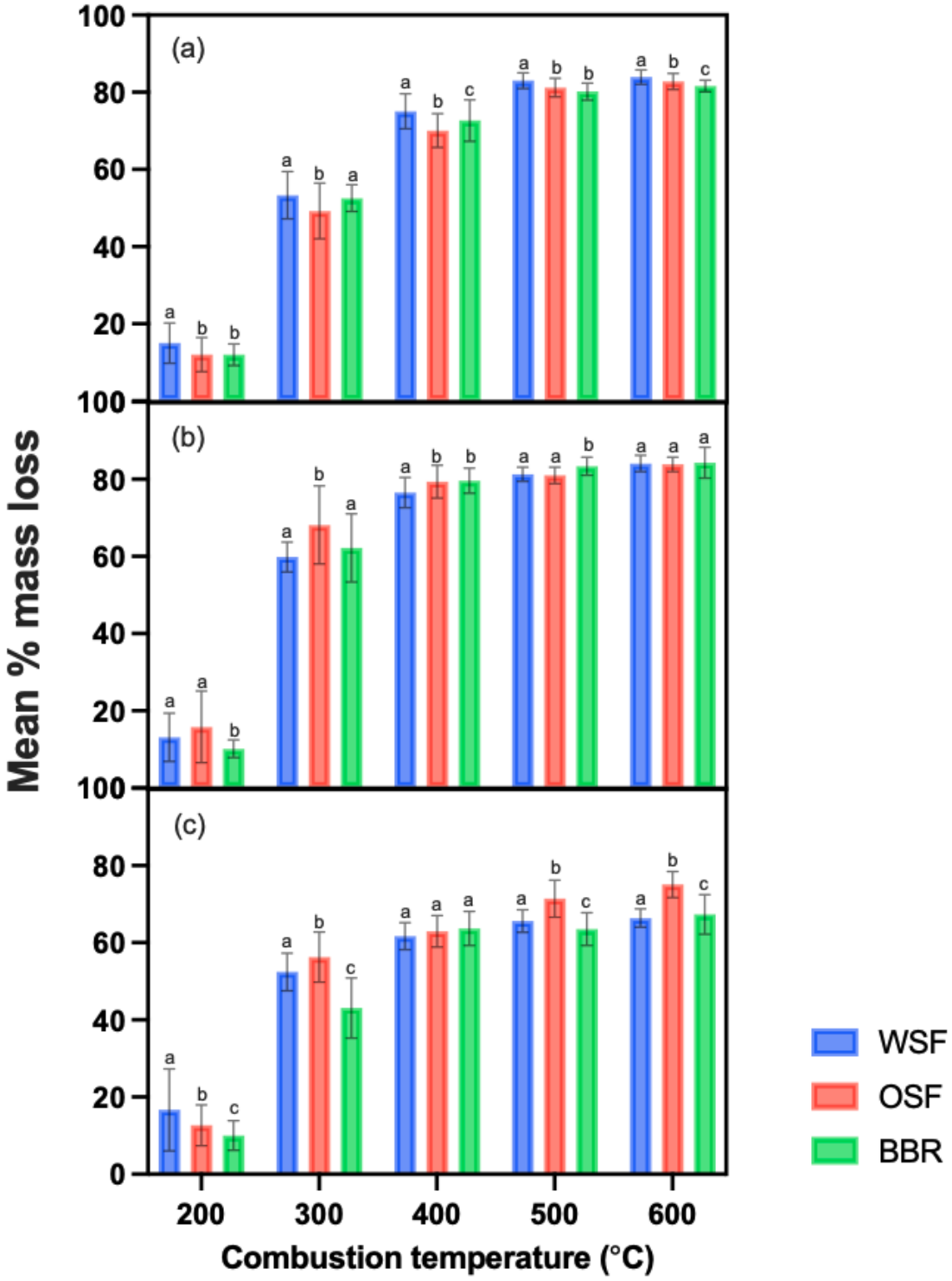

Figure 4.3: Percentage mass loss (%ML) of surface fuel litter (leaf litter, twigs, and surface fine fuel litter) after muffle furnace combustion at 200, 300, 400, 500, and 600 °C. (a) %ML of leaf litter; (b) twigs; and (c) surface fine fuel litter. Surface fuel litter was collected from Wombat State Forest (Wombat SF; blue bars), Orbost State Forest (Orbost SF; red bars), and Big Bit Road (BBR; green bars). Bars represent mean value and error bars indicate standard deviation (n = 40). Statistical comparison among sites was identified using one-way ANOVA and Games-Howell Post-Hoc test. For each surface fuel litter type and combustion temperature, means with the same letter are not significantly different ($p > 0.05$).

All LMMs demonstrated excellent model fits, with marginal R^2 of 0.96 and conditional R^2 ranging from 0.96 to 0.97 (Table 4.1). The fixed effects alone explained 96% of the variance, while the inclusion of random effects only explained a small proportion of variance in all models. The linear mixed model that included position as random effects (LMM_positional) was slightly better than the LMM_batch model (LMM; conditional R^2 = 0.97 and 0.96, respectively; Table 4.1). However, the full model that included both random effects did not improve the model performance and had the same conditional R^2 as the LMM_positional model (conditional R^2 = 0.97). This is likely due to the low intra-class correlation coefficient (ICC) value of batch effects (LMM; ICC = 0.013; Table 4.2), indicating the variation between batches was small and did not have strong influence on the total variance. Positional effects which accounted for the variation within batch, also had minimal influence on total variance and improved the overall model fit by only 0.01% (LMM; ICC = 0.16; Table 4.2). In addition, high residual variance (LMM; σ = 20.66; Table 4.2) indicated that a large proportion of variance was unexplained by both the fixed and random effects that were considered in the model.

The Fixed effects Omnibus tests results indicated that site of origin (LMM; F = 51.5; p < 0.001; Table 4.3), litter type (LMM; F = 786.6; p < 0.001; Table 4.3), and combustion temperature (LMM; F = 11218.6; p < 0.001; Table 4.3) had a highly significant effect on litter %ML (Table 4.3). More importantly, the interactions among the three factors were also highly statistically significant (LMM; p < 0.001; Table 4.3).

Table 4.1: Linear mixed models (LMM) were used to investigate the effects of site of sample origin (Wombat State Forest (SF), Orbost SF, and Big Bit Road), litter type (leaf litter, twigs, and surface fine fuel litter), combustion temperature (200, 300, 400, 500, and 600 °C), and their combined effects on litter percentage mass loss (%ML). %ML was treated as the response variable in all models, while site of origin, litter type, combustion temperature, and their combined effects were included as fixed effects. Batch effects and positional effects were included as random effects. Marginal R^2 represents the proportion of variance explained by fixed effects, while condition R^2 represents the proportion of variance explained by both fixed and random effects.

Model name	Variables	Marginal R^2	Conditional R^2
LMM_batch	%ML ~ 1+ site of origin + litter type + combustion temperature + site of origin + litter type + site of origin: combustion temperature + litter type: combustion temperature + site of origin: litter type: combustion temperature (1|batch effects)	0.96	0.96
LMM_positional	%ML~ 1+ site of origin + litter type + combustion temperature + site of origin + litter type + site of origin: combustion temperature + litter type: combustion temperature + site of origin: litter type: combustion temperature (1|positional effects)	0.96	0.97
Full LMM	%ML ~ 1+ site of origin + litter type + combustion temperature + site of origin + litter type + site of origin: combustion temperature + litter type: combustion temperature + site of origin: litter type: combustion temperature (1|batch effects) + (1+|positional effects)	0.96	0.97

Table 4.2: Summary of random effects from the full linear mixed model (LMM). Variance, standard deviation (SD), and intra-class correlation coefficient (ICC) of positional and batch random intercept are presented.

Groups	Name	Variance (σ)	SD	ICC
Position	(Intercept)	3.78	1.94	0.16
Batch	(Intercept)	0.28	0.53	0.013
Residual		20.66	4.55	

Table 4.3: Fixed effects Omnibus tests showing the effects of site of origin (Wombat State Forest (SF), Orbost SF, and Big Bit Road), litter type (leaf litter, twigs, and surface fine fuel litter), combustion temperature (200, 300, 400, 500, and 600 °C), and their combined effects on litter percentage mass loss (%ML).

Effect	*F* value	df	*p* value
Site of origin	60.8	2	< 0.001
Litter type	924.7	2	< 0.001
Combustion temperature	13181.5	4	< 0.001
Site of origin × Litter type	69.3	4	< 0.001
Site of origin × Combustion temperature	17.2	8	< 0.001
Litter type × Combustion temperature	103.1	8	< 0.001
Site of origin × Litter type × Combustion temperature	19.9	16	< 0.001

4.3.2 Independent site characteristics

A total of 19 surface fuel litter and topsoil samples (0-10 cm) were collected from BBR, 4 years after the 2019/2020 Black Summer bushfires. All forest litter fractions had broadly similar TC content, except for decomposing litter which was slightly lower (Table 4.4). Total C content of surface fuel litter ranged from 37% (surface fine fuel litter) to nearly 50% (leaf litter). For TN content, understorey litter was highest (1.0%), closely matched with surface fine fuel litter (0.8%). The carbon:nitrogen (C/N) ratios of the fractions of surface fuel litter varied considerably with C/N of leaf litter being approximately double compared to surface fine fuel litter and understorey litter (Table 4.4). Surface soil (0-10 cm) had comparatively low TN (0.19%) and TC (4.9%).

Table 4.4: Total carbon (TC), total nitrogen (TN), and carbon:nitrogen (C/N) ratio in surface fuel litter and topsoil (0-10 cm) samples collected from the study area in Big Bit Road (n = 19). Data are presented as mean ± standard deviation.

	N	TC (%)	TN (%)	C/N
Overstorey leaves	19	49.66 ± 1.11	0.58 ± 0.07	87.29 ± 11.95
Twigs	19	45.01 ± 1.64	0.53 ± 0.18	93.47 ± 27.37
Bark	17	41.02 ± 3.69	0.54 ± 0.18	82.95 ± 28.03
Fine fuel litter	19	37.14 ± 6.36	0.80 ± 0.19	47.49 ± 8.21
Understorey litter	15	45.10 ± 2.68	1.03 ± 0.18	44.87 ± 7.88
Soil	19	4.87 ± 1.38	0.19 ± 0.06	25.55 ± 3.30

4.3.3 Initial carbon and nitrogen content of surface fuel litter

Across the three study sites, leaf litter consistently had the highest TC content and decomposing litter had the lowest, although there were differences in TC and TN among sites (Table 4.5). Conversely, surface fine fuel litter had the greatest amount of N, and twig litter had the least. Among litter types, surface fine fuel litter had the highest TN content at all sites; Wombat SF and BBR (0.87% and 0.82%, respectively) had significantly higher values than Orbost SF (One-way ANOVA; $p < 0.001$; Table 4.5). In contrast, twigs had the lowest TN content among all litter types; total N in twigs from Wombat SF was approximate four times greater compared to twigs from BBR and Orbost SF (0.15% and 0.17%, respectively; One-way ANOVA; $p < 0.001$; Table 4.5). Leaf litter had moderate TN content but there were still significant differences among study sites (One-way ANOVA; $p < 0.001$, Table 4.5). Total C content in leaf litter followed the same pattern, with significant differences found across all study sites: Orbost SF > Wombat SF > BBR (One-way ANOVA; $p < 0.001$, Table 4.5). Total C content of twigs from all study sites were similar and within a narrow range of 44.7-47.4% (One-way ANOVA; $p > 0.05$, Table 4.5). Surface fine fuel litter had the lowest TC content among study sites and litter types (One-way ANOVA; $p < 0.001$, Table 4.5). Carbon:nitrogen ratios generally varied significantly among study sites and litter types (One-way ANOVA; $p < 0.001$-0.017, Table 4.5).

Table 4.5: Summary statistics of total carbon (TC), total nitrogen (TN), and carbon:nitrogen ratio (C/N) for leaf litter, twigs, and surface fine fuel litter collected from Wombat State Forest (SF), Orbost SF, and Big Bit Road (BBR). Data is presented as mean ± standard deviation (n = 5). Statistical comparisons among sites were done using one-way ANOVA and Games-Howell Post-Hoc test. For each litter type and chemical quality, mean values with the same superscript letter within a column are not significantly different ($p > 0.05$).

	Litter type	**TC (%)**	**TN (%)**	**C/N ratio**
Wombat SF	Leaf litter	52.61 ± 0.22^{a}	0.69 ± 0.047^{a}	76.1 ± 4.77^{a}
	Twigs	46.11 ± 0.45^{a}	0.40 ± 0.039^{a}	115 ± 12.35^{a}
	Surface fine fuel	$39.22 \pm 1.00^{\underline{a}}$	$0.87 \pm 0.034^{\underline{a}}$	$45.2 \pm 1.11^{\underline{a}}$
Orbost SF	Leaf litter	54.95 ± 0.45^{b}	0.37 ± 0.073^{b}	150.7 ± 24.75^{b}
	Twigs	47.36 ± 0.22^{a}	0.17 ± 0.015^{b}	274 ± 22.62^{b}
	Surface fine fuel	$35.16 \pm 0.22^{\underline{b}}$	$0.56 \pm 0.01^{\underline{b}}$	$63.1 \pm 0.80^{\underline{b}}$
BBR	Leaf litter	50.70 ± 0.20^{c}	0.48 ± 0.06^{c}	107.8 ± 12.22^{c}
	Twigs	44.7 ± 0.17^{a}	0.15 ± 0.032^{b}	313.3 ± 90.7^{b}
	Surface fine fuel	$22.47 \pm 2.40^{\underline{c}}$	$0.82 \pm 0.054^{\underline{a}}$	$27.5 \pm 1.105^{\underline{c}}$

4.3.4 Changes in carbon and nitrogen during combustion

Combustion of surface fuel litter types (leaf litter, twigs, and surface fine fuel litter) from Wombat SF, Orbost SF, and BBR resulted in a significant decrease in TC and TN content as combustion temperature increased (Figure 4.4). In general, TC and TN content decreased gradually as combustion temperature increased, with small differences in losses at lower temperatures. Among the three litter components, decomposing litter retained more TC and TN content than leaf and twig litter along the temperature gradient.

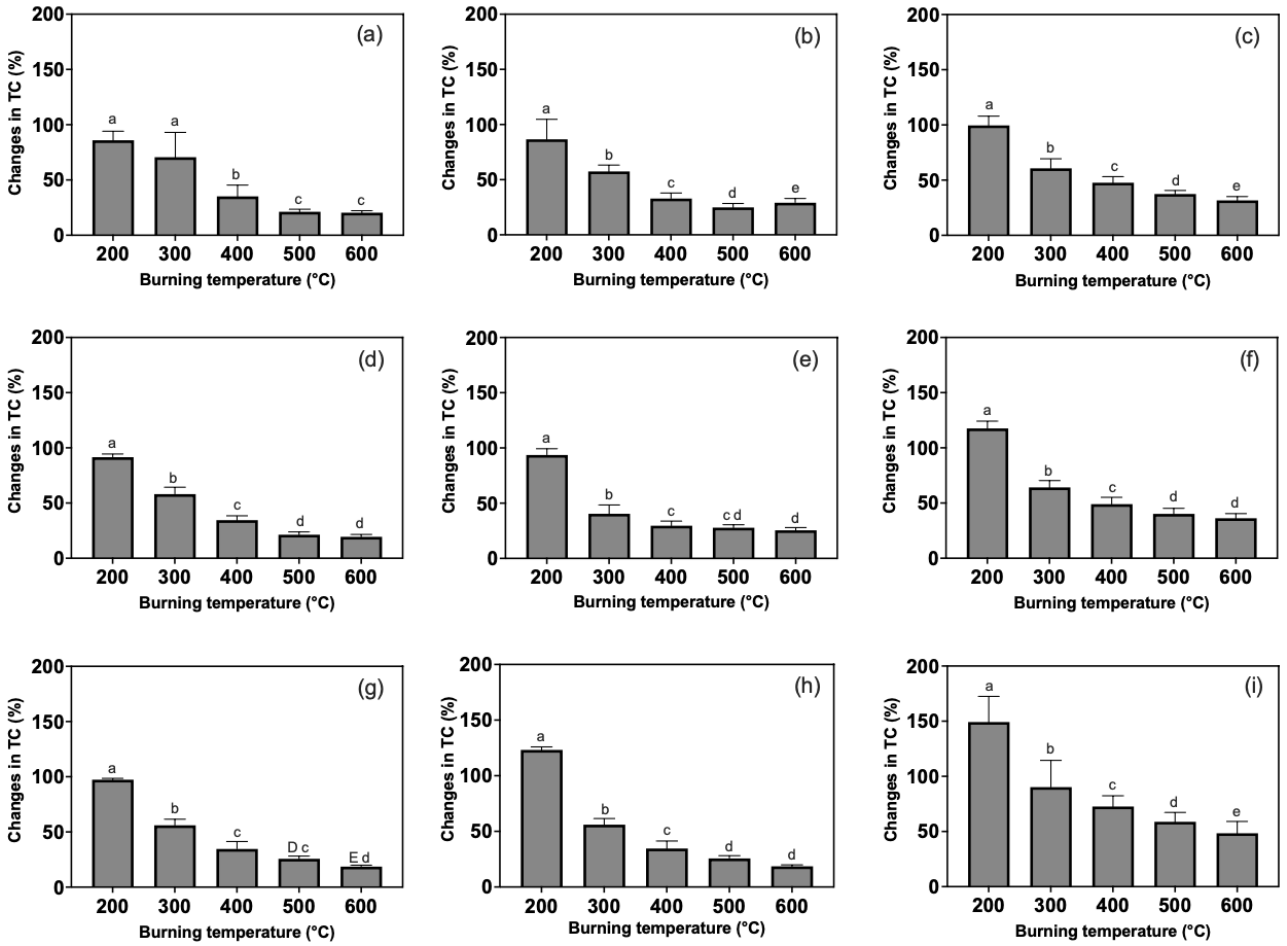

Figure 4.4: Percentage of total carbon (TC) remaining in combustion residues after muffle furnace combustion at 200, 300, 400, 500, and 600 °C. Bars represent mean value and error bars indicate standard deviation (n = 20). Panels show the percentage of TC in (a) leaf litter; (b) twigs; and (c) surface fine fuel litter from Wombat State Forest (SF); (d) leaf litter; (e) twigs; and (f) surface fine fuel litter from Orbost SF, and (g) leaf litter; (h) twigs; and (i) surface fine fuel litter from Big Bit Road (BBR). For each litter type, means with the same letter within a column are not significantly different ($p > 0.05$).

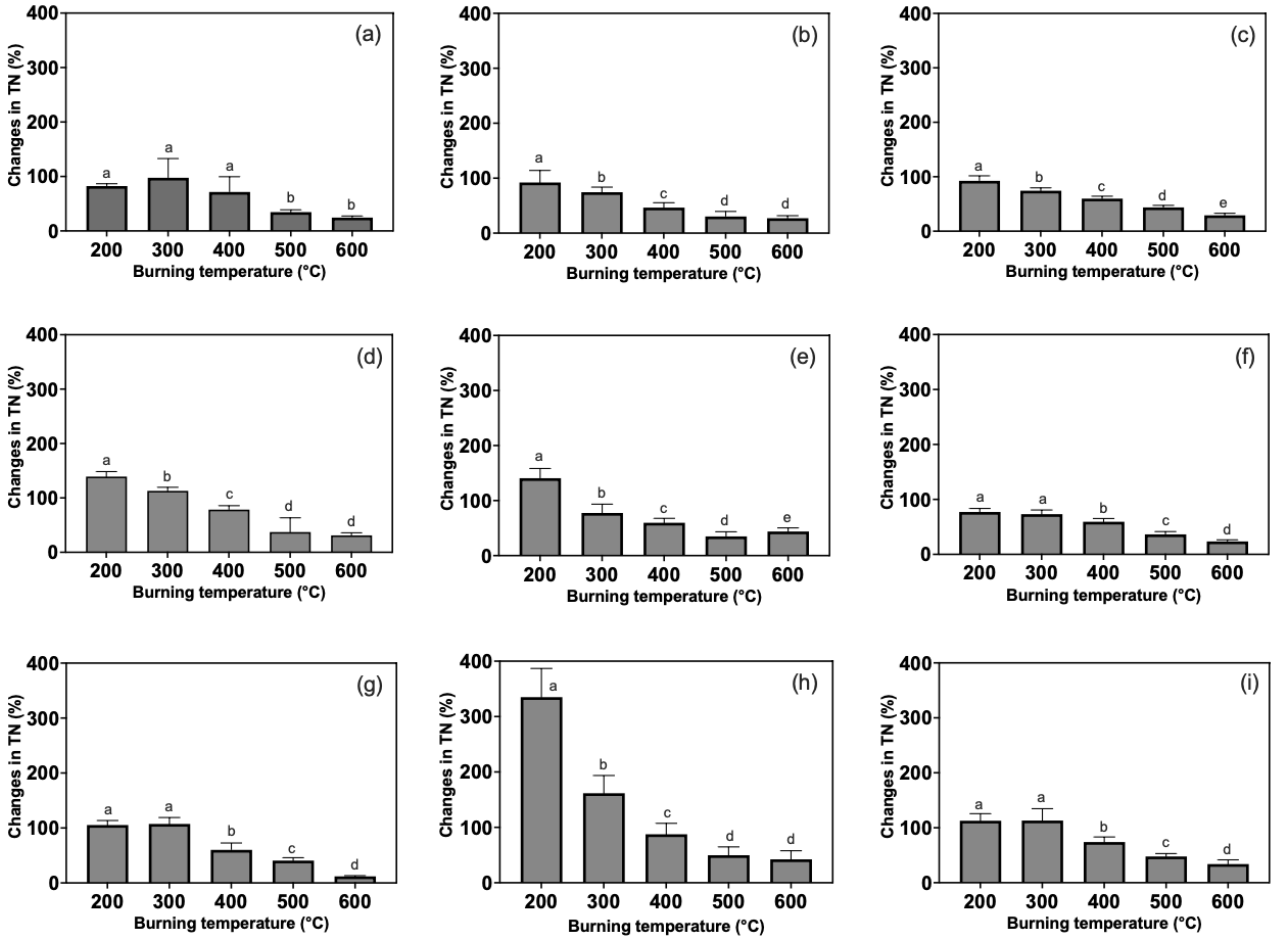

Figure 4.5: Percentage of total carbon (TN) remaining in combustion residues after muffle furnace combustion at 200, 300, 400, 500, and 600 °C. Bars represent mean values and error bars indicate standard deviation (n = 20). Panels show the percentage of TN in (a) leaf litter; (b) twigs; and (c) surface fine fuel litter from Wombat State Forest (SF); (d) leaf litter; (e) twigs; and (f) surface fine fuel litter from Orbost SF, and (g) leaf litter; (h) twigs; and (i) surface fine fuel litter from Big Bit Road (BBR). For each litter type, means with the same letter within a column are not significantly different ($p > 0.05$).

Leaf litter, twigs, and surface fine fuel litter followed the same consistent pattern of total carbon (TC) lost with increasing temperature. At 200 °C, approximately 10% of TC was lost in most litter types. Exceptions to this were twigs from BBR (23%), and decomposing litter from Orbost SF (17%) and BBR (49%). Between 200 and 300 °C, TC content declined significantly across all litter types, with remaining TC ranging from 40-70% (One-way ANOVA; $p < 0.001$-0.008, Figure 4.4), except for surface fine fuel litter from BBR, which retained 90% of its TC at 300 °C (Figure 4.4i). As temperature increased to 400°C, the remaining TC content dropped significantly to approximately 30% for leaf litter and twigs, and below 50% for surface fine fuel litter from Wombat SF and Orbost SF (One-way ANOVA; $p < 0.001$-0.006, Figure 4.4). Surface fine fuel litter from BBR also showed a significant decline in TC content (One-way ANOVA; $p < 0.001$, Figure 4.4i), but approximately 72% of the initial TC remained (Figure 4.3.3i). Between 400-500 °C, TC continued to decline

significantly across all litter types (One-way ANOVA; 0.002 $p < 0.001$, Figure 4.4), except for twigs from Orbost SF (One-way ANOVA; $p > 0.05$; Figure 4.4e). Loss of TC reached a plateau from 500-600 °C, with statistically similar levels of TC remaining in most litter types (One-way ANOVA; $p > 0.05$, Figure 4.4). The few exceptions were twigs from Wombat SF, leaf litter from BBR and surface fine fuel litter from Wombat SF and BBR (One-way ANOVA; $p < 0.001$-0.040; Figure 4.4b, c, g, i). However, combustion residues produced at 600 °C showed considerable variation in TC, with a range of 18-48%.

TN in surface fuel litter had a different pattern to TC, especially at lower temperature (200-300 °C). When combusted to 200 °C, an increase in TN content was found for most litter types, except for twigs from Wombat SF and decomposing litter from Wombat SF and Orbost SF (Figure 4.5b, c, f). In particular, twigs from BBR showed exceptionally high level of TN at 200 °C (Figure 4.5h). Following combustion at 200°C, TN content in surface fuel litter declined when heated at 300 °C. The exceptions were leaf litter from Wombat SF, and leaf and surface fine fuel litter collected from BBR where there was a slight increase in TN (Figure 4.5a, g, i). A statistically significant decrease in TN was found at 400 °C in all surface fuel litter types (One-way ANOVA; $p < 0.001$, Figure 4.5), except for leaf litter from Wombat SF (One-way ANOVA; $p > 0.05$, Figure 4.5a). Between 500-600 °C, all litter types showed a decrease in TN, except for twigs from Orbost SF, which increased in TN content (34.9 to 43.8%, Figure 4.5e).

4.3.5: Predicting chemical quality of combustion residues with spectroscopy

Calibration and validation dataset

The calibration dataset for Model 5 comprised a total of 337 litterbags samples (see Chapter 3 for details). This dataset covered a large range of TC content (30.5-51.3%, mean = 44.4%), however it did not fully cover the TC range observed in the validation dataset which construct of residues samples (13.4-77.5%, mean = 56.6%). Similarly, the calibration dataset also did not capture the large variation of TN in the validation dataset (0.2-2.3%, mean = 0.8%). The validation dataset for TN covered a range of lower N values compared to the calibration dataset, however the median, mean, and 3rd quartile values were similar (Table 4.6).

The calibration dataset for Model 6 included a total of 595 composite samples originating from two long-unburnt forests (Wombat SF and Orbost SF). This dataset captured a wide range of variation in both TC and TN content in combustion residues and was considered to be sufficiently large enough for development of a calibration model. In this dataset, the mean TC value was 57.7%, with a range of 29.0-77.5%, while the mean TN value was 0.8%, with a range of 0.2-1.9%. The

validation dataset includes a total of 298 composite residue samples collected from a recently burnt forest (BBR). The validation dataset has a similarly broad distribution of TC and TN content, with the exception of a lower minimum TC content (13.4%) and slightly higher maximum TN content (2.3%) than the calibration dataset (Table 4.6). These values were found in the samples that were derived from surface fine fuel litter.

Table 4.6: Descriptive statistics of total carbon (TC) and total nitrogen (TN) content in combustion residues. The calibration model developed in Chapter 3 (Model 3; see Section 3.3.3) was used in Model 5, while the validation dataset represents combustion residues from Wombat State Forest (Wombat SF; long-unburnt site), Orbost State Forest (Orbost SF; long-unburnt site), and Big Bit Road (BBR; recently burnt site). The calibration dataset of Model 6 was constructed using samples from WSF and OSF, while the validation dataset represents samples from BBR. Abbreviations: *N* = number of samples; Min = minimum, 1st Qu = first quartile; 3rd Qu = third quartile; Max = maximum.

Model 5: Generalised model using litterbag samples (from Chapter 3)

	N	Min	1st Qu	Median	Mean	3rd Qu	Max
Total carbon							
Whole dataset	1,230	13.43	44.78	51.38	53.21	63.25	77.51
Calibration	337	30.51	41.95	44.83	44.36	47.21	51.33
Validation	893	13.43	49.35	59.89	56.56	64.73	77.51
Total nitrogen							
Whole dataset	1,230	0.23	0.61	0.84	0.85	1.02	2.29
Calibration	337	0.50	0.78	0.86	0.89	0.97	1.64
Validation	893	0.23	0.55	0.79	0.84	1.05	2.29

Model 6: Sample-specific model using combustion residues from Wombat SF and Orbost SF

	N	Min	1st Qu	Median	Mean	3rd Qu	Max
Total carbon							
Whole dataset	893	13.43	49.42	59.87	56.56	64.71	77.51
Calibration	595	28.99	50.14	60.12	57.73	64.77	77.51
Validation	298	13.43	44.92	58.81	54.24	64.63	73.30
Total nitrogen							
Whole dataset	893	0.23	0.55	0.79	0.84	1.05	2.29
Calibration	595	0.23	0.54	0.75	0.81	1.00	1.93
Validation	298	0.23	0.56	0.93	0.90	1.14	2.29

Model performance

Model evaluation statistics from calibration and validation datasets suggested that partial least square regression (PLSR) models outperformed bootstrap PLSR, Cubist, and random forest (RF) in predicting TC and TN in combustion residues, as evidence by higher R^2 and LCCC, and lower RMSE (Table 4.7; Figure 4.5; Figure 4.6). The application of spectral pre-processing techniques including

Savitzky-Golay (SG) smoothing, standard normal variate (SNV) transformation, and genetic algorithm (GA) feature selection did not lead to an improvement in model accuracy. The exception was the generalised model (Model 5), where pre-processed ATR-FTIR spectra produced better TC predictions, while pre-processed vis-NIR and NIR spectra provided more accurate predictions for TN (Table 4.7). In these cases, the PLSR model using SG smoothing (window size = 3) combined with SNV transformation was the best. In all other cases, the model built with raw and trimmed spectra performed better than those built from pre-processed spectra, particularly for the sample-specific model (Model 6; Table 4.7).

For both calibration models, PLSR models built using ATR-FTIR spectra yielded the most accurate prediction of TC and TN in combustion residues (Table 4.7). All ATR-FTIR models had excellent performance, with R^2v higher than 0.91, low RMSEV, and high LCCC values. Among them, Model 6, which constructed using residues samples, provided the most reliable TC and TN predictions, as evident by excellent cross-validation and validation statistics (Table 4.7). However, both models were unable to accurately prediction TC values below 30% (Figure 4.5c; Figure 4.6c) or TN values above 1.5% (Figure 4.5f; Figure 4.6f).

Compared with ATR-FTIR spectra, vis-NIR and NIR models were less accurate, particularly the generalised model (Model 5). For TC content, although validated predictions from vis-NIR and NIR were fair (R^2 < 0.61-0.81; Table 4.7), calibration performance of these models was weak, with low R^2 values of 0.39 and 0.06, respectively. In contrast, the sample-specific model (Model 6), which used raw and trimmed vis-NIR and NIR spectra, had good TC prediction (R^2v > 0.82; Table 4.7). However, both the generalised model (Model 5) and the sample-specific model (Model 6) tended to over-predict TC when actual values were below 30% (Figure 4.5a, b and Figure 4.6a, b).

Considering both models, vis-NIR predictions of TN were poor (Table 4.7; Figure 4.5; Figure 4.6). In particular, the generalised model (Model 5) produced very weak results with both cross-validation and validation model yielded R^2 < 0.1 (Table 4.7). Although the performance of sample-specific model (Model 6) was better, its validation accuracy remained low, leading to poor model performance. In contrast, NIR spectroscopy showed a far stronger performance, especially for the sample-specific model (Model 6), which produced fair TN prediction (0.61 < R^2 < 0.81; Table 4.7). However, Model 5, constructed with litterbag samples (Chapter 3), did not provide accurate predictions for TN when using pre-processed NIR spectra.

Table 4.7: Comparative performance of the best models selected from vis-NIR, NIR, and ATR-FTIR spectra for predicting total carbon (TC), total nitrogen (TN) content in combustion residues from surface fuel litter: leaf litter, twigs, and surface fine fuel litter. Calibration models were developed using multivariate modelling analysis including partial least squared regression (PLSR), bootstrap PLSR, Cubist, and random forest (RF). Models were selected based on the highest coefficient of determination (R^2), the lowest root mean squared error (RMSE), and the highest Lins's Concordance Correlation Coefficient (LCCC) value after testing different pre-processing combinations (raw spectra, Savitzky-Golay smoothing, standard normal variate transformation, and genetic algorithm feature wavelength selection). SG = Savitzky-Golay smoothing; *w* = window size (number following indicate the size of the applied window); *k* = polynomial order; SNV = standard normal variate transformation; R^2cv = coefficient of determination of cross-validation model; RMSECV = root mean squared error of cross-validation model; LCCCcv = Lin's Concordance Correlation Coefficient of cross-validation model; R^2v = coefficient of determination of validation model; RMSEV = root mean squared error of validation model; LCCCv = Lin's Concordance Correlation Coefficient of validation model.

Model 5: Generalised model using litterbag samples (from Chapter 3)

	Spectra	Best model	Pre-processing technique	Calibration dataset			Validation dataset		
				R^2cv	RMSECV	LCCCcv	R^2v	RMSEV	LCCCv
Carbon	vis-NIR[a]	PLSR	Raw trimmed vis-NIR spectra	0.39	3.40	0.62	0.75	5.70	0.85
	NIR[b]	PLSR	Raw trimmed NIR spectra	0.06	4.59	0.24	0.73	6.00	0.82
	ATR-FTIR[c]	PLSR	SG (w = 3, k = 2), SNV	0.69	2.08	0.81	0.95	2.38	0.98
Nitrogen	vis-NIR[a]	PLSR	SG (w = 3, k = 2), SNV	0.01	0.18	-0.01	0.09	0.36	0.16
	NIR[b]	PLSR	SG (w = 3, k = 2), SNV	0.11	0.18	0.33	0.54	0.26	0.69
	ATR-FTIR[c]	PLSR	Raw ATR-FTIR spectra	0.63	0.11	0.79	0.91	0.11	0.95

Table 4.7 continued.

Model 6: Sample-specific model using combustion residues from Wombat SF and Orbost SF

	Spectra	Best model	Pre-processing technique	Calibration dataset			Validation dataset		
				R^2cv	RMSECV	LCCCcv	R^2v	RMSEV	LCCCv
Carbon	vis-NIR[a]	PLSR	Raw trimmed vis-NIR spectra	0.71	5.30	0.84	0.86	5.19	0.91
	NIR[b]	PLSR	Raw trimmed NIR spectra	0.72	5.26	0.84	0.88	4.91	0.92
	ATR-FTIR[c]	PLSR	Raw ATR-FTIR spectra	0.94	2.38	0.97	0.97	2.29	0.99
Nitrogen	vis-NIR[a]	PLSR	Raw trimmed vis-NIR spectra	0.26	0.30	0.42	0.34	0.36	0.47
	NIR[b]	PLSR	Raw trimmed NIR spectra	0.57	0.23	0.73	0.71	0.23	0.82
	ATR-FTIR[c]	PLSR	Raw ATR-FTIR spectra	0.93	0.10	0.96	0.93	0.12	0.96

[a] The wavelength range for the vis-NIR spectral regions was 500.5-1,000 nm
[b] The wavelength range for the NIR spectral region was 1,000.5-1,650 nm
[c] The wavenumber range for the MIR infrared region was 4,000-650 cm^{-1} (wavelength: 2,500-25,000 nm)

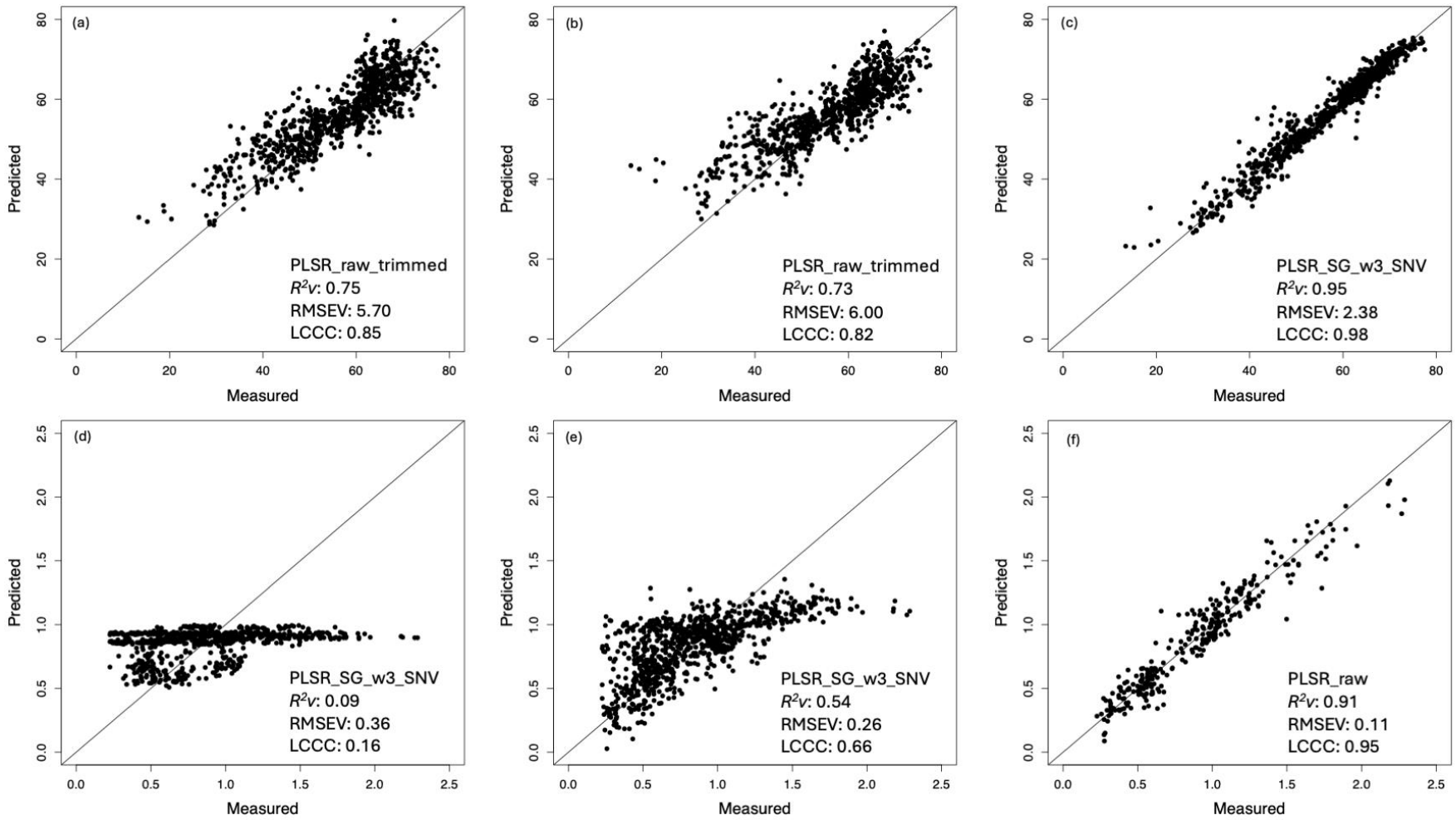

Figure 4.5: Validation results for prediction of total carbon (TC) and total nitrogen (TN) content in combustion residues using litterbag samples from Chapter 3 (Model 5; as a generalised model) with vis-NIR, NIR, and ATR-FTIR spectra. Calibration models were developed using a train-test data split. Scatterplots show measured values against predicted values for the validation dataset. The top row shows the best-performing models for prediction TC using (a) vis-NIR, (b) NIR, and (c) ATR-FTIR spectra. The bottom row shows the best performing models for predicting TN content using (d) vis-NIR, (e) NIR, and (f) ATR-FTIR spectra. In each panel, the solid line represents the 1:1 line. PLSR = partial least square regression; SG = Savitzky-Golay smoothing; *w* = window size; SNV = standard normal variate transformation; R^2v = coefficient of determination of validation model; RMSEV = root mean squared error of validation model; LCCC = Lin's Concordance Correlation Coefficient.

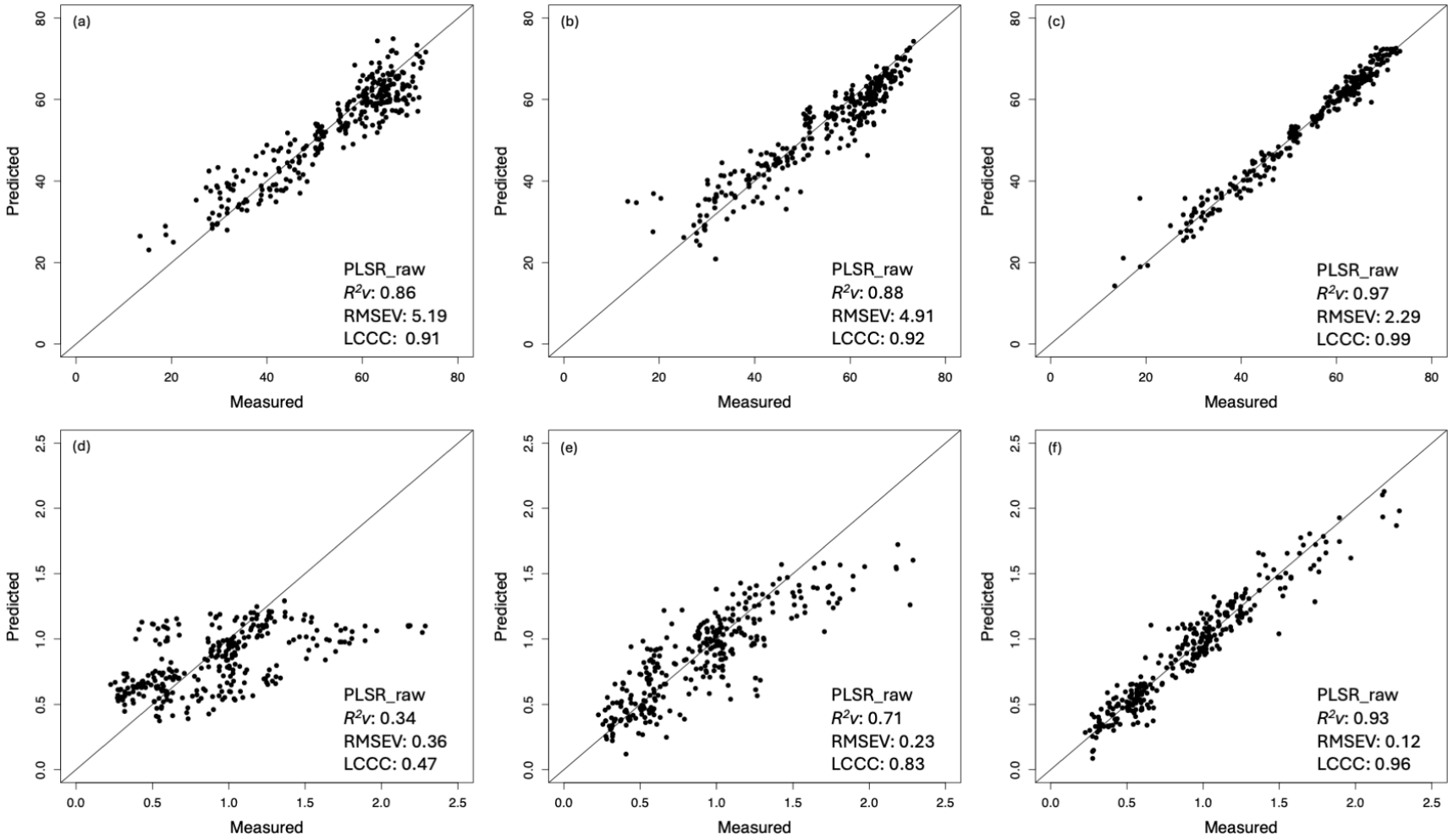

Figure 4.6: Validation results for prediction of total carbon (TC) and total nitrogen (TN) content in combustion residues produced from BBR litter (as an external independent test dataset) with vis-NIR, NIR, and ATR-FTIR spectra. Calibration models were developed using a train-test data split. Scatterplots show measured values against predicted values for the validation dataset. The top row shows the best-performing models for prediction of TC content using (a) vis-NIR; (b) NIR; and (c) ATR-FTIR spectra. The bottom row shows the best performing models for prediction TN content using (d) vis-NIR; (e) NIR; and (f) ATR-FTIR spectra. In each panel, the solid line represents the 1:1 line. PLSR = partial least square regression; R^2v = coefficient of determination of validation model; RMSEV = root mean squared error of validation model; LCCC = Lin's Concordance Correlation Coefficient.

4.4 Discussion

Prescribed burning has become an essential management practice in DSFs in Australia to mitigate the risks of catastrophic bushfires. Biological decomposition and prescribed burning both reduce the amount of litter accumulated on the forest floor, but they operate at vastly different timescales. Prescribed burning can have deleterious influences on nutrient pools in forests at single points in time altering nutrient availability for plant growth, particularly N, decomposition is a far slower process and ultimately increases plant and microbial access to C and N. Although numerous studies have examined the effects of prescribed burning on litter chemical and physical properties, these studies focused primarily on leaves (e.g., Toberman et al., 2014; Butler et al., 2017b). In reality, the forest floor consists of a heterogeneous mixture of leaves, twigs, and partially decomposed materials of different ages (e.g., Burrows, 2001). This raises questions regarding mass loss and nutrient changes of surface fine fuel litter derived from forests with different disturbance histories.

4.4.1 Changes in litter mass during combustion

The observed patterns of litter mass loss with increasing combustion temperatures were consistent with previous studies (Gray and Dighton, 2006; Úbeda et al., 2009; Hougue and Inglett, 2012). However, mass loss reported here was lower than other studies, particularly at 200 °C. *Eucalyptus* litter showed substantially lower mass loss compared to pine, oak, and herbaceous species (Gray and Dighton, 2006; Úbeda et al., 2009; Hougue and Inglett, 2012), likely due to the abundance of lignocellulosic compounds in *Eucalyptus* litter (Paul and Polglase, 2004). Cellulose, hemicellulose, and lignin degrade at temperatures above 290 °C (Barneto et al., 2011), suggesting that the rapid mass loss at 300 °C may result from the combustion of lignocellulosic compounds.

Variations in experimental design may partially explain differences in litter mass loss compared to other studies. For example, Gray and Dighton (2006) pre-ground leaf litter to ensure a highly homogenous sample size to facilitate heat transfer during combustion. Sample weight and combustion time is also noted to be different among studies (Úbeda et al., 2009; Hogue and Inglett, 2012). Initial litter weight, particle size, combustion duration, and fuel arrangement (depth) can substantially affect litter mass loss, especially at lower temperature (Gould et al., 2011; McCaw et al., 2012; Ganteaume et al., 2014). At higher temperatures, litter mass loss is comparable with previous studies, with an average of 80% of initial mass lost regardless of litter type or fire history. This underscores the critical role of combustion temperature in fuel reduction practices.

Litter mass loss for leaves and twigs was generally similar, except at lower temperature where twigs combusted more efficiently. The rapid mass loss for *Eucalyptus* leaf and twig litter is consistent with fine twigs (< 4 mm) being considered to be the most flammable component of the forest floor in DSFs (Burrows, 2001). Surface fine fuel litter consistently showed lower and more variable mass loss across the temperature gradient. Heterogeneity in the composition and particle size of surface fine fuel litter can have a substantial influence on flammability and combustion dynamics (Ganteaume et al., 2014). This knowledge is particularly relevant since surface fuel litter is the primary source for fire ignitions. Understanding fuel load and combustion behaviour of surface fuel litter is important for predicting litter consumption, fire rate, and fire spread.

4.4.2 Changes in nutrient pools during combustion

Ecologists are particularly interested in quantifying how fire affects N cycling since it is a primary limiting nutrient for forest growth and productivity (Adams and Attiwill, 1984). It is well established that fire redistributes nutrients within ecosystems – nutrients in plant material are lost to the atmosphere through volatilisation (in gaseous form) or to the forest floor through ash deposition (in solid form). In general, fire reduce C, N, and P in litter through volatilisation, while increase the available cation such as Ca, K, and Mn through ash deposition (Raison et al., 1985a; Raison et al., 1985b; Gillon and Rapp, 1989; O'Connell and McCaw, 1997; Wanthongchai et al., 2008; Úbeda et al., 2009; Yusiharni and Gilkes, 2012).

Prior to combustion, TC and TN in *Eucalyptus* leaf litter, twigs, and surface fine fuel litter differed considerably among long-unburnt and recently burnt sites suggesting that the nutrient pool held in surface litter is more likely to be influenced by site characteristics than by fire history. As discussed in Chapter 2, TC and TN content of freshly fallen litterfall from two long-unburnt forests were similar (see Section 2.3.1). It is therefore surprising that there were differences in TC and TN in litter components from sites with broadly similar fire history. These discrepancies may be attributed to variations in tree species composition and differences in the rate of early leaching of soluble compounds (Taylor, 1998). Despite low TN in leaf litter, the low C/N ratios in surface fine fuel litter from the recently burnt site suggest that organic matter breakdown was fast and more potentially efficient compared to long-unburnt sites (Bui and Henderson, 2013). This empirical data indicates potential enhancement of N post-fire to support regeneration of vegetation through stimulation of decomposition and presence of understorey vegetation such as N-fixing *Acacia* spp. (Adams and Attiwill, 1984).

Despite initial differences in nutrient content, TC and TN in surface litter followed broadly similar patterns across combustion temperatures. This is consistent with previous studies reporting a decrease in TC and TN as combustion temperature increases (e.g., Raison et al., 1985b; Gray and Dighton, 2006; Wanthongchai et al., 2008; Hogue and Inglett, 2012). However, changes in TC and TN were highly variable at lower temperatures. A sharp decline in TC and TN was evident as combustion temperature increased with greater volatilisation of N than C at lower temperature (e.g., Hogue and Inglett, 2012). Despite this overall pattern, an increased in TN was detected following combustion at 200-300 °C. A substantial proportion of N was retained in twigs and fine fuel litter at 600 °C. Collectively, these findings suggested that low-temperature combustion of surface fine fuel at low temperature may enhance N availability in the form of combustion residues. In addition, when combined with information on fuel load, fuel type, and fire intensity, this information is valuable for forest management in estimating C and nutrient loss regarding prescribed burning in DSFs.

The physical and chemical quality of combustion residues produced in laboratory conditions may not be equivalent to residues formed *in-situ* during prescribed burning or open-air combustion where the rate and duration of combustion are strongly influenced by oxygen availability, humidity, and air movement (e.g., Hogue and Inglett, 2012). Nevertheless, results from this study are comparable with an *in-situ* study conducted by Raison et al. (1985b) where 72% of fine fuel (< 6 mm) and 66% of N were lost during a low-intensity prescribed burning in *Eucalyptus* forests in Australia. Similarly, a meta-analysis found that both prescribed burning and bushfire significantly reduced litter N, with an average loss of 71% in broad-leaved forests (Wan et al., 2001). Compared to other ecosystems, the percentage loss of TC and TN reported here is lower than for herbaceous litter (99%; Hogue and Inglett, 2012). These differences likely reflect variations in litter type and combustion duration. Future studies could quantify the changes of other essential elements such as P, Ca, and K during prescribed burning.

4.4.3 Predictive power of vis-NIR, NIR-, and ATR-FTIR spectroscopy

To the author's knowledge, this is the first study to employ vis-NIR, NIR, and ATR-FTIR spectroscopy to predict TC and TN content in char and ash derived from plant litter. The following section discusses whether a generalised model can be broadly applied for prediction of changes during biological and thermal decomposition processes, or if a sample-specific model is required for characterising combustion residues produced from *Eucalyptus* forest litter.

As discussed in Chapters 2 and 3, generalised models built using representative samples with ATR-FTIR spectra can provide reliable predictions of the chemical quality of unknown litter samples

(see Sections 2.4.1 and 3.4.4). However, the use of synthetic mixtures and litterfall samples built using vis-NIR and NIR spectra to predict the chemical quality of decomposing samples (Model 3) was unsatisfactory (see Section 3.3.4). Because of this, litterbag samples from the *in-situ* decomposing trial were used to construct a generalised model to predict the TC and TN content of combustion residues (Model 5). The aim of this was to explore the feasibility of using a generalised model to predict the chemical quality of litter material existing in range of different forms and conditions (i.e., transformed through decomposition and combustion). Similar to findings from Chapter 3 (see Section 3.3.4), a generalised model using ATR-FTIR spectroscopy was found to be capable to provide a promising model for prediction on TC and TN in combustion residues. More importantly, the performance of the ATR-FTIR generalised model was highly comparable with the ATR-FTIR sample-specific model (constructed using combustion residue samples only). This further highlights the robustness and reliability of the use of ATR-FTIR spectroscopy. Although the performance of the generalised model and the sample-specific model are highly similar, the sample-specific model yielded better cross-validation results (Table 4.7). This suggests that a generalised model built using ATR-FTIR spectra is a suitable option for rapid, broad-scale predictions, however a sample-specific model is recommended if greater accuracy is required.

Importantly, this study further demonstrated that vis-NIR and NIR spectroscopy are not sensitive enough for the development of generalised model. Although the models based on vis-NIR and NIR yielded fair predictions for C, their performance using the cross-validation dataset were unsatisfactory. The large discrepancy between the cross-validation and the validation results indicates potential model overfitting and C predictions using the generalised model would not be reliable. In contrast to generalised and sample-specific models developed using vis-NIR and NIR spectroscopy to predict N content in litterfall and litterbags (see Sections 2.3.2 and 3.3.3) did not lead to accurate or reliable predictions of N content in combustion residues. This can be attributed to the N content in combustion residues exceeding those in litterbag samples, which limited the performance of vis-NIR and NIR spectroscopy. Another possible reason is that combustion may alter the chemical structure in litter materials reducing the ability of vis-NIR and NIR spectroscopy for detecting spectral signals related to N in combustion residues. Further testing will be necessary before any strong conclusions can be made regarding the effectiveness of vis-NIR and NIR spectroscopy in analysing the chemical quality of combustion residues.

Collectively, this study showed that ATR-FTIR spectroscopy is a powerful technique that can be used to develop generalised models for a wider ecological application. However, when highly accurate predictions are required, sample-specific models are preferable, and the use of external independent datasets for validation is recommended for broader application. Visible-NIR and NIR

spectroscopy are not recommended for the development of generalised models and is only recommended for prediction of C when used in conjunction with a sample-specific calibration model.

Chapter 5

General discussion: The fate of *Eucalyptus* litter in fire-prone ecosystems

---

5.1 Introduction

Dry sclerophyll forests (DSFs) in Australia, dominated by flammable *Eucalyptus* and often dense understorey vegetation, are highly susceptible to intense bushfire posing risks to both human populations and terrestrial ecosystems (e.g., Ashton and Attiwill, 1994). For example, the catastrophic 2019/20 Australian Black Summer bushfires burnt more than 5.8 million hectares of *Eucalyptus* dominated forests in New South Wales and Victoria (Bowman et al., 2020; Abram et al., 2021). Future climate projections for Australia postulate an increase in extreme fire weather conditions (Sharples et al., 2016; Di Virgilio et al., 2020). To reduce the socio-ecological impacts of bushfires, prescribed burning has been used extensively to manage forest fuel loads (Raison et al., 1983; Fernandes and Botelho, 2003; Burrows and McCaw, 2013; Dixon et al. 2018). In recent decades, a substantial body of literature investigating both the short- and long-term effects of prescribed burning on soil properties, understorey vegetation, and microbial activities has been amassed. However, less is known about how prescribed burning shapes litter dynamics in both long-unburnt and recently burnt forest ecosystems through fire-induced changes in litter types, and litter quantity and quality. Understanding how fire influences *Eucalyptus* litter dynamics and the balance of nutrient pools is crucial for developing strategic and sustainable forest and fuel management approaches in fire-prone ecosystems.

A second consideration in this thesis is that analysing plant materials using traditional laboratory methods is expensive and time-consuming. As an emerging analytical technique, visible-near-infrared (vis-NIR) and attenuated total reflectance Fourier transform (ATR-FTIR) offer promising alternatives for providing reliable compositional data (e.g., Parsons et al., 2011; Prananto et al., 2021). Accordingly, the overall aim of this thesis was to extend the current knowledge of compositional dynamics of *Eucalyptus* litter under current climate and fire regimes using spectroscopy. To facilitate this goal, the chemical quality of *Eucalyptus* litter at different stages, including freshly fallen litter, decomposing litter, combusted litter, and in combination with litter from understorey species, was investigated. The 2019/20 bushfire event provided an opportunity to

investigate and compare the chemical quality of litter in long-unburnt and bushfire-affected ecosystems. This final chapter presents and synthesises the major research findings in relation to the ecological importance of *Eucalyptus* litter and showcases the potential applications of spectroscopy in broader ecological and practical contexts.

5.2 Overview of research

The meta-analysis in Chapter 1 highlighted that, although research describing the effects of fire in terrestrial ecosystems is increasing, relatively few studies have examined how fire-induced changes in litter chemical quality influence rates of post-fire decomposition. Given that traditional laboratory analyses are expensive and time-consuming, Chapter 2 demonstrated the potential of vis-NIR, NIR, and ATR-FTIR spectroscopy as high-throughput and cost-effective alternatives for quantifying the chemical quality of *Eucalyptus* leaf and bark as litterfall. Purified cellulose, hemicellulose, and lignin were used as the main basic chemical constituents of litterfall to develop rudimentary calibration models for litter chemical quality. Building on this, Chapter 3 investigated the effects of prescribed burning on litter chemical quality and subsequent decomposition dynamics. Chapter 3 recognised the depth of research done to understand biological decomposition in forests and, in the process, highlighted that much of this work has been done using litter from a single species or of a single type. The study addressed this shortfall using litter mixtures and demonstrated the value of spectroscopic methods, particularly ATR-FTIR, in characterising the chemical quality of decomposing litter. Chapter 4 extended this work by examining how thermal decomposition affects the litter mass and chemical quality of *Eucalyptus* litter. It was further demonstrated that ATR-FTIR can accurately predict carbon and nitrogen content in combustion residues through generalised and sample-specific calibration models. Prescribed burning in DSFs in Australia was used as a background to demonstrate the application of predictive models.

5.2.1 An ecological perspective – Telling the overSTOREY

How the overSTOREY begins: cracking the chemical code in Eucalyptus *litterfall*

Throughout this thesis, Orbost State Forest (Orbost SF), Victoria, was used as a case study to showcase the complex fate of *Eucalyptus* litter (Figure 2.1b). This story begins with the natural senescence of *Eucalyptus* plant materials in long-unburnt DSFs. In these forests, litter dynamics are most often predicted using the Olson model (Olson, 1963). However, the use of this model has recently generated intense discussion, as it assumes constant litterfall and decomposition rate across

forests, without accounting for spatial and temporal variability (Zazali et al., 2020; Adams and Neumann, 2024; Sharples et al., 2025). This variability was demonstrated by investigating the annual litterfall pattern in Orbost SF (a coastal forest) and how it compared to an inland DSF, Wombat State Forest (Wombat SF; Chapter 2; Figure 2.1a). However, differences in litterfall patterns and site characteristics did not result in differences in leaf litter C/N. Given the similarity of chemical quality of *Eucalyptus* leaf litter across the two DSFs, future research efforts could pay particular attention to bark litterfall, which contributes 10-20% to the annual litterfall and showed great variability in C/N ratio and lignocellulosic compound content (Chapter 2; O'Connell, 1997). As for leaf litterfall, these variations will certainly be due to differences in tree species composition but are also likely due to the seasonal pattern of bark litterfall. This information is an important component in understanding litter dynamics as leaves and woody parts represent a large proportion of the annual litterfall and, once it has been shed, the surface fine fuel litter (Ashton, 1975; Neumann et al., 2021). The chemical composition of surface litter is likely to strongly influence forest litter decomposition and subsequent nutrient cycling (O'Connell, 1987b; Guo and Sims, 1999; Paudel et al., 2015; Wang et al., 2019b). This information, together with empirical data on annual litterfall production, could improve the accuracy of predicting litter dynamics in long-unburnt forests across the Australian landscape.

Plot twist: prescribed burning as the codebreaker of surface fine fuel decomposition

Once litterfall reaches the forest floor, the interplay of climate, litter chemical quality, and microbial activity begins, although their effects take time to become fully apparent (e.g., O'Connell, 1987a). This was evident in the carbon and nitrogen content of freshly fallen *Eucalyptus* leaf litterfall collected in Orbost SF in winter 2018 (Chapter 2) being comparable to leaf litter collected from the forest floor in summer of the same year (Chapter 4). This suggests that TC and TN content of litter are not strongly influenced by seasonal effects. This also suggests that N leaching does not occur as quickly as for other plant species or forest types, such as *Populus tremuloides* (Aspen) litter where up to 24% of N was lost through early leaching (Parsons et al., 1990). *Eucalyptus* litter contains high amount of readily soluble components that are more susceptible to early leaching than N (O'Connell, 1987a). In the current study, during *Eucalyptus* litter decomposition, most N was retained within the litter and increased with the degree of litter fragmentation, while C content decreased slowly over time (Chapter 3).

The rate of litter decomposition is predominately regulated by climate (Coûteaux et al., 1995; Zhang et al., 2008) and in most cases, increases with temperature and rainfall. In this sense, climate is the protagonist in the story of litter decomposition in *Eucalyptus* forests. This was demonstrated in

the *in-situ* litterbag decomposition trial where rapid initial mass loss happened during the wet and warm summer months (Chapter 3). The role of initial litter chemical quality (the deuteragonist second main character) is more important at a regional scale (Aerts, 1997). Under the same climate and environmental conditions, litter with high initial C/N ratios and lignin content decomposes slower than N-rich litter (e.g., Melillo et al., 1982; Zhang et al., 2019; Paul and Polglase, 2004). This was also evident in the *in-situ* litterbag decomposition trial, where the mass loss of *Eucalyptus* leaf litter was substantially slower than N-rich litter, such as elevated fuel (i.e., understorey biomass) and surface fine fuel litter (Chapter 3). In natural environments, N-rich litter materials in the surface fine fuel layer act as the deuteragonist to facilitate the decomposition of *Eucalyptus* litter through microbial respiration and nutrient transfer (e.g., Xiang and Bahus, 2007; Ferreira et al., 2012; Lummer et al., 2012). This is supported by the results in Chapter 3 where the presence of elevated fuel and surface fine fuel litter accelerated the decomposition rate of more recalcitrant *Eucalyptus* leaf litter.

Under current risk management scenarios and potentially in response to changing climates, an increased use of prescribed burning has putatively reduced the extent of long-unburnt areas, creating a mosaic of recently burnt patches in Australian forests (Burrows and McCaw, 2013; van Takach et al., 2022). This shift can affect litter dynamics through changes in vegetation composition, litter quantity, and microbial activity (Guinto et al., 2011; Lewis et al., 2012; Butler et al., 2020). Comparing the chemical quality of surface fine fuel litter (i.e., overstorey leaf, elevated fuel, and surface fine fuel litter) collected before and 1-year after a prescribed burning in Orbost SF (Chapter 3) has helped to unravel how time-since-fire influences litter chemical quality and subsequent litter decomposition rate (Chapter 1). *Eucalyptus* leaf litter and elevated fuel produced after fire was found to have significantly lower C/N ratios, reflecting increased nutrient availability for overstorey vegetation (Dijkstra and Adams, 2015) and the growth of N-rich species including *Acacia* and ferns. This supports the hypothesis of a 'nutrient kick' following fire (O'Connell, 1986; Gordon et al., 2017). However, the chemical quality of decomposing litter before and 1-year after a prescribed burn was similar (Chapter 3). It may take several years for post-fire overstorey and understorey vegetation to contribute inputs to this layer (Hosseini Bai et al., 2013; Gordon et al., 2017).

Importantly, variations in initial litter chemical quality and time-since-fire did not significantly affect litter decomposition rate. With the exception that *Eucalyptus* leaf litter collected 1-year after fire had a higher decomposition rate constant (*k*-value) than those from the pre-fire collection (mean *k*-value = 0.35 yr^{-1} and 0.29 yr^{-1}, respectively; see Chapter 1 Equation 1.1 and Chapter 3). This result contrasts vividly with other Australian-based studies, where leaf litter from prescribed-burnt sites typically decomposed slower than unburnt sites (mean *k*-value = 0.57 yr^{-1} and 0.77 yr^{-1}, respectively; Chapter 1). The influence of time-since-fire on litter nutrient dynamics was

more substantial. At the end of the decomposition trial, surface fine fuel litter collected after fire retained more C and N than litter collected prior to fire. This may be explained in part by the presence of charred materials in the surface fine fuel litter layer after a prescribed fire (Chapter 4). These charred materials are a C-rich pyrogenic residues that are highly resistant to decomposition (Shindo, 1991; Baldock and Smernik, 2002; Preston and Schmidt, 2006; Makoto and Koike, 2020). If the pre-fire surface fine fuel litter layer is not completely combusted during fire, which is likely during low-intensity prescribed burning, the slower rate of decomposition of this layer post-fire can potentially lead to more subtle changes in post-fire nutrient dynamics.

How the overSTOREY ends: what is lost in the fire is found in the ash

In the absence of fire, litter decomposition is slow. In contrast, thermal decomposition during fire accelerates the transformation of litter (which is often referred to as surface fine fuel in the context of fire and combustion) resulting in a heterogenous layer of char and ash. This layer offers valuable insight into the past, present, and future dynamics of litter. During prescribed burning, nutrients retained in surface fine fuel are redistributed through volatilisation and mineralisation (Guinto et al., 2011; Certini, 2005; Muqaddas et al., 2015). Carbon accumulates at low temperature in the form of char, while cations such as K^+ and Ca^{2+} are concentrated in ash that is produced at higher temperature (Bodí, 2014). This indicates that when prescribed burning is used as a management tool is not only valuable in fuel reduction for risk mitigation but also has a vital role in forest nutrient cycling.

Estimating the effects of bushfire and prescribed burning on litter dynamics and nutrient cycling is challenging because the magnitude of fuel reduction and nutrient alteration depends on the interaction of fuel type, spatial variability, and combustion temperature (Chapter 4). On a broad scale, the proportion of fuel consumed by prescribed burning in DSFs ranges from 22 to 87% (Price et al., 2022). At a much finer scale, this study showed that at 600 °C, mass loss of leaf and twig litter was similar (82-84%), whereas surface fine fuel litter (< 9 mm) showed much lower mass loss (66-75%; Chapter 4). As a result, combustion residues from surface fine fuel litter were richer in C and N compared to those of leaf and twig litter. Collectively, combustion of surface fuel litter demonstrated that charred litter produced at lower temperature was not only C-rich but can also be rich in N. Although C and N content declined with increasing combustion temperature, a substantial proportion remained in residues produced at 600 °C. This result can be extrapolated to suggest that fire in DSFs could enhance N availability through char and ash to support ecosystem productivity and plant growth.

5.2.2: Spectroscopy – revealing hidden secrets in *Eucalyptus* litter

Seeing the invisible: using vis-NIR, NIR, and ATR-FTIR spectroscopy to decode litter chemistry

As a sequel to the story, the three experimental chapters each showed that spectroscopy is a reliable analytical technique that can be used confidently to predict the chemical quality of *Eucalyptus* litter at different stages, including freshly fallen litter (Chapter 2), decomposing litter (Chapter 3), and combusted litter (Chapter 4). Traditional chemical analysis showed that litter chemical quality varied considerably among litter types and throughout both natural and thermal decomposition. Variations in litter C and N content, which were sometimes quite small, were successfully detected by spectroscopic approaches due to its sensitivity to C-H, C-O, and C=C bonds. Compared to laboratory analysis, the main advantages of vis-NIR, NIR, and ATR-FTIR spectroscopy in ecological studies are: (1) minimal to no sample preparation is required, (2) measurements are simple, repeatable and can be done as high-throughput, and (3) aside from the cost of equipment (Chapter 2), sample analysis is inexpensive. Despite these advantages, the use of spectroscopy is strongly dependent on knowledge of chemometrics and multivariate statistical analysis to develop robust calibration models.

Throughout this thesis, the ranked performance and effectiveness of spectroscopic techniques was ATR-FTIR > NIR > vis-NIR. Visible-NIR and NIR spectroscopy were found to be useful for predicting the chemical quality of freshly fallen litter (Chapter 2), while ATR-FTIR spectroscopy was more broadly applicable, providing reliable predictions of C and N in *Eucalyptus* litterfall, decomposing litter, and combustion residues with high accuracy. This demonstrates that spectroscopy is a powerful tool when used alongside with laboratory analysis to understand chemical transformation of forest litter. The use of spectroscopy in combination with surrogates of lignocellulosic compounds showed promising results for predicting litter cellulose and lignin content in plant material (Chapter 2). This approach not only serve as a feasibility alternative to costly chemical analysis of lignocellulosic compounds but also promotes sustainable research without the use of harmful chemicals. The use of spectroscopy enables researchers to see the 'invisible' chemical composition of forest litter in a quick and reliable way.

Generalised versus sample-specific models: which one is the best detective?

The prediction accuracy of spectroscopy is highly dependent on both the representativeness and size of the calibration model. Broadly speaking, sample-specific models performed better than generalised models due to their high similarity with the validation dataset. However, predictions made using calibration models trained on a specific dataset may not be suitable for predicting other sample types without data manipulation (Chapter 3; Chapter 4; Esbensen and Geladi, 2010; Li et al., 2021).

This was evident from the three experimental chapters where the performance of a generalised model and a sample-specific model were compared and evaluated. Overall, the sample-specific model yielded more accurate predictions than the generalised model, especially using vis-NIR and NIR spectroscopy. For example, when applying the generalised calibration model to predict the chemical quality of litterbag samples (Chapter 3) and combustion residues (Chapter 4), the outputs were unsatisfactory. In contrast, ATR-FTIR spectroscopy showed stronger potential for developing a generalised model and appeared to compensate for some of the limitations of generalised model, at least for prediction of N. This was evident in the study presented in Chapter 4 where N prediction using the generalised model built using ATR-FTIR spectra from *in situ* decomposition (litterbag trial) yielded excellent accuracy for N prediction. While promising, further investigation is required to validate this to ensure model reproducibility across different litter types.

To facilitate the use of spectroscopy and optimise model accuracy, Figure 5.1 provides an easy-to-follow workflow summarising the process involved in developing spectroscopic predictive models. As shown in Figure 5.1, cross-validation and validation are important steps for both generalised and sample-specific models. As discussed above, although sample-specific models provide predictions closer to the measured values, the risk of overfitting is substantially high. For applications across Australian DSFs, a generalised model built with ATR-FTIR spectra and supplemented by a representative subset of litter materials for different genera (e.g., *Eucalyptus* and *Acacia*) and plant functional groups (e.g., ferns and grasses) is preferable. At the same time, sample-specific models are valuable as benchmarks for assessing the performance and robustness of generalised models.

Practical implications: linking spectroscopy to forest and fire management

This thesis explicitly demonstrated the usefulness and effectiveness of vis-NIR, NIR, and ATR-FTIR spectroscopy in quantifying the chemical quality of *Eucalyptus* litter. The successful application of predictive models to determine the chemical quality of litterfall, decomposing litter, and combusted residues highlight the potential for using spectroscopic techniques in forest and fuel management of surface fine fuel (e.g., McLellan et al., 1991b; Gillon et al., 1999; Parsons et al., 2011). For example, the use of spectroscopy in quantifying C content in combustion residues can provide empirical data to facilitate the accuracy of the estimation of C emissions during bushfires and prescribed burning in DSFs (Possell et al., 2015). Fire severity is routinely mapped post-fire using broadband spectral indices, such as the differenced Normalized Burn Ratio (dNBR) from Landsat imagery (Holden et al., 2009; Soveral et al., 2010; Dixon et al., 2022). Other combinations of imaging

spectroscopy and statistical modelling have been used to improve the accuracy and precision of fire severity (e.g., Morgan et al., 2014; Veraverbeke et al., 2014; He et al., 2024). Similarly, imaging spectroscopy has been used to characterise fuels to assist in predicting fire behaviour (Stavros et al., 2018). The growing body of literature describing the use of and uptake of spectroscopic techniques in forest and fire management indicates the willingness of adoption of new technologies at research level as well as an operational one.

With the rapid advancement of spectroscopic technology, affordable research-grade spectrometers are now available as dual-purpose benchtop and portable devices. These instruments can unlock the potential for real-time, *in-situ* field measurements, allowing long-term routine monitoring. With an increase in fire frequency, handheld spectrometers could be applied in *in-situ* field conditions to quantifying C and N content in char and ash produced from prescribed burning and bushfire. From a management perspective, this information would be important in predicting the rate of forest recovery and understorey species richness based on post-fire nutrient availability. Together with litter decomposition data, this information could be particularly useful for decision makers to determine the best intervals for prescribed burning optimise the desired outcomes of fuel management, at the same time to promote ecological health.

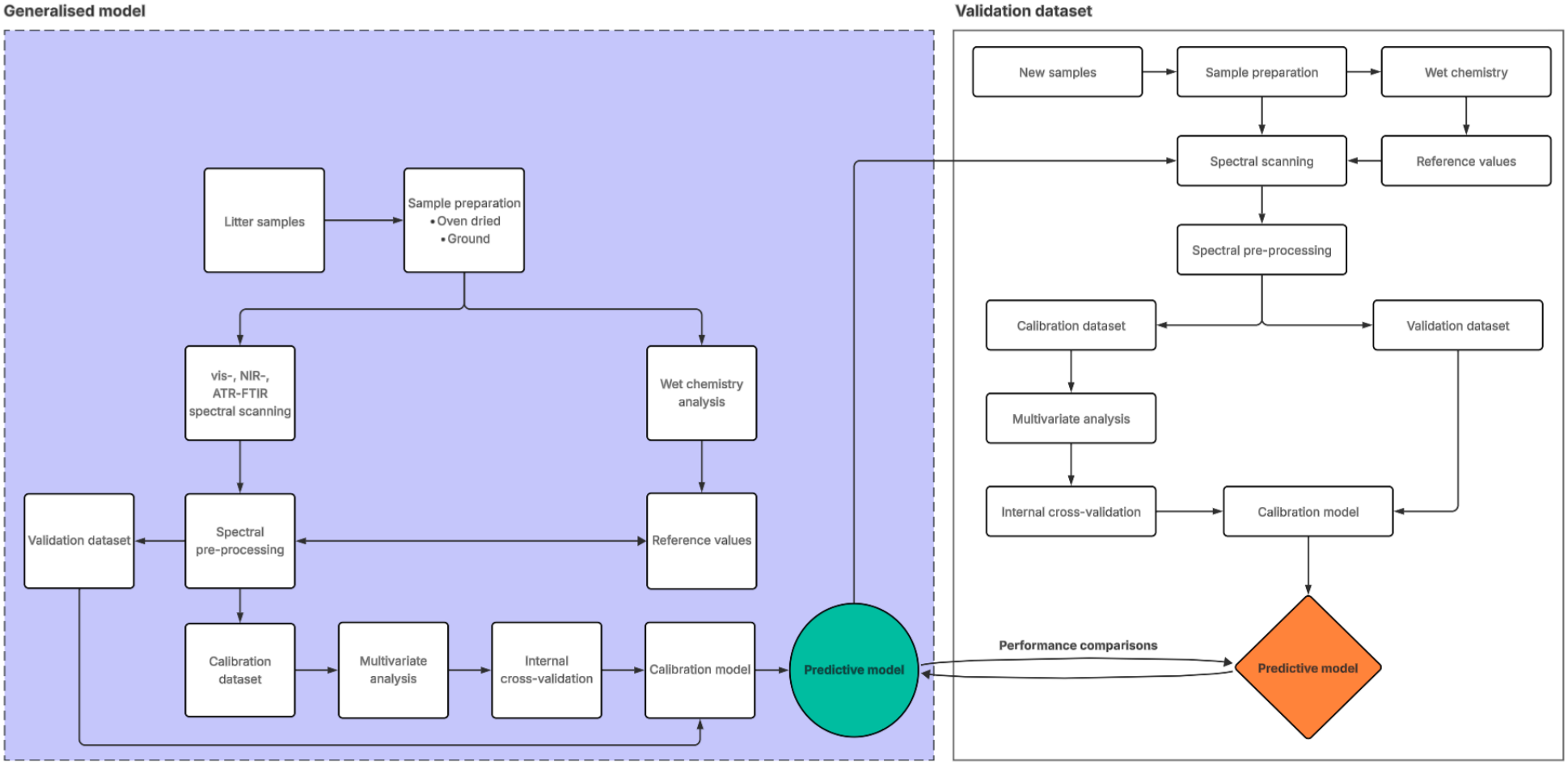

Figure 5.1: Schematic overview of the spectroscopic workflow used throughout this thesis (Chapter 2, 3, and 4) to analyse litter chemical quality using visible-near-infrared (vis-NIR), near-infrared (NIR), and attenuated total reflectance Fourier transform infrared (ATR-FTIR). The left panel shows the procedures used in building a generalised calibration model (detailed in Chapters 2 and 3) and the right panel shows the steps involves in building a validation model using new sample sets (detailed in Chapters 3 and 4). The green circle represents the generalised model, and the orange diamond represents the sample-specific model referred to throughout the thesis.

5.3: The final chapter of the story - future plot lines for research

5.3.1: Improving understanding of long-term decomposition processes

Due to time constraints, *in-situ* litterbag decomposition was limited to 15 months and, arguably, only reflects the short-term dynamics of decomposition. Long-term studies (more than 2 years) are required to improve our understanding of litter decomposition and nutrient cycling under current climate and fire regimes (Prescott, 2015; Krishna and Mohan, 2017; Prescott and Vesterdal, 2021; Sun et al., 2024). Future decomposition studies could also examine changes in other important indicators of chemical quality of litter such as phosphorus content and lignocellulosic compounds (e.g., Aerts, 1997; Krishna and Mohan, 2017; Santos et al., 2018; Wang et al., 2022b). While decomposition studies conducted under 'home-field' conditions have provided valuable insight into the interactions among climate, litter chemical quality, microbial communities, vegetation and microclimate, uncertainties remain regarding how changes in climate and fire regimes influence litter chemical quality and subsequent decomposition rates (e.g., Guo and Sim, 1999; Rachid et al., 2023). Building on the methodology used in the present study, future research could consider conducting litterbag decomposition in controlled *in-situ* field environments. This approach allows researchers to examine the effects of climate and litter chemical quality by minimising the influences of other site-specific ecological factors such as vegetation composition and soil properties. If, as projected, rainfall is becoming more variable (e.g., Abram et al., 2021; Huang et al., 2025), manipulating soil moisture levels through programmed irrigation systems could be used to simulate future climate scenarios to fully understand forest litter dynamics into the future. When integrated with localised climate predictions, empirical data describing litterfall and litter decomposition could be used to develop site-specific fine fuel models to aid future fire management.

5.3.2: Spectroscopic analysis for character development

Standardised wet chemical analysis

As discussed in Chapter 2, there is considerable variation in methods presently used to determine litter chemical quality, particularly for the determination of lignocellulosic compounds (Table 2.4). The three most common approaches for quantifying cellulose, hemicellulose, and lignin are fibre analysis, UV/VIS spectrophotometry, and the Klason method. These techniques involve the use of chemical reagents, and laboratory procedures can vary, leading to potential measurement bias. For example, McLellan et al. (1991a) reported concerning analytical errors in nitrogen, cellulose, and lignin content when comparing results from five different laboratories. Among the five laboratories,

only one employed a different analytical technique for lignin measurement, which led to further variation in lignin content. Although NIR spectroscopy helped to reduce the inter-laboratory variations, biases remained high. This highlights the importance of developing universal guidelines for laboratory analysis protocols in combination with spectroscopy to ensure consistency within and among studies. Importantly, calibration models developed using values obtained from a particular laboratory method should only be validated and applied against the same method to reduce bias.

Standardised model evaluation metrics

In spectroscopy, the ratio of performance to deviation (RPD) is commonly used to assess model quality, particularly in assessing the performance and applicability of calibration models (Chang et al., 2001). For example, the RPD has been widely used in soil science as a model evaluation metric (e.g., Chang et al., 2001; Zornoza et al., 2008; Canero et al., 2024). Generally speaking, a RPD value less than 1.5 indicates poor prediction, while RPD values between 1.5 and 2.0 indicate a fair performance, and a model with a RPD greater than 2.0 suggests good to excellent predictivity (Nduwamungu et al., 2009). However, some studies have adjusted RPD standard according to their findings (e.g., Malley et al., 1999; Chang et al., 2001; Dunn et al., 2002; Coûteaux et al., 2003; Terhoeven-Urselmans et al., 2006; Van Vuuren et al., 2006; Nduwamungu et al., 2009), leading to inconsistencies in the use of RPD values. Another common problem is the description of model performance which in some contexts, the word “good” and “excellent” are somewhat interchangeable for describing a RPD close to and greater than 2.0 (e.g., Chang et al., 2001; Dunn et al., 2002; Van Vuuren et al., 2006).

The inconsistency in the use of RPD values has led to serious confusion and thus promotes debate in using RPD as an important model evaluation metric in soil science (Minasny and McBratney, 2013). More seriously, RPD values are also commonly used in forestry and agricultural research, however the standard is somewhat different from those used in soil science. For example, Parsons et al. (2011) have considered a RPD value between 2.5 and 3.0 as ‘acceptable’, while Elle et al. (2019) have considered a RPD value greater than 2.5-3.0 as ‘good’, and a value greater than 3.0 as ‘excellent’. These values are higher than indicative numbers used in soil science. Such inconsistent use of RPD values highlights the notion that a systematic model evaluation metric is required to allow sophisticated and useful comparisons among different studies to fully understand the effectiveness and reliability of spectroscopy in analysing plant and forest litter materials over a broad spatial and temporal scales. As with the call made above for the development for universal guidelines for

laboratory analysis and spectroscopy protocols, a further challenge for consistency in use of RDP or development of other methods to assess model performance is made here.

5.3.3 Cast credits: spectroscopy linking litter, decomposition, and fire

In summary, this study demonstrates the potential of spectroscopy (vis-NIR, NIR, and ATR-FTIR) in analysing carbon and nitrogen in litterfall, decomposing litter, char and ash derived from litter biomass. This study also unveils the dominance of climate with initial litter chemical quality (i.e., C/N ratios) as the local regulator on *in-situ* litter mixture decomposition. In addition, this study underscores the influences of prescribed burning on litter decomposition. Prescribed burning immediately transforms surface fuel litter into heterogenous residues (i.e., char and ash) and subsequently affect litter decomposition through alteration in litter chemical quality. More importantly, this study shows that spectroscopy is a useful and reliable technique for understanding the changes in C and N during both biological and thermal litter decomposition but sample-specific models are recommended for accurate predictions. Future studies could explore the feasibility of using spectroscopy to predict litter chemical quality in field conditions.

THE END

References

Australian Bureau of Agricultural and Resource Economics and Sciences (2023) Australia's forests and forestry glossary, v.1.2.0Australian Bureau of Agricultural and Resource Economics and Sciences, Canberra. CC BY 4.0. doi.org/10.25814/5ef43d15f69cc.

Abbott, I., Heurck, P. V., & Wong, L. (1984). Responses to long-term fire exclusion: physical, chemical and faunal features of litter and soil in a Western Australian forest. *Australian Forestry*, *47*(4), 237-242.

Abram, N. J., Henley, B. J., Sen Gupta, A., Lippmann, T. J., Clarke, H., Dowdy, A. J., Sharples, J. J., Nolan, R. H., Zhang, T., Wooster, M. J., Wurtzel, J. B., Meissner, K. J., Pitman, A. J., Ukkola, A. M., Murphy, B. P., Tapper, N. J., & Boer, M. M. (2021). Connections of climate change and variability to large and extreme forest fires in southeast Australia. *Communications Earth & Environment*, *2*(1), 8.

Adams, M. A., & Attiwill, P. M. (1986). Nutrient cycling and nitrogen mineralization in eucalypt forests of south-eastern Australia: II. Indices of nitrogen mineralization. *Plant and Soil*, *92*(3), 341-362.

Adams, M. A., & Neumann, M. (2024). Perspective: Flawed assumptions behind analysis of litter decomposition, steady state and fire risks in Australia. *Forest Ecology and Management*, *556*, 121741.

Aerts, R. (1997). Climate, leaf litter chemistry and leaf litter decomposition in terrestrial ecosystems: a triangular relationship. *Oikos*, 439-449.

Agbeshie, A. A., Abugre, S., Atta-Darkwa, T., & Awuah, R. (2022). A review of the effects of forest fire on soil properties. *Journal of Forestry Research*, *33*(5), 1419-1441.

Agelet, L. E., & Hurburgh Jr, C. R. (2010). A tutorial on near infrared spectroscopy and its calibration. *Critical Reviews in Analytical Chemistry*, *40*(4), 246-260.

Águas, A., Incerti, G., Saracino, A., Lanzotti, V., Silva, J. S., Rego, F. C., Mazzoleni, S., Bonanomi, G. (2018). Fire effects on litter chemistry and early development of *Eucalyptus globulus*. *Plant and Soil*, *422*(1), 495-514.

Ai, N., Jiang, Y., Omar, S., Wang, J., Xia, L., & Ren, J. (2022). Rapid measurement of cellulose, hemicellulose, and lignin content in *Sargassum horneri* by near-infrared spectroscopy and characteristic variables selection methods. *Molecules*, *27*(2), 335.

Akpor, O. B., Okoh, A. I., & Babalola, G. O. (2006). Culturable microbial population dynamics during decomposition of *Theobroma cacao* leaf litters in a tropical soil setting. *Journal of Biological Sciences*, *6*(4), 768-774.

Alchanatis, V., Schmilovitch, Z., & Meron, M. J. P. A. (2005). In-field assessment of single leaf nitrogen status by spectral reflectance measurements. *Precision Agriculture*, *6*(1), 25-39.

Alexis, M. A., Rasse, D. P., Knicker, H., Anquetil, C., & Rumpel, C. (2012). Evolution of soil organic matter after prescribed fire: a 20-year chronosequence. *Geoderma*, *189*, 98-107.

Altangerel, K., & Kull, C. A. (2013). The prescribed burning debate in Australia: conflicts and compatibilities. *Journal of Environmental Planning and Management*, *56*(1), 103-120.

Ashton, D. H. (1975). Studies of litter in *Eucalyptus regnans* forests. *Australian Journal of Botany*, *23*(3), 413-433.

Ashton D.H. and Attiwill P.M. (1994) Tall open-forests. In: *Australian Vegetation* (ed. R.H. Groves), pp. 157-196. Cambridge University Press, Cambridge.

Attiwill, P. M. (1994). Ecological disturbance and the conservative management of eucalypt forests in Australia. *Forest Ecology and Management*, *63*(2-3), 301-346.

Attiwill, P. M. (1968). The loss of elements from decomposing litter. *Ecology*, *49*(1), 142-145.

Attiwill, P. M., Guthrie, H. B., & Leuning, R. (1978). Nutrient cycling in a *Eucalyptus obliqua* (L'Herit.) forest. I. Litter production and nutrient return. *Australian Journal of Botany*, *26*(1), 79-91.

Attiwill, P. M., & Adams, M. A. (2013). Mega-fires, inquiries and politics in the eucalypt forests of Victoria, south-eastern Australia. *Forest Ecology and Management*, *294*, 45-53.

Attiwill, P. M., Ryan, M. F., Burrows, N., Cheney, N. P., McCaw, L., Neyland, M., & Read, S. (2014). Timber harvesting does not increase fire risk and severity in wet eucalypt forests of southern Australia. *Conservation Letters*, *7*(4), 341-354.

Bachega, L. R., Bouillet, J. P., de Cássia Piccolo, M., Saint-André, L., Bouvet, J. M., Nouvellon, Y., Gonçalves, J. L. de M., Robin, A., & Laclau, J. P. (2016). Decomposition of *Eucalyptus grandis* and *Acacia mangium* leaves and fine roots in tropical conditions did not meet the Home Field Advantage hypothesis. *Forest Ecology and Management*, *359*, 33-43.

Baietto, A., Hernández, J., & del Pino, A. (2021). Comparative dynamics of above-ground litter production and decomposition from *Eucalyptus grandis* Hill ex Maiden and *Pinus taeda* L., and their contribution to soil organic carbon. *Forests*, *12*(3), 349.

Baker, T. G., & Attiwill, P. M. (1985). Above-ground nutrient distribution and cycling in *Pinus radiata D. Don* and *Eucalyptus obliqua L'Herit*. forests in southeastern Australia. *Forest Ecology and Management*, *13*(1-2), 41-52.

Barker, J. W., & Price, O. F. (2018). Positive severity feedback between consecutive fires in dry eucalypt forests of southern Australia. *Ecosphere*, *9*(3), e02110.

Baldock, J. A., & Smernik, R. J. (2002). Chemical composition and bioavailability of thermally altered *Pinus resinosa* (Red pine) wood. *Organic Geochemistry*, *33*(9), 1093-1109.

Bani, A., Borruso, L., Matthews Nicholass, K. J., Bardelli, T., Polo, A., Pioli, S., Gómez-Brandón, M., Insam, H., Bumbrell, A. J., & Brusetti, L. (2019). Site-specific microbial decomposer communities do not imply faster decomposition: results from a litter transplantation experiment. *Microorganisms*, *7*(9), 349.

Bao, J., Yu, M., Li, J., Wang, G., Tang, Z., & Zhi, J. (2024). Determination of leaf nitrogen content in apple and jujube by near-infrared spectroscopy. *Scientific Reports*, *14*(1), 20884.

Barnes, R. J., Dhanoa, M. S., & Lister, S. J. (1989). Standard normal variate transformation and de-trending of near-infrared diffuse reflectance spectra. *Applied Spectroscopy*, *43*(5), 772-777.

Barneto, A. G., Hernández, R. B., & Berenguer, J. M. (2011). Thermogravimetric characterization of *Eucalyptus* wood. *O Papel*, *72*(7), 53-56.

Barotto, A. J., Martínez-Meier, A., Segura, V., Monteoliva, S., Charpentier, J. P., Gyenge, J., Sergent, A. S., Milier, F., Rozenberg, P., & Fernández, M. E. (2023). Use of near-infrared spectroscopy to estimate physical, anatomical and hydraulic properties of *Eucalyptus* wood. *Tree Physiology*, *43*(3), 501-514.

Bassett, M., Leonard, S. W., Chia, E. K., Clarke, M. F., & Bennett, A. F. (2017). Interacting effects of fire severity, time since fire and topography on vegetation structure after wildfire. *Forest Ecology and Management*, *396*, 26-34.

Bauhus, J., Khanna, P. K., & Menden, N. (2000). Aboveground and belowground interactions in mixed plantations of *Eucalyptus globulus* and *Acacia mearnsii*. *Canadian Journal of Forest Research*, *30*(12), 1886-1894.

Beard, J. S. (1977). Tertiary evolution of the Australian flora in the light of latitudinal movements of the continent. *Journal of Biogeography*, *4*(1), 111-118.

Ben-Dor, E., & Banin, A. (1995). Near-infrared analysis as a rapid method to simultaneously evaluate several soil properties. *Soil Science Society of America Journal*, *59*(2), 364-372.

Berg, B., & McClaugherty, C. (1989). Nitrogen and phosphorus release from decomposing litter in relation to the disappearance of lignin. *Canadian Journal of Botany*, *67*(4), 1148-1156.

Berglund, S. L., & Ågren, G. I. (2012). When will litter mixtures decompose faster or slower than individual litters? A model for two litters. *Oikos*, *121*(7), 1112-1120.

Bernhard-Reversat, F. (1999). The leaching of *Eucalyptus* hybrids and *Acacia auriculiformis* leaf litter: laboratory experiments on early decomposition and ecological implications in Congolese tree plantations. *Applied Soil Ecology*, *12*(3), 251-261.

Birk, E. M. (1979). Disappearance of overstorey and understorey litter in an open eucalypt forest. *Australian Journal of Ecology*, *4*(2), 207-222.

Birk, E. M., & Simpson, R. W. (1980). Steady state and the continuous input model of litter accumulation and decomposition in Australian eucalypt forests. *Ecology*, *61*(3), 481-485.

Birk, E. M., & Bridges, R. G. (1989). Recurrent fires and fuel accumulation in even-aged blackbutt (*Eucalyptus pilularis*) forests. *Forest Ecology and Management*, *29*(1-2), 59-79.

Blum, M. M., & John, H. (2012). Historical perspective and modern applications of attenuated total reflectance–Fourier transform infrared spectroscopy (ATR-FTIR). *Drug Testing and Analysis*, *4*(3-4), 298-302.

Bodí, M. B., Martin, D. A., Balfour, V. N., Santín, C., Doerr, S. H., Pereira, P., Cerdà, A., & Mataix-Solera, J. (2014). Wildland fire ash: Production, composition and eco-hydro-geomorphic effects. *Earth Science Reviews*, *130*, 103-127.

Bokhorst, S., & Wardle, D. A. (2013). Microclimate within litter bags of different mesh size: Implications for the 'arthropod effect' on litter decomposition. *Soil Biology and Biochemistry*, *58*, 147-152.

Bowman, D. M. (1998). The impact of Aboriginal landscape burning on the Australian biota. *The New Phytologist*, *140*(3), 385-410.

Bowman, D. M., Balch, J. K., Artaxo, P., Bond, W. J., Carlson, J. M., Cochrane, M. A., D'Antonio, C. M., Defries, R. S., Doyle, J. C., Harrison, S. P., Johnston, F. H., Keeley, J. E., Krawchuk, M. A., Kull, C. A., Marston, J. B., Moritz, M. A., Prentice, I. C., Roos, C. I., Scott, A. C., Swetnam, T. W., van der Werf G. R., & Pyne, S. J. (2009). Fire in the Earth system. *Science*, *324*(5926), 481-484.

Bowman, D. M., Williamson, G. J., Abatzoglou, J. T., Kolden, C. A., Cochrane, M. A., & Smith, A. M. (2017). Human exposure and sensitivity to globally extreme wildfire events. *Nature Ecology & Evolution*, *1*(3), 0058.

Bowman, D. M., Kolden, C. A., Abatzoglou, J. T., Johnston, F. H., van der Werf, G. R., & Flannigan, M. (2020). Vegetation fires in the Anthropocene. *Nature Reviews Earth & Environment*, *1*(10), 500-515.

Bradford, M. A., Tordoff, G. M., Eggers, T., Jones, T. H., & Newington, J. E. (2002). Microbiota, fauna, and mesh size interactions in litter decomposition. *Oikos*, *99*(2), 317-323.

Bradstock, R. A., Hammill, K. A., Collins, L., & Price, O. (2010). Effects of weather, fuel and terrain on fire severity in topographically diverse landscapes of south-eastern Australia. *Landscape Ecology*, *25*(4), 607-619.

Bradford, M. A., Berg, B., Maynard, D. S., Wieder, W. R., & Wood, S. A. (2016). Future directions: understanding the dominant controls on litter decomposition. *Journal of Ecology*, *104*(1), 229-238.

Breiman, L. (2001). Random forests. *Machine Learning*, *45*(1), 5-32.

Brennan, K. E., Christie, F. J., & York, A. (2009). Global climate change and litter decomposition: more frequent fire slows decomposition and increases the functional importance of invertebrates. *Global Change Biology*, *15*(12), 2958-2971.

Bridges, R. G. (2004). Fine fuel in the dry sclerophyll forests of south-eastern New South Wales. *Australian Forestry*, *67*(2), 88-100.

Briggs, S. V., & Maher, M. T. (1983). Litter fall and leaf decomposition in a river red gum (*Eucalyptus camaldulensis*) swamp. *Australian Journal of Botany*, *31*(3), 307-316.

Briones, M. J. I., & Ineson, P. (1996). Decomposition of *Eucalyptus* leaves in litter mixtures. *Soil Biology and Biochemistry*, *28*(10-11), 1381-1388.

Brockerhoff, E. G., Barbaro, L., Castagneyrol, B., Forrester, D. I., Gardiner, B., González-Olabarria, J. R., O'B.Lyver, P., Meurisse, N., Oxbrough, A., Taki, H.,Thompson, I. D., van der Plas, F. & Jactel, H. (2017). Forest biodiversity, ecosystem functioning and the provision of ecosystem services. *Biodiversity and Conservation*, *26*(13), 3005-3035.

Brown, C. D., Vega-Montoto, L., & Wentzell, P. D. (2000). Derivative preprocessing and optimal corrections for baseline drift in multivariate calibration. *Applied Spectroscopy*, *54*(7), 1055-1068.

Buckingham, S., Murphy, N., & Gibb, H. (2015). The effects of fire severity on macroinvertebrate detritivores and leaf litter decomposition. *PLoS One*, *10*(4), e0124556.

Bunnell, F. L., & Tait, D. E. N. (1974). Mathematical simulation models of decomposition processes. *Soil organisms and decomposition in tundra*, 207-225.

Burrows, N. D. (2001). Flame residence times and rates of weight loss of eucalypt forest fuel particles. *International Journal of Wildland Fire*, *10*(2), 137-143.

Burrows, N., & McCaw, L. (2013). Prescribed burning in southwestern Australian forests. *Frontiers in Ecology and the Environment*, *11*(s1), e25-e34.

Burrows, N., Wills, A., & Densmore, V. (2023). Fuel weight and understorey hazard dynamics in mature karri (*Eucalyptus diversicolor*) forests in southwest Western Australia. *Australian Forestry*, *86*(2), 68-81.

Butler, O. M., Lewis, T., & Chen, C. (2017a). Fire alters soil labile stoichiometry and litter nutrients in Australian eucalypt forests. *International Journal of Wildland Fire*, *26*(9), 783-788.

Butler, O. M., Lewis, T., & Chen, C. (2017b). Prescribed fire alters foliar stoichiometry and nutrient resorption in the understorey of a subtropical eucalypt forest. *Plant and Soil*, *410*(1), 181-191.

Butler, O.M., Lewis, T., Rezaei Rashti, M., Maunsell, S.C., Elser, J.J. and Chen, C. (2019). The stoichiometric legacy of fire regime regulates the roles of micro-organisms and invertebrates in decomposition. *Ecology*, *100*(7), p.e02732.

Butler, O.M., Lewis, T., Rezaei Rashti, M. and Chen, C. (2020). Long-term fire regime modifies carbon and nutrient dynamics in decomposing *Eucalyptus pilularis* leaf litter. *Frontiers in Forests and Global Change*, *3*, 22.

Campbell, C. D., Cameron, C. M., Bastias, B. A., Chen, C., & Cairney, J. W. (2008). Long term repeated burning in a wet sclerophyll forest reduces fungal and bacterial biomass and responses to carbon substrates. *Soil Biology and Biochemistry*, *40*(9), 2246-2252.

Canero, F. M., Rodriguez-Galiano, V., & Aragones, D. (2024). Machine Learning and Feature Selection for soil spectroscopy. An evaluation of Random Forest wrappers to predict soil organic matter, clay, and carbonates. *Heliyon*, *10*(9), e30228.

Cannon, P. J., & Clement, S. (2025). Why do we burn? Examining arguments underpinning the use of prescribed burning to manage wildfire risk. *People and Nature*.

Cawson, J. G., & Duff, T. J. (2019). Forest fuel bed ignitability under marginal fire weather conditions in *Eucalyptus* forests. *International Journal of Wildland Fire*, *28*(3), 198-204.

Cawson, J. G., Duff, T. J., Tolhurst, K. G., Baillie, C. C., & Penman, T. D. (2017). Fuel moisture in Mountain Ash forests with contrasting fire histories. *Forest Ecology and Management*, *400*, 568-577.

Cawson, J. G., Duff, T. J., Swan, M. H., & Penman, T. D. (2018). Wildfire in wet sclerophyll forests: the interplay between disturbances and fuel dynamics. *Ecosphere*, *9*(5), e02211.

Cawson, J. G., & Duff, T. J. (2019). Forest fuel bed ignitability under marginal fire weather conditions in Eucalyptus forests. *International Journal of Wildland Fire*, *28*(3), 198-204.

Cécillon, L., Barthès, B. G., Gomez, C., Ertlen, D., Génot, V., Hedde, M., Stevens, A., & Brun, J. J. (2009). Assessment and monitoring of soil quality using near-infrared reflectance spectroscopy (NIRS). *European Journal of Soil Science*, *60*(5), 770-784.

Certini, G. (2005). Effects of fire on properties of forest soils: a review. *Oecologia*, *143*(1), 1-10.

Chambers, D. P., & Attiwill, P. M. (1994). The ash-bed effect in *Eucalyptus regnans* forest: chemical, physical and microbiological changes in soil after heating or partial sterilisation. *Australian Journal of Botany*, *42*(6), 739-749.

Chander, K., Goyal, S., & Kapoor, K. K. (1995). Microbial biomass dynamics during the decomposition of leaf litter of poplar and eucalyptus in a sandy loam. *Biology and Fertility of Soils*, *19*(4), 357-362.

Chang, C. W., Laird, D. A., Mausbach, M. J., & Hurburgh, C. R. (2001). Near-infrared reflectance spectroscopy–principal components regression analyses of soil properties. *Soil Science Society of America Journal*, *65*(2), 480-490.

Chen, H., Ferrari, C., Angiuli, M., Yao, J., Raspi, C., & Bramanti, E. (2010). Qualitative and quantitative analysis of wood samples by Fourier transform infrared spectroscopy and multivariate analysis. *Carbohydrate Polymers*, *82*(3), 772-778.

Chen, C., Luo, J., Qin, W., & Tong, Z. (2014). Elemental analysis, chemical composition, cellulose crystallinity, and FT-IR spectra of *Toona sinensis* wood. *Monatshefte für Chemie-Chemical Monthly*, *145*(1), 175-185.

Cheng, J. H., & Sun, D. W. (2017). Partial least squares regression (PLSR) applied to NIR and HSI spectral data modelling to predict chemical properties of fish muscle. *Food Engineering Reviews*, *9*(1), 36-49.

Cheng, C. H., Chen, Y. S., Huang, Y. H., Chiou, C. R., Lin, C. C., & Menyailo, O. V. (2013). Effects of repeated fires on ecosystem C and N stocks along a fire induced forest/grassland gradient. *Journal of Geophysical Research: Biogeosciences*, *118*(1), 215-225.

Cheney, N. P. (1976). Bushfire disasters in Australia, 1945–1975. *Australian Forestry*, *39*(4), 245-268.

Chintala, R., Clay, D. E., Schumacher, T. E., Malo, D. D., & Julson, J. L. (2013). Optimization of oxygen parameters for determination of carbon and nitrogen in biochar materials. *Analytical Letters*, *46*(3), 532-538.

Chodak, M. (2008). Application of Near Infrared Spectroscopy for Analysis of Soils, Litter and Plant Materials. *Polish Journal of Environmental Studies*, *17*(5), 631-642.

Close, D. C., Davidson, N. J., & Swanborough, P. W. (2011). Fire history and understorey vegetation: water and nutrient relations of *Eucalyptus gomphocephala* and *E. delegatensis* overstorey trees. *Forest Ecology and Management*, *262*(2), 208-214.

Coops, N., Dury, S., Smith, M. L., Martin, M., & Ollinger, S. (2002). Comparison of green leaf eucalypt spectra using spectral decomposition. *Australian Journal of Botany*, *50*(5), 567-576.

Corbeels, M., O'Connell, A. M., Grove, T. S., Mendham, D. S., & Rance, S. J. (2003). Nitrogen release from eucalypt leaves and legume residues as influenced by their biochemical quality and degree of contact with soil. *Plant and Soil*, *250*(1), 15-28.

Cornelissen, J. H. C. (1996). An experimental comparison of leaf decomposition rates in a wide range of temperate plant species and types. *Journal of Ecology*, *84*(4), 573-582.

Cornelissen, J. H. C., & Thompson, K. (1997). Functional leaf attributes predict litter decomposition rate in herbaceous plants. *New Phytologist*, *135*(1), 109-114.

Cornelissen, J. H., Grootemaat, S., Verheijen, L. M., Cornwell, W. K., van Bodegom, P. M., van der Wal, R., & Aerts, R. (2017). Are litter decomposition and fire linked through plant species traits? *New Phytologist*, *216*(3), 653-669.

Cornwell, W. K., Cornelissen, J. H., Amatangelo, K., Dorrepaal, E., Eviner, V. T., Godoy, O., Hobbie, S. E., Hoorens, B., Kurokawa, H., Pérez-Harguindeguy, N., Quested, H. M., Santiago, L. S., Wardle, D. A., Wright, I. J., Aerts, R., Allison, S. D., Bodegom, P. V., Brovkin, V., Chatain, Al., Callaghan, T. V., Díaz, S., Garnier, E., Gurvich, D. E., Kazakou, E., Klein, J. A., Read, J., Riech, P. B., Soudzilovskaia, N. A., Vaieretti, M. V., & Westoby, M. (2008). Plant species traits are the predominant control on litter decomposition rates within biomes worldwide. *Ecology Letters*, *11*(10), 1065-1071.

Constantine IV, M., Mooney, S., Hibbert, B., Marjo, C., Bird, M., Cohen, T., Forbes, M., McBeath, A., Rich, A., & Stride, J. (2021). Using charcoal, ATR FTIR and chemometrics to model the intensity of pyrolysis: Exploratory steps towards characterising fire events. *Science of the Total Environment*, *783*, 147052.

Coûteaux, M. M., Bottner, P., & Berg, B. (1995). Litter decomposition, climate and litter quality. *Trends in Ecology & Evolution*, *10*(2), 63-66.

Coûteaux, M. M., Berg, B., & Rovira, P. (2003). Near infrared reflectance spectroscopy for determination of organic matter fractions including microbial biomass in coniferous forest soils. *Soil Biology and Biochemistry*, *35*(12), 1587-1600.

Crockford, R. H., & Richardson, D. P. (1998a). Litterfall, litter and associated chemistry in a dry sclerophyll eucalypt forest and a pine plantation in south-eastern Australia: 1. Litterfall and litter. *Hydrological Processes*, *12*(3), 365-384.

Crockford, R. H., & Richardson, D. P. (1998b). Litterfall, litter and associated chemistry in a dry sclerophyll eucalypt forest and a pine plantation in south-eastern Australia: 2. Nutrient recycling by litter, throughfall and stemflow. *Hydrological Processes*, *12*(3), 385-400.

Crockford, R. H., & Richardson, D. P. (2002). Decomposition of litter in a dry sclerophyll eucalypt forest and a *Pinus radiata* plantation in southeastern Australia. *Hydrological Processes*, *16*(17), 3317-3327.

Crous, K. Y., Wujeska-Klause, A., Jiang, M., Medlyn, B. E., & Ellsworth, D. S. (2019). Nitrogen and phosphorus retranslocation of leaves and stemwood in a mature *Eucalyptus* forest exposed to 5 years of elevated CO2. *Frontiers in Plant Science*, *10*, 664.

Cruz, M. G., Gould, J. S., Hollis, J. J., & McCaw, W. L. (2018). A hierarchical classification of wildland fire fuels for Australian vegetation types. *Fire*, *1*(1), 13.

Cuchietti, A., Marcotti, E., Gurvich, D. E., Cingolani, A. M., & Harguindeguy, N. P. (2014). Leaf litter mixtures and neighbour effects: low-nitrogen and high-lignin species increase decomposition rate of high-nitrogen and low-lignin neighbours. *Applied Soil Ecology*, *82*, 44-51.

D'heer, B. G., De Boever, J. L., Kanacker, J. M., & Boucqué, C. V. (2000). The filter bag versus the conventional filtration technique for the determination of crude fibre and Van Soest cell wall constituents. *Journal of Animal and Feed Sciences*, *9*(3), 513-526.

Dangal, S. R., Sanderman, J., Wills, S., & Ramirez-Lopez, L. (2019). Accurate and precise prediction of soil properties from a large mid-infrared spectral library. *Soil Systems*, *3*(1), 11.

Davey, S. M., & Sarre, A. (2020). the 2019/20 Black Summer bushfires. *Australian Forestry*, *83*(2), 47-51.

De Alencar Figueiredo, L. F., Davrieux, F., Fliedel, G., Rami, J. F., Chantereau, J., Deu, M., Courtois, B., & Mestres, C. (2006). Development of NIRS equations for food grain quality traits through exploitation of a core collection of cultivated sorghum. *Journal of Agricultural and Food chemistry*, *54*(22), 8501-8509.

Department of Agriculture, Fisheries and Forestry. (2023). Australia's state of the forests report 2023: Synthesis. Australian Government. Retrieved from: https://www.agriculture.gov.au/sites/default/files/documents/Australias_State_of_the_Forests_Report_Synthesis_2023.pdf.

Department of Sustainability and Environment. (2004a). EVC/Bioregion Benchmark for Vegetation Quality Assessment, Victorian, Volcanic Plain bioregion, EVC 16: Lowland Forest. Department of Sustainability and Environment, East Melbourne.

Department of Sustainability and Environment (2004b). EVC/Bioregion Benchmark for Vegetation Quality Assessment, Victorian, Volcanic Plain bioregion, EVC 20: Heathy Dry Forest. Department of Sustainability and Environment, East Melbourne.

Denham, A. J., Vincent, B. E., Clarke, P. J., & Auld, T. D. (2016). Responses of tree species to a severe fire indicate major structural change to *Eucalyptus–Callitris* forests. *Plant Ecology*, *217*(6), 617-629.

Di Virgilio, G., Hart, M. A., & Jiang, N. B. (2018). Meteorological controls on atmospheric particulate pollution during hazard reduction burns. *Atmospheric Chemistry and Physics*, *18*(9), 6585–6599.

Di Virgilio, G., Evans, J. P., Blake, S. A., Armstrong, M., Dowdy, A. J., Sharples, J., & McRae, R. (2019). Climate change increases the potential for extreme wildfires. *Geophysical Research Letters*, *46*(14), 8517-8526.

Di Virgilio, G., Evans, J. P., Clarke, H., Sharples, J., Hirsch, A. L., & Hart, M. A. (2020). Climate change significantly alters future wildfire mitigation opportunities in southeastern Australia. *Geophysical Research Letters*, *47*(15), e2020GL088893.

Dijkstra, F. A., & Adams, M. A. (2015). Fire eases imbalances of nitrogen and phosphorus in woody plants. *Ecosystems*, *18*(5), 769-779.

Dixon, K. M., Cary, G. J., Worboys, G. L., Seddon, J., & Gibbons, P. (2018). A comparison of fuel hazard in recently burned and long-unburned forests and woodlands. *International Journal of Wildland Fire*, *27*(9), 609-622.

Dixon, D. J., Callow, J. N., Duncan, J. M., Setterfield, S. A., & Pauli, N. (2022). Regional-scale fire severity mapping of Eucalyptus forests with the Landsat archive. *Remote Sensing of Environment*, *270*, 112863.

Dlapa, P., Bodí, M. B., Mataix-Solera, J., Cerdà, A., & Doerr, S. H. (2013). FT-IR spectroscopy reveals that ash water repellence is highly dependent on ash chemical composition. *Catena*, *108*, 35-43.

Dooley, S. R., & Treseder, K. K. (2012). The effect of fire on microbial biomass: a meta-analysis of field studies. *Biogeochemistry*, *109*(1), 49-61.

Dos Santos, C. A. T., Lopo, M., Páscoa, R. N., & Lopes, J. A. (2013). A review on the applications of portable near-infrared spectrometers in the agro-food industry. *Applied Spectroscopy*, *67*(11), 1215-1233.

Duboc, O., Zehetner, F., Djukic, I., Tatzber, M., Berger, T. W., & Gerzabek, M. H. (2012). Decomposition of European beech and Black pine foliar litter along an Alpine elevation gradient: mass loss and molecular characteristics. *Geoderma*, *189*, 522-531.

Dūdaitė, J., Baltrėnaitė, E., Pereira, P., & Úbeda, X. (2011). Temperature effects on the ash colour of forest litter. *Mokslas–Lietuvos ateitis/Science–Future of Lithuania*, *3*(5), 18-23.

Dunn, B. W., Batten, G. D., Beecher, H. G., & Ciavarella, S. (2002). The potential of near-infrared reflectance spectroscopy for soil analysis — a case study from the Riverine Plain of south-eastern Australia. *Australian Journal of Experimental Agriculture*, *42*(5), 607-614.

Elle, O., Richter, R., Vohland, M., & Weigelt, A. (2019). Fine root lignin content is well predictable with near-infrared spectroscopy. *Scientific Reports*, *9*(1), 6396.

Elvidge, C. D. (1990). Visible and near infrared reflectance characteristics of dry plant materials. *Remote Sensing*, *11*(10), 1775-1795.

Engel, J., Gerretzen, J., Szymańska, E., Jansen, J. J., Downey, G., Blanchet, L., & Buydens, L. M. (2013). Breaking with trends in pre-processing? *Trends in Analytical Chemistry*, *50*, 96-106.

Esbensen, K. H., & Geladi, P. (2010). Principles of proper validation: use and abuse of re-sampling for validation. *Journal of Chemometrics*, *24*(3-4), 168-187.

Etchells, H., O'Donnell, A. J., McCaw, W. L., & Grierson, P. F. (2020). Fire severity impacts on tree mortality and post-fire recruitment in tall eucalypt forests of southwest Australia. *Forest Ecology and Management*, *459*, 117850.

Fan, Y., Cai, Y., Li, X., Jiao, L., Xia, J., & Deng, X. (2017). Effects of the cellulose, xylan and lignin constituents on biomass pyrolysis characteristics and bio-oil composition using the Simplex Lattice Mixture Design method. *Energy Conversion and Management*, *138*, 106-118.

Fernandes, P. M., & Botelho, H. S. (2003). A review of prescribed burning effectiveness in fire hazard reduction. *International Journal of Wildland Fire*, *12*(2), 117-128.

Ferreira, G. W., Roque, J. V., Soares, E. M., Silva, I. R., Silva, E. F., Vasconcelos, A. A., & Teófilo, R. F. (2018). Temporal decomposition sampling and chemical characterization of *Eucalyptus* harvest residues using NIR spectroscopy and chemometric methods. *Talanta*, *188*, 168-177.

Ficken, C. D., & Wright, J. P. (2017). Effects of fire frequency on litter decomposition as mediated by changes to litter chemistry and soil environmental conditions. *PloS One*, *12*(10), e0186292.

Flannigan, M. D., Krawchuk, M. A., de Groot, W. J., Wotton, B. M., & Gowman, L. M. (2009). Implications of changing climate for global wildland fire. *International Journal of Wildland Fire*, *18*(5), 483-507.

Foley, W. J., McIlwee, A., Lawler, I., Aragones, L., Woolnough, A. P., & Berding, N. (1998). Ecological applications of near infrared reflectance spectroscopy–a tool for rapid, cost-effective prediction of the composition of plant and animal tissues and aspects of animal performance. *Oecologia*, *116*(3), 293-305.

Food and Agriculture Organization of the United Nations. (2025). Global forest resources assessment 2025: Terms and definitions (FAO Forest Resources Assessment Working Paper No. 194). FAO. https://www.fao.org/forest-resources-assessment.

Fox, B. J., Fox, M. D., & McKay, G. M. (1979). Litter accumulation after fire in a eucalypt forest. *Australian Journal of Botany*, *27*(2), 157-165.

Fox, M. D., & Fox, B. J. (1986). The effect of fire frequency on the structure and floristic composition of a woodland understorey. *Australian Journal of Ecology*, *11*(1), 77-85.

Freitag, S., Sulyok, M., Logan, N., Elliott, C. T., & Krska, R. (2022). The potential and applicability of infrared spectroscopic methods for the rapid screening and routine analysis of mycotoxins in food crops. *Comprehensive Reviews in Food Science and Food Safety*, *21*(6), 5199-5224.

Führer, E. (2000). Forest functions, ecosystem stability and management. *Forest Ecology and Management*, *132*(1), 29-38.

Elser, J. J., Bracken, M. E., Cleland, E. E., Gruner, D. S., Harpole, W. S., Hillebrand, H., Ngai, J. T., Seabloom, E. W., & Smith, J. E. (2007). Global analysis of nitrogen and phosphorus limitation of primary producers in freshwater, marine and terrestrial ecosystems. *Ecology Letters*, *10*(12), 1135-1142.

Gabet, E. J., & Bookter, A. (2011). Physical, chemical and hydrological properties of Ponderosa pine ash. *International Journal of Wildland Fire*, *20*(3), 443-452.

Galang, M. A., Markewitz, D., & Morris, L. A. (2010). Soil phosphorus transformations under forest burning and laboratory heat treatments. *Geoderma*, *155*(3-4), 401-408.

Gałuszka, A., Migaszewski, Z. M., & Namieśnik, J. (2015). Moving your laboratories to the field–Advantages and limitations of the use of field portable instruments in environmental sample analysis. *Environmental Research*, *140*, 593-603.

Ganteaume, A., Jappiot, M., Curt, T., Lampin, C., & Borgniet, L. (2014). Flammability of litter sampled according to two different methods: comparison of results in laboratory experiments. *International Journal of Wildland Fire*, *23*(8), 1061-1075.

Gartner, T. B., & Cardon, Z. G. (2004). Decomposition dynamics in mixed-species leaf litter. *Oikos*, *104*(2), 230-246.

Gharun, M., Possell, M., Bell, T. L., & Adams, M. A. (2017). Optimisation of fuel reduction burning regimes for carbon, water and vegetation outcomes. *Journal of Environmental Management*, *203*, 157-170.

Gholz, H. L., Wedin, D. A., Smitherman, S. M., Harmon, M. E., & Parton, W. J. (2000). Long-term dynamics of pine and hardwood litter in contrasting environments: toward a global model of decomposition. *Global Change Biology*, *6*(7), 751-765.

Gill, A. M. (1975). Fire and the Australian flora: a review. *Australian Forestry*, *38*(1), 4-25.

Gillon, D., Joffre, R., & Dardenne, P. (1993). Predicting the stage of decay of decomposing leaves by near infrared reflectance spectroscopy. *Canadian Journal of Forest Research*, *23*(12), 2552-2559.

Gillon, D., Joffre, R., & Ibrahima, A. (1999). Can litter decomposability be predicted by near infrared reflectance spectroscopy?. *Ecology*, *80*(1), 175-186.

Gillon, D., & David, J. F. (2001). The use of near infrared reflectance spectroscopy to study chemical changes in the leaf litter consumed by saprophagous invertebrates. *Soil Biology and Biochemistry*, *33*(15), 2159-2161.

Goforth, B. R., Graham, R. C., Hubbert, K. R., Zanner, C. W., & Minnich, R. A. (2005). Spatial distribution and properties of ash and thermally altered soils after high-severity forest fire, southern California. *International Journal of Wildland Fire*, *14*(4), 343-354.

Gomat, H. Y., Bengo, D. M., Ifo, S. A., Mayassi, C. T. B., Bokaketi, E., Mayinguidi, U., Mabiala, P., Santenoise, P., & Epa, C. (2024). Comparison of MIR Spectral Signatures of Soils from *Acacia*, *Eucalyptus*, and *Cassava* Plantations in the Tropical Region of the Batéké Plateau (Republic of Congo). *Open Journal of Ecology*, *14*(12), 914-923.

Gordon, C. E., Price, O. F., Tasker, E. M., & Denham, A. J. (2017). *Acacia* shrubs respond positively to high severity wildfire: implications for conservation and fuel hazard management. *Science of the Total Environment*, *575*, 858-868.

Gould, J. S., McCaw, W. L., & Cheney, N. P. (2011). Quantifying fine fuel dynamics and structure in dry eucalypt forest (*Eucalyptus marginata*) in Western Australia for fire management. *Forest Ecology and Management*, *262*(3), 531-546.

Goya, J. F., Frangi, J. L., Pérez, C., & Dalla Tea, F. (2008). Decomposition and nutrient release from leaf litter in *Eucalyptus grandis* plantations on three different soils in Entre Ríos, Argentina. *Bosque*, *29*(3), 217-226.

Gray, D. M., & Dighton, J. (2006). Mineralization of forest litter nutrients by heat and combustion. *Soil Biology and Biochemistry*, *38*(6), 1469-1477.

Guinto, D. F., Xu, Z. H., House, A. P. N., & Saffigna, P. G. (2001). Soil chemical properties and forest floor nutrients under repeated prescribed-burning in eucalypt forests of south-east Queensland, Australia. *New Zealand Journal of Forestry Science*, *31*(2), 170-187.

Guo, Y., Bustin, R.M. 1998. FTIR spectroscopy and reflectance of modern charcoals and fungal decayed woods: implications for studies of inertinite in coals. *International Journal of Coal Geology. 37*, 29–53.

Guo, L. B., & Sims, R. E. H. (1999). Litter decomposition and nutrient release via litter decomposition in New Zealand eucalypt short rotation forests. *Agriculture, Ecosystems and Environment*, *75*(1-2), 133-140.

Guo, L. B., & Sims, R. E. H. (2002). Eucalypt litter decomposition and nutrient release under a short rotation forest regime and effluent irrigation treatments in New Zealand: II. Internal effects. *Soil Biology and Biochemistry*, *34*(7), 913-922.

Gupta, V., Reinke, K., & Jones, S. (2013). Changes in the spectral features of fuel layers of an Australian dry sclerophyll forest in response to prescribed burning. *International Journal of Wildland Fire*, *22*(6), 862-868.

Haberhauer, G., & Gerzabek, M. H. (1999). Drift and transmission FT-IR spectroscopy of forest soils: an approach to determine decomposition processes of forest litter. *Vibrational Spectroscopy*, *19*(2), 413-417.

Hamilton, S. D., Lawrie, A. C., Hopmans, P., & Leonard, B. V. (1991). Effects of fuel-reduction burning on a *Eucalyptus obliqua* forest ecosystem in Victoria. *Australian Journal of Botany*, *39*(3), 203-217.

Han, L., Sun, K., Yang, Y., Xia, X., Li, F., Yang, Z., & Xing, B. (2020). Biochar's stability and effect on the content, composition and turnover of soil organic carbon. *Geoderma*, *364*, 114184.

Hart, D. M. (1995). Litterfall and decomposition in the Pilliga State Forests, New South Wales, Australia. *Australian Journal of Ecology*, *20*(2), 266-272.

Hashida, Y., Lewis, D. J., & Cummins, K. (2025). Prescribed fires as a climate change adaptation tool. *Journal of Environmental Economics and Management*, *130*, 103081.

Hättenschwiler, S., Tiunov, A. V., & Scheu, S. (2005). Biodiversity and litter decomposition in terrestrial ecosystems. *Annual Review of Ecology, Evolution, and Systematics, 36*(1), 191-218.

He, K., Shen, X., Merow, C., Nikolopoulos, E., Gallagher, R. V., Yang, F., & Anagnostou, E. N. (2024). Improving fire severity prediction in south-eastern Australia using vegetation-specific information. *Natural Hazards and Earth System Sciences*, *24*(10), 3337-3355.

Hernández, D. L., & Hobbie, S. E. (2008). Effects of fire frequency on oak litter decomposition and nitrogen dynamics. *Oecologia*, *158*(3), 535-543.

Hingston, F. J., Dimmock, G. M., & Turton, A. G. (1980). Nutrient distribution in a jarrah (*Eucalyptus marginata Donn ex Sm.)* ecosystem in south-west Western Australia. *Forest Ecology and Management*, *3*, 183-207.

Hobley, E. U., Brereton, A. J. L. G., & Wilson, B. (2017). Forest burning affects quality and quantity of soil organic matter. *Science of the Total Environment*, *575*, 41-49.

Hogue, B. A., & Inglett, P. W. (2012). Nutrient release from combustion residues of two contrasting herbaceous vegetation types. *Science of the Total Environment*, *431*, 9-19.

Holden, Z. A., Morgan, P., & Evans, J. S. (2009). A predictive model of burn severity based on 20-year satellite-inferred burn severity data in a large southwestern US wilderness area. *Forest Ecology and Management*, *258*(11), 2399-2406.

Hollis, J. J., Gould, J. S., Cruz, M. G., & Lachlan McCaw, W. (2015). Framework for an Australian fuel classification to support bushfire management. *Australian Forestry*, *78*(1), 1-17.

Hollis, J. J., Cruz, M. G., McCaw, W. L., Gould, J. S., & Samson, S. A. (2025). An efficient and comprehensive field protocol for assessing fuel characteristics for fire behaviour modelling in Australian open forests. *MethodsX*, *14*, 103345.

Holsinger, L., Parks, S. A., & Miller, C. (2016). Weather, fuels, and topography impede wildland fire spread in western US landscapes. *Forest Ecology and Management*, *380*, 59-69.

Hooda, N. (1998). Effect of site and fertiliser treatment on nutrient cycling and productivity in *Eucalyptus globulus* plantations. Ph.D. Thesis. University of Melbourne.

Hosseini Bai, S., Sun, F., Xu, Z., & Blumfield, T. J. (2013). Ecophysiological status of different growth stage of understorey *Acacia leiocalyx* and *Acacia disparrima* in an Australian dry sclerophyll forest subjected to prescribed burning. *Journal of Soils and Sediments*, *13*(8), 1378-1385.

Huang, W., Xu, Z., Chen, C., Zhou, G., Liu, J., Abdullah, K. M., Reverchon, F., & Liu, X. (2013). Short-term effects of prescribed burning on phosphorus availability in a suburban native forest of subtropical Australia. *Journal of Soils and Sediments*, *13*(5), 869-876.

Huang, W., Xie, T., Huang, L., Hao, S., & Duan, Y. (2025). Why are extreme precipitation events becoming more frequent in a warming world?. *Fundamental Research*, *5*(4), 1631-1632.

Hutengs, C., Seidel, M., Oertel, F., Ludwig, B., & Vohland, M. (2019). In situ and laboratory soil spectroscopy with portable visible-to-near-infrared and mid-infrared instruments for the assessment of organic carbon in soils. *Geoderma*, *355*, 113900.

Hutson, B. R. (1985). Rates of litterfall and organic matter turnover at three South Australian indigenous forest sites. *Australian Journal of Ecology*, *10*(3), 351-359.

Ishizuka, S., Sakai, Y., & Tanaka-Oda, A. (2014). Quantifying lignin and holocellulose content in coniferous decayed wood using near-infrared reflectance spectroscopy. *Journal of Forest Research*, *19*(1), 233-237.

Janik, L. J., Soriano-Disla, J. M., Forrester, S. T., & McLaughlin, M. J. (2016). Effects of soil composition and preparation on the prediction of particle size distribution using mid-infrared spectroscopy and partial least-squares regression. *Soil Research*, *54*(8), 889-904.

Javier-Astete, R., Jimenez-Davalos, J. and Zolla, G. (2021). Determination of hemicellulose, cellulose, holocellulose and lignin content using FTIR in *Calycophyllum spruceanum* (Benth.) K. Schum. and *Guazuma crinita* Lam. *PLoS One*, *16*(10), p.e0256559.

Jenkins, M. E., Bell, T. L., Poon, L. F., Aponte, C., & Adams, M. A. (2016). Production of pyrogenic carbon during planned fires in forests of East Gippsland, Victoria. *Forest Ecology and Management*, *373*, 9-16.

Jenny, H., Gessel, S. P., & Bingham, F. T. (1949). Comparative study of decomposition rates of organic matter in temperate and tropical regions. *Soil science*, *68*(6), 419-432.

Jeon, S. H., Jang, H. J., Ng, W., Minasny, B., Kim, S. H., Shim, J. H., Roh, A., Kwon, S., & Yun, J. J. (2024). Predicting soil properties for fertiliser recommendation in South Korea using MIR spectroscopy. *Geoderma Regional*, *39*, e00901.

Jimenez, R. R., & Ladha, J. K. (1993). Automated elemental analysis: A rapid and reliable but expensive measurement of total carbon and nitrogen in plant and soil samples. *Communications in Soil Science and Plant Analysis*, *24*(15-16), 1897-1924.

Joffre, R., Gillon, D., Dardenne, P., Agneessens, R., & Biston, R. (1992). The use of near-infrared reflectance spectroscopy in litter decomposition studies. *Annales Des Sciences Forestières*. *49*(5), 481-488.

Johnson, J. B., El Orche, A., & Naiker, M. (2022). Prediction of anthocyanin content and variety in plum extracts using ATR-FTIR spectroscopy and chemometrics. *Vibrational Spectroscopy*, *121*, 103406.

Jones, T. P., Chaloner, W. G., & Kuhlbusch, T. A. J. (1997). Proposed bio-geological and chemical based terminology for fire-altered plant matter. In *Sediment records of biomass burning and global change* (pp. 9-22). Berlin, Heidelberg: Springer Berlin Heidelberg.

Kaal, J., Schneider, M. P., & Schmidt, M. W. (2012). Rapid molecular screening of black carbon (biochar) thermosequences obtained from chestnut wood and rice straw: A pyrolysis-GC/MS study. *Biomass and Bioenergy*, *45*, 115-129.

Kazanis, D., Xanthopoulos, G., & Arianoutsou, M. (2012). Understorey fuel load estimation along two post-fire chronosequences of *Pinus halepensis* Mill. forests in Central Greece. *Journal of Forest Research*, *17*(1), 105-109.

Keane, R. E. (2013). Describing wildland surface fuel loading for fire management: a review of approaches, methods and systems. *International Journal of Wildland Fire*, *22*(1), 51-62.

Keeley, J. E., Pausas, J. G., Rundel, P. W., Bond, W. J., & Bradstock, R. A. (2011). Fire as an evolutionary pressure shaping plant traits. *Trends in Plant Science*, *16*(8), 406-411.

Keith, A., Singh, B., Dijkstra, F. A., & van Ogtrop, F. (2016). Biochar field study: greenhouse gas emissions, productivity, and nutrients in two soils. *Agronomy Journal*, *108*(5), 1805-1815.

Kimber, R. G., & Friedel, M. H. (2015). Challenging the concept of Aboriginal mosaic fire practices in the Lake Eyre Basin. *The Rangeland Journal*, *37*(6), 623-630.

Khanna, P. K., Raison, R., & Falkiner, R. (1994). Chemical properties of ash derived from *Eucalyptu*s litter and its effects on forest soils. *Forest Ecology and Management*, *66*(1-3), 107-125.

Knicker, H. (2007). How does fire affect the nature and stability of soil organic nitrogen and carbon? A review. *Biogeochemistry*, *85*(1), 91-118.

Kostryukov, S. G., Matyakubov, H. B., Masterova, Y. Y., Kozlov, A. S., Pryanichnikova, M. K., Pynenkov, A. A., & Khluchina, N. A. (2023). Determination of lignin, cellulose, and hemicellulose in plant materials by FTIR spectroscopy. *Journal of Analytical Chemistry*, *78*(6), 718-727.

Kothari, S., Hobbie, S. E., & Cavender-Bares, J. (2024). Rapid estimates of leaf litter chemistry using reflectance spectroscopy. *Canadian Journal of Forest Research*, *54*(9), 978-991.

Krasznai, D. J., Champagne, P., & Cunningham, M. F. (2012). Quantitative characterization of lignocellulosic biomass using surrogate mixtures and multivariate techniques. *Bioresource Technology*, *110*, 652-661.

Krishna, M. P., & Mohan, M. (2017). Litter decomposition in forest ecosystems: a review. *Energy, Ecology and Environment*, *2*(4), 236-249.

Kumar, L. (2007). High-spectral resolution data for determining leaf water content in *Eucalyptus* species: Leaf level experiments. *Geocarto International*, *22*(1), 3-16.

Lam, W. N., Lian, J. J., Chan, P. J., Ting, Y. Y., Chong, R., Rahman, N. E., Tan, L. W. A., Ho, Q. Y., Ramchunder, S. J., Peh, K. S. -H., Cai, Y., & Chong, K. Y. (2021). Leaf litter decomposition

in tropical freshwater swamp forests is slower in swamp than non-swamp conditions. *Biotropica*, *53*(3), 920-929.

Lamb, R. J. (1985). Litter fall and nutrient turnover in two eucalypt woodlands. *Australian Journal of Botany*, *33*(1), 1-14.

Lambrakis, D. P. (1968). Experiments with mixtures: A generalization of the simplex-lattice design. *Journal of the Royal Statistical Society: Series B (Methodological)*, *30*(1), 123-136.

Lammers, K., Arbuckle-Keil, G., & Dighton, J. (2009). FT-IR study of the changes in carbohydrate chemistry of three New Jersey pine barrens leaf litters during simulated control burning. *Soil Biology and Biochemistry*, *41*(2), 340-347.

Landuyt, D., De Lombaerde, E., Perring, M. P., Hertzog, L. R., Ampoorter, E., Maes, S. L., Frenne, P. D., Ma, S., Proesmans, W., Blondeel, H., Sercu, B. K., Wang, B., Wasof, S., & Verheyen, K. (2019). The functional role of temperate forest understorey vegetation in a changing world. *Global Change Biology*, *25*(11), 3625-3641.

Lawrence, I., & Lin, K. (1989). A concordance correlation coefficient to evaluate reproducibility. *Biometrics*, *45*(1), 255-268.

Lee, K. E., & Correll, R. L. (1978). Litter fall and its relationship to nutrient cycling in a South Australian dry sclerophyll forest. *Australian Journal of Ecology*, *3*(3), 243-252.

Lee, L. C., Liong, C. Y., & Jemain, A. A. (2017). A contemporary review on Data Preprocessing (DP) practice strategy in ATR-FTIR spectrum. *Chemometrics and Intelligent Laboratory Systems*, *163*, 64-75.

Lestander, T. A., Leardi, R., & Geladi, P. (2003). Selection of near infrared wavelengths using genetic algorithms for the determination of seed moisture content. *Journal of Near Infrared Spectroscopy*, *11*(6), 433-446.

Lewis, T., & Debuse, V. J. (2012). Resilience of a eucalypt forest woody understorey to long-term (34–55 years) repeated burning in subtropical Australia. *International Journal of Wildland Fire*, *21*(8), 980-991.

Lewis, T., Reif, M., Prendergast, E., & Tran, C. (2012). The effect of long-term repeated burning and fire exclusion on above-and below-ground Blackbutt (*Eucalyptus pilularis*) forest vegetation assemblages. *Austral Ecology*, *37*(7), 767-778.

Lewis, T. (2020). Very frequent burning encourages tree growth in sub-tropical Australian eucalypt forest. *Forest Ecology and Management*, *459*, 117842.

Li, X., Li, Z., Yang, X., & He, Y. (2021). Boosting the generalization ability of Vis-NIR-spectroscopy-based regression models through dimension reduction and transfer learning. *Computers and Electronics in Agriculture*, *186*, 106157.

Li, R., Yang, Q., Guan, X., Chen, L., Wang, Q., Wang, S., & Zhang, W. (2022). High quality litters with faster initial decomposition produce more stable residue remaining in a subtropical forest ecosystem. *Catena*, *213*, 106134.

Liechty, H. O., & Reinke, M. (2020). The influence of repeated prescribed fire on decomposition and nutrient release in uneven-aged loblolly–shortleaf pine stands. *Fire Ecology*, *16*(1), 6.

Linn, R., Winterkamp, J., Edminster, C., Colman, J. J., & Smith, W. S. (2007). Coupled influences of topography and wind on wildland fire behaviour. *International Journal of Wildland Fire*, *16*(2), 183-195.

Liu, Y., Stanturf, J., & Goodrick, S. (2010). Trends in global wildfire potential in a changing climate. *Forest Ecology and Management*, *259*(4), 685-697.

Liu, J., Liu, X., Song, Q., Compson, Z. G., LeRoy, C. J., Luan, F., Wang, H., Hu, Y., & Yang, Q. (2020). Synergistic effects: a common theme in mixed-species litter decomposition. *New Phytologist*, *227*(3), 757-765.

Liu, Y., Zhang, A., Li, X., Kuang, W., & Islam, W. (2024). Litter decomposition rate response to multiple global change factors: A meta-analysis. *Soil Biology and Biochemistry*, *195*, 109474.

Louzada, J. N., Schoereder, J., & De Marco Jr, P. (1997). Litter decomposition in semideciduous forest and *Eucalyptu*s spp. crop in Brazil: a comparison. *Forest Ecology and Management*, *94*(1-3), 31-36.

Lucà, F., Conforti, M., Castrignanò, A., Matteucci, G., & Buttafuoco, G. (2017). Effect of calibration set size on prediction at local scale of soil carbon by Vis-NIR spectroscopy. *Geoderma*, *288*, 175-183.

Lummer, D., Scheu, S., & Butenschoen, O. (2012). Connecting litter quality, microbial community and nitrogen transfer mechanisms in decomposing litter mixtures. *Oikos*, *121*(10), 1649-1655.

Maheswaran, J., & Attiwill, P. M. (1987). Loss of organic matter, elements, and organic fractions in decomposing *Eucalyptus microcarpa* leaf litter. *Canadian Journal of Botany*, *65*(12), 2601-2606.

Makkar, H. P. S., Borowy, N. K., Becker, K., & Degen, A. (1995). Some problems in fiber determination of a tannin-rich forage (*Acacia saligna* leaves) and their implications in in vivo studies. *Animal Feed Science and Technology*, *55*(1-2), 67-76.

Makoto, K., & Koike, T. (2021). Charcoal ecology: Its function as a hub for plant succession and soil nutrient cycling in boreal forests. *Ecological Research*, *36*(1), 4-12.

Malley, D. F., Yesmin, L., Wray, D., & Edwards, S. (1999). Application of near-infrared spectroscopy in analysis of soil mineral nutrients. *Communications in Soil Science and Plant Analysis*, *30*(7-8), 999-1012.

Manheim, J., Doty, K. C., McLaughlin, G., & Lednev, I. K. (2016). Forensic hair differentiation using attenuated total reflection Fourier transform infrared (ATR FT-IR) spectroscopy. *Applied spectroscopy*, *70*(7), 1109-1117.

Martins, R. C., Queirós, C., Silva, F. M., Santos, F., Barroso, T. G., Tosin, R., Cunha, M., Leão, M., Damásio, M., Martins, P., & Silvestre, J. (2024). Spectral data augmentation for leaf nutrient uptake quantification. *Biosystems Engineering*, *246*, 82-95.

Matthews, S. (2014). Dead fuel moisture research: 1991–2012. *International Journal of Wildland Fire*, *23*(1), 78-92.

McArthur, C. (1988). Variation in neutral detergent fiber analysis of tannin-rich foliage. *The Journal of Wildlife Management*, *52*(2), 374-378.

McCaw, W. L., Neal, J. E., & Smith, R. H. (1996). Fuel accumulation following prescribed burning in young even-aged stands of karri (*Eucalyptus diversicolor*). *Australian Forestry*, *59*(4), 171-177.

McCaw, W. L., Gould, J. S., Cheney, N. P., Ellis, P. F., & Anderson, W. R. (2012). Changes in behaviour of fire in dry eucalypt forest as fuel increases with age. *Forest Ecology and Management*, *271*, 170-181.

McCaw, W. L. (2013). Managing forest fuels using prescribed fire–a perspective from southern Australia. *Forest Ecology and Management*, *294*, 217-224.

McCaw, W. L., Neal, J. E., & Smith, R. H. (2002). Stand characteristics and fuel accumulation in a sequence of even-aged Karri (*Eucalyptus diversicolor*) stands in south-west Western Australia. *Forest Ecology and Management*, *158*(1-3), 263-271.

McCarty, G. W., Reeves, J. B., Reeves, V. B., Follett, R. F., & Kimble, J. M. (2002). Mid-infrared and near-infrared diffuse reflectance spectroscopy for soil carbon measurement. *Soil Science Society of America Journal*, *66*(2), 640-646.

McColl, J. G. (1966). Accession and decomposition of litter in spotted gum forests. *Australian Forestry*, *30*(3), 191-198.

McKee, G. A., Soong, J. L., Caldéron, F., Borch, T., & Cotrufo, M. F. (2016). An integrated spectroscopic and wet chemical approach to investigate grass litter decomposition chemistry. *Biogeochemistry*, *128*(1), 107-123.

McLellan, T. M., Martin, M. E., Aber, J. D., Melillo, J. M., Nadelhoffer, K. J., & Dewey, B. (1991a). Comparison of wet chemistry and near infrared reflectance measurements of carbon-fraction chemistry and nitrogen concentration of forest foliage. *Canadian Journal of Forest Research*, *21*(11), 1689-1693.

McLellan, T. M., Aber, J. D., Martin, M. E., Melillo, J. M., & Nadelhoffer, K. J. (1991b). Determination of nitrogen, lignin, and cellulose content of decomposing leaf material by near infrared reflectance spectroscopy. *Canadian Journal of Forest Research*, *21*(11), 1684-1688.

Md Salim, R., Asik, J., & Sarjadi, M. S. (2021). Chemical functional groups of extractives, cellulose and lignin extracted from native *Leucaena leucocephala* bark. *Wood Science and Technology*, *55*(2), 295-313.

Meentemeyer, V. (1978). Macroclimate and lignin control of litter decomposition rates. *Ecology*, *59*(3), 465-472.

Meira-Castro, A., Shakesby, R. A., Espinha Marques, J., Doerr, S. H., Meixedo, J. P., Teixeira, J., & Chaminé, H. I. (2015). Effects of prescribed fire on surface soil in a *Pinus pinaster* plantation, northern Portugal. *Environmental Earth Sciences*, *73*(6), 3011-3018.

Melillo, J. M., Aber, J. D., & Muratore, J. F. (1982). Nitrogen and lignin control of hardwood leaf litter decomposition dynamics. *Ecology*, *63*(3), 621-626.

Minasny, B., & McBratney, A. B. (2008). Regression rules as a tool for predicting soil properties from infrared reflectance spectroscopy. *Chemometrics and Intelligent Laboratory Systems*, *94*(1), 72-79.

Minasny, B., & McBratney, A. (2013). Why you don't need to us RPD. *Pedometron*, *33*(600), 14-15.

Minatre, K. L., Arienzo, M. M., Moosmüller, H., & Maezumi, S. Y. (2024). Charcoal analysis for temperature reconstruction with infrared spectroscopy. *Frontiers in Earth Science*, *12*, 1354080.

Morgan, P., Hardy, C. C., Swetnam, T. W., Rollins, M. G., Long, D. G. (2001). Mapping fire regimes across time and space: understanding coarse and fine-scale fire patterns. *International Journal of Wildland Fire, 10*, 329–342.

Morgan, P., Keane, R. E., Dillon, G. K., Jain, T. B., Hudak, A. T., Karau, E. C., Sikkink, P. G., Holden, Z. A. & Strand, E. K. (2014). Challenges of assessing fire and burn severity using field measures, remote sensing and modelling. *International Journal of Wildland Fire*, *23*(8), 1045-1060.

Mould, E. D., & Robbins, C. T. (1981). Evaluation of detergent analysis in estimating nutritional value of browse. *The Journal of Wildlife Management*, *45*(4), 937-947.

Mukherjee, A., Zimmerman, A. R., & Harris, W. (2011). Surface chemistry variations among a series of laboratory-produced biochars. *Geoderma*, *163*(3-4), 247-255.

Muscarella, R., Kolyaie, S., Morton, D. C., Zimmerman, J. K., & Uriarte, M. (2020). Effects of topography on tropical forest structure depend on climate context. *Journal of Ecology*, *108*(1), 145-159.

Muqaddas, B., Zhou, X., Lewis, T., Wild, C., & Chen, C. (2015). Long-term frequent prescribed fire decreases surface soil carbon and nitrogen pools in a wet sclerophyll forest of Southeast Queensland, Australia. *Science of the Total Environment*, *536*, 39-47.

Muqaddas, B., Chen, C., Lewis, T., & Wild, C. (2016). Temporal dynamics of carbon and nitrogen in the surface soil and forest floor under different prescribed burning regimes. *Forest Ecology and Management*, *382*, 110-119.

Muqaddas, B., Lewis, T., Esfandbod, M., & Chen, C. (2019). Responses of labile soil organic carbon and nitrogen pools to long-term prescribed burning regimes in a wet sclerophyll forest of southeast Queensland, Australia. *Science of the Total Environment*, *647*, 110-120.

Murphy, J. A. M. E. S., & Riley, J. P. (1962). A modified single solution method for the determination of phosphate in natural waters. *Analytica Chimica Acta*, *27*, 31-36.

Myers-Pigg, A. N., Grieger, S., Roebuck Jr, J. A., Barnes, M. E., Bladon, K. D., Bailey, J. D., Barton, R., Chu, R. K., Graham, E. B., Homolka, K. K., Kew, W., Lipton, A. S., Scheibe, T., Toyoda, J. G., & Wagner, S. (2024). Experimental open air burning of vegetation enhances organic matter chemical heterogeneity compared to laboratory burns. *Environmental Science & Technology*, *58*(22), 9679-9688.

Nault, J. R., Preston, C. M., Trofymow, J. T., Fyles, J., Kozak, L., Siltanen, M., & Titus, B. (2009). Applicability of diffuse reflectance Fourier transform infrared spectroscopy to the chemical analysis of decomposing foliar litter in Canadian forests. *Soil Science*, *174*(3), 130-142.

Nduwamungu, C., Ziadi, N., Parent, L. É., Tremblay, G. F., & Thuriès, L. (2009). Opportunities for, and limitations of, near infrared reflectance spectroscopy applications in soil analysis: A review. *Canadian Journal of Soil Science*, *89*(5), 531-541.

Neumann, M., Turner, J., Lewis, T., McCaw, L., Cook, G., & Adams, M. A. (2021). Dynamics of necromass in woody Australian ecosystems. *Ecosphere*, *12*(8), e03693.

Ng, W., Minasny, B., Mendes, W. D. S., & Demattê, J. A. (2019). Estimation of effective calibration sample size using visible near infrared spectroscopy: Deep learning vs machine learning. *Soil Discussions*, *2019*, 1-21.

Nguyen, T. H., Jones, S., Reinke, K. J., & Soto-Berelov, M. (2024). Estimating fine fuel loads in Eucalypt forests using forest inventory data and a modelling approach. *Forest Ecology and Management*, *561*, 121851.

Nolan, R. H., Boer, M. M., Collins, L., Resco de Dios, V., Clarke, H., Jenkins, M., Kenny, B., & Bradstock, R. A. (2020). Causes and consequences of eastern Australia's 2019–20 season of mega-fires. *Global Change Biology*, *26*(3), 1039.

NSW Government. (2025). *NSW Government Data Portal - Seed 2025*. Retrieved from https://datasets.seed.nsw.gov.au/dataset/fire-extent-and-severity-mapping-fesm.

O'Connell, A. M., & Menage, P. M. A. (1982). Litter fall and nutrient cycling in karri (*Eucalyptus diversicolor* F. Muell.) forest in relation to stand age. *Australian Journal of Ecology*, *7*(1), 49-62.

O'Connell L, A. M., & Menage, P. (1983). Decomposition of litter from three major plant species of jarrah (*Eucalyptus marginata* Donn ex Sm.) forest in relation to site fire history and soil type. *Australian Journal of Ecology*, *8*(3), 277-286.

O'Connell, A. M. (1986). Effect of legume understorey on decomposition and nutrient content of eucalypt forest litter. *Plant and Soil*, *92*(2), 235-248.

O'Connell, A. M. (1987a). Litter decomposition, soil respiration and soil chemical and biochemical properties at three contrasting sites in karri (*Eucalyptus diversicolor* F. Muell.) forests of south-western Australia. *Australian Journal of Ecology*, *12*(1), 31-40.

O'Connell, A. M. (1987b). Litter dynamics in Karri (*Eucalyptus diversicolor*) forests of south-western Australia. *The Journal of Ecology*, *75*(3), 781-796.

O'Connell, A. M. (1988). Nutrient dynamics in decomposing litter in karri (*Eucalyptus diversicolor* F. Muell.) forests of south-western Australia. *The Journal of Ecology*, *76*(4), 1186-1203.

O'Connell, A. M. (1989). Nutrient accumulation in and release from the litter layer of karri (*Eucalyptus diversicolor*) forests of southwestern Australia. *Forest Ecology and Management*, *26*(2), 95-111.

O'Connell, A. M. (1997). Decomposition of slash residues in thinned regrowth eucalypt forest in Western Australia. *Journal of Applied Ecology*, *34*(1), 111-122.

Oh, S. Y., Yoo, D. I., Shin, Y., Kim, H. C., Kim, H. Y., Chung, Y. S., Park, W. H., & Youk, J. H. (2005). Crystalline structure analysis of cellulose treated with sodium hydroxide and carbon dioxide by means of X-ray diffraction and FTIR spectroscopy. *Carbohydrate research*, *340*(15), 2376-2391.

Oliveira, L. F. R. D., Santana, R. C., & Oliveira, M. L. R. D. (2019). Non-destructive estimation of leaf nutrient concentrations in *Eucalyptus* plantations. *Cerne*, *25*(2), 184-194.

Olson, J. S. (1963). Energy storage and the balance of producers and decomposers in ecological systems. *Ecology*, *44*(2), 322-331.

Ono, K., Hiraide, M., & Amari, M. (2003). Determination of lignin, holocellulose, and organic solvent extractives in fresh leaf, litterfall, and organic material on forest floor using near-infrared reflectance spectroscopy. *Journal of Forest Research*, *8*(3), 191-198.

Ono, K., Hasegawa, M., Araki, M., Amari, M., & Hiraide, M. (2007). Spectrophotometrical characteristics in the near infrared region in beech (*Fagus crenata*) and pine (*Pinus densiflora*) litters at the various decomposing stages. *Journal of forest research*, *12*(4), 255-261.

Ono, K., Miki, K., Amari, M., & Hirai, K. (2008). Near-infrared reflectance spectroscopy for the determination of lignin-derived compounds in the decomposed and humified litters of coniferous and deciduous temperate forests in Northern Kanto District, Central Japan. *Soil Science & Plant Nutrition*, *54*(2), 188-196.

Parsons, W. F., Taylor, B. R., & Parkinson, D. (1990). Decomposition of aspen (*Populus tremuloides*) leaf litter modified by leaching. *Canadian Journal of Forest Research*, *20*(7), 943-951.

Parsons, S. A., Lawler, I. R., Congdon, R. A., & Williams, S. E. (2011). Rainforest litter quality and chemical controls on leaf decomposition with near-infrared spectrometry. *Journal of Plant Nutrition and Soil Science*, *174*(5), 710-720.

Parsons, S. A., Congdon, R. A., Storlie, C. J., Shoo, L. P., & Williams, S. E. (2012). Regional patterns and controls of leaf decomposition in Australian tropical rainforests. *Austral Ecology*, *37*(7), 845-854.

Partheepan, S., Sanati, F., & Hassan, J. (2025). Modelling bushfire severity and predicting future trends in Australia using remote sensing and machine learning. *Environmental Modelling & Software*, *188*, 106377.

Paudel, E., Dossa, G. G., de Blécourt, M., Beckschäfer, P., Xu, J., & Harrison, R. D. (2015). Quantifying the factors affecting leaf litter decomposition across a tropical forest disturbance gradient. *Ecosphere*, *6*(12), 1-20.

Paul, K. I., & Polglase, P. J. (2004). Prediction of decomposition of litter under eucalypts and pines using the FullCAM model. *Forest Ecology and Management*, *191*(1-3), 73-92.

Pausas, J. G., Keeley, J. E., & Schwilk, D. W. (2017). Flammability as an ecological and evolutionary driver. *Journal of Ecology*, *105*(2), 289-297.

Penman, T. D., & York, A. (2010). Climate and recent fire history affect fuel loads in *Eucalyptus* forests: Implications for fire management in a changing climate. *Forest Ecology and Management*, *260*(10), 1791-1797.

Penman, T. D., Christie, F. J., Andersen, A. N., Bradstock, R. A., Cary, G. J., Henderson, M. K., Price, O., Tran, C., Wardle, G. M., Williams, R. J. & York, A. (2011). Prescribed burning: how can it work to conserve the things we value?. *International Journal of Wildland Fire*, *20*(6), 721-733.

Pereira, P., Úbeda, X., & Martin, D. A. (2012). Fire severity effects on ash chemical composition and water-extractable elements. *Geoderma*, *191*, 105-114.

Pereira, P., Úbeda, X., Martin, D., Mataix-Solera, J., Cerdà, A., & Burguet, M. (2014). Wildfire effects on extractable elements in ash from a *Pinus pinaster* forest in Portugal. *Hydrological Processes*, *28*(11), 3681-3690.

Pereira, P., Bogunovic, I., Zhao, W., & Barcelo, D. (2021). Short-term effect of wildfires and prescribed fires on ecosystem services. *Current Opinion in Environmental Science and Health*, *22*, 100266.

Pitman, R. M. (2006). Wood ash use in forestry – a review of the environmental impacts. *Forestry*, *79*(5), 563-588.

Poke, F. S., Wright, J. K., & Raymond, C. A. (2005). Predicting extractives and lignin contents in *Eucalyptus globulus* using near infrared reflectance analysis. *Journal of Wood Chemistry and Technology*, *24*(1), 55-67.

Polglase, P. J., Attiwill, P. M., & Adams, M. A. (1992). Nitrogen and phosphorus cycling in relation to stand age of *Eucalyptus regnans* F. Muell: III. Labile inorganic and organic P, phosphatase activity and P availability. *Plant and Soil*, *142*(2), 177-185.

Pook, E. W., Gill, A. M., & Moore, P. H. R. (1997). Long-term variation of litter fall, canopy leaf area and flowering in a Eucalyptus maculata forest on the south coast of New South Wales. *Australian Journal of Botany*, *45*(5), 737-755.

Popescu, M. C., Popescu, C. M., Lisa, G., & Sakata, Y. (2011). Evaluation of morphological and chemical aspects of different wood species by spectroscopy and thermal methods. *Journal of Molecular Structure*, *988*(1-3), 65-72.

Possell, M., Jenkins, M., Bell, T. L., & Adams, M. A. (2015). Emissions from prescribed fires in temperate forest in south-east Australia: implications for carbon accounting. *Biogeosciences*, *12*(1), 257-268.

Prananto, J. A., Minasny, B., & Weaver, T. (2021). Rapid and cost-effective nutrient content analysis of cotton leaves using near-infrared spectroscopy (NIRS). *PeerJ*, *9*, e11042.

Prescott, C. E., & Vesterdal, L. (2021). Decomposition and transformations along the continuum from litter to soil organic matter in forest soils. *Forest Ecology and Management*, *498*, 119522.

Prescott, C. E. (2005). Do rates of litter decomposition tell us anything we really need to know?. *Forest Ecology and Management*, *220*(1-3), 66-74.

Pressland, A. J. (1982). Litter production and decomposition from an overstorey of *Eucalyptus* spp. on two catchments in the New England region of New South Wales. *Australian Journal of Ecology*, *7*(2), 171-180.

Preston, C. M., & Schmidt, M. W. (2006). Black (pyrogenic) carbon: a synthesis of current knowledge and uncertainties with special consideration of boreal regions. *Biogeosciences*, *3*(4), 397-420.

Price, O. H., Nolan, R. H., & Samson, S. A. (2022). Fuel consumption rates in resprouting eucalypt forest during hazard reduction burns, cultural burns and wildfires. *Forest Ecology and Management*, *505*, 119894.

Prieto, I., Almagro, M., Bastida, F., & Querejeta, J. I. (2019). Altered leaf litter quality exacerbates the negative impact of climate change on decomposition. *Journal of Ecology*, *107*(5), 2364-2382.

Qian, Y., Miao, S. I., Gu, B., & Li, Y. C. (2008). Effects of burn temperature on ash nutrient forms and availability from cattail (*Typha domingensis*) and sawgrass (*Cladium jamaicense*) in the Florida Everglades. *Journal of Environmental Quality*, *38*(2), 451-464.

Quinlan, J. R. (1993). Combining instance-based and model-based learning. In: Proceedings of the Tenth International Conference on Machine Learning pp. 236-243. San Mateo, CA.

Rachid, C. T., Balieiro, F. C., Peixoto, R. S., Fonseca, E. S., Jesus, H. E., Novotny, E. H., Chaer, G. M., Santos, F. M., Tiedje, J. M. & Rosado, A. S. (2023). Mycobiome structure does not affect field litter decomposition in *Eucalyptus* and *Acacia* plantations. *Frontiers in Microbiology*, *14*, 1106422.

Rahman, M. M., Tsukamoto, J., Tokumoto, Y., & Shuvo, M. A. R. (2013). The role of quantitative traits of leaf litter on decomposition and nutrient cycling of the forest ecosystems. *Journal of Forest and Environmental Science*, *29*(1), 38-48.

Raison, R. J., Woods, P. V., & Khanna, P. K. (1983). Dynamics of fine fuels in recurrently burnt eucalypt forests. *Australian Forestry*, *46*(4), 294-302.

Raison, R. J., Khanna, P. K., & Woods, P. V. (1985). Transfer of elements to the atmosphere during low-intensity prescribed fires in three Australian subalpine eucalypt forests. *Canadian Journal of Forest Research*, *15*(4), 657-664.

Raison, R. J., Woods, P. V., & Khanna, P. K. (1986). Decomposition and accumulation of litter after fire in sub-alpine eucalypt forests. *Australian Journal of Ecology*, *11*(1), 9-19.

Ramalho, F. M. G., Hein, P. R. G., Andrade, J. M., & Napoli, A. (2017). Potential of near-infrared spectroscopy for distinguishing charcoal produced from planted and native wood for energy purpose. *Energy and Fuels 31*, 1593–1599.

Ramírez, P. B., Calderón, F. J., Jastrow, J. D., Ping, C. L., & Matamala, R. (2023). Applying NIR and MIR spectroscopy for C and soil property prediction in northern cold-region ecosystems. Which approach works better?. *Geoderma Regional*, *32*, e00617.

Ramirez-Lopez, L., Wadoux, A. C., Franceschini, M. H., Terra, F. S., Marques, K. P. P., Sayão, V. M., & Demattê, J. A. M. (2019). Robust soil mapping at the farm scale with vis–NIR spectroscopy. *European Journal of Soil Science*, *70*(2), 378-393.

Raymond, C. A., & Schimleck, L. R. (2002). Development of near infrared reflectance analysis calibrations for estimating genetic parameters for cellulose content in *Eucalyptus globulus*. *Canadian Journal of Forest Research*, *32*(1), 170-176.

Reichenbächer, M., & Popp, J. Chapter 2: Vibrational Spectroscopy. *Challenges in molecular structure determination*, 63-143.

Reverchon, F., Xu, Z., Blumfield, T. J., Chen, C., & Abdullah, K. M. (2012). Impact of global climate change and fire on the occurrence and function of understorey legumes in forest ecosystems. *Journal of Soils and Sediments*, *12*(2), 150-160.

Ribeiro, C., Madeira, M., & Araújo, M. C. (2002). Decomposition and nutrient release from leaf litter of *Eucalyptus globulus* grown under different water and nutrient regimes. *Forest Ecology and Management*, *171*(1-2), 31-41.

Richards, K. R., & Stokes, C. (2004). A review of forest carbon sequestration cost studies: a dozen years of research. *Climatic Change*, *63*(1), 1-48.

Richardson, A. D., & Reeves Iii, J. B. (2005). Quantitative reflectance spectroscopy as an alternative to traditional wet lab analysis of foliar chemistry: near-infrared and mid-infrared calibrations compared. *Canadian Journal of Forest Research*, *35*(5), 1122-1130.

Richardson, A. D., Reeves III, J. B., & Gregoire, T. G. (2004). Multivariate analyses of visible/near infrared (VIS/NIR) absorbance spectra reveal underlying spectral differences among dried, ground conifer needle samples from different growth environments. *New Phytologist*, *161*(1), 291-301.

Rinnan, Å., Van Den Berg, F., & Engelsen, S. B. (2009). Review of the most common pre-processing techniques for near-infrared spectra. *Trends in Analytical Chemistry*, *28*(10), 1201-1222.

Rogers, R. W., & Westman, W. E. (1977). Seasonal nutrient dynamics of litter in a subtropical eucalypt forest, North Stradbroke Island. *Australian Journal of Botany*, *25*(1), 47-58.

Roger, J. M., Chauchard, F., & Bellon-Maurel, V. (2003). EPO–PLS external parameter orthogonalisation of PLS application to temperature-independent measurement of sugar content of intact fruits. *Chemometrics and Intelligent Laboratory Systems*, *66*(2), 191-204.

Rotbart, N., Schmilovitch, Z., Cohen, Y., Alchanatis, V., Erel, R., Ignat, T., Shenderey, C., Dag, A., & Yermiyahu, U. (2013). Estimating olive leaf nitrogen concentration using visible and near-infrared spectral reflectance. *Biosystems Engineering*, *114*(4), 426-434.

Roy, D. P., Boschetti, L., Maier, S. W., & Smith, A. M. (2010). Field estimation of ash and char colour-lightness using a standard grey scale. *International Journal of Wildland Fire*, *19*(6), 698-704.

Ryan, R., Thomas, Z., Simkovic, I., Dlapa, P., Worthy, M., Wasson, R., Bradstock, R., Mooney, S., Haynes, K., & Dosseto, A. (2024). Assessing changes in high-intensity fire events in south-eastern Australia using Fourier Transform Infra-red (FITR) spectroscopy. *International Journal of Wildland Fire*, *33*(9), WF24064.

Ryan, R., Dosseto, A., Dlapa, P., Thomas, Z., Simkovic, I., Mooney, S., & Bradstock, R. (2025). Using Fourier Transform Infrared spectroscopy to produce high-resolution centennial records of past high-intensity fires from organic-rich sediment deposits. *International Journal of Wildland Fire*, *34*(1), WF23175.

Safdari, M. S., Rahmati, M., Amini, E., Howarth, J. E., Berryhill, J. P., Dietenberger, M., Weise, D. R., & Fletcher, T. H. (2018). Characterization of pyrolysis products from fast pyrolysis of live and dead vegetation native to the Southern United States. *Fuel*, *229*, 151-166.

Salamanca, E. F., Kaneko, N., Katagiri, S., & Nagayama, Y. (1998). Nutrient dynamics and lignocellulose degradation in decomposing Quercus serrata leaf litter. *Ecological Research*, *13*(2), 199-210.

Sanchez-Garcia, C., Santín, C., Neris, J., Sigmund, G., Otero, X. L., Manley, J., González-Rodríguez, G., Belcher, C. M., Cerdà, A., Marcotte, A. L., Murphy, S. F., Rhoades, C. C., Sheridan, G., Strydom, T., Robichaud, P. R., & Doerr, S. H. (2023). Chemical characteristics of wildfire ash across the globe and their environmental and socio-economic implications. *Environment International*, *178*, 108065.

Sandak, J., Sandak, A., Zitek, A., Hintestoisser, B., & Picchi, G. (2020). Development of low-cost portable spectrometers for detection of wood defects. *Sensors*, *20*(2), 545.

Sangha, K. K., Jalota, R. K., & Midmore, D. J. (2006). Litter production, decomposition and nutrient release in cleared and uncleared pasture systems of central Queensland, Australia. *Journal of Tropical Ecology*, *22*(2), 177-189.

Santín, C., Doerr, S. H., Otero, X. L., & Chafer, C. J. (2015). Quantity, composition and water contamination potential of ash produced under different wildfire severities. *Environmental Research*, *142*, 297-308.

Santín, C., Doerr, S. H., Merino, A., Bucheli, T. D., Bryant, R., Ascough, P., Gao, X., & Masiello, C. A. (2017). Carbon sequestration potential and physicochemical properties differ between wildfire charcoals and slow-pyrolysis biochars. *Scientific Reports*, *7*(1), 11233.

Santos, F. M., Balieiro, F. D. C., Fontes, M. A., & Chaer, G. M. (2018). Understanding the enhanced litter decomposition of mixed-species plantations of *Eucalyptus* and *Acacia mangium*. *Plant and Soil*, *423*(1), 141-155.

Savitzky, A., & Golay, M. J. (1964). Smoothing and differentiation of data by simplified least squares procedures. *Analytical Chemistry*, *36*(8), 1627-1639.

Scheffé, H. (1958). Experiments with mixtures. *Journal of the Royal Statistical Society: Series B (Methodological)*, *20*(2), 344-360.

Schimel, J. P., & Hättenschwiler, S. (2007). Nitrogen transfer between decomposing leaves of different N status. *Soil Biology and Biochemistry*, *39*(7), 1428-1436.

Schimleck, L. R., Raymond, C. A., Beadle, C. L., Downes, G. M., Kube, P. D., & French, J. (2000). Applications of NIR spectroscopy to forest research. *Appita Journal: Journal of the Technical Association of the Australian and New Zealand Pulp and Paper Industry*, *53*, 458-464.

Senger, C. C., Kozloski, G. V., Sanchez, L. M. B., Mesquita, F. R., Alves, T. P., & Castagnino, D. S. (2008). Evaluation of autoclave procedures for fibre analysis in forage and concentrate feedstuffs. *Animal Feed Science and Technology*, *146*(1-2), 169-174.

Shammas, K., O'connell, A. M., Grove, T. S., McMurtrie, R., Damon, P., & Rance, S. J. (2003). Contribution of decomposing harvest residues to nutrient cycling in a second rotation *Eucalyptus globulus* plantation in south-western Australia. *Biology and Fertility of Soils*, *38*(4), 228-235.

Sharples, J. J., Cary, G. J., Fox-Hughes, P., Mooney, S., Evans, J. P., Fletcher, M. S., Fromm, M., Grierson, P. F., McRae, R., & Baker, P. (2016). Natural hazards in Australia: extreme bushfire. *Climatic Change*, *139*(1), 85-99.

Sharples, J. J., & Towers, I. N. (2025). Modelling litter accumulation and fire risks in Australia using Olson models: Commentary on Adams and Neumann (2024). *Forest Ecology and Management*, *578*, 122443.

Shindo, H. (1991). Elementary composition, humus composition, and decomposition in soil of charred grassland plants. *Soil Science and Plant Nutrition*, *37*(4), 651-657.

Simmons, D., & Adams, R. (1986). Fuel dynamics in an urban fringe dry sclerophyll forest in Victoria. *Australian Forestry*, *49*(3), 149-154.

Skorupa, A. L. A., Barros, N. F. D., & Neves, J. C. L. (2015). Forest litter decomposition as affected by *Eucalyptus* stand age and topography in south-eastern Brazil. *Revista Árvore*, *39*(6), 1055-1064.

Song, H. H., Yan, T., & Zeng, D. H. (2019). Establishment of mixed plantations of *Pinus sylvestris* var. *mongolica* and *Populus* × Xiaozhuanica may not be appropriate: evidence from litter decomposition. *Journal of Plant Ecology*, *12*(5), 857-870.

Soriano-Disla, J. M., Janik, L. J., Viscarra Rossel, R. A., Macdonald, L. M., & McLaughlin, M. J. (2014). The performance of visible, near-, and mid-infrared reflectance spectroscopy for prediction of soil physical, chemical, and biological properties. *Applied Spectroscopy Reviews*, *49*(2), 139-186.

Soriano-Disla, J. M., Janik, L., McLaughlin, M. J., Forrester, S., Kirby, J. K., Reimann, C., & EuroGeoSurveys GEMAS Project Team. (2013). Prediction of the concentration of chemical elements extracted by aqua regia in agricultural and grazing European soils using diffuse reflectance mid-infrared spectroscopy. *Applied Geochemistry*, *39*, 33-42.

Spain, A. V. (1984). Litterfall and the standing crop of litter in three tropical Australian rainforests. *The Journal of Ecology*, *72*(3), 947-961.

Spain, A. V., & Le Feuvre, R. P. (1987). Breakdown of four litters of contrasting quality in a tropical Australian rainforest. *Journal of Applied Ecology*, *24*(1), 279-288.

Specht, R. L. (1970). Vegetation. In 'The Australian Environment'. 4th edn. (Ed. GW Leeper.) pp. 44–67.

Spence, R. J., & Baxter, G. S. (2006). Effects of fire on the structure and composition of open eucalypt forests. *Austral Ecology*, *31*(5), 638-646.

Stanton, P., Parsons, M., Stanton, D., & Stott, M. (2014). Fire exclusion and the changing landscape of Queensland's Wet Tropics Bioregion 2. The dynamics of transition forests and implications for management. *Australian Forestry*, *77*(1), 58-68.

Stavros, E. N., Coen, J., Peterson, B., Singh, H., Kennedy, K., Ramirez, C., & Schimel, D. (2018). Use of imaging spectroscopy and LIDAR to characterize fuels for fire behaviour prediction. *Remote Sensing Applications: Society and Environment*, *11*, 41-50.

Stein, B. R., Thomas, V. A., Lorentz, L. J., & Strahm, B. D. (2014). Predicting macronutrient concentrations from loblolly pine leaf reflectance across local and regional scales. *GIScience & Remote Sensing*, *51*(3), 269-287.

Steinwandter, M., Schlick-Steiner, B. C., Steiner, F. M., & Seeber, J. (2019). One plus one is greater than two: mixing litter types accelerates decomposition of low-quality alpine dwarf shrub litter. *Plant and Soil*, *438*(1), 405-419.

Storey, M., Price, O., & Tasker, E. (2016). The role of weather, past fire and topography in crown fire occurrence in eastern Australia. *International Journal of Wildland Fire*, *25*(10), 1048-1060.

Sullivan, A. L., McCaw, W. L., Cruz, M. G., Matthews, S., & Ellis, P. F. (2012). Fuel, fire weather and fire behaviour in Australian ecosystems. Flammable Australia: fire regimes, biodiversity and ecosystems in a changing world, *1*, 51-77.

Sun, T., Dong, L., Zhang, Y., Hättenschwiler, S., Schlesinger, W. H., Zhu, J., Berg, B., Adair, E. C., & Hobbie, S. E. (2024). General reversal of N-decomposition relationship during long-term decomposition in boreal and temperate forests. *Proceedings of the National Academy of Sciences*, *121*(20), e2401398121.

Tahir, P. M., Halip, J. A., & Lee, S. H. (2019). Tannin-based bioresin as adhesives. In *Lignocellulose for Future Bioeconomy* (pp. 109-133). Elsevier.

Tahmasbian, I., Xu, Z., Nguyen, T. T. N., Che, R., Omidvar, N., Lambert, G., & Bai, S. H. (2019). Short-term carbon and nitrogen dynamics in soil, litterfall and canopy of a suburban native forest subjected to prescribed burning in subtropical Australia. *Journal of Soils and Sediments*, *19*(12), 3969-3981.

Talbot, J. M., & Treseder, K. K. (2012). Interactions among lignin, cellulose, and nitrogen drive litter chemistry–decay relationships. *Ecology*, *93*(2), 345-354.

Talbot, J. M., Yelle, D. J., Nowick, J., & Treseder, K. K. (2012). Litter decay rates are determined by lignin chemistry. *Biogeochemistry*, *108*(1), 279-295.

Tang, Y., Jones, E., & Minasny, B. (2020). Evaluating low-cost portable near infrared sensors for rapid analysis of soils from South Eastern Australia. *Geoderma Regional*, *20*, e00240.

Taylor, B. R., Parkinson, D., & Parsons, W. F. (1989). Nitrogen and lignin content as predictors of litter decay rates: a microcosm test. *Ecology*, *70*(1), 97-104.

Terhoeven-Urselmans, T., Michel, K., Helfrich, M., Flessa, H., & Ludwig, B. (2006). Near-infrared spectroscopy can predict the composition of organic matter in soil and litter. *Journal of Plant Nutrition and Soil Science*, *169*(2), 168-174.

Thomas, P. B., Watson, P. J., Bradstock, R. A., Penman, T. D., & Price, O. F. (2014). Modelling surface fine fuel dynamics across climate gradients in eucalypt forests of south-eastern Australia. *Ecography*, *37*(9), 827-837.

Toberman, H., Chen, C., Lewis, T., & Elser, J. J. (2014). High-frequency fire alters C: N: P stoichiometry in forest litter. *Global Change Biology*, *20*(7), 2321-2331.

Tolhurst, K., Shields, B., & Chong, D. (2008). Phoenix: development and application of a bushfire risk management tool. *Australian Journal of Emergency Management*, *23*(4), 47-54.

Trouvé, R., Oborne, L., & Baker, P. J. (2021). The effect of species, size, and fire intensity on tree mortality within a catastrophic bushfire complex. *Ecological Applications*, *31*(6), e0238.

Tsuchikawa, S., Inagaki, T., & Ma, T. (2023). Application of near-infrared spectroscopy to forest and wood products. *Current Forestry Reports*, *9*(6), 401-412.

Turner, J., & Lambert, M. J. (2002). Litterfall and forest floor dynamics in *Eucalyptus pilularis* forests. *Austral Ecology*, *27*(2), 192-199.

Úbeda, X., Pereira, P., Outeiro, L., & Martin, D. A. (2009). Effects of fire temperature on the physical and chemical characteristics of the ash from two plots of cork oak (*Quercus suber*). *Land Degradation & Development*, *20*(6), 589-608.

Van Soest, P. J. (1963). Ruminant fat metabolism with particular reference to factors affecting low milk fat and feed efficiency. A review. *Journal of Dairy Science*, *46*(3), 204-216.

Van Vuuren, J. A. J., Meyer, J. H., & Claassens, A. S. (2006). Potential use of near infrared reflectance monitoring in precision agriculture. *Communications in Soil Science and Plant Analysis*, *37*(15-20), 2171-2184.

Vávrová, P., Stenberg, B., Karsisto, M., Kitunen, V., Tapanila, T., & Laiho, R. (2008). Near infrared reflectance spectroscopy for characterization of plant litter quality: Towards a simpler way of predicting carbon turnover in Peatlands?. In *Wastewater treatment, plant dynamics and management in constructed and natural wetlands* (pp. 65-87). Dordrecht: Springer Netherlands.

Veraverbeke, S., Stavros, E. N., & Hook, S. J. (2014). Assessing fire severity using imaging spectroscopy data from the Airborne Visible/Infrared Imaging Spectrometer (AVIRIS) and comparison with multispectral capabilities. *Remote Sensing of Environment*, *154*, 153-163.

Vitousek, P. M. (1994). Beyond global warming: ecology and global change. *Ecology*, *75*(7), 1861-1876.

Vogel, K. P., Pedersen, J. F., Masterson, S. D., & Toy, J. J. (1999). Evaluation of a filter bag system for NDF, ADF, and IVDMD forage analysis. *Crop Science*, *39*(1), 276-279.

Wadoux, A. M. C., Malone, B., Minasny, B., Fajardo, M., & McBratney, A. B. (2021). *Soil spectral inference with R*. Berlin/Heidelberg, Germany: Springer.

Wadoux, A. M. C. (2023). Interpretable spectroscopic modelling of soil with machine learning. *European Journal of Soil Science*, *74*(3), e13370.

Walsh, K. B., Blasco, J., Zude-Sasse, M., & Sun, X. (2020). Visible-NIR 'point' spectroscopy in postharvest fruit and vegetable assessment: The science behind three decades of commercial use. *Postharvest Biology and Technology*, *168*, 111246.

Wang, Y., Zheng, J., Xu, Z., Abdullah, K. M., & Zhou, Q. (2019a). Effects of changed litter inputs on soil labile carbon and nitrogen pools in a *Eucalyptus*-dominated forest of southeast Queensland, Australia. *Journal of Soils and Sediments*, *19*(4), 1661-1671.

Wang, Y., Zheng, J., Boyd, S. E., Xu, Z., & Zhou, Q. (2019b). Effects of litter quality and quantity on chemical changes during *Eucalyptus* litter decomposition in subtropical Australia. *Plant and Soil*, *442*(1), 65-78.

Wang, Y., Xiang, J., Tang, Y., Chen, W., & Xu, Y. (2022a). A review of the application of near-infrared spectroscopy (NIRS) in forestry. *Applied Spectroscopy Reviews*, *57*(4), 300-317.

Wang, L., Zhou, Y., Chen, Y., Xu, Z., Zhang, J., Liu, Y., & Joly, F. X. (2022b). Litter diversity accelerates labile carbon but slows recalcitrant carbon decomposition. *Soil Biology and Biochemistry*, *168*, 108632.

Wanthongchai, K., Bauhus, J., & Goldammer, J. G. (2008). Nutrient losses through prescribed burning of aboveground litter and understorey in dry dipterocarp forests of different fire history. *Catena*, *74*(3), 321-332.

Wardle-Johnson et al. (2017). Wet Sclerophyll Forests. In: Australian Vegetation (ed. D. A. Keith), pp. 281-. Cambridge Univ. Press, Cambridge.

Webb, L. J. (1959). A physiognomic classification of Australian rain forests. *The Journal of Ecology*, *47*(3), 551-570.

Wedderburn, M. E., & Carter, J. (1999). Litter decomposition by four functional tree types for use in silvopastoral systems. *Soil Biology and Biochemistry*, *31*(3), 455-461.

Williamson, G. J., Prior, L. D., Jolly, W. M., Cochrane, M. A., Murphy, B. P., & Bowman, D. M. (2016). Measurement of inter-and intra-annual variability of landscape fire activity at a continental scale: the Australian case. *Environmental Research Letters*, *11*(3), 035003.

Wilm, H. G. (1946). The design and analysis of methods for sampling microclimatic factors. *Journal of the American Statistical Association*, *41*(234), 221-232.

Wiltshire, R.J.E. (2004). Eucalypts. *Encyclopedia of Forest Sciences 4 Volume Set*, *1*(1), p.2000, pp. 1687–1699.

Wold, S., Sjöström, M., & Eriksson, L. (2001). PLS-regression: a basic tool of chemometrics. *Chemometrics and Intelligent Laboratory Systems*, *58*(2), 109-130.

Wood, T. (1974). Synopsis: Field investigations on the decomposition of leaves of *Eucalyptus delegatensis* in relation to environmental factors. *Pedobiologia, 14*(1), 79-80.

Woods, P. V., & Raison, R. J. (1983). Decomposition of litter in sub-alpine forests of *Eucalyptus delegatensis, E. pauciflora* and *E. dives*. *Australian Journal of Ecology*, *8*(3), 287-299.

Wood, D. L., & Storer, A. J. (2009). Forest habitats. In Encyclopedia of insects (pp. 386-396). Academic Press.

Wright, I. J., & Westoby, M. (2003). Nutrient concentration, resorption and lifespan: leaf traits of Australian sclerophyll species. *Functional Ecology*, *17*(1), 10-19.

Wu, Q., Ni, X., Sun, X., Chen, Z., Hong, S., Berg, B., Zheng, M., Chen, J., Zhu, J., Ai, L., Zhang, Y., & Wu, F. (2025). Substrate and climate determine terrestrial litter decomposition. *Proceedings of the National Academy of Sciences*, *122*(7), e2420664122.

Xiang, W., & Bauhus, J. (2007). Does the addition of litter from N-fixing *Acacia mearnsii* accelerate leaf decomposition of *Eucalyptus globulus*?. *Australian Journal of Botany*, *55*(5), 576-583.

Xiao, Q., Wu, N., Tang, W., Zhang, C., Feng, L., Zhou, L., Shen, J., Zhang, Z., Gao, P., & He, Y. (2022). Visible and near-infrared spectroscopy and deep learning application for the qualitative and quantitative investigation of nitrogen status in cotton leaves. *Frontiers in Plant Science*, *13*, 1080745.

Xiaobo, Z., Jiewen, Z., Povey, M. J., Holmes, M., & Hanpin, M. (2010). Variables selection methods in near-infrared spectroscopy. *Analytica Chimica Acta*, *667*(1-2), 14-32.

Xie, Y. (2020). A meta-analysis of critique of litterbag method used in examining decomposition of leaf litters. *Journal of Soils and Sediments*, *20*(4), 1881-1886.

Xu, X., Xie, L., & Ying, Y. (2019). Factors influencing near infrared spectroscopy analysis of agro-products: a review. *Frontiers of Agricultural Science and Engineering*, *6*(2), 105-115.

Yang, Z., Nie, G., Pan, L., Zhang, Y., Huang, L., Ma, X., & Zhang, X. (2017). Development and validation of near-infrared spectroscopy for the prediction of forage quality parameters in *Lolium multiflorum*. *PeerJ*, *5*, e3867.

Yusiharni, E., & Gilkes, R. (2012). Minerals in the ash of Australian native plants. *Geoderma*, *189*, 369-380.

Zazali, H. H., Towers, I. N., & Sharples, J. J. (2020). A critical review of fuel accumulation models used in Australian fire management. *International Journal of Wildland Fire*, *30*(1), 42-56.

Zhang, D., Hui, D., Luo, Y., & Zhou, G. (2008). Rates of litter decomposition in terrestrial ecosystems: global patterns and controlling factors. *Journal of Plant Ecology*, *1*(2), 85-93.

Zhang, M., Cheng, X., Geng, Q., Shi, Z., Luo, Y., & Xu, X. (2019). Leaf litter traits predominantly control litter decomposition in streams worldwide. *Global Ecology and Biogeography*, *28*(10), 1469-1486.

Zhang, X., Xue, J., Xiao, Y., Shi, Z., & Chen, S. (2023). Towards optimal variable selection methods for soil property prediction using a regional soil vis-NIR spectral library. *Remote Sensing*, *15*(2), 465.

Zhang, Y., Dong, X., Liu, H., Gao, T., Ren, Y., Meng, Y., Teng, C., & Zhang, J. (2024). A novel approach for predicting the carbon content of birch leaf litter using Fourier transform infrared (FTIR) spectroscopy. *Microchemical Journal*, *200*, 110262.

Zhao, L., Hu, Y. L., Lin, G. G., Gao, Y. C., Fang, Y. T., & Zeng, D. H. (2013). Mixing effects of understory plant litter on decomposition and nutrient release of tree litter in two plantations in Northeast China. *PLoS One*, *8*(10), e76334.

Zhao, X., Zhao, D., Wang, J., & Triantafilis, J. (2022). Soil organic carbon (SOC) prediction in Australian sugarcane fields using Vis–NIR spectroscopy with different model setting approaches. *Geoderma Regional*, *30*, e00566.

Zhou, G., Taylor, G., & Polle, A. (2011). FTIR-ATR-based prediction and modelling of lignin and energy contents reveals independent intra-specific variation of these traits in bioenergy poplars. *Plant Methods*, *7*(1), 9.

Zhou, C., Jiang, W., Via, B. K., Fasina, O., & Han, G. (2015). Prediction of mixed hardwood lignin and carbohydrate content using ATR-FTIR and FT-NIR. *Carbohydrate Polymers*, *121*, 336-341.

Zimmermann, B., & Kohler, A. (2013). Optimizing Savitzky–Golay parameters for improving spectral resolution and quantification in infrared spectroscopy. *Applied Spectroscopy*, *67*(8), 892-902.

Zornoza, R., Guerrero, C., Mataix-Solera, J., Scow, K. M., Arcenegui, V., & Mataix-Beneyto, J. (2008). Near infrared spectroscopy for determination of various physical, chemical and biochemical properties in Mediterranean soils. *Soil Biology and Biochemistry*, *40*(7), 1923-1930.

Zou, N., Zhang, R., Wu, Y., Lei, P., Xiang, W., Ouyang, S., Chen, L., & Yan, W. (2024). Model Exploration and Application of Near-Infrared Spectroscopy for Species Separation and Quantification during Mixed Litter Decomposition in Subtropical Forests of China. *Forests*, *15*(4), 637.

Zylstra, P., Wardell-Johnson, G., Falster, D., Howe, M., McQuoid, N., & Neville, S. (2023). Mechanisms by which growth and succession limit the impact of fire in a south-western Australian forested ecosystem. *Functional Ecology*, *37*(5), 1350-1365.

Appendix A: Supplementary materials for Chapter 1

Table A1. Summary table of literature reviewed in this study. Studies that conducted in the same forest were coded with the same alphabet to account for site-specific variables. LAT = latitude; LONG = longitude; NP = National Park; NSW = New South Wales; DSF = dry sclerophyll forest; SF = State Forest; WSF = wet sclerophyll forest; VIC = Victoria; QLD = Queensland; WA = Western Australia; ACT = Australian Capital Territory; TAS = Tasmania. LA = litter accumulation; LDp = litter decomposition prediction; LBD = litterbag decomposition; LF = litterfall; LCQ = litter chemical quality; FS = foliage stoichiometry; FR = fuel reduction; VC = vegetation composition; USV = understorey vegetation; IV = invertebrates; MBC = microbial community; SN = soil nutrient.

Reference	Code	Author and year	Forest and location	LAT	LONG	Elevation (m asl)	Inland/ Coastal	Distance from coast (km)	Forest type	Type of variable studies
1	A	Birk and Bridges, 1989	Manning River NP, NSW	31.48°S	152.36°E	31	Coastal	50	WSF	LA; LDp; LF; FR
2	B	Brennan et al., 2009	Lorne SF, NSW	31.33°S	152.38°E	240	Coastal	20	WSF	LBD; IV
3	C	Bridges, 2004	Ben Boyd NP, NSW	37.10°S	149.58°E	< 500	Coastal	< 10	DSF	LA; LF
4	D	Buckingham et al., 2015	Kinglake NP, VIC	37.34°S	140.30°E	479	Inland	50	WSF	LBD; IV
5	E	Butler et al., 2019	Peachester SF, QLD	26.52°S	152.51°E	137	Coastal	30	WSF	LBD; MBC; IV
6	F	Butler et al., 2017a	Toohey Forest, QLD	27.53°S	150.04°E	108	Coastal	42	DSF	SN
7	G	Butler et al., 2017a	White Rock Spring Mountain Conservation Estate, QLD	27.71°S	152.60°E	79	Coastal	60	WSF	SN
8	E	Butler et al., 2020	Peachester SF, QLD	26.52°S	152.51°E	137	Coastal	30	WSF	LBD; LCQ; MBC

Table A1 continued.

Reference	Code	Author and year	Forest and location	LAT	LONG	Elevation (m asl)	Inland/ Coastal	Distance from coast (km)	Forest type	Type of variable studies
9	H	Cawson et al., 2018	Central Highland forest, VIC		-	-	Inland	543	WSF	FA
10	E	Toberman et al., 2014	Peachester SF, QLD	26.52°S	152.51°E	137	Coastal	30	WSF	LBD; MBC; LCQ
11	I	Fox et al., 1979	Myall Lakes NP, NSW	32.28°S	152.30°E	56	Coastal	< 10	WSF	LA; LDp
12	E	Gunito et al., 2001	Peachester SF, QLD	26.52°S	152.51°E	137	Coastal	30	WSF	LCQ; SN
13	J	Gunito et al., 2001	Bauple SF, QLD	25.48°S	152.37°E	60	Coastal	40	DSF	LCQ; SN
14	K	Hobley et al., 2017	Guy Fawkes River NP, NSW	29.30°S	152.14°E	1095	Inland	90	DSF	SN
15	F	Huang et al., 2013	Toohey Forest, QLD	27.30°S	135.00°E	108	Coastal	42	DSF	SN
16	E	Muqaddas et al., 2015	Peachester SF, QLD	26.52°S	152.51°E	137	Coastal	30	WSF	SN
17	E	Muqaddas and Lewis, 2020	Peachester SF, QLD	26.52°S	152.51°E	137	Coastal	30	WSF	LF; LCQ
18	L	O'Connell et al., 1979	Dwellingup SF, WA	32.58°S	116.41°E	340	Coastal	42	DSF	LF; LCQ
19	M	O'Connell, 1987a	Pine Creek, WA	34.24°S	115.59°E	104	Coastal	20	DSF	LBD; LDp; LCQ; SN
20	M	O'Connell, 1987b	Big Brook Forest, WA	34.24°S	115.59°E	104	Coastal	20	WSF	LBD; LDp; LA;

Table A1 continued.

Reference	Code	Author and year	Forest and location	LAT	LONG	Elevation (m asl)	Inland/ Coastal	Distance from coast (km)	Forest type	Type of variable studies
21	M	O'Connell, 1988	Big Brook Forest, WA	34.24°S	115.59°E	104	Coastal	20	WSF	LBD; LDp; LCQ; SN
22	B	Penman and York, 2010	Lorne SF, NSW	31.33°S	152.38°E	240	Coastal	30	WSF	LA; LDp;
23	N	Woods and Raison, 1983	Brindabella Range, ACT	35.21°S	148.48°E	1125	Inland	153	DSF	LBD; LCQ; LDp
24	N	Raison et al., 1986	Brindabella Range, ACT	35.21°S	148.48°E	1125	Inland	153	DSF	LA; LBD; LF; LDp
25	D	Simmon and Adam, 1986	Kinglake NP, VIC	37.34°S	140.30°E	479	Inland	50	WSF	LA
26	L	O'Connell and Menage, 1983	Dwellingup SF, WA	32.58°S	116.41°E	340	Coastal	42	DSF	LBD; LCQ
27	E	Bastias et al., 2016	Peachester SF, QLD	26.52°S	152.51°E	137	Coastal	30	WSF	SN
28	O	Krishnaeaj et al., 2016	Otwat Range, VIC	38.48°S	143.50°E	266	Coastal	22	DSF	SN; LCQ
29	P	Abbott et al., 1984	Jarrahdale SF, WA	32.20°S	116.50°E	292	Coastal	33	DSF	LCQ; SN; VC

Table A1 continued.

Reference	Code	Author and year	Forest and location	LAT	LONG	Elevation (m asl)	Inland/ Coastal	Distance from coast (km)	Forest type	Type of variable studies
30	Q	Close et al., 2011	Mount Maurice, TAS	41.17°S	147.34°E	850	Inland	35	WSF	VC; SN; LCQ
31	R	Close et al., 2011	Yalgorup NP, WA	32.55°S	115.41°E	23	Coastal	< 10	DSF	VC; SN; LCQ
32	S	Fensham, 1992	Mount Wellington, TAS	42.53°S	147.13°E	1189	Coastal	< 10	WSF	LDp; VC;
33	T	Etchells et al., 2012	Northcliffe, WA	33.53°S	116.26°E	530	Coastal	< 20	WSF	VC; SN

Table A2. Summary table of literature that investigated fire effects on understorey composition, microclimate, litter quantity and quality, soil properties, and microbial activity. NSW = New South Wales; DSF = dry sclerophyll forest; SF = State Forest; WSF = wet sclerophyll forest; VIC = Victoria; QLD = Queensland; WA = Western Australia; ACT = Australian Capital Territory; TAS = Tasmania. TSF = time-since-fire; NP = National Park; SF = State Forest; DRY = dry sclerophyll forest; WET = wet sclerophyll forest; PB = prescribed burning; BF = Bushfire; 2yB = burnt every 2 years; 4yB = burnt every 4 years; UB = unburnt; RB = recently burnt; WRSMCE = White Rock Spring Mountain Conservation Estate; MBC = microbial biomass C; MBN = microbial biomass N; MBP = microbial biomass P; OC = organic C; PyC = pyrogenic carbon.

Understorey composition/ microclimate

Study	Study site	Forest type	Fire type	TSF (year)	Significance
Birk and Bridges, 1989	Manning River NP, NSW	WSF	PB	1, 2, 4, 6	Fire frequency affected understorey composition. Tall woody shrubs in 2yB site were replaced by grasses.
Buckingham et al., 2015	Kinglake NP, VIC	WSF	BF	2, 20	BF significantly affected the forest floor microhabitat. Crown burnt site had higher moss cover.
Fox et al., 1979	Myall Lakes NP, NSW	WSF	PB	2, 4, 7, 10	The height of vegetation increased with TSF. Post-fire understorey regeneration was rapid under high rainfall and mild temperature conditions. The height growth rate of understorey in Myall Lakes was three times higher than that of Blue Mountains.
Lewis et al., 2012	Peachester SF, QLD	WSF	PB	2 (2yB), 4 (4yB)	Fire regime did not significantly affect understorey species richness but had strong impacts on understorey composition and density. Burnt sites had higher grass species richness than UB sites. Specifically, herbaceous taxa, resprouting shrubs and bracken fern were higher in 2yB site, while rainforest trees, tall shrubs, and vines were higher in UB sites. 4yB site had high species diversity. Frequent fires (2yB) inhibited the growth of woody plants.

Table A2 continued.

Study	Study site	Forest type	Fire type	TSF (year)	Significance
Muqaddas and Lewis, 2020	Peachester SF, QLD	WSF	PB	3.5, 5.5	PB altered the vegetation structure and composition. Frequently burnt sites (2yB) were dominated by grassy understorey and had a lower density of woody shrub (> 3 m in height), and rainforest associated vegetation.
O'Connell, 1987a	Big Brook Forest, WA	WSF	PB	2, 6	PB removed most of the live ground cover and killed understorey vegetation, but understorey regrowth was rapid in the winter following fire (less than a year).
Abbott et al., 1984	Jarrahdale SF, WA	DSF	PB	0.75, 45	PB did not significantly affect vegetation ground cover and number of plant species.
Close et al., 2011	Mount Maurice, TAS	WSF	PB	40, > 100	UB site was dominated by moss, fern, and woody debris, while RB site was dominated by shrub, herb, and grass.
	Yalgorup NP, WA	DSF	PB	40, < 10	UB site was dominated by understorey, midstorey and *Eucalyptus* species. RB site was dominated by woody debris, herb, and litter.
Etchells et al., 2020	Northcliffe, WA	WSF	BF	1.08, 1.42, 30	Fire severity significantly affected mature tree mortality and vegetation composition. Tree mortality was significantly higher in high severity sites than low severity and UB sites. *Clematis pubescens* (a climber) was the only species that was observed at all sites. *Trymaliun odoratissimum* (understorey shrub) was the most abundant understorey in low severity and UB sites and was entirely absent at high severity sites.

Table A2 continued.

Litter dynamics

Study	Study site	Forest type	Fire type	TSF (year)	Significance
Birk and Bridges, 1989	Manning River NP, NSW	WSF	PB	1, 2, 4, 6	PB had no effect on litterfall production but significantly reduced fuel load and retarded rate of decomposition and thus lead to rapid litter accumulation.
			BF	6	BF significantly affected fuel load, litterfall, litter accumulation, and decomposition. Litter accumulation after BF was rapid in the first few months due to the large contribution of scorched overstorey leaves and twigs. However, litter accumulated to only 73% of pre-fire level 6 years after fire and contained more understorey litter.
Brennan et al., 2009	Bull Ground Study Area, NSW	DSF	PB	2, 6	The interaction between fire regime and litter bag mesh size significantly affects litter mass loss. Litter decomposed faster in UB site than burnt sites with the same bag mesh size. PB slower the rate of decomposition by lowering litter N ratio.
Bridges, 2004	Ben Boyd NP, NSW	DSF	PB	1, 2, 3, 5	Annual litterfall was 3.3-4.8 t ha^{-1}, similar to other Australian forests. Fine fuel accumulated rapidly after PB and was likely to be caused by disruption of litter decomposition process. It is estimated that the forest floor would reach 95% of the steady state in about 8 years after fire.

Table A2 continued.

Study	Study site	Forest type	Fire type	TSF (year)	Significance
Bridges, 2004	Ben Boyd NP, NSW	DSF	BF	3, 11, 22	Fine fuel accumulated rapidly after BF, with a high proportion of twigs (41%) and a small proportion of leaf (4%) were observed. The weight of fine fuel is estimated to reach a peak 10 years after BF. Hence, the contribution of non-leaf materials decreased with TSF.
Buckingham et al., 2015	Kinglake NP, VIC	WSF	BF	2, 20	BF (severity) did not significantly affect rate of litter decomposition.
Butler et al., 2019	Peachester SF, QLD	WSF	PB	2.3	Fire regimes do not have strong influences on litter decomposition in the presence of a decomposer community. However, the rate of microbially-driven decomposition was higher in UB than 4yB litter. The rate of litter decomposition was associated with fire frequency: UB > 2yB > 4yB.
Butler et al., 2020	Peachester SF, QLD	DSF	PB	2.3	The rate of litter decomposition was associated with fire frequency: UB > 2yB > 4yB.
Toberman et al., 2014	Peachester SF, QLD	WSF	PB	3.5, 5.5	Litter decomposition was higher for freshly fallen leaf litter than older mixed-age leaf litter. For both litter types, 2yB leaf litter decomposed slower than 4yB and UB leaf litter.
Fox et al., 1979	Myall Lakes NP, NSW	WSF	PB	2, 4, 7, 10	Litter accumulation increase with TSF. A large amount of bark contributed to the forest floor immediately after fire. Leaf litter was the main contributor to the litter layer from 2 to 9 years after fire, after which twigs litter dominated the litter layer.

Table A2 continued.

Study	Study site	Forest type	Fire type	TSF (year)	Significance
Muqaddas and Lewis, 2020	Peachester SF, QLD	WSF	PB	3.5, 5.5	PB significantly reduced monthly and annual total litterfall, yet the litterfall was still highest in summer. Overall, burnt sites (2yB and 4yB) had lower litterfall than UB sites, while no significant differences were observed between sites with different fire frequency.
O'Connell et al., 1979	Dwellingup SF, WA	DSF	PB (high intensity)	0-2	Litterfall amount and pattern were significantly affected by high intensity fire. Large amounts of scorched leaves and branches contributed to the total litterfall in the burnt site during the first year after fire. However, litterfall in the burnt site was significantly less than that in the control site in the second year after fire.
O'Connell, 1987a	Pine Creek, WA	DSF	PB	2, 6	Litter mass loss in the first 30 weeks was correlated with the initial readily soluble material concentration. Hence, subsequent litter mass loss was related to the initial lignin and cellulose concentration. Karri leaf litter decomposed more rapidly than non-leaf litter and was predicted to make up only 1/3 of the total litter layer. The accumulation of leaf litter decreased with TSF, while that of twig, bark and fruit increased with TSF.
O'Connell, 1987b	Big Brook Forest, WA	WSF	PB	2, 6	After 82 weeks, litter mass loss was similar between RB site (55%) and UB site (54%).
Penman and York, 2010	Lorne SF, NSW	WSF	PB	3, 22	In UB sites, fuel loads increased with time. A significant reduction in fuel loads can be observed immediately after fire. Litter accumulation was rapid and accumulated to the UB level within 3 years.

Table A2 continued.

Study	Study site	Forest type	Fire type	TSF (year)	Significance
Muqaddas and Lewis, 2020	Peachester SF, QLD	WSF	PB	3.5, 5.5	PB significantly reduced monthly and annual total litterfall, yet the litterfall was still highest in summer. Overall, burnt sites (2yB and 4yB) had lower litterfall than UB sites, while no significant differences were observed between sites with different fire frequency.
Raison et al., 1986	Brindabella Range, ACT	DSF	PB	4, 5	Low intensity PB did not alter the pattern and amount of litterfall. Partially burnt litter decomposed rapidly. Leaf litter decomposition varied among *Eucalyptus* species. *E. pauciflora* and *E. delegatensis* leaf litter decomposition was higher in UB site than burnt site. However, leaf litter decomposition of *E. dives* was not affected by PB. Winter leaf litter had higher decay rate due to higher initial [N]. Litter accumulation after fire was rapid and will reach a mass of 10-15 t ha^{-1} within 5 years.
Simmon and Adam, 1986	Kinglake NP, VIC	DSF	PB	0.5, 2, 3.5, 23	Fuel loads (t ha^{-1}) increased with TSF but the proportion of leaves and twigs (< 6 mm in diameter) decreased slightly with TSF. The proportion of twigs was at maximum 3.5 years after fire. Leaf litter decomposition was rapid compared to twigs. Hence, the latter became increasingly dominant. Post-fire litter accumulation was rapid in the first few years after fire and may increase the risk of future fire.
Krishnaraj et al., 2016	Otway Range, VIC	DSF	PB	0.019	PB significantly reduced the mass of 2-25 mm litter and increased the mass of < 2 mm litter.

Table A2 continued.

Study	Study site	Forest type	Fire type	TSF (year)	Significance
O'Connell and Menage, 1983	Dwellingup SF, WA	DSF	PB	1, 6	Fire regimes altered individual species decomposition. In general, leaf litter from Jarrah decomposed faster than from Marri. No significant difference in mass loss of Marri litter found between burnt and UB treatment at 18 months. After 18 months, Marri litter from burnt sites (intense and cool) decomposed faster than litter from UB sites. While the mass of Jarrah litter from intense burnt sites decreased significantly than litter from cool and UB sites. Litter mass loss was slower in finer mesh bags than litter in coarse mesh bags.
Abbott et al., 1984	Jarrahdale SF, WA	DSF	PB	0.75, 45	PB significantly reduced litterfall production and the depth of the litter layer.
O'Connell, 1988	Big Brook Forest	WSF	PB	6	Leaf litter decomposed faster than non-leaf litter. After 82 weeks, the rate of decomposition decreased in the order: leaves > bark = fruit > twigs.

Table A2 continued.

Decomposer activity

Study	Study site	Forest type	Fire type	TSF (year)	Significance
Brennan et al., 2009	Bull Ground Study Area, NSW	WSF	PB	2, 6	Litterbag mesh size was highly associated with invertebrate abundance and composition, a large number of invertebrates were observed in coarse mesh litterbags. Invertebrate composition was more variables within finer mesh bags, yet these invertebrates did not have significant impacts on litter decomposition.
Buckingham et al., 2015	Kinglake NP, NSW	WSF	BF	2, 20	Macroinvertebrates had a vital role in litter decomposition. The abundance and body size of macroinvertebrate were induced by fire severity as a result of changes in habitat structure; however, the effects were short-lived.
Butler et al., 2019	Peachester SF, QLD	WSF	PB	2.3	Microbial C, N and P were not affected by PB and fire frequency. Litter in 4yB has lower microbial N and P than litter in 2yB and UB.
Butler et al., 2020	Peachester SF, QLD	WSF	PB	2.3	Fire regimes did not affect litter MBC, yet MBN was high in UB litter than 2yB and 4yB litter. Litter in UB and 2yB treatment had higher MBP than litter 4yB.
Toberman et al., 2014	Peachester SF, QLD	WSF	PB	3.5, 5.5	Fire frequency has significant influence on litter microbial biomass. 2yB litter microbial biomass was significantly higher than UB for freshly fallen litter and older mixed-age litter, but there was no significant difference between 4yB and UB microbial biomass C:N. 2yB litter microbial biomass N:P ratios was significantly lower than 4yB and UB.

Table A2 continued.

Study	Study site	Forest type	Fire type	TSF (year)	Significance
Huang et al., 2013	Toohey Forest, QLD	DSF	PB	-15, 0.033, 0.052, 0.13	PB induced changes in soil P fractions also affected microbial biomass C and P. However, the restoration of soil microbial biomass C and P was rapid.
Muqaddas et al., 2015	Peachester SF, QLD	WSF	PB	4, 6, 42	MBC content was positively correlated with MBN. MBC and MBN were significantly lower in 2yB site than UB and 4yB site.
Abbott et al., 1984	Jarrahdale SF	DSF	PB	0.75, 45	UB site had high number of invertebrate than burnt site, but the abundance of invertebrates was not significantly affected by fire regime. Differences in invertebrate abundance were highly associated with seasonal variables. For both sites, the most abundant animals were Isoptera, Formicidae and Araneae.

Table A2 continued.

Litter chemical quality

Study	Study site	Forest type	Fire type	TSF (year)	Significance
Butler et al., 2019	Peachester SF	WSF	PB	2.3	Fire frequency has a significant influence on litter chemical quality (C, N, P ratio). Litter in 2yB site has lower total N:P ratio than litter in UB and 4yB sites. Total C:N ratio in UB litter was significantly lower than 2yB and 4yB litter. Litter pH and EC were not affected by fire frequency.
Toberman et al., 2014	Peachester SF, QLD	WSF	PB	3.5, 5.5	Fire frequency influenced litter chemical quality. Total C:N ratio in freshly fallen leaf litter increased significantly with fire frequency: 2yB > 4yB > NB and was significantly higher for 2yB than UB for older mixed-age litter.
Butler et al., 2017b	Toohey Forest & WRSMCE	DSF & WSF	PB & BF	0.5, 1.1, 4.4, 14.7, 14.9, >15	Fire history did not have consistent influence on litter HWE and total C:N:P ratio. Fire regimes (RB vs. UB) did not have significant impacts on litter N:P ratio.
Butler et al., 2020	Peachester SF, QLD	WSF	PB	2.3	In general, litter nutrient depletion was correlated with increased fire frequency. PB and fire frequency did not affect litter total and soluble C. However, litter total [N] was significantly influenced by fire regimes, litter [N] increased during decomposition in both 2yB and 4yB. Litter in UB has higher total [N] than litter in 2yB and 4yB. Litter [P] was significantly affected by fire regimes, while UB and 2yB litter had higher total and soluble [P].
Guinto et al., 2001	Bauple SF, QLD	DSF	PB	2, 5, 48	PB did not have a significant influence on litter [N] and [K]. However, annual burnt sites had significantly higher [P], [Ca] and [Mg] than UB.

Table A2 continued.

Study	Study site	Forest type	Fire type	TSF (year)	Significance
Guinto et al., 2001	Peachester SF, QLD	WSF	PB	3, 5, 25	Litter [N] and [Ca] were significantly lower in burnt sites than UB. However, litter [P] and [Mg] were not affected by PB.
Muqaddas and Lewis, 2020	Peachester SF, QLD	WSF	PB	3.5, 5.5	PB significantly affected litter C:N ratio with lower litter C and fruit N ratio than UB sites. Litter in 4yB has significantly higher leaf and fruit N than litter in 2yB. The latter had higher leaf litter C:N ratio than 4yB and UB. Leaf litter had the highest C concentration compared to other litter components. Litter N concentration was highly associated with water availability which often led to reduce in N plant uptake from soil and withdrawal of N in the leaves before leaf abscission.
O'Connell et al., 1979	Dwellingup SF	DSF	PB (high intensity)	0-2	Scorched litter had 2x higher [N] and [P] than unburnt litter in the first year after fire. However, [K] in scorched litter was half that in unburnt litter. Litter [Ca] was similar at both sites. Scorched litter had lower [Mg], [Na] and [Cl] than unburnt litter. Differences between nutrient concentration in litter from the two sites were much smaller in the second year after fire except for [P] which was still 50% higher in litter from burnt site.
Woods and Raison, 1983	Brindabella Range	DSF	BF	4.5, 30	Significant positive linear relationships were found between the initial leaves [N], [P] and mass loss after 12 months of decomposition. [Soluble carbon] and litter mass decreased rapidly in the first 20 weeks of decomposition.

Table A2 continued.

Study	Study site	Forest type	Fire type	TSF (year)	Significance
O'Connell, 1987b	Big Brook Forest	WSF	PB	2, 6	The release of nutrient was similar between site: Na > Cl > K > Mg > S > Ca > N > P.
Raison et al., 1986	Brindabella Range	DSF	PB	4, 5	Leaf litter from burnt sites had lower moisture content than UB site
O'Connell, 1988	Big Brook Forest	WSF	PB	6	Nutrient release in leaf litter decreased in the order: Na > Cl > K > Mg > S > Ca > N > P. Karri litter tended to accumulate N during decomposition.
O'Connell and Menage, 1983	Dwellingup SF	DSF	PB	1, 6	Nutrient release of Jarrah and Marri leaf litter were similar and followed the order: Na > K > Cl > Mg > S > Ca > N > P. The [N] and [P] on the forest floor increased with time of decomposition.
Krishnaraj et al., 2016	Otway Range	DSF	PB	0.019	High intensity PB significantly increased litter total [C] and litter [N]. Litter from high intensity PB site had the highest charred OM.
Abbott et al., 1984	Jarrahdale SF	DSF	PB	0.75, 45	Chemical composition of leaf litter from both UB and burnt sites was similar, however UB site had higher [Ca], [Mg] and [Mn] than burnt site.
Close et al., 2011	Mount Maurice, TAS	WSF	PB	40, > 100	Chemical composition of litter from UB and RB sites were similar; however, RB site had significantly higher foliar P than UB site.
Close et al., 2011	Yalgorup NP, WA	DSF	PB	40, < 10	UB site had significantly lower foliage N, Cu, and Mn content than RB site.

Table A2 continued.

Soil quality

Study	Study site	Forest type	Fire type	TSF (year)	Significance
Butler et al., 2017b	Toohey Forest & WRSMCE, QLD	DSF & WSF	PB & BF	0.5, 1.1, 4.4, 14.7, 14.9, >15	Fire history did not affect soil (0-10 cm) pH, soil total C, N and N:P ratio. However, fire regimes (RB vs. UB) altered soil labile stoichiometry, RB sites had lower soil labile C:P, and N:P ratio.
Butler et al., 2020	Peachester SF, QLD	WSF	PB	2.3	Soil nutrient (0-10 cm) depletion correlated with increased fire frequency. High frequency fire may reduce the rate of soil C accumulation as a result of the decomposition rate.
Guinto et al., 2001	Bauple SF	DSF	PB	2, 5, 48	Soil pH increased with fire frequency and was significantly higher than UB sites. Topsoil (0-10 cm) chemical properties were strongly affected by PB. Soil in periodically burnt sites had slightly higher OC than UB, PB did not significantly reduce total N. Burnt sites had higher total P than UB but the differences were not significant. Acid-extractable P increased with fire frequency. Frequent burning increased soil P availability.

Table A2 continued.

Study	Study site	Forest type	Fire type	TSF (year)	Significance
Butler et al., 2017b	Peachester SF, QLD	WSF	PB	3, 5, 25	Soil (0-10 cm) pH increased with fire frequency and were significantly higher than UB sites. PB reduced topsoil OC and total N, the effect was more profound in 2yB. Acid-extractable P increased with fire frequency.
Huang et al., 2013	Toohey Forest, QLD	DSF	PB	-15, 0.033, 0.052, 0.13	PB temporally changed soil properties (0-10 cm). Soil pH increased immediately after fire, but the effect was short-lived. PB also lowered soil organic P.
Muqaddas et al., 2015	Peachester SF, QLD	WSF	PB	4, 6, 42	Soil (0-10 cm) C and N pools were negatively correlated with soil pH and were positively correlated with soil moisture content. Soil of 2yB site had significantly higher pH and lower total C, N, labile HCl-C and N than UB and 4yB. Soil [N] did not vary between UB and 4yB. 2yB site had significantly lower charcoal level than 4yB. Yet, fire regimes did not significantly affect charcoal-N and charcoal-C:N ratio.
Bastias et al., 2006	Peachester SF, QLD	WSF	PB	5, 7, 50	2yB site had lower total soil (0-10 and 10-20 cm) [C] and [N] than 4yB and UB sites. Soil pH increased with fire frequency, while soil mineral N decreased with fire frequency.
Krishnaraj et al., 2016	Otway Range	DSF	PB	0.019	High intensity Pb significantly increased soil total [C], soil 0-2 cm carbon stock and soil total [N]. PB did not have impact on the carbon stock of 2-4 cm soil. Soil [PyC] increased with fire intensity.

Table A2 continued.

Study	Study site	Forest type	Fire type	TSF (year)	Significance
Butler et al., 2017b	Peachester SF, QLD	WSF	PB	3, 5, 25	Soil (0-10 cm) pH increased with fire frequency and were significantly higher than UB sites. PB reduced topsoil (0-10 cm) OC and total N, the effect was more profound in 2yB. Acid-extractable P increased with fire frequency.
Abbott et al., 1984	Jarrahdale SF, WA	DSF	PB	0.75, 45	UB site had higher soil moisture content, extractable N and lower soil total [P] and [K] than soil in burnt site.
Close et al., 2011	Mount Maurice, TAS	WSF	PB	40, > 100	UB site had significantly lower soil (0-5 cm) pH, total P, and higher soil Al than RB site.
	Yalgorup NP, WA	DSF	PB	< 10	UB site had significantly higher soil (0-5 cm) pH, soil nitrate content and soil total N than RB site.

Appendix B: Supplementary materials for Chapter 2

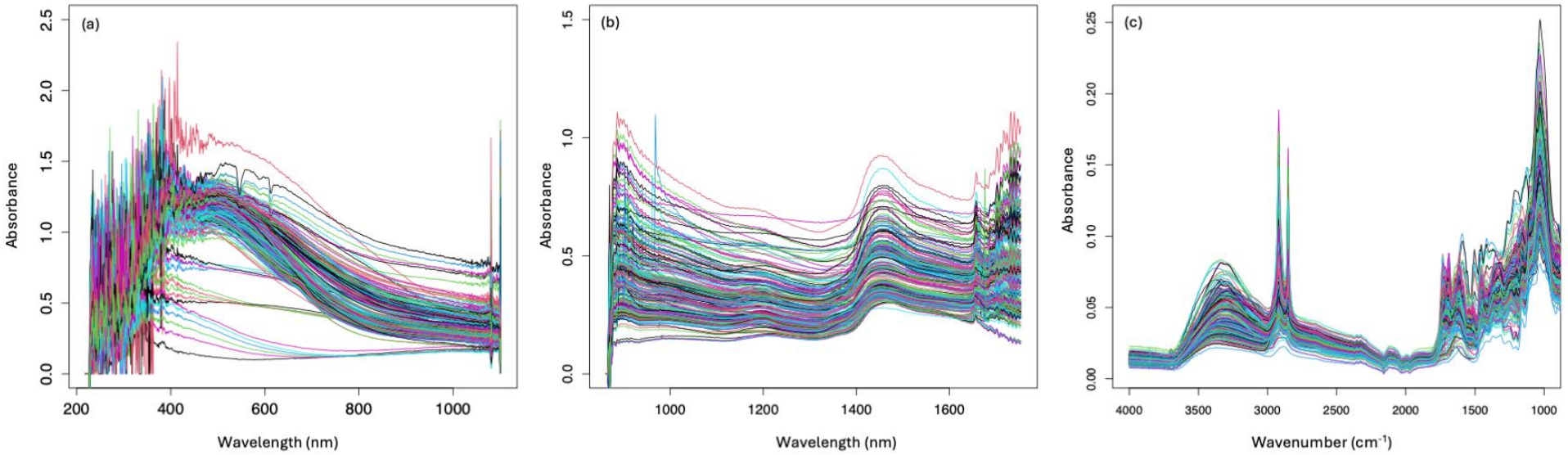

Figure B1: Example of raw (a) visible-near infrared (vis-NIR); (b) near-infrared (NIR); and attenuated total reflectance Fourier transform infrared (ATR-FTIR) spectra of synthetic mixtures, and leaf and bark litterfall samples from Wombat State Forest (Wombat SF) and Orbost State Forest (Orbost SF).

Table B1: Result from the best five models selected from vis-NIR, NIR, and ATR-FTIR spectra for predicting total carbon (TC), total nitrogen (TN), cellulose, hemicellulose, and lignin content in *Eucalyptus* litterfall (see Chapter 2). Models were developed using multivariate modelling analysis including partial least square regression (PLSR), bootstrap PLSR, Cubist, and random forest (RF). Models were selected based on the highest coefficient of determination (R^2), the lowest root mean squared error (RMSE), and the highest Lin's Concordance Correlation Coefficient (LCCC) value after testing different pre-processing combinations (raw spectra, SG smoothing, SNV, and GA feature wavelength selection). SG = Savitzky-Golay smoothing; w = window size; k = polynomial order; SNV = standard normal variate transformation; R^2cv = coefficient of determination of cross-validation model; RMSECV = root mean squared error of cross-validation model; LCCCcv = Lin's Concordance Correlation Coefficient of cross-validation model; R^2v = coefficient of determination of validation model; RMSEV = root mean squared error of validation model; LCCCv = Lin's Concordance Correlation Coefficient of validation model.

Spectra	Variable	Pre-processing technique	Model	Calibration dataset			Validation dataset		
				R²cv	**RMSECV**	**LCCCcv**	***R²v***	**RMSEV**	**LCCCv**
vis-NIR	Carbon	Raw data	PLSR	0.02	6.44	0.16	0.48	5.02	0.63
		SG (w = 3, k = 2), SNV	PLSR	0.00	6.92	0.03	0.16	6.43	0.23
		SG (w = 5, k = 2), SNV	PLSR	0.00	6.92	0.03	0.16	6.43	0.23
		SG (w = 7, k = 2), SNV	PLSR	0.00	6.92	0.03	0.16	6.43	0.23
		Raw data, GA	RF	0.88	2.52	0.86	0.09	8.73	0.12
vis-NIR	Nitrogen	SG (w = 3, k = 2), SNV	PLSR	0.65	0.13	0.80	0.61	0.11	0.73
		SG (w = 5, k = 2), SNV	PLSR	0.65	0.13	0.80	0.61	0.11	0.73
		Raw data	PLSR	0.65	0.13	0.80	0.61	0.11	0.73
		SG (w = 7, k = 2), SNV	PLSR	0.65	0.13	0.80	0.60	0.11	0.73
		SG (w = 7, k = 2), SNV, GA	Bootstrap	0.55	0.13	0.71	0.16	0.19	-0.16
vis-NIR	Cellulose	Raw data	PLSR	0.74	15.02	0.84	0.62	5.32	0.78
		SG (w = 3, k = 2), SNV	PLSR	0.34	23.61	0.54	0.41	7.77	-0.17
		SG (w = 5, k = 2), SNV	PLSR	0.34	23.61	0.54	0.41	7.77	-0.17
		SG (w = 7, k = 2), SNV	PLSR	0.34	23.61	0.54	0.41	0.77	-0.17
		SG (w = 7, k = 2), SNV	RF	0.95	8.66	0.95	0.44	21.69	-0.02

Table B1 continued.

Spectra	Variable	Pre-processing technique	Model	Calibration dataset			Validation dataset		
				R^2cv	RMSECV	LCCCcv	R^2v	RMSEV	LCCCv
vis-NIR	Hemicell-ulose	SG (w = 3, k = 2), SNV	PLSR	0.70	16.31	0.80	0.36	5.88	0.35
		SG (w = 5, k = 2), SNV	PLSR	0.55	19.61	0.71	0.13	4.97	0.27
		SG (w = 5, k = 2), SNV	Bootstrap	0.44	36.75	0.60	0.13	10.99	0.11
		SG (w = 7, k = 2), SNV	PLSR	0.69	16.50	0.80	0.36	5.84	0.35
		Raw data, GA	RF	0.87	12.85	0.87	0.44	23.85	-0.07
vis-NIR	Lignin	Raw data, GA	PLSR	0.99	3.04	0.99	0.83	2.49	0.91
		SG (w = 3, k = 2), SNV	PLSR	0.43	22.21	0.62	0.41	5.22	0.40
		SG (w = 5, k = 2), SNV	PLSR	0.43	22.21	0.62	0.41	5.22	0.40
		SG (w = 7, k = 2), SNV	PLSR	0.43	22.21	0.62	0.41	5.22	0.40
		SG (w = 3, k = 2), SNV	Bootstrap	0.43	22.03	0.64	0.41	8.42	0.22
NIR	Carbon	Raw data	PLSR	0.12	5.83	0.33	0.60	4.40	0.75
		SG (w = 7, k = 2), SNV	PLSR	0.14	5.91	0.34	0.60	4.41	0.74
		SG (w = 5, k = 2), SNV	PLSR	0.14	5.93	0.34	0.60	4.43	0.74
		SG (w = 3, k = 2), SNV	PLSR	0.14	5.91	0.34	0.60	4.44	0.74
		SG (w = 7, k = 2), SNV	Cubist	0.72	3.25	0.85	0.12	9.45	0.29
NIR	Nitrogen	SG (w = 5, k = 2), SNV	PLSR	0.72	0.11	0.78	0.51	0.12	0.69
		SG (w = 7, k = 2), SNV	PLSR	0.72	0.11	0.78	0.51	0.12	0.69
		SG (w = 3, k = 2), SNV	PLSR	0.73	0.11	0.78	0.51	0.12	0.69
		Raw data	PLSR	0.61	0.13	0.66	0.42	0.13	0.62
		Raw data	Bootstrap	0.79	0.09	0.89	0.11	0.38	0.24

Table B1 continued.

Spectra	Variable	Pre-processing technique	Model	Calibration dataset			Validation dataset		
				R^2cv	RMSECV	LCCCcv	R^2v	RMSEV	LCCCv
NIR	Cellulose	SG (w = 3, k = 2), SNV	PLSR	1.00	2.00	1.00	0.89	2.44	0.94
		SG (w = 5, k = 2), SNV	PLSR	1.00	2.02	1.00	0.89	2.44	0.94
		SG (w = 7, k = 2), SNV	PLSR	1.00	1.79	1.00	0.79	3.35	0.89
		SG (w = 5, k = 2), SNV	Bootstrap	1.00	1.28	1.00	0.72	20.73	0.39
		SG (w = 3, k = 2), SNV	Bootstrap	1.00	1.28	1.00	0.72	20.74	0.39
NIR	Hemicell-ulose	Raw data	PLSR	0.99	3.07	0.99	0.32	2.53	0.55
		SG (w = 3, k = 2), SNV	PLSR	1.00	2.08	1.00	0.31	2.99	0.50
		SG (w = 5, k = 2), SNV	PLSR	1.00	2.09	1.00	0.31	2.99	0.50
		SG (w = 7, k = 2), SNV	PLSR	1.00	2.09	1.00	0.31	3.00	0.50
		SG (w = 3, k = 2), SNV, GA	PLSR	1.00	1.74	1.00	0.66	18.14	0.44
NIR	Lignin	SG (w = 3, k = 2), SNV	PLSR	1.00	2.00	1.00	0.89	2.44	0.94
		SG (w = 5, k = 2), SNV	PLSR	1.00	2.02	1.00	0.89	2.44	0.94
		Raw data	PLSR	1.00	1.93	1.00	0.73	3.87	0.86
		SG (w = 7, k = 2), SNV	PLSR	1.00	1.79	1.00	0.79	3.35	0.89
		SG (w = 3, k = 2), SNV	Bootstrap	1.00	1.93	1.00	0.73	3.87	0.86
ATR-FTIR	Carbon	SG (w = 7, k = 2), SNV	PLSR	0.07	5.52	0.24	0.72	3.96	0.80
		Raw data	PLSR	0.07	5.22	0.26	0.68	3.89	0.80
		SG (w = 3, k = 2), SNV	PLSR	0.07	5.52	0.24	0.67	3.96	0.80
		SG (w = 5, k = 2), SNV	PLSR	0.07	5.52	0.24	0.67	3.96	0.80
		SG (w = 3, k = 2), SNV	Bootstrap	0.25	3.94	0.44	0.35	8.63	0.23

Table B1 continued.

Spectra	Variable	Pre-processing technique	Model	Calibration dataset			Validation dataset		
				R^2cv	RMSECV	LCCCcv	R^2v	RMSEV	LCCCv
ATR-FTIR	Nitrogen	SG (w = 5, k = 2), SNV	PLSR	0.77	0.10	0.86	0.51	0.13	0.66
		SG (w = 7, k = 2), SNV	PLSR	0.77	0.10	0.86	0.51	0.13	0.66
		SG (w = 3, k = 2), SNV	PLSR	0.79	0.10	0.87	0.43	0.14	0.60
		Raw data	PLSR	0.72	0.11	0.84	0.42	0.14	0.58
		Raw data	Cubist	0.91	0.05	0.95	0.23	0.20	0.32
ATR-FTIR	Cellulose	SG (w = 5, k = 2), SNV, GA	RF	0.96	6.36	0.97	0.77	5.30	0.82
		SG (w = 3, k = 2), SNV	RF	0.97	5.74	0.98	0.73	6.04	0.74
		Raw data	PLSR	0.91	8.97	0.95	0.68	5.36	0.80
		SG (w = 3, k = 2), SNV	PLSR	0.97	5.59	0.98	0.62	5.06	0.79
		SG (w = 5, k = 2), SNV	PLSR	0.97	5.59	0.98	0.62	5.06	0.79
ATR-FTIR	Hemicell-ulose	SG (w = 3, k = 2), SNV	PLSR	0.97	4.68	0.99	0.30	2.94	0.50
		SG (w = 5, k = 2), SNV	PLSR	0.97	4.68	0.99	0.30	2.94	0.50
		SG (w = 7, k = 2), SNV	PLSR	0.97	4.68	0.99	0.29	2.94	0.50
		Raw data	PLSR	0.95	6.52	0.97	0.36	3.70	0.47
		Raw data	Bootstrap	0.98	4.55	0.99	0.59	25.52	0.10
ATR-FTIR	Lignin	Raw data	PLSR	0.94	7.04	0.97	0.45	4.74	0.68
		SG (w = 3, k = 2), SNV	PLSR	0.97	5.09	0.98	0.40	4.95	0.64
		SG (w = 5, k = 2), SNV	PLSR	0.97	5.08	0.98	0.40	4.95	0.64
		SG (w = 7, k = 2), SNV	PLSR	0.97	5.08	0.99	0.40	4.95	0.64
		SG (w = 5, k = 2), SNV	RF	0.95	6.43	0.98	0.43	17.38	0.36

[a] The wavelength range for the vis-NIR spectral regions was 500.5-1,000 nm.
[b] The wavelength range for the NIR spectral region was 1,000.5-1,650 nm.
[c] The wavenumber range for the MIR infrared region was 4,000-650 cm^{-1} (wavelength: 2,500-25,000 nm).

Appendix C: Supplementary materials for Chapter 3

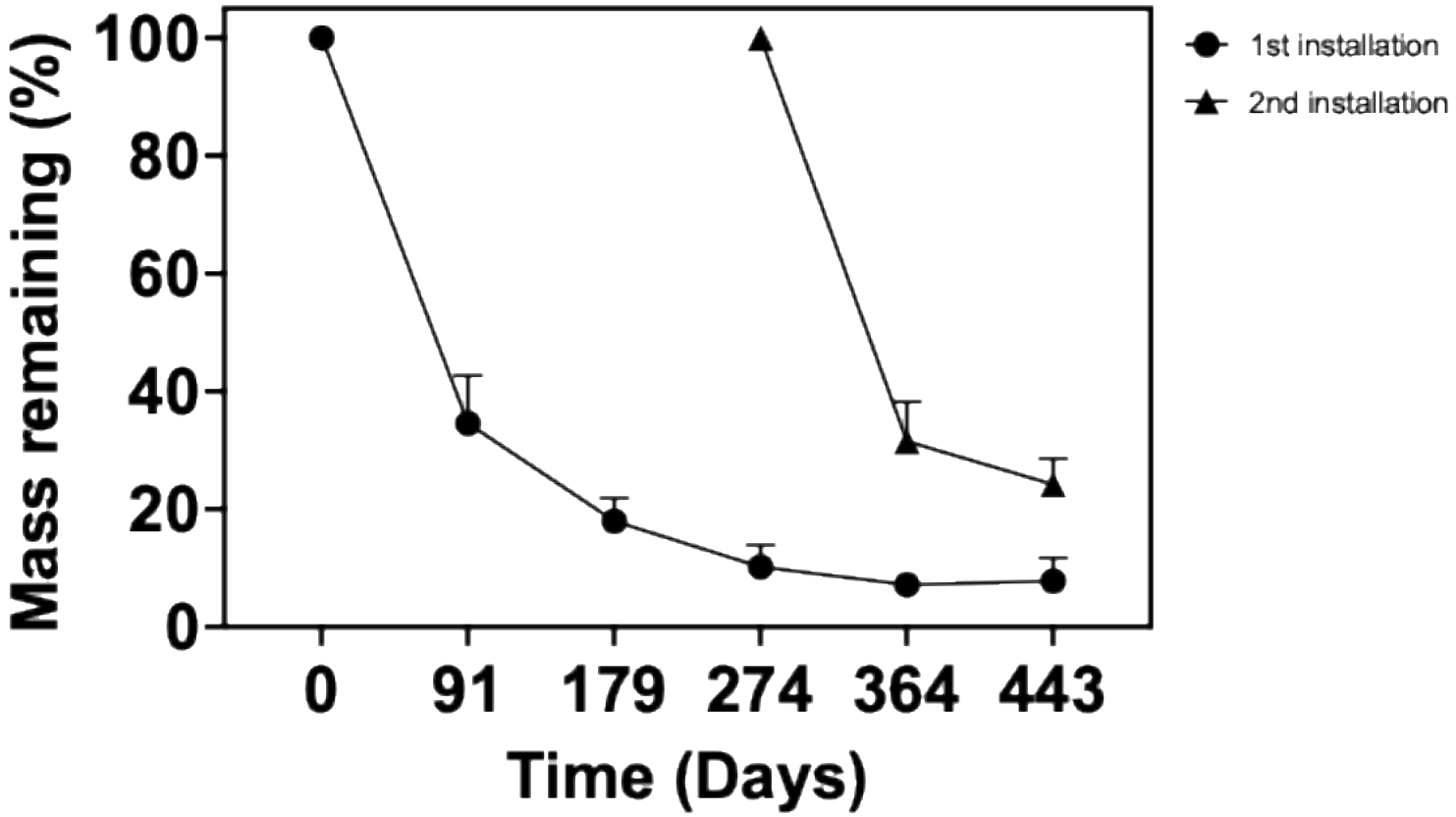

Figure C1: Percentage of the initial litter mass remaining (%LMR) of litterbag filled with lucerne hay (10g; see Section 3.2.2) over the course of 15 months of *in-situ* litterbag decomposition. Each point represents the mean %LMR and the error bars indicating standard deviation. Points in circle represent lucerne litterbag installed in the beginning of the trial (11 September 2023; 1st installation), while points in triangle represent lucerne litterbag installed in the middle of the trial (11 June 2024; 2nd installation). Lucerne hay was used as a positive control to make sure biological litter decomposition happened.

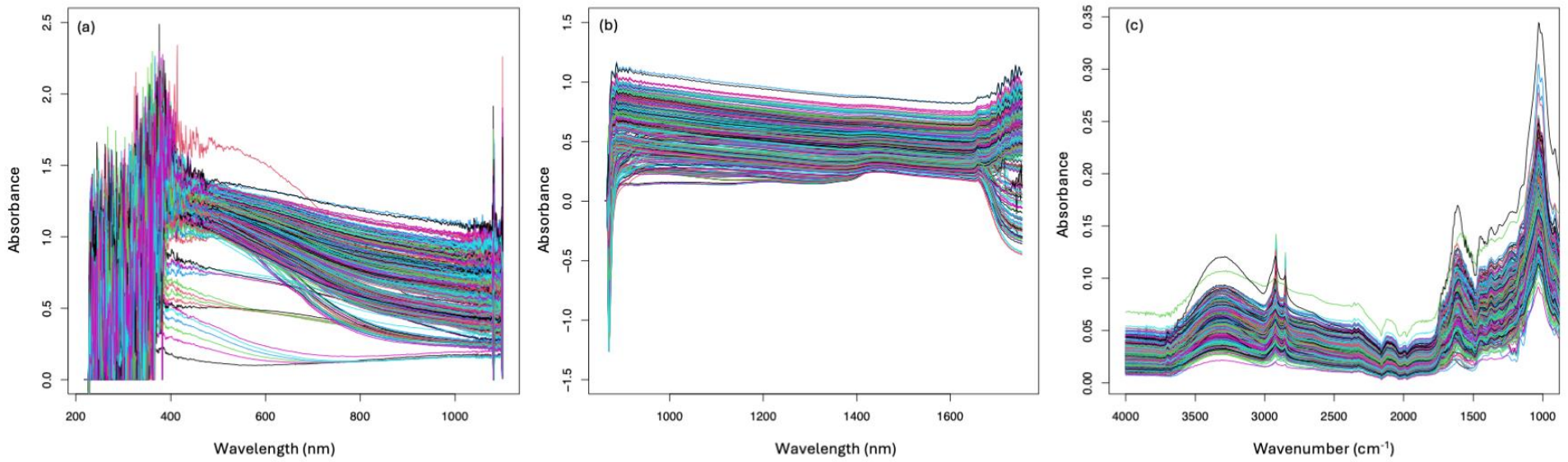

Figure C2: Example of raw (a) visible-near-infrared (vis-NIR); (b) near-infrared (NIR); and attenuated total reflectance Fourier transform infrared (ATR-FTIR) spectra of synthetic mixture, litterfall samples, and decomposing litter mixture from *in-situ* litterbag decomposition trial.

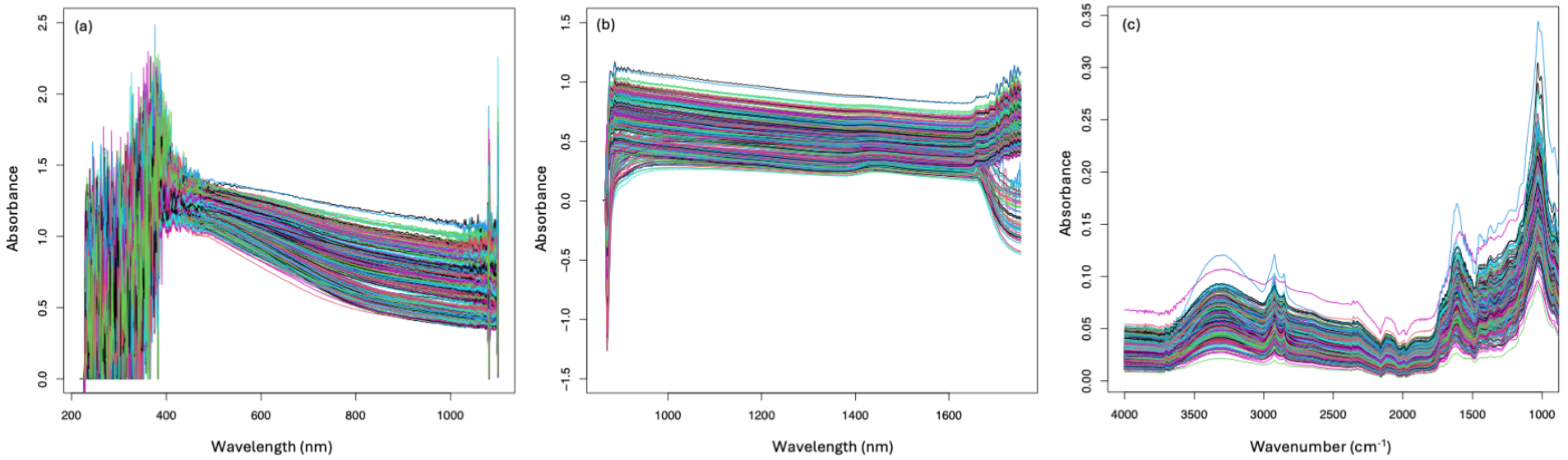

Figure C3: Example of raw (a) visible-near-infrared (vis-NIR); (b) near-infrared (NIR); and attenuated total reflectance Fourier transform infrared (ATR-FTIR) spectra of decomposing litter mixture from *in-situ* litterbag decomposition trial.

Table C1: Results of the best five models selected from vis-NIR, NIR, and ATR-FTIR spectra for predicting total carbon (TC) and total nitrogen (TN) in decomposing litter mixture from *in-situ* litterbag decomposition trial (see Chapter 3). Models were developed using multivariate modelling analysis including partial least square regression (PLSR), bootstrap PLSR, Cubist, and random forest (RF). Models were selected based on the highest coefficient of determination (R^2), the lowest root mean squared error (RMSE), and the highest Lin's Concordance Correlation Coefficient (LCCC) value after testing different pre-processing combinations (raw spectra, SG smoothing, SNV, and GA feature wavelength selection). SG = Savitzky-Golay smoothing; w = window size; k = polynomial order; SNV = standard normal variate transformation; R^2cv = coefficient of determination of cross-validation model; RMSECV = root mean squared error of cross-validation model; LCCCcv = Lin's Concordance Correlation Coefficient of cross-validation model; R^2v = coefficient of determination of validation model; RMSEV = root mean squared error of validation model; LCCCv = Lin's Concordance Correlation Coefficient of validation model.

Model 3: Generalised model using synthetic mixture and litterfall samples (from Chapter 2)

Spectra	Variable	Pre-processing technique	Model	Calibration dataset			Validation dataset		
				R²cv	**RMSECV**	**LCCCcv**	***R²v***	**RMSEV**	**LCCCv**
vis-NIR	Carbon	SG (w = 7, k = 2), SNV	PLSR	0.19	5.04	0.34	0.58	2.43	0.73
		SG (w = 5, k = 2), SNV	PLSR	0.19	5.02	0.35	0.57	2.45	0.73
		SG (w = 3, k = 2), SNV	PLSR	0.16	5.11	0.32	0.56	2.47	0.72
		Raw data	PLSR	0.03	5.71	0.16	0.38	2.94	0.52
		SG (w = 5, k = 2), SNV, GA	Bootstrap	0.14	5.19	0.24	0.29	4.43	-0.13
vis-NIR	Nitrogen	SG (w = 7, k = 2), SNV	PLSR	0.43	0.18	0.63	0.33	0.14	0.54
		SG (w = 3, k = 2), SNV	PLSR	0.49	0.17	0.67	0.31	0.14	0.51
		Raw data	PLSR	0.39	0.18	0.61	0.30	0.14	0.49
		SG (w = 5, k = 2), SNV	PLSR	0.48	0.17	0.67	0.29	0.14	0.51
		Raw data	Cubist	0.79	0.09	0.88	0.08	0.77	0.03
NIR	Carbon	SG (w = 3, k = 2), SNV	PLSR	0.07	5.58	0.10	0.05	3.64	0.10
		Raw data	PLSR	0.06	5.62	0.05	0.04	3.66	0.09
		SG (w = 5, k = 2), SNV	PLSR	0.08	5.48	0.13	0.04	3.65	0.10
		SG (w = 7, k = 2), SNV	PLSR	0.08	5.48	0.13	0.04	3.65	0.10
		Raw data	Bootstrap	0.21	4.98	0.32	0.04	10.92	-0.08

Table C1 continued.

Spectra	Variable	Pre-processing technique	Model	Calibration dataset			Validation dataset		
				R^2cv	RMSECV	LCCCcv	R^2v	RMSEV	LCCCv
NIR	Nitrogen	Raw data	PLSR	0.71	0.11	0.83	0.46	0.12	0.64
		SG (w = 5, k = 2), SNV	PLSR	0.69	0.09	0.83	0.45	0.12	0.62
		SG (w = 7, k = 2), SNV	PLSR	0.70	0.11	0.83	0.45	0.12	0.62
		SG (w = 3, k = 2), SNV	PLSR	0.49	0.17	0.67	0.31	0.14	0.51
		SG (w = 5, k = 2), SNV	Bootstrap	0.97	0.04	0.98	0.12	0.77	-0.06
ATR-FTIR	Carbon	SG (w = 7, k = 2), SNV	PLSR	0.33	3.77	0.55	0.67	2.13	0.80
		Raw data	PLSR	0.28	3.88	0.49	0.66	2.16	0.79
		SG (w = 3, k = 2), SNV	PLSR	0.27	3.93	0.49	0.66	2.16	0.79
		SG (w = 5, k = 2), SNV	PLSR	0.27	3.94	0.49	0.66	2.16	0.79
		Raw data	PLSR	0.32	3.72	0.50	0.30	7.28	-0.38
ATR-FTIR	Nitrogen	SG (w = 5, k = 2), SNV	PLSR	0.84	0.08	0.92	0.77	0.08	0.87
		SG (w = 3, k = 2), SNV	PLSR	0.84	0.08	0.92	0.77	0.08	0.87
		Raw data	PLSR	0.71	0.11	0.84	0.75	0.08	0.85
		SG (w = 7, k = 2), SNV	PLSR	0.84	0.08	0.91	0.76	0.08	0.87
		SG (w = 3, k = 2), SNV	Bootstrap	0.96	0.04	0.98	0.15	0.62	0.03

Model 4: Sample-specific model using litterbag samples (train-test split)

Spectra	Variable	Pre-processing technique	Model	Calibration dataset			Validation dataset		
				R^2cv	RMSECV	LCCCcv	R^2v	RMSEV	LCCCv
vis-NIR	Carbon	SG (w = 7, k = 2), SNV	PLSR	0.51	2.62	0.67	0.48	2.67	0.66
		Raw data	PLSR	0.51	2.61	0.67	0.44	2.77	0.63
		SG (w = 3, k = 2), SNV	PLSR	0.47	2.73	0.64	0.47	2.70	0.63
		SG (w = 5, k = 2), SNV	PLSR	0.47	2.73	0.64	0.47	2.71	0.63
		SG (w = 3, k = 2), SNV, GA	PLSR	0.50	2.63	0.67	0.44	2.82	0.62
vis-NIR	Nitrogen	SG (w = 3, k = 2), SNV	PLSR	0.50	0.12	0.64	0.35	0.13	0.57
		SG (w = 5, k = 2), SNV	PLSR	0.50	0.12	0.64	0.35	0.13	0.57
		SG (w = 7, k = 2), SNV	PLSR	0.50	0.12	0.64	0.35	0.13	0.57
		SG (w = 3, k = 2, m = 2), SNV	PLSR	0.50	0.12	0.64	0.35	0.13	0.57
		SG (w = 5, k = 2, m = 2), SNV	PLSR	0.50	0.12	0.64	0.35	0.13	0.57

Table A4 continued.

Spectra	Variable	Pre-processing technique	Model	Calibration dataset			Validation dataset		
				R^2cv	RMSECV	LCCCcv	R^2v	RMSEV	LCCCv
NIR	Carbon	SG (w = 3, k = 2, m = 2), SNV	PLSR	0.51	2.62	0.68	0.55	2.41	0.71
		SG (w = 5, k = 2, m = 2), SNV	PLSR	0.49	2.69	0.66	0.51	2.54	0.67
		SG (w = 7, k = 2, m = 2), SNV	PLSR	0.46	2.77	0.63	0.51	2.53	0.67
		Raw data	Cubist	0.46	2.76	0.64	0.38	2.89	0.59
		SG (w = 5, k = 2), SNV	Cubist	0.56	2.49	0.71	0.39	2.83	0.58
NIR	Nitrogen	SG (w = 5, k = 2, m = 2), SNV	PLSR	0.49	2.69	0.66	0.51	2.54	0.67
		SG (w = 7, k = 2, m = 2), SNV	PLSR	0.46	2.77	0.63	0.51	2.53	0.67
		Raw data	Cubist	0.46	2.76	0.64	0.38	2.89	0.59
		SG (w = 5, k = 2), SNV	Cubist	0.56	2.49	0.71	0.39	2.83	0.58
		Raw data	PLSR	0.55	0.12	0.70	0.40	0.12	0.60
ATR-FTIR	Carbon	SG (w = 5, k = 2), SNV	PLSR	0.73	1.94	0.84	0.68	2.04	0.81
		Raw data	PLSR	0.71	2.02	0.83	0.68	2.06	0.81
		SG (w = 3, k = 2), SNV	PLSR	0.73	1.94	0.85	0.68	2.07	0.81
		SG (w = 7, k = 2), SNV	PLSR	0.73	1.95	0.84	0.67	2.08	0.81
		Raw	Bootstrap	0.74	1.97	0.84	0.64	2.19	0.78
ATR-FTIR	Nitrogen	SG (w = 3, k = 2), SNV	PLSR	0.76	0.08	0.86	0.73	0.08	0.85
		SG (w = 7, k = 2), SNV	PLSR	0.79	0.08	0.88	0.73	0.08	0.85
		SG (w = 5, k = 2), SNV	PLSR	0.77	0.08	0.87	0.71	0.08	0.84
		SG (w = 3, k = 2), SNV	Bootstrap	0.77	0.08	0.87	0.68	0.09	0.82
		SG (w = 3, k = 2), SNV	Cubist	0.83	0.07	0.91	0.69	0.09	0.83

[a] The wavelength range for the vis-NIR spectral regions was 500.5-1,000 nm.
[b] The wavelength range for the NIR spectral region was 1,000.5-1,650 nm.
[c] The wavenumber range for the MIR infrared region was 4,000-650 cm^{-1} (wavelength: 2,500-25,000 nm).

Appendix D: Supplementary materials for Chapter 4

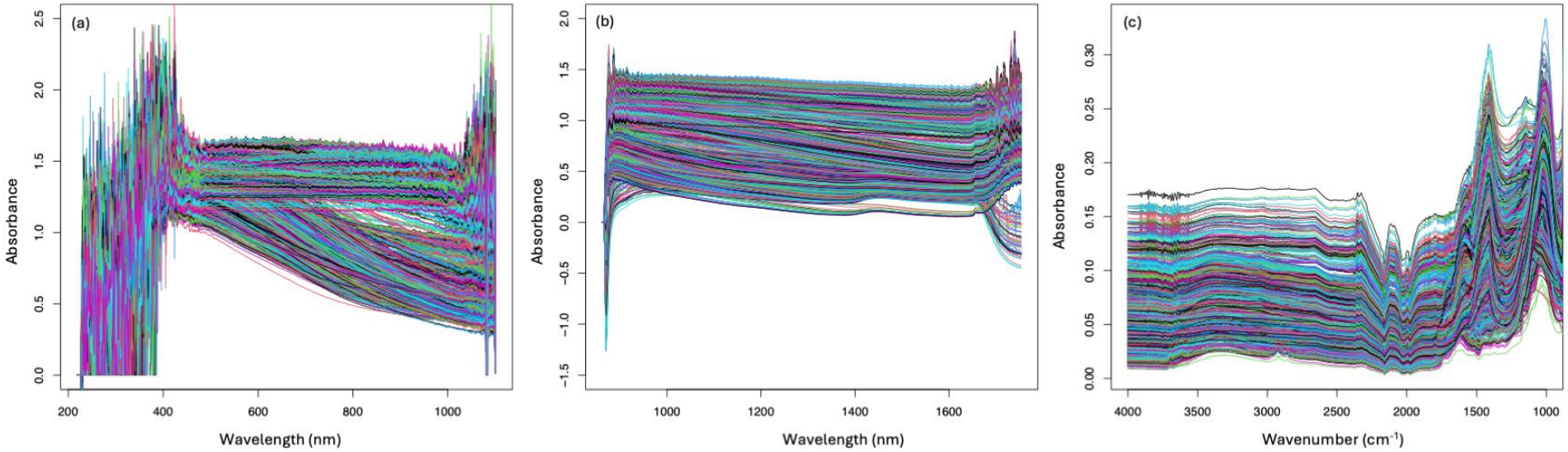

Figure D1: Example of raw (a) visible-near-infrared (vis-NIR); (b) near-infrared (NIR); and attenuated total reflectance Fourier transform infrared (ATR-FTIR) spectra of decomposing litter mixture from *in-situ* litterbag decomposition trial and combustion residues from surface fuel litter: leaf litter, twigs, and surface fine fuel.

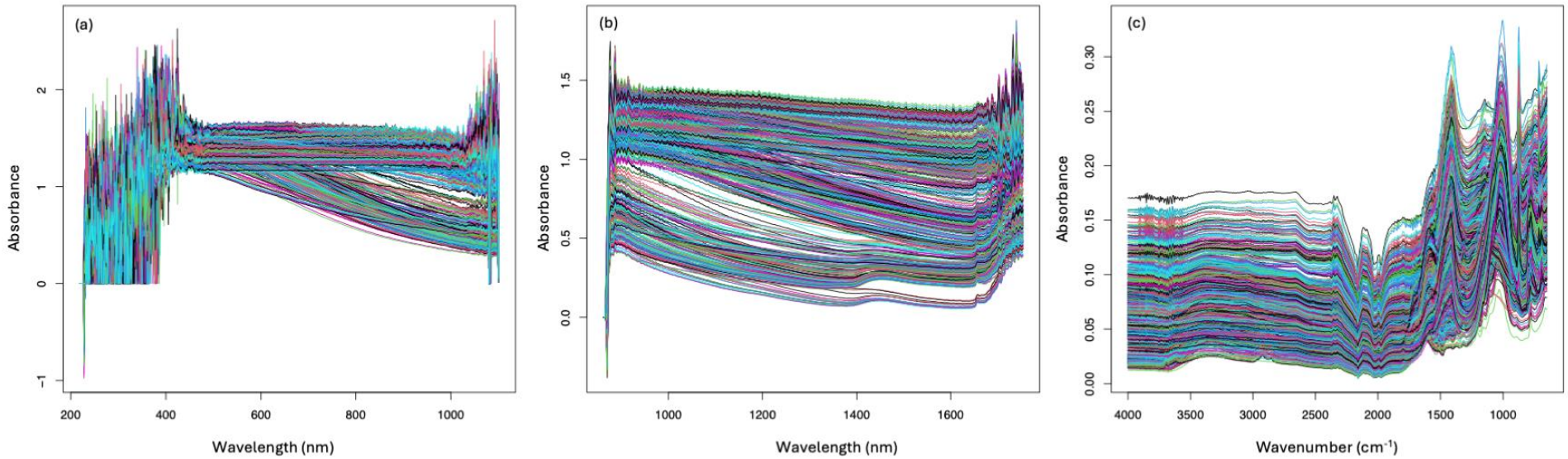

Figure D2: Example of raw (a) visible-near-infrared (vis-NIR); (b) near-infrared (NIR); and attenuated total reflectance Fourier transform infrared (ATR-FTIR) spectra combustion residues from surface fuel litter: leaf litter, twigs, and surface fine fuel.

Table D1: Result of the best five models selected from vis-NIR, NIR, and ATR-FTIR spectra for predicting total carbon (TC) and total nitrogen (TN) in combustion residues from surface fuel litter: leaf litter, twigs, and surface fine fuel (see Chapter 4). Models were developed using multivariate modelling analysis including partial least square regression (PLSR), bootstrap PLSR, Cubist, and random forest (RF). Models were selected based on the highest coefficient of determination (R^2), the lowest root mean squared error (RMSE), and the highest Lin's Concordance Correlation Coefficient (LCCC) value after testing different pre-processing combinations (raw spectra, SG smoothing, SNV, and GA feature wavelength selection). SG = Savitzky-Golay smoothing; w = window size; k = polynomial order; SNV = standard normal variate transformation; R^2cv = coefficient of determination of cross-validation model; RMSECV = root mean squared error of cross-validation model; LCCCcv = Lin's Concordance Correlation Coefficient of cross-validation model; R^2v = coefficient of determination of validation model; RMSEV = root mean squared error of validation model; LCCCv = Lin's Concordance Correlation Coefficient of validation model.

Model 5: Generalised model using litterbag samples (from Chapter 3)

Spectra	Variable	Pre-processing technique	Model	Calibration dataset			Validation dataset		
				R²cv	**RMSECV**	**LCCCcv**	***R²v***	**RMSEV**	**LCCCv**
vis-NIR	Carbon	Raw data	PLSR	0.39	3.40	0.62	0.75	5.70	0.85
		SG (w = 3, k = 2), SNV	PLSR	0.27	3.39	0.38	0.71	6.10	0.82
		SG (w = 5, k = 2), SNV	PLSR	0.27	3.39	0.38	0.71	6.11	0.82
		SG (w = 7, k = 2), SNV	PLSR	0.24	3.39	0.35	0.67	6.45	0.79
		SG (w = 3, k = 2), SNV, GA	PLSR	0.50	2.63	0.67	0.24	16.72	0.40
vis-NIR	Nitrogen	SG (w = 3, k = 2), SNV	PLSR	0.01	0.18	-0.01	0.09	0.36	0.16
		SG (w = 5, k = 2), SNV	PLSR	0.01	0.18	-0.10	0.09	0.36	0.16
		SG (w = 7, k = 2), SNV	PLSR	0.01	0.18	-0.01	0.08	0.36	0.15
		Raw data	PLSR	0.01	0.20	0.88	0.08	0.28	0.40
		SG (w = 3, k = 2), SNV, GA	RF	0.95	0.05	0.93	0.16	0.40	-0.07
NIR	Carbon	Raw data	PLSR	0.06	4.59	0.24	0.73	6.00	0.82
		SG (w = 3, k = 2), SNV	PLSR	0.18	4.52	0.41	0.55	7.68	0.66
		SG (w = 5, k = 2), SNV	PLSR	0.13	4.69	0.35	0.56	7.59	0.68
		SG (w = 7, k = 2), SNV	PLSR	0.12	4.71	0.34	0.56	7.55	0.68
		Raw data	RF	0.46	2.76	0.64	0.19	12.31	0.43

Table D1 continued.

Spectra	Variable	Pre-processing technique	Model	Calibration dataset			Validation dataset		
				R^2cv	RMSECV	LCCCcv	R^2v	RMSEV	LCCCv
NIR	Nitrogen	SG (w = 3, k = 2), SNV	PLSR	0.11	0.18	0.33	0.54	0.26	0.69
		Raw data	PLSR	0.19	0.17	0.42	0.48	0.27	0.64
		SG (w = 5, k = 2), SNV	PLSR	0.20	0.16	0.41	0.29	0.32	0.44
		SG (w = 7, k = 2), SNV	PLSR	0.23	0.16	0.42	0.26	0.32	0.41
		SG (w = 5, k = 2), SNV	RF	0.94	0.06	0.93	0.18	0.42	-0.17
ATR-FTIR	Carbon	SG (w = 3, k = 2), SNV	PLSR	0.69	2.08	0.81	0.95	2.38	0.95
		Raw data	PLSR	0.63	2.27	0.78	0.95	2.47	0.95
		SG (w = 5, k = 2), SNV	PLSR	0.69	2.09	0.81	0.95	2.39	0.95
		SG (w = 7, k = 2), SNV	PLSR	0.70	2.06	0.83	0.86	2.37	0.98
		Raw data	Cubist	0.80	1.68	0.89	0.72	6.59	0.76
ATR-FTIR	Nitrogen	Raw data	PLSR	0.63	0.11	0.79	0.91	0.11	0.95
		SG (w = 3, k = 2), SNV	PLSR	0.63	0.11	0.78	0.90	0.12	0.95
		SG (w = 5, k = 2), SNV	PLSR	0.64	0.10	0.80	0.90	0.12	0.95
		SG (w = 7, k = 2), SNV	PLSR	0.65	0.10	0.80	0.90	0.12	0.95
		Raw data	Cubist	0.80	0.08	0.88	0.21	0.36	0.40

Model 6: Sample-specific model using combustion residues from Wombat SF and Orbost SF

Spectra	Variable	Pre-processing technique	Model	Calibration dataset			Validation dataset		
				R^2cv	RMSECV	LCCCcv	R^2v	RMSEV	LCCCv
Vis-NIR	Carbon	Raw data	PLSR	0.71	5.30	0.84	0.86	5.19	0.91
		SG (w = 3, k = 2), SNV	PLSR	0.69	5.50	0.82	0.73	7.05	0.82
		SG (w = 5, k = 2), SNV	PLSR	0.69	5.51	0.82	0.73	7.07	0.82
		SG (w = 7, k = 2), SNV	PLSR	0.69	5.52	0.82	0.72	7.09	0.82
		Raw data	RF	0.97	1.92	0.98	0.71	7.36	0.81

Table A5 continued.

Spectra	Variable	Pre-processing technique	Model	Calibration dataset			Validation dataset		
				R^2cv	RMSECV	LCCCcv	R^2v	RMSEV	LCCCv
Vis-NIR	Nitrogen	Raw data	PLSR	0.26	0.30	0.42	0.34	0.36	0.47
		SG (w = 3, k = 2), SNV	RF	0.97	0.08	0.97	0.28	0.40	0.37
		SG (w = 5, k = 2), SNV	RF	0.97	0.08	0.97	0.28	0.39	0.37
		SG (w = 7, k = 2), SNV	RF	0.97	0.08	0.97	0.28	0.40	0.37
		SG (w = 3, k = 2), SNV	Cubist	0.87	0.13	0.93	0.21	0.43	0.43
NIR	Carbon	Raw data	PLSR	0.72	5.26	0.84	0.88	4.91	0.92
		SG (w = 3, k = 2), SNV	PLSR	0.60	6.27	0.76	0.79	6.42	0.85
		SG (w = 5, k = 2), SNV	PLSR	0.60	6.29	0.76	0.78	6.55	0.85
		SG (w = 7, k = 2), SNV	PLSR	0.60	6.27	0.77	0.77	6.68	0.84
		Raw data, GA	PLSR	0.71	5.25	0.83	0.69	8.33	0.76
NIR	Nitrogen	Raw data	PLSR	0.57	0.23	0.73	0.71	0.23	0.82
		SG (w = 3, k = 2), SNV	PLSR	0.37	0.28	0.55	0.53	0.30	0.67
		SG (w = 5, k = 2), SNV	PLSR	0.36	0.28	0.55	0.53	0.30	0.66
		SG (w = 7, k = 2), SNV	PLSR	0.36	0.28	0.55	0.51	0.31	0.64
		Raw data, GA	PLSR	0.49	0.25	0.66	0.62	0.45	0.21
ATR-FTIR	Carbon	Raw data	PLSR	0.94	2.49	0.97	0.97	2.19	0.99
		SG (w = 3, k = 2), SNV	PLSR	0.94	2.46	0.97	0.94	2.46	0.98
		SG (w = 5, k = 2), SNV	PLSR	0.94	2.42	0.97	0.97	2.35	0.98
		SG (w = 7, k = 2), SNV	PLSR	0.94	2.37	0.97	0.97	2.28	0.99
		SG (w = 3, k = 2), SNV	Bootstrap	0.94	2.39	0.97	0.96	2.75	0.98
ATR-FTIR	Nitrogen	Raw data	PLSR	0.92	0.10	0.96	0.93	0.12	0.96
		SG (w = 3, k = 2), SNV	PLSR	0.91	0.10	0.96	0.92	0.12	0.96
		SG (w = 5, k = 2), SNV	PLSR	0.91	0.10	0.95	0.92	0.12	0.96
		SG (w = 7, k = 2), SNV	PLSR	0.91	0.10	0.95	0.92	0.12	0.96
		Raw data	Bootstrap	0.93	0.01	0.97	0.86	0.18	0.89

[a] The wavelength range for the vis-NIR spectral regions was 500.5-1,000 nm.
[b] The wavelength range for the NIR spectral region was 1,000.5-1,650 nm.
[c] The wavenumber range for the MIR infrared region was 4,000-650 cm^{-1} (wavelength: 2,500-25,000 nm).